



DCU

**Ion Chromatographic Analysis
of Disinfectant By-Products**

For the award of
Doctor of Philosophy

Leon Barron

**School of Chemical Sciences
Student ID: 97311006**

Table of Contents

<i>Declaration</i>	11
<i>List of Figures</i>	12
<i>List of Tables</i>	20
<i>List of Abbreviations</i>	22
<i>List of Publications</i>	23
<i>List of Poster Presentations</i>	24
<i>List of Oral Presentations</i>	25
<i>List of Honours and Awards</i>	25
<i>Acknowledgements</i>	26
Abstract	28
Chapter 1.0 Literature Review	30
1.0 Background	31
1.1 Current Water Treatment Methods	32
1.1.1 Ozonation	32
1.1.2 Chlorination	35
1.2 Factors Affecting the Formation of Disinfectant By-Products	36
1.2.1 pH	36
1.2.2 Contact Time	37
1.2.3 Temperature and Season	37
1.2.4 Concentration and Properties of Natural Organic Matter	37
1.2.5 Concentration of Chlorine and Residual Chlorine	38
1.2.6 Concentration of Bromide	38

1.3	The Haloacetic Acids	39
1.3.1	<i>Chlorinated Acetic Acids</i>	39
1.3.1.1	<i>Physical and Chemical Properties</i>	39
1.3.1.2	<i>Effects on Laboratory Animals and/or Humans</i>	39
1.3.2	<i>Brominated Acetic Acids</i>	40
1.3.2.1	<i>Physical Properties</i>	40
1.3.2.2	<i>Effect on Laboratory Animals and/or Humans</i>	41
1.4	Chromatographic Determination of Haloacetic Acids	42
1.4.1	<i>Introduction to chromatographic theory</i>	42
1.4.2	<i>Band broadening in chromatography</i>	45
1.4.2.1	<i>Multiple path lengths</i>	45
1.4.2.3	<i>Molecular diffusion</i>	46
1.4.2.4	<i>Mass transfer</i>	47
1.4.2.5	<i>The van Deemter equation</i>	47
1.5	Ion Exchange Chromatography	48
1.5.1	<i>The Ion Exchange Process</i>	49
1.5.1.1	<i>Cation Exchange</i>	49
1.5.1.2	<i>Anion Exchange</i>	49
1.5.2	<i>Ion Exchange Stationary Phases</i>	51
1.5.2.1	<i>Polymeric exchangers</i>	52
1.5.2.2	<i>Dionex micro-bore anion exchangers suited to HA and oxyhalide analysis</i>	53
1.5.2.3	<i>Acrylic polymer based phases</i>	55
1.6	Ion Chromatography Instrumentation	55
1.6.1	<i>Eluent delivery and pumping systems</i>	56
1.6.2	<i>Injection systems</i>	58
1.6.3	<i>Detection Techniques in Ion Chromatography</i>	58
1.6.3.1	<i>Ultra Violet Detection</i>	58
1.6.3.2	<i>Conductivity Detection</i>	59
1.6.3.2.1	<i>Suppressed conductivity detection in anion exchange chromatography</i>	64

1.6.3.3	<i>Electrospray Ionisation-Mass Spectrometric Detection (ESI-MS)</i>	67
1.6.3.3.1	<i>Principles of Electrospray Ionisation (ESI)</i>	67
1.6.3.3.2	<i>Negative ion, positive ion and neutral modes</i>	68
1.6.3.3.3	<i>Considerations for practical hyphenation to ion chromatography</i>	69
1.6.3.3.4	<i>The Ion trap mass analyser</i>	73
1.7	Applications of IC to DBP Analysis	75
1.7.1	<i>Chloral Hydrate</i>	75
1.7.2	<i>Oxyhalides of Chloride and Bromide</i>	76
1.7.3	<i>Application of IC to the determination of HAs</i>	84
1.7.3.1	<i>Ion-interaction chromatography</i>	84
1.7.3.2	<i>Ion exchange chromatography</i>	85
1.7.3.3	<i>Ion-exclusion chromatography</i>	86
1.7.3.4	<i>IC-ESI-MS</i>	87
1.7.3.5	<i>IC-ICP-MS</i>	89
1.7.4	<i>Preconcentration methods for HAs</i>	92
1.7.4.1	<i>Solid phase extraction (SPE)</i>	93
1.7.4.1.1	<i>Problems with SPE</i>	93
1.7.4.1.2	<i>Comparison of stationary phases</i>	94
1.7.4.1.3	<i>Interference elimination</i>	95
1.8	References	100

3.3.1	<i>Extraction and elution of HAs using LiChrolut EN SPE cartridges</i>	147
3.3.2	<i>Determination of the eluting agent</i>	148
3.3.3.	<i>Sample load rate and recoveries</i>	149
3.3.4	<i>Durability of the LiChrolut EN cartridge</i>	152
3.3.5	<i>Capacity of LiChrolut EN cartridge</i>	154
3.3.6	<i>Analysis of real samples</i>	156
3.3.7	<i>Standard Addition</i>	160
3.4	Conclusion	162
3.5	References	163

Chapter 4.0 Reagentless Ion Exchange Chromatography of Haloacetates and Separations with an AS16 Column **164**

4.1	Introduction	165
4.2	Experimental	168
	4.2.1 <i>Instrumentation</i>	168
	4.2.2 <i>Reagents</i>	168
4.3	Results and Discussion	169
	4.3.1. <i>Initial Separations and Comparison of EG40 to Manually Prepared Eluents</i>	169
	4.3.2 <i>Reproducibility of retention time with electrolytically generated eluents</i>	172
	4.3.3 <i>Limits of Detection</i>	175
	4.3.4 <i>Analysis of Real Samples with Preconcentration and EG40 System Separation</i>	177
	4.3.5 <i>Separation of inorganic chloride and MBA</i>	181
	4.3.6 <i>Effect of Temperature</i>	186
	4.3.7 <i>Comparison of Limits of Detection of AS16 and AS11-HC column methods</i>	189
	4.3.8 <i>Repeatability of AS16 Method</i>	192
	4.3.9 <i>Linearity of AS16 method</i>	193

4.4	Conclusions	194
4.5	References	195

Chapter 5.0	Trace Detection of HAs with Monolithic Cation Exchange Type Suppressor and Investigation into the Effect of LiChrolut EN Sorbent Mass	196
--------------------	--	------------

5.1	Introduction	197
5.2	Experimental	199
	5.2.1 <i>Instrumentation</i>	199
	5.2.2 <i>Chemicals</i>	199
	5.2.3 <i>Sample collection and treatment</i>	200
5.3	Results and Discussion	201
	5.3.1 <i>Improvements in sensitivity with Atlas suppressor</i>	201
	5.3.2 <i>Inclusion of DCBA and CDBA</i>	204
	5.3.3 <i>Sample pre-treatment and removal of interferent ions</i>	204
	5.3.4 <i>Analysis of drinking water samples</i>	209
	5.3.4.1 <i>HAs in drinking water without using preconcentration procedure</i>	209
	5.3.4.2 <i>Preconcentration and HA determination in drinking water supplies</i>	212
	5.3.5 <i>Investigation into LiChrolut EN sorbent mass</i>	218
5.4	Conclusions	227
5.5	References	228

Chapter 6.0	Alternative Detection Modes to Suppressed Conductivity Detection for HA Analysis	229
6.1	Introduction	230
6.2	Experimental	232
	6.2.1 <i>Instrumentation</i>	232
	6.2.2 <i>Chemicals</i>	232
6.3	Results and Discussion	234
	6.3.1 <i>UV detection – wavelength optimisation</i>	234
	6.3.2 <i>UV detector linearity and low limit sensitivity</i>	237
	6.3.3 <i>Direct Infusion – Mass Spectrometry</i>	239
	6.3.4 <i>Ion chromatography-mass spectrometry optimisation</i>	249
	6.3.4.1 <i>Elimination of background interference</i>	249
	6.3.4.2 <i>Optimum parameters for simultaneous detection of nine HAs</i>	251
	6.3.4.3 <i>Addition of volatilising solvent</i>	253
	6.3.4.4 <i>Optimisation of % MeOH in total flow</i>	254
	6.3.5.5 <i>Improvement in UV chromatogram with manually prepared eluent</i>	256
	6.3.5 <i>Trends in observed ion types for each HA</i>	257
	6.3.6 <i>Analysis of a drinking water sample using suppressed ion chromatography with conductivity, UV and ESI-MS detection</i>	260
6.4	Conclusion	264
6.5	References	265


Chapter 7.0 Use of Temperature Programming to Improve Resolution of Inorganic Anions, Haloacetates and Oxyhalides by Suppressed IC-ESI-MS	267
7.1 Introduction	268
7.2 Experimental	270
7.2.1 <i>Apparatus</i>	270
7.2.2 <i>Reagents</i>	271
7.2.3 <i>Procedure</i>	271
7.3 Results and Discussion	273
7.3.1 <i>Effect of temperature on ion chromatography – theoretical considerations</i>	273
7.3.1.1 <i>Ion-exchanger</i>	274
7.3.1.2 <i>Mobile phase</i>	275
7.3.1.3 <i>Solutes</i>	276
7.3.2 <i>Van't Hoff plots</i>	276
7.3.3 <i>Alteration of existing IC gradient method for separation of oxyhalides from HAs</i>	282
7.3.4 <i>Effect of elevated temperature upon gradient IC separation</i>	283
7.3.5 <i>Column oven performance</i>	285
7.3.6 <i>Application of temperature program</i>	288
7.3.7 <i>Optimum method for suppressed ion chromatography with conductivity and electrospray mass spectrometry.</i>	291
7.3.8 <i>Analytical performance data for suppressed IC-ESI-MS and conductivity detection</i>	292
7.3.8.1 <i>Retention time reproducibility of dual gradient method</i>	292
7.3.8.2 <i>Linearity for suppressed conductivity and ESI-MS</i>	294
7.3.8.3 <i>LOD for conductivity detection</i>	298
7.3.8.4 <i>ESI-MS of oxyhalides and limit of detection</i>	302
7.3.8.5 <i>ESI-MS Reproducibility</i>	305

7.3.9	<i>Application to real samples</i>	306
7.3.9.1	<i>Application to HA and oxyhalide determinations in soil</i>	306
7.3.9.2	<i>Suppressed IC-conductivity-ESI-MS of drinking water sample</i>	309
7.4	Conclusions	315
7.5	References	316
Chapter 8.0	Final Conclusions and Summations	318
Appendix A.1		322
Appendix A.2		326
Appendix A.3		328
Appendix A.4		333
Appendix A.5		337
Appendix A.6		339
Appendix A.7	Poster Presentations	343

I hereby certify that this material, which I now submit for assessment on the programme of study leading to the award of

Doctor of Philosophy

is entirely my own work and has not been taken from the work of others save and to the extent that such work has been cited and acknowledged within the text of my work.

Signed:  ID No.: 97311006

Date: 26th May, 2005

List of Figures

- Fig. 1.1 Bromate formation pathways during ozonation
- Fig. 1.2 Relative composition of other DBP classifications associated with ozonation as a proportion of assimilable total organic carbon. Note: This does not include the oxyhalides as they are non-carbon containing DBPs.
- Fig. 1.3 Classification and relative proportion of halogenated DBPs to total organic carbon in chlorinated drinking water.
- Fig. 1.4 Typical chromatogram for the separation of two species showing retention time and peak asymmetry (A_s).
- Fig. 1.5 Calculating the resolution of two adjacent peaks, where W and t_r are measured in decimal minutes.
- Fig. 1.6 Schematic of eddy diffusion of solute molecules causing band broadening in chromatographic separations.
- Fig. 1.7 Van Deemter Plot to determine the optimum flow rate for a chromatographic system.
- Fig. 1.8 Structure of an ion exchange resin
- Fig. 1.9 Cross-linked polymeric ion exchanger
- Fig. 1.10 Schematic of an IC system showing reciprocating pump, injector valve, guard and analytical columns and detector. Only conductivity detector cells are located inside the column oven. UV and mass spectrometric detectors lie external to column oven.
- Fig. 1.11 Schematic of a variable wavelength detector with deuterium lamp, diffraction grating, sample cell and photocell.
- Fig. 1.12 Suppressed ion chromatography in auto suppression and external water modes.
- Fig. 1.13 Chemical suppression of hydroxide eluent with sulphuric acid. No electrical potential is required in this mode. All hydroxide is neutralised by hydronium ions to form water. Sodium ions cross membrane to the regenerant chamber to waste.
- Fig. 1.14 Hiraoka and Hewlett-Packard/Bruker Daltonics design schematic for orthogonal sample introduction into ion source.
-
- Fig. 2.1 Initial isocratic separation of 25 μ L of 0.1 mM of the seven HAs at 0.38 mL/min, and 30 mM NaOH eluent. Elution order: 1 = MCA, 2 = MBA, 3 = TFA, 4 = DCA, 5 = CDFA, 6 = DBA, 7 = TCA.
- Fig. 2.2 Linear gradient of 30-100 mM NaOH eluent showing separation and improved peak shape for the HAs. Elution order: 1 = MCA, 2 = MBA, 3 = TFA, 4 = DCA, 5 = CDFA, 6 = DBA, 7 = TCA.
- Fig. 2.3 Conductivity trace of 0.05 μ M of seven HAs with 0.06 μ M spike of Cl^- , BrO_3^- , NO_2^- , NO_3^- , SO_4^{2-} and 0.1 μ M PO_4^{3-} . Elution order: 1 = MCA, 2 = BrO_3^- and Cl^- , 3 = NO_2^- , 4 = PO_4^{3-} , 5 = TFA, 6 = DCA, 7 = NO_3^- , 8 = CDFA, 9 = SO_4^{2-} , 10 = DBA, 11 = TCA. Flow rate: 0.38 mL/min; Loop size: 25 μ L.

- Fig. 2.4 UV trace of HAs and interfering inorganic anions at 230 nm. Elution Order: 1 = MCA, 2 = MBA, 3 = NO₂⁻, 4 = TFA, 5 = DCA, 6 = NO₃⁻, 7 = CDFA, 8 = DBA, 9 = TCA.
- Fig. 2.5 Gradient of 10-100 mM NaOH after 10 minutes. Elution order: 1 = MCA, 2 = MBA, 3 = TFA, 4 = DCA, 5 = CDFA, 6 = DBA, 7 = TCA.
- Fig. 2.6 Gradient separation of the seven HAs using 10 – 100 mM NaOH at a flow rate of 0.30 mL/min. Elution Order: 1 = MCA, 2 = MBA, 3 = TFA, 4 = DCA, 5 = CDFA, 6 = DBA, 7 = TCA.
- Fig. 2.7 Gradient separation of 0.1 mM of seven HAs in Milli-Q water spiked with commonly occurring inorganic anions. Elution order: 1 = F (2 mg/L), 2 = MCA, 3 + 4 = Cl⁻ (2 mg/L) and MBA, 5 = TFA, 6 = DCA, 7 = NO₃⁻ (1 mg/L), 8 = CDFA, 9 + 10 = SO₄²⁻ (2 mg/L) and DBA, 11 = TCA. Flow rate: 0.30 mL/min; Injection volume: 25 µL. Gradient Parameters: 10 mM NaOH for 15 minutes; 10-100 mM NaOH over 15 minutes; 100 mM NaOH for a further 10 minutes. Post-acquisition parameters and equilibration: 100-10 mM NaOH for 5 minutes; 10 mM NaOH for a further 5 minutes. Detection: Suppressed conductivity at 50 mA.
- Fig. 2.8 Van't Hoff Plots for fluoride ($R^2 = 0.8399$; $m = -669.25$), MCA ($R^2 = 0.9825$; $m = -646.53$), chloride ($R^2 = 0.9419$; $m = -257.17$), MBA ($R^2 = 0.9520$; $m = -481.32$), DCA ($R^2 = 0.9755$; $m = -393.18$), nitrate ($R^2 = 0.6974$, $m = 351.77$), DBA ($R^2 = 0.9035$, $m = -190.95$) and sulphate ($R^2 = 0.9948$, $m = -2000.10$) using a 30 mM NaOH isocratic gradient at a flow rate of 0.30 mLmin⁻¹ over a temperature range of 21-45 °C.
- Fig. 2.9 The effect of temperature on the retention of the seven HAs and two inorganic anions in eluent gradient of 10-100 mM NaOH.
- Fig. 2.10 The effect of temperature on the retention behaviour of seven HAs and 5 inorganic anions. Elution Order: 1 = fluoride, 2 = MCA, 3 = chloride/MBA, 4 = TFA, 5 = nitrate, 6 = DCA, 7 = CDFA, 8 = DBA, 9 = sulphate, 10 = TCA. [HA] = 0.1 mM. Note: 23°C trace does not contain DBA, to illustrate the retention of sulphate.
- Fig. 2.11 The effect of temperature on nitrate retention. 1 = TFA, 2 = nitrate, 3 = DCA.
- Fig. 2.12 Optimum separation of 50 µM of seven HAs and five inorganic anions at an oven temperature of 40°C. Elution order: 1 = fluoride (2 mg/L), 2 = MCA, 3 + 4 = MBA/chloride (0.5 mg/L), 5 = nitrite (1 mg/L), 6 = TFA, 7 = nitrate (1 mg/L), 8 = DCA, 9 = CDFA, 10 = DBA, 11 = sulphate (5 mg/L), 12 = TCA.
- Fig. 2.13 A: Standard of 5, 5, 7.5, 7.5, 15, 15, and 25 µM of the seven HAs respectively of elution order and just above LOD of S:N of 3:1. B: One-tenth concentration of A representing the MDL for the seven HAs. Elution Order: 1 = MCA, 2 = MBA/chloride, 3 = TFA, 4 = DCA, 5 = CDFA, 6 = DBA, 7 = sulphate, 8 = TCA.
- Fig. 2.14 Separation of 0.1 mM of seven HAs in drinking water using the optimum methodology. Elution Order: 1 = fluoride, 2 = MCA, 3

- = MBA/chloride, 4 = TFA, 5 = nitrate, 6 = DCA, 7 = CDFA, 8 = DBA, 9 = sulphate, 10 = TCA. Loop: 25 μ L.
- Fig. 2.15 Near LOD trace for four of the seven HAs. Elution Order: 1 = fluoride, 2 = MCA (2 μ M), 3 = chloride/MBA (2 μ M), 4 = TFA (3 μ M), 5 = nitrate, 6 = carbonate, 7 = CDFA (6 μ M), 8 = sulphate. Inset: TCA near LOD peak (70 μ M).
- Fig. 3.1 Percent recoveries and elution profiles for HAs within each 0.5 mL fraction of eluate at three preconcentration flow rates on LiChrolut EN SPE cartridges. Eluent = 10 mM NaOH; (a) eluent = 1 mL/min; (b) eluent = 2 mL/min; (c) eluent = 3 mL/min sample loading flow rate.
- Fig. 3.2 Capacity study for LiChrolut EN cartridge. Volumes of 10, 20, 50 and 250 mL of 5 μ M MCA, MBA, TFA and DCA and 10 μ M CDFA, DBA and TCA preconcentrated to 2 mL NaOH with LiChrolut EN cartridge.
- Fig. 3.3 Chromatograms of preconcentration of drinking water using LiChrolut EN solid phase extraction cartridges from (A) Dublin City University showing MCA, DCA and TCA with inset enlarged to the right (B) Drumcondra showing MCA and DCA (C) Ballsbridge showing DCA and (D) Celbridge Co. Kildare showing levels of DCA.
- Fig. 3.4 Standard addition curve for DCA found in Dublin City University drinking water source. [DCA] = 0.29 μ M or 34 μ g/L.
- Fig. 3.5 Preconcentrated unspiked sample of Dublin City University drinking water source. Standard addition shows that DCA was present at a concentration of 34 μ g/L on that date.
- Fig. 4.1 Schematic of the eluent generation process.
- Fig. 4.2 Schematic of the continuously regenerated anion trap column (CR-ATC).
- Fig. 4.3 Comparison of electrolytically generated eluents with manually prepared hydroxide eluents with respect to baseline stability, retention matching and noise level. Elution Order: 1 = MCA (0.5 μ M), 2 = MBA (0.5 μ M)/Chloride, 3 = TFA (0.75 μ M), 4 = Nitrate, 5 = DCA (0.75 μ M), 6 = CDFA (1.5 μ M), 7 = DBA (1.5 μ M), 8 = sulphate, 9 = TCA (3.0 μ M).
- Fig. 4.4 Reproducibility of A: peak height; B: t_r and C: t_r for TCA in particular. [HA] = 10 μ M with electrolytic eluent generation system (n = 25).
- Fig. 4.5 Near LOD trace of seven HAs. 1 = Fluoride, 2 = MCA (0.5 μ M), 3 = Chloride/MBA (0.5 μ M), 4 = TFA (0.8 μ M), 5 = Nitrate, 6 = DCA (0.8 μ M), 7 = CDFA (1.5 μ M), 8 = DBA (1.5 μ M), 9 = sulphate, 10 = TCA (3 μ M).
- Fig. 4.6 Sample taken 1st September 2003 from laboratory water supply showing out of specification levels for MCA (113 μ g/L) and TFA (35 μ g/L).

- Fig. 4.7 Preconcentration of Drumcondra sample taken on 1st September 2003 showing levels of DCA(24.97 µg/L), CDFA (17.51 µg/L) and TCA (<LOD).
- Fig. 4.8 Sample of drinking water taken on the 2nd September 2003 showing levels of DCA (17.2 µg/L).
- Fig. 4.9 Sample taken on the 3rd September 2003 showing levels of MCA (<LOD), DCA (31 µg/L), CDFA (20 µg/L) and TCA (<LOD).
- Fig. 4.10 Sample taken on 4th September 2003 showing levels of DCA (19.86 µg/L) and TCA (<LOD).
- Fig. 4.11 (a) Gradient of 10 – 100 mM KOH at 15 minutes for a duration of 15 minutes at 45°C (b) Gradient of 5 – 100 mM KOH at 15 minutes for a duration of 15 minutes at 45°C (c) Gradient of 2.5 – 100 mM KOH at 10 minutes for a duration of 5 minutes at 45°C. Elution Order: 1 = fluoride, 2 = MBA, 3 = chloride, 4 = MBA, 5 = TFA, 6 = nitrate, 7 = DCA, 8 = CDFA, 9 = DBA, 10 = sulphate, 11 = TCA. [HA] = 15 µM.
- Fig. 4.12 Gradient separation of 2.5 mM – 20 mM KOH at 10 minutes over a duration of 5 minutes of 15 µM of the seven HAs at 45°C. Elution order: 1 = fluoride, 2 = MCA, 3 = chloride, 4 = MBA, 5 = TFA, 6 = nitrate, 7 = DCA, 8 = CDFA, 9 = DBA, 10 = sulphate, 11 = TCA.
- Fig. 4.13 The effect of temperature on AS16 HA separations. Elution order: 1 = fluoride, 2 = MCA, 3 = chloride (2 mg/L), 4 = MBA, 5 = TFA, 6 = nitrate, 7 = DCA, 8 = CDFA, 9 = DBA, 10 = sulphate, 11 = TCA. [HA] = 15 µM
- Fig 4.14 Optimised separation of HAs and inorganic anions on AS16 column. Flow rate: 0.30 mL/min; loop size: 100 µL; gradient: 2.5 – 20 mM KOH at 10 minutes for a duration of 5 minutes; suppressor current: 50 mA. Elution Order: 1= fluoride, 2 = MCA, 3 = chloride, 4 = MBA, 5 = TFA, 6 = nitrate, 7 = DCA, 8 = CDFA, 9 = DBA, 10 = carbonate, 11 = sulphate, 12 = TCA. [HA] = 15 µM.
- Fig. 4.15 Black Trace: Near LOD trace of 0.5 µM of seven HAs with the optimum method. Grey Trace: 5 µM standard of seven HAs with optimum AS16 method. Elution order: 1 = MCA, 2 = MBA, 3 = TFA, 4 = DCA, 5 = CDFA, 6 = DBA, 7 = TCA.
- Fig 4.16 Overlay of preconcentrated drinking water sample (black trace) spiked with 1 µM of seven HAs and expected 100 % 25 µM standard in Milli-Q (grey trace). Elution order and % recoveries: 1 = fluoride, 2 = MCA (102 %), 3 = chloride, 4 = MBA (71 %), 5 = TFA (13 %), 6 = nitrate, 7 = DCA (110 %), 8 = CDFA (111 %), 9 = DBA (123 %), 10 = sulphate, 11 = TCA (104 %).
- Fig 4.17 Overlay of 1st, 10th and 20th repeat injection of 10 µM of seven HAs with AS16 and EG40 methods. Elution Order: 1 = MCA, 2 = chloride, 3 = MBA, 4 = TFA, 5 = nitrate, 6 = DCA, 7 = CDFA, 8 = DBA, 9 = carbonate, 10 = sulphate, 11 = TCA.

- Fig. 5.1 Schematic of the Dionex AEES Atlas suppressor
- Fig. 5.2 Comparisons of HA separations with both Atlas and ASRS Ultra suppressors. 5.2(a) Elution Order: 1 = fluoride, 2 = formate, 3 = chlorite, 4 = MCA, 5 = chloride, 6 = MBA, 7 = nitrite, 8 = TFA, 9 = nitrate, 10 = DCA, 11 = CDFA, 12 = DBA, 13 = carbonate, 14 = sulphate, 15 = TCA, 16 = DCBA, 17 = phthalate, 18 = CDBA, [HA] = 2 μ M. 5.2(b) Enlargement of region I and II. Other conditions; 2.5 mM KOH for 10 minutes, then ramped linearly to 20 mM for 5 minutes and kept at 20 mM KOH for a further 20 minutes (eluent flow rate = 0.3 mL/min).
- Fig. 5.3 (a) Non-preconcentrated sample of New Ross drinking water supply passed through chloride and sulphate removal cartridges and run on IC with overlay of 0.8 μ M HA spiked water sample. Elution Order: 1 = fluoride, 2 = formate, 3 = chlorite, 4 = MCA, 5 = chloride, 6 = MBA, 7 = TFA, 8 = nitrate, 9 = CDFA, 10 = DBA, 11 = sulphate, 12 = TCA, 13 = DCBA, 14 = phthalate (int. std), 15 = CDBA, 16 = phosphate. Other conditions as Fig. 5.1. Fig. 5.3(b). Non-preconcentrated Dublin City University drinking water sample passed through chloride and sulphate removal cartridges and run on IC overlaid with 1 μ M standard solution prepared in Milli-Q water. Elution Order: 1 = fluoride, 2 = formate, 3 = chlorite, 4 = MCA, 5 = chloride, 6 = MBA, 7 = TFA, 8 = nitrate, 9 = DCAA, 10 = CDFA, 11 = DBA, 12 = carbonate, 13 = sulphate, 14 = thiosulphate, 15 = TCAA, 16 = DCBA, 17 = phthalate, 18 = CDBA. Other conditions as Fig. 5.1.
- Fig. 5.4 Standard addition of HAs in drinking water from Drogheda, Co. Louth, Ireland. Sample and spiked samples preconcentrated 25 fold using SPE (LiChrolut EN). Elution Order: 1 = fluoride, 2 = formate, 3 = MCA, 4 = chloride, 5 = MBA, 6 = nitrite, 7 = TFA, 8 = nitrate, 9 = DCAA, 10 = CDFA, 11 = DBA, 12 = sulphate, 13 = thiosulphate, 14 = TCA, 15 = DCBA, 16 = phthalate (Int. Std), 17 = CDBA. Concentration range = 0 – 0.8 μ M HA.
- Fig. 5.5 Elution profiles for eight HAs using 400 mg sorbent mass (double commercially available sorbent mass) in stepwise fractions of 0.5 mL of 10 mM NaOH.
- Fig. 5.6 (a) Elution profiles for 8 HAs when using 20 mM NaOH as the eluting agent (b) the effect of increasing fraction number on excess sulphate removal associated with acidification step.
- Fig. 6.1 UV absorbance wavelength optimisation for 4 μ M standard of all HAs
- Fig. 6.2 Chromatograms at each wavelength for a 4 μ M standard of 9 HAs. Offset 0.02 AU for clarity. Elution order: 1 = acetate, 2 = MCA, 3 = chloride, 4 = MBA, 5 = TFA, 6 = nitrate, 7 = DCA, 8 = CDFA, 9 = DBA, 10 = carbonate, 11 = system peak, 12 = sulphate, 13 = TCA, 14 = DCBA, 15 = CDBA.
- Fig. 6.3 A 4 μ M standard of 9 HAs with UV detection showing interference from chloride combined with background contaminant making integration of MBA and MCA difficult at low

levels along with significant background signal rise over gradient run. Elution order: 1 = acetate, 2 = MCA, 3 = chloride, 4 = MBA, 5 = TFA, 6 = nitrate, 7 = DCA, 8 = CDFA, 9 = DBA, 10 = TCA, 11 = DCBA, 12 = CDBA.

- Fig. 6.4 Observed pseudo molecular ion $[M-H]$, decarboxylated $[M-COOH]$ and dimerised forms $[2M-H]$ of each HA where X = F, Cl, Br or H.
- Fig. 6.5 Linear superposition of bromine and chlorine peak patterns
- Fig. 6.6 Mass spectra for directly infused standard of MCA, DCA and TCA.
- Fig. 6.7 Direct infusion mass spectra for MBA and DBA at 250 $\mu\text{L}/\text{hour}$
- Fig. 6.8 Direct infusion mass spectra for TFA and CDFA (Flow rate = 250 $\mu\text{L}/\text{hour}$).
- Fig. 6.9 TIC and SIM traces of interferent species at m/z 182.9 resulting from leached styrene sulphonate into the electrolytically generated eluent during a separation of 100 μM standard of nine HAs. Elution order: 1 = fluoride, 2 = MCA, 3 = MBA, 4 = TFA, 5 = DCA, 6 = CDFA, 7 = DBA, 8 = TCA, 9 = DCBA, 10 = CDBA.
- Fig. 6.10 Comparison of intensities at average MS conditions for all nine HAs versus TCA optimum conditions.
- Fig. 6.11 Optimisation of total flow to electrospray needle comprising of 0.30 mL/min IC eluate (fixed) and additional 0.05, 0.075, 0.1, 0.12, 0.15 and 0.2 mL/min MeOH.
- Fig. 6.12 Effect of % MeOH on signal intensity at total flow rate
- Fig. 6.13 Improvement in baseline stability for UV detection with manually prepared eluents.
- Fig. 6.14 TIC and SIM traces for 15 μM standard of 9 HAs. Elution order: 1 = fluoride, 2 = MCA (SIM m/z 92.9), 3 = MBA (SIM m/z 136.9), 4 = TFA (SIM m/z 112.9, 68.9, 226.8), 5 = DCA (SIM m/z 126.9, 128.9, 92.9, 254.8), 6 = CDFA (SIM m/z 128.9, 84.9, 258.8), 7 = DBA (SIM m/z 216.9, 172.9, 434.4), 8 = TCA (SIM m/z 162.9, 118.8, 326.6), 9 = DCBA (SIM m/z 206.8, 162.9, 414.6) 10 = CDBA (SIM m/z 251.2, 206.8, 503.4).
- Fig. 6.15 Figure left: TIC and SIM chromatograms for a preconcentration of drinking water spiked with nine HAs at 1 μM . Elution order: 1 = m/z 88.9, 2 = m/z 174.6, 3 = MCA, 4 = MBA, 5 = m/z 124.9, 6 = TFA, 7 = DCA, 8 = CDFA, 9 = DBA, 10 = m/z 198.8, 11 = sulphate, 12 = TCA, 13 = DCBA, 14 = m/z 164.8, 15 = CDBA, 16 = m/z 172.8, 17 = m/z 200.8. Figure right: SIM traces for most abundant ion for each HA. SIM traces smoothed with 2.5 point Gaussian averaging.
- Fig. 6.16 Preconcentration of 1 μM spiked drinking water with (a) conductivity detection (overlaid with 15 μM standard offset by 2 μS) and (b) UV detection (overlaid with same 15 μM standard offset by 0.01 AU). Elution order: 1 = acetate, 2 = fluoride, 3 = MCA, 4 = chloride, 5 = MBA, 6 = nitrite, 7 = TFA, 8 = nitrate, 9 = bromide, 10 = DCA, 11 = CDFA, 12 = DBA, 13 = sulphate, 14 = TCA, 15 = DCBA, 16 = phthalate, 17 = CDBA.

- Fig. 7.1 Van't Hoff plots for 4 oxyhalides, 9 HAs and 4 inorganic anions using AS16 column with isocratic elution. Eluent = 20 mM NaOH.
- Fig. 7.2 (a) Plot showing the slope from van't Hoff plot against mean $\ln k$ for each HA over the temperature range 35 – 45 °C. Data shown in brackets = $\log P$ value or each anion. (b) Plot showing the slope from van't Hoff plot against $\log P$ for each HA.
- Fig. 7.3 Optimised gradient of 1 mM hydroxide for 20 mins, then linearly ramped to 4 mM over 20 mins followed by 5 minute linear increase to 20 mM hydroxide all at 35°C. Elution order: 1 = fluoride, 2 = iodate, 3 = MCA, 4 = bromate, 5 = chloride/MBA, 6 = TFA, 7 = nitrate, 8 = chlorate, 9 = DCA, 10 = CDFA, 11 = DBA, 12 = sulphate, 13 = TCA, 14 = DCBA, 15 = CDBA, 16 = perchlorate.
- Fig. 7.4 Effect of increased column temperature upon the isothermal gradient separation of inorganic anions, oxyhalides and HAs. Eluent conditions = 1 mM NaOH 0 - 20 minutes, increased to 4 mM hydroxide over next 20 minute, then increased to 20 mM hydroxide over next 5 minutes. Peaks; 1 = acetate 2 = fluoride, 3 = MCA, 4 = bromate, 5 = chloride, 6 = MBA, 7 = TFA, 8 = nitrate, 9 = bromide, 10 = chlorite 11 = DCA, 12 = CDFA, 13 = DBA, 14 = carbonate, 15 = sulphate, 16 = TCA, 17 = BDCA, 18 = CDBA, 19 = perchlorate.
- Fig. 7.5 (a-b) Column temperatures for columns held within column ovens during temperature programming cycles, recorded using iButton temperature sensor adhered to column surface. (c) Difference between the column oven readout and the column surface temperature. (d) Difference between the column oven readout and the column oven wall temperature.
- Fig. 7.6 Separation of HAs and oxyhalides in a drinking water sample (20 μM spike of each HAs and oxyhalide, ex. CDBA = 32 μM , BDCA = 40 μM) using a hydroxide gradient with applied column temperature programming. Peaks; 1 = fluoride, 2 = iodate, 3 = chlorite 4 = MCA, 5 = bromate, 6 = chloride, 7 = MBA, 8 = TFA, 9 = nitrate, 10 = chlorate, 11 = DCA, 12 = CDFA, 13 = DBA, 14 = carbonate, 15 = sulphate, 16 = TCA, 17 = BDCA, 18 = CDBA, 19 = perchlorate.
- Fig. 7.7 Chromatograms showing the hydroxide gradient separation of inorganic anions, organic acids, oxyhalide and HAs in a chlorinated drinking water (a), and the same sample following preconcentration (b). Hydroxide gradient – as Fig. 7.3.
- Fig. 7.8 Optimum method for use with conductivity combined with ESI-MS detection using temperature program from 30-45°C at 20 minutes for a duration of 10 minutes. Also included is the hydroxide gradient profile (highlighted in grey). Elution order: 1 = fluoride, 2 = iodate, 3 = MCA, 4 = bromate, 5 = chloride, 6 = MBA, 7 = TFA, 8 = nitrate, 9 = chlorate, 10 = DCA, 11 = CDFA, 12 = DBA, 13 = carbonate, 14 = TCA, 15 = DCBA, 16 = CDBA, 17 = perchlorate. [Analytes] = 20 μM .

- Fig. 7.9 *Retention time repeatability for 30 repeat gradient runs with applied temperature programme using conductivity detection.*
- Fig. 7.10 *Separation of 20 μM standard of all analytes with BCA and chlorite (in bold). Elution order: 1 = acetate, 2 = iodate, 3 = chlorite, 4 = MCA, 5 = bromate, 6 = chloride, 7 = MBA, 8 = TFA, 9 = nitrate/bromide, 10 = chlorate, 11 = DCA, 12 = CDFA, 13 = BCA, 14 = DBA, 15 = carbonate, 16 = TCA, 17 = DCBA, 18 = CDBA, 19 = perchlorate.*
- Fig. 7.11 *(a) eluent injection (b) near limit of detection 50 nM standard and (c) Milli-Q water injection. Elution order: 1 = iodate, 2 = MCA, 3 = bromate, 4 = TFA, 5 = nitrate, 6 = chlorate, 7 = DCA, 8 = CDFA, 9 = BCA, 10 = TCA, 11 = DCBA, 12 = CDBA, 13 = perchlorate.*
- Fig. 7.12 *Overlay of (a) 80 nM standard with suppression in auto-recycling mode and (b) same standard with suppression in external water mode. Elution order: 1 = fluoride, 2 = iodate, 3 = chlorite, 4 = MCA, 5 = bromate, 6 = chloride, 7 = TFA, 8 = nitrate, 9 = chlorate, 10 = DCA, 11 = CDFA, 12 = BCA, 13 = DBA, 14 = sulphate, 15 = TCA, 16 = DCBA, 17 = CDBA, 18 = perchlorate.*
- Fig. 7.13 *Extracted ion chromatograms for 10 μM standard of all analytes. Elution order: 1 = iodate, 2 = MCA, 3 = bromate, 4 = MBA, 5 = TFA, 6 = chlorate, 7 = DCA, 8 = CDFA, 9 = BCA, 10 = DBA, 11 = TCA, 12 = DCBA, 13 = CDBA, 14 = perchlorate.*
- Fig. 7.14 *(a) Unspiked soil extract (b) 0.5 μM spiked soil extract. Elution order: 1 = MCA, 2 = bromate, 3 = TFA, 4 = DCA, 5 = BCA, 6 = DBA, 7 = DCBA, 8 = CDBA, 9 = perchlorate.*
- Fig. 7.15 *Extracted ion chromatograms for each ion in TIC. (Right) mass spectrum for peak corresponding to perchlorate.*
- Fig. 7.16 *Standard addition curve for perchlorate in soil. Best fit curve for all data points shown in black, and for curve directed through unspiked sample data point in grey.*
- Fig. 7.17 *(a) neat drinking water sample with sulphate and chloride removed with Alltech SPE cartridges (b) preconcentrated neat drinking water sample. Elution order: 1 = MCA, 2 = MBA, 3 = TFA, 4 = chlorate, 5 = DCA, 6 = CDFA, 7 = BCA, 8 = DBA, 9 = DCBA, 10 = CDBA, 11 = perchlorate.*
- Fig. 7.18 *Extracted ion chromatograms for laboratory drinking water preconcentrated 25-fold showing presence of DCA, CDFA, DBA, chlorate, perchlorate, CDBA and possibly some DCBA and MBA.*

List of Tables

- Table 1.1 *Physical properties of chlorinated acetic acids [27]*
- Table 1.2 *Physical and chemical properties of brominated acetic acids*
- Table 1.3 *Limiting equivalent ionic conductances in aqueous solution at 25°C*
- Table 1.4 *Observed/measured ions (m/z) for HAs using ESI-MS. Most abundant ions for each HA are highlighted in bold.*
- Table 1.5 *Ion chromatographic methods for HAs, separation and detection conditions and detection limits.*
- Table 1.6 *Haloacetic acids (HAs) and known pK_a values*
- Table 1.7 *Variation in recovery data for HAs on LiChrolut EN SPE cartridges*
-
- Table 2.1 *Elution order, retention time and resolution of HAs*
- Table 2.2 *Resolution of seven HAs using linear gradient from 30-100 mM NaOH.*
- Table 2.3 *Resolution of seven HAs using a gradient of 10 – 100 mM NaOH after 10 minutes*
- Table 2.4 *Collected data for observed peaks in Fig 2.7 above.*
- Table 2.5 *Correlation coefficients, slopes, intercepts and standard deviations for n = 3 replicate linearity standard runs of the seven HAs*
- Table 2.6 *Reproducibility of optimum ion exchange methodology for the seven HAs where n = 7.*
- Table 2.7 *LOD (S:N = 3) values for the developed ion exchange methodology.*
- Table 2.8 *LOD values for 4 detected HAs in a spiked water sample.*
-
- Table 3.1 *Effect of NaOH concentration on % recovery*
- Table 3.2 *Recovery and precision data for preconcentration of HAs on LiChrolut EN SPE cartridges.*
- Table 3.3 *Identification and quantification of HAs from four sources in Dublin City and Co. Kildare.*
-
- Table 4.1 *Reproducibility of Eluent Generation Methodology where n = 25.*
- Table 4.2 *Comparison of Absolute LOD values for both EG40 and manually prepared eluent systems*
- Table 4.3 *HAs observed in 5 drinking water samples and their concentrations*
- Table 4.4 *Comparison of AS11-HC and AS16 column packing specifications [3,4].*
- Table 4.5 *Retention and resolution data for three AS16 gradient separations*
- Table 4.6 *Comparison of LODs for AS16 and AS11-HC methods*
- Table 4.7 *Repeatability of AS16 method for 20 successive injections*
- Table 4.8 *Linearity data for AS16 column method*

- Table 5.1 Analytical performance data for KOH gradient IC method for HAs and LODs with Atlas and ASRS Ultra suppressors and overall method LOD including preconcentration.*
- Table 5.2 Recovery and precision data for Maxi Clean cartridge series for nine HAs including SPE preconcentration data for DCBA and CDBA.*
- Table 5.3 HAs observed in three chlorinated drinking water supplies*
- Table 5.4 Comparison of single vs double sorbent mass as well as two-step elution*
- Table 6.1 Linearity data for Dionex AD20 UV detector for 2, 5, 7.5, 10, 15, 20 and 25 μM of all nine HAs run in triplicate along with MDL.*
- Table 6.2 Optimised mass spectrometer conditions for HA analysis. All optimised parameters carried out at 8 L/min drying gas, 300°C dry gas temperature and 55 psi nebulizer pressure.*
- Table 6.3. % Intensity of each fragment for all nine HAs*
- Table 7.1 Slope data from van't Hoff plots, correlation coefficients, and ΔH values for oxyhalides, haloacetates and inorganic anions.*
- Table 7.2 Peak area and peak height reproducibility for $n = 10$ replications of a 2 μM standard of all analytes*
- Table 7.3 Linearity data for conductivity detection over 50 – 500 nM analyte concentration.*
- Table 7.4 Linearity data for extracted ion chromatograms for ESI-MS over 5 – 30 μM analyte concentration*
- Table 7.5 Limits of detection for combined temperature and hydroxide gradient method.*
- Table 7.6 Limits of detection for all analytes with ESI-MS.*
- Table 7.7 Reproducibility for peak intensities of a 20 μM oxyhalide and HA standard for $n = 6$ replicate runs.*
- Table 7.8. Semi-quantitative standard addition of HAs in laboratory drinking water sample.*

List of Abbreviations

AEES	Anion Atlas Electrolytic Suppressor
APCI	Atmospheric Pressure Chemical Ionisation
API	Atmospheric Pressure Ionisation
ASRS	Anion Self Regenerating Suppressor
BCA	Bromochloroacetic Acid
BDCA	Bromodichloroacetic Acid
CDFA	Chlorodifluoroacetic Acid
CE	Capillary Electrophoresis
CR-ATC	Continuously Regenerating Anion Trap Column
CTACI	Cetyltrimethylammonium Chloride
DBA	Dibromoacetic Acid
DBCA	Dibromochloroacetic Acid
DBP	Disinfectant By-Product
DBuA	Dibutylamine
DCA	Dichloroacetic Acid
DDAB	Didodecyldimethylammonium Bromide
DMBA	Dimethylbutylamine
DOC	Dissolved Organic Carbon
DVB	Divinylbenzene
ECD	Electron Capture Detection
EG	Eluent Generator
EIC	Extracted Ion Chromatogram
EPA	Environmental Protection Agency
ESI	Electrospray Ionisation
DWCEU	Drinking Water Commission of the European Union
EVB-DVB	Ethylvinylbenzene-Divinylbenzene
GC	Gas Chromatography
HA	Haloacetic Acid
HPLC	High Performance Liquid Chromatography
IC	Ion Chromatography
ICP	Inductively Coupled Plasma
IIR	Ion Interaction Reagent
IPA	Isopropyl Alcohol
IP-Fluo	Ion-Pair Fluorescence
ISO	International Standards Organisation
LOD	Limit of Detection
MBA	Monobromoacetic Acid
MCA	Monochloroacetic Acid
MCG	Maximum Contaminant Goal
MCL	Maximum Contaminant Limit
MDL	Maximum Detectable Limit
MS	Mass Spectrometry
MTBE	Methyl <i>tert</i> -Butyl Ether
NOM	Natural Organic Matter
ODA	<i>o</i> -Dianisidine
ODS	Octadecyl Silica
PCR	Post-Column Reaction
PEEK	Polyether Ether Ketone

PS-DVB	Polystyrene-Divinylbenzene
RP	Reversed Phase
RSD	Relative Standard Deviation
S:N	Signal to Noise Ratio
SIM	Single Ion Monitoring
SLMME	Supported Liquid Micromembrane Extraction
SPE	Solid Phase Extraction
TBA	Tribromoacetic Acid
TBACl	Tetrabutylammonium Chloride
TBuA	Tributylamine
TCA	Trichloroacetic Acid
TEA	Triethylamine
TFA	Trifluoroacetic Acid
THM	Trihalomethane
TOX	Total Organic Halide
USEPA	United States Environmental Protection Agency
UV	Ultra Violet
VWD	Variable Wavelength Detector
WHO	World Health Organisation

List of Publications

1. Leon Barron, Pavel N. Nesterenko and Brett Paull,
Combined hydroxide and temperature gradients to improve resolution of inorganic anions, haloacetic acids and oxyhalides in drinking water by suppressed ion chromatography.
Journal of Chromatography A, 1072 (2005), 207-215.
2. Leon Barron and Brett Paull,
Direct detection of trace haloacetates in drinking water using micro-bore ion chromatography. Improved detector sensitivity using a hydroxide gradient and a monolithic ion-exchange type suppressor.
Journal of Chromatography A, 1047(2):205-212, 2004.
3. Leon Barron and Brett Pauli,
Determination of haloacetic acids in drinking water using suppressed micro-bore ion chromatography with solid phase extraction.
Analytica Chimica Acta. 522(2):153-161, 2004.
4. Brett Paull and Leon Barron,
Using ion chromatography to monitor haloacetic acids in drinking water: A review of current technologies.
Journal of Chromatography. A. 1046(1-2):1-9, 2004.
5. Damian Connolly, Leon Barron and Brett Paull,
Determination of urinary thiocyanate and nitrate using fast ion interaction chromatography.
Journal of Chromatography. B. 767(1):175-180, 2002.
6. Brett Paull, Leon Barron and Pavel Nesterenko,
The determination of phosphates in environmental samples by ion chromatography.
Chromatographic Analysis of the Environment, Third Edition, 2005, CRC Press, *in press*.

List of Poster Presentations

1. Leon Barron, Pavel Nesterenko and Brett Paull,
Use of temperature programming to improve resolution of haloacetic acids and oxyhalides in drinking water by suppression ion chromatography,
Pittcon 2005, Orlando, Florida, USA, February 2005.
2. Leon Barron and Brett Paull,
Is our water safe to drink? Ion chromatography-electrospray mass spectrometry of haloacetates in drinking water.
15th Irish Environmental Researchers' Colloquium, IT Sligo, Poster Presentation, January 2005.
3. Leon Barron and Brett Paull,
Direct detection of trace haloacetates in drinking water using micro-bore ion chromatography,
3rd Biennial Conference on Analytical Science in Ireland, University College Cork, September 2004.
4. Leon Barron and Brett Paull,
Reagentless IC of haloacetic acids in drinking water and preconcentration with SPE,
International Ion Chromatography Symposium, San Diego, CA, USA, September 2003.
5. Leon Barron and Brett Paull,
Suppressed Ion Chromatography of haloacetic acids in drinking waters and preconcentration using solid phase extraction,
RSC Analytical Research Forum, Sunderland, UK. July 2003.
6. Leon Barron and Brett Paull,
IC-MS of haloacetic acids,
RSC Analytical Research Forum, Kingston, London, UK, July 2002.

(see also Appendix A.7 for reprints of posters 1-5)

List of Oral Presentations

1. Leon Barron and Brett Paull,
Micro-bore suppressed ion chromatography of Haloacetic acids in drinking waters using conductivity, UV and mass spectrometric detection.
International Ion Chromatography Symposium, University of Trier, Germany. 21 Sep 2004.
2. Leon Barron and Brett Paull,
Direct Detection of Trace Haloacetates in Drinking water using Suppressed Ion Chromatography; Improved Detector Sensitivity using a Hydroxide Gradient and a Monolithic Cation Exchange Suppressor,
RSC Analytical Research Forum, Preston, UK, July 2004.

List of Honours and Awards

1. Colin Barnes' Award for Outstanding Postgraduate Contribution to Chemical Research, School of Chemical Sciences, Dublin City University, 2005.
2. Awarded the Student Travel Bursary (\$500) to travel and present at the 17th International Ion Chromatography Symposium in Trier, Germany in September 2004.

Acknowledgements

First and foremost, I would like to thank my supervisor Dr Brett Pauli for his advice and encouragement in the area of ion chromatography and for the opportunity to carry out this work with him and his research group, all of which are fine chemists. Also, to Prof. Pavel Nesterenko, for his guidance on the dual gradient work.

Secondly, I would like to thank Enterprise Ireland for funding this project. I hope you are satisfied with the results and benefit you in your own research.

For all those who helped and encouraged me over the past few years as a post-graduate student, I thank you sincerely. Most importantly, I would like to thank my parents, PJ and Angela Barron and my dear sister Laura. Without the three of you, I would not have come this far, not only because I have completed a PhD in analytical chemistry, but my progress in all facets of life. I know you would have supported me even if I decided to be a rock star! I owe it all to you and love you very much.

I would like to thank Ms Wendy Hein for believing in me and sticking with me through my years in DCU. A large part of my enthusiasm and drive to do this was the result of your encouragement. To my friends at home in New Ross, Co. Wexford, Joan Devereux and Damien Fallon, you believed in me and listened to my stories of success and woe without a judgemental eye and made sure that my feet stayed permanently on terra firma. For the same reason, I would like to thank my close friends in Dublin outside the world of DCU, Eoin Hanley, John Hoolahan and Neville Mullally.

Within the labyrinth that is DCU, I would like to thank Darragh Lucey and Dr Thomas F McEvoy for jovial banter and good friendship over the course of my studies and wish you the best in whatever path you decide. To Damien McGuirk for countless hours playing rock music in the technicians office in DCU as part of *The Keytones* and other ventures. I've been educated now McGuirk, no longer a Padawan! To the technical staff in DCU, you keep this place alive and without you we would all be lost. To all the postgraduates in DCU, most of which have offered friendship that I will always remember and cherish.

To all the members of the Youth Augustinian Partnership of Ireland, my time with you and support you have given me for my chosen path has benefited me immensely. To the German Society committee for the effort they have put in over the past three years even when I was not available. To Mustaine *et al.*, Joe Satriani and Steve Vai for providing inspiration and to whose music I escaped to when chemistry became too tough. To all I have forgotten or omitted, I thank you too.

Leon Barron

For my mother and father

Abstract

The complete development of chromatographic methods to determine daily concentrations of the haloacetates (HAs) monochloro- (MCA), dichloro- (DCA), trichloro- (TCA), monobromo- (MBA), dibromo- (DBA), chlorodifluoro- (CDFA) trifluoro- (TFA), dichlorobromo- (DCBA) and chlorodibromoacetates (CDBA) as well as the oxyhalides bromate, chlorate, perchlorate and iodate are presented. This work is divided into seven sections. Firstly, Chapter 1.0 deals with a full understanding of the background to disinfectant by-product formation and analysis, including explanation of all instrumentation required to complete the area of research. Following this, a review of current technologies for the determination of HAs and oxyhalides in modern treated drinking water is discussed. Chapter 2.0 investigates a micro-bore Dionex IonPac AS11-HC as a possible column of choice for ion exchange chromatography of the first seven HAs listed only. The method utilises suppressed conductivity detection with a gradient of sodium hydroxide. Analytical performance characteristics for linearity, reproducibility and limits of detection are presented also. In a brief study, the effect of column temperature was investigated for the developed method with this column and van't Hoff plots are included here. For determinations of HAs in real drinking water samples, Chapter 3.0 offers solid phase extraction as a possible solution and was investigated using a solid phase extraction cartridge with a stationary phase of hyper-crosslinked polystyrene-divinylbenzene copolymer. Selectivity, percent recovery, capacity and reproducibility studies were carried out on LiChrolut EN cartridges. Under optimised conditions average recoveries for MCA, DCA, TCA, MBA and CDFA spiked in drinking water samples ranged from 62 to 88 %, with an optimum preconcentration factor of 25. The reproducibility of recovery data for the above HAs was found to range from 12 to 29 % based upon six repeat recovery experiments. This method coupled with the IC method in Chapter 2.0 was then applied to the analysis of some real drinking water samples. Improvements in sensitivity are tackled in Chapter 4.0 with addition of Dionex eluent generation and carbonate removal modules. Noise levels decreased by a factor of one third with this new instrumentation. The reproducibility and accuracy of eluent preparation is assessed and compared with manually prepared eluents. The developed method was then applied to the analysis of 5 drinking water samples. Separations with a micro-bore Dionex IonPac AS16 are also shown here. Once more, analytical performance characteristics of linearity, reproducibility and limits of detection are presented along with a brief investigation of the effect column temperature on separation. This new method was then combined with the SPE method in Chapter 2.0 for the determination of HAs in a drinking water sample. Chapter 5.0 deals further with improvements in sensitivity with the use of a monolithic cation exchange type suppressor. Noise levels were dramatically reduced and direct detection of HAs was possible without preconcentration. However, some SPE was carried out along with this IC method and was sensitive to the range of HAs typically expected in drinking water. The effect of doubling the ethylvinylbenzene-divinylbenzene copolymer sorbent was investigated showing a requirement for double the reagent volumes for effective preconcentration and was virtually independent of eluting agent concentration. Chapter 6.0 presents results gathered from UV and MS detectors as alternatives to suppressed conductivity.

UV wavelength optimisation, linearity, limits of detection and reproducibility are presented. For IC-MS a suitable interface for coupling the IC eluate to the electrospray chamber is presented along with optimisation of all parameters for maximum sensitivity to HAs. The developed suppressed conductivity-UV-MS method was then applied to a spiked drinking water sample. Chapter 7.0 discusses the possibility of separating both oxyhalides and HAs on one column with the use of combined temperature and eluent concentration gradients. This chapter discusses in detail the effect of temperature on the separation of HAs and oxyhalides on the AS16 column and measured versus actual column temperatures are presented. Full optimisation of the dual temperature and eluent concentration gradient for conductivity detection only are presented and applied to a drinking water sample. Following on from this, analytical performance data for reproducibility for $n = 30$ replicates, LOD and linearity for both suppressed conductivity and mass spectrometric detection is presented. The method was then applied to the analysis of HAs and oxyhalides in a soil sample and a drinking water sample using both detectors.

Chapter 1.0

Literature Review

"There's no recess and no rules in the school of life. If you listen very closely you'll see what it's like. Have cool, will travel" – Dave Mustaine, Cryptic Writings, 1997, Capitol Records

1.0 Background

Disinfectant by-products (DBPs) are of major concern when assessing the quality of drinking waters, as it is known that the presence of these DBPs has a potential for carcinogenic and mutagenic effects in humans. Initial concern arose upon the realisation of the hazards associated with the formation of trihalomethanes (THMs) in the early 1970s. These compounds were subsequently studied in detail, often not associating the presence of other DBPs, such as the haloacetic acids (HAs), with similar health risks to humans. As a result, identification, classification and toxicological studies into other DBPs were overlooked until recently, even though in some cases the concentration of some HAs, namely trichloroacetic acid, were greater than that of chloroform [1].

Research over the past few years has linked the formation of these compounds, for the most part, to the chlorination and/or ozonation of water as part of its treatment process, as well as inorganic bromide found in ground and surface waters [1-5]. Waters with high levels of *natural organic matter* (NOM) were found to undergo oxidation by the disinfectant halogen ions or ozonation processes to form a wide variety of DBPs. Cause for concern lies in the fact that only approximately 40 % of all DBPs have been classified. Moreover, only THMs are currently covered by legislation in Europe and are limited to a maximum of 150 µg/L for total THMs by the European Union until further review in 2008 where this limit is to be reduced to 100 µg/L. The USEPA has imposed a maximum contamination limit (MCL) for some of these DBPs. Trihalomethanes are the most common form of identified DBP found in chlorinated drinking waters (20.1 %) and are their regulated USEPA MCL is 80 µg/L in total. This is to be assessed and reduced to 40 µg/L in the coming years [6]. For the next most commonly occurring chlorination DBP, the HAs, it is proposed that the MCL for five commonly occurring HAs, namely, monochloro- (MCA), monobromo- (MBA), dichloro- (DCA), dibromo- (DBA) and trichloroacetic acids (TCA) should not exceed 60 µg/L in total. Again, this is to be lowered in the coming years to 30 µg/L. Within this regulation, DCA should

never be present, and TCA concentrations should not amount to more than 30 µg/L.

The content of this section will cover the aspects of DBP formation and distribution, with an emphasis on the HAs and, to a lesser extent, the oxyhalides. An evaluation of current technologies for the determination of these DBPs in a modern laboratory environment is also included here.

1.1 Current Water Treatment Methods

The primary requirements for water treatment systems are to remove humic and fulvic matter, inorganic species, micropollutants and the preservation of the freshly purified water from toxic microorganisms to a purity fit for human consumption. However, as part of this water treatment, many of the disinfection procedures currently employed often result in undesired by-product formation.

1.1.2 Ozonation

In recent years, ozonation of drinking water has been used as a successful method of disinfection. It offers a wide range of advantages over chlorination. Ozonation is a suitable disinfectant due to its high oxidation potential. Chemical oxidant exposure occurs in three steps throughout the treatment process, i.e. pre-oxidation, intermediate oxidation and final disinfection [7]. Pre-oxidation serves to remove any mineral compounds, turbidity and suspended solids. Additionally, microorganisms are inactivated and coagulation-flocculation-decantation stages are improved as a result of this step. The second stage is of more importance to DBP formation. Intermediate oxidation attempts to remove trihalomethane precursors and any toxic micropollutants. Since disinfectants react with humic and fulvic matter, the final disinfection stage removes any traces of remaining microorganisms and residual organic matter and thus aims to minimise the DBP formation process as much as possible. It has been observed that ozone to dissolved organic carbon (DOC) dosage ratios of 1:1 are optimum and increases in ozone

dosages do not significantly remove additional DOC. Variances in pH of ozonation processes do not seem to affect the overall outcome of the treatment and this allows for bromate control at low pH values [18].

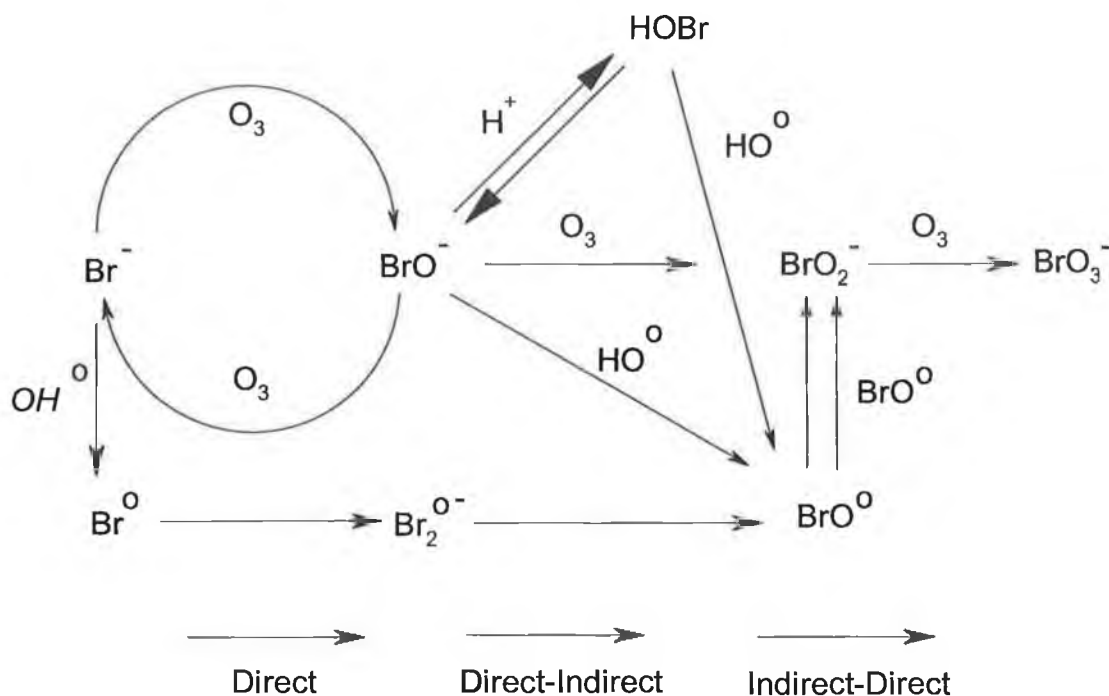


Fig. 1.1 Bromate formation pathways during ozonation [30]

The majority of inorganic species are removed by pre-oxidation. However, in the presence of residual inorganic bromide, ammonia may decompose to nitrogen gas and, as a result, rapidly oxidise bromide to hypobromous acid, HOBr [8,9], which reacts with additional ammonia to yield nitrogen gas and bromide. This cycle acts to rapidly remove ammonia from drinking water. However, the formation of HOBr also yields hypobromite (BrO^-) and hence bromate (BrO_3^-) with increased ozone contact time. Bromate is a potential carcinogen, which classifies it as a hazardous DBP [10]. The World Health Organisation (WHO) limit is $0.5 \mu\text{g/L}$ for bromate and formation must be reduced by carefully optimising the ozonation process with regard to contact time and ozone dosage for a particular concentration of residual bromide.

A mechanism by which bromate is formed can be seen in *Fig. 1.1* and was proposed by Legube *et al.* [30]. According to these researchers, the reactions between ozone, bromide and hypobromite are relatively slow at low temperatures. Additionally, the factors determining the HOBr/BrO⁻ ratio are preponderant because only hypobromite is a precursor of bromate formation by molecular ozone. On the other hand, ozone reacts quite quickly with natural organic matter, as does bromide with ammonia. Ozonation of cool waters should therefore reduce the level of bromate formation, but also is dependent on pH, natural organic matter and ammonia levels in water.

There have been attempts to reduce the level of bromate formation, such as that of Kirisits *et al.*, in which a large H₂O₂/O₃ ratio was employed to cause reduction of the HOBr/BrO⁻ and thus curbing bromate formation with an end product of bromide [2, 11]. Kimbrough *et al.* proposed the electrochemical removal of inorganic bromide and reduction of the THM formation potential as a result. This method, although carried out on a laboratory scale, showed promise for future work, but needed to be applied to production scale treatment to ensure complete confidence in the methodology [25]. In the final disinfection stage of the water treatment process, natural organic matter (NOM) is selectively removed, as it is known to form THMs. The same problem exists here as with the removal of ammonia. Although ozonation reduces the overall quantity of NOM, there will still exist a residual concentration of inorganic bromide, which if exposed to ozone for extended periods of time, will form brominated disinfectant by-products such as bromohydrins [12]. A list of some of the other ozonated by-products is shown in *Fig. 1.2*.

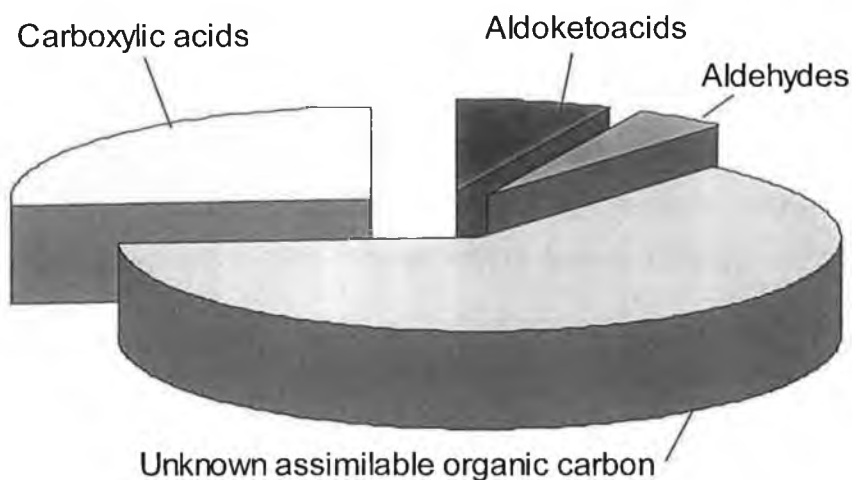


Fig. 1.2 Relative composition of other DBP classifications associated with ozonation as a proportion of assimilable total organic carbon [29]. Note: This does not include the oxyhalides as they are non-carbon containing DBPs.

1.2.2 Chlorination [13]

Chlorination is currently the most widespread method for disinfection and has been in use since the early 20th century and its advantage over ozonation is its simplicity of operation. Water treatment plants do not require operators with extensive chemical competency and so can be run quite economically and efficiently. Chlorine is an effective disinfectant against a wide range of bacteria, viruses and other pathogenic organisms. Many treatment plants that do not rely solely on chlorination processes still require backup chlorination equipment. Moreover, chlorination is by far the most effective method for disinfection, as the method is the only of its kind to supply adequate residual disinfection to preserve waters from potential post-treatment microbial growth after distribution. In addition to this, it serves as the most effective method to meet the standards put forward by the USEPA, WHO and other regulatory bodies. Since the discovery of potentially hazardous DBPs in 1974, measures have been taken to try to reduce the levels of DBP formation in

chlorinated waters. Such measures include a reduction in chlorine dosage, the repositioning of the chlorine addition in the process, changes in the type of chlorine used and a more extensive removal of NOM. Other methodologies suggest a safer alternative, such as the aforementioned ozonation procedure, although water suppliers need to use chlorine at some step in the process to administer the residual disinfectant chlorine for water preservation. As can be seen in *Fig. 1.3*, a wide range of DBPs are formed from chlorination of waters, many of which have suspected carcinogenic and mutagenic effects. Even now, 62.4 % of all halogenated by-products of disinfection have not yet been classified.

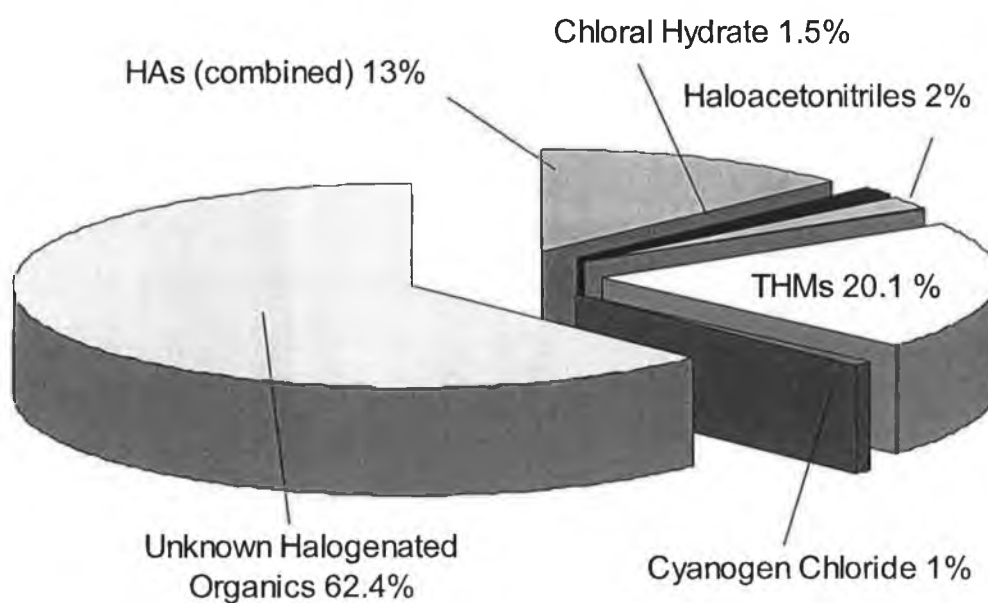


Fig 1.3 Classification and relative proportion of halogenated DBPs to total organic carbon in chlorinated drinking water [29].

1.2 Factors Affecting the Formation of DBPs [26]

1.2.1 pH

There are several factors that affect the formation of halogenated organics, the first of which is pH. There is an inverse relationship between the formation of HAs and an increase in pH. Many halogenated organics hydrolyse at high pH values and total organic halide (TOX) concentrations have been reported to be halved at pH 12 compared with TOX at pH 7 over a period of 72 hours and at 20°C [14]. However, as pH decreases, the formation of trihalomethanes (THMs) decreases to a lower concentration than existing HAs according to Pourmoghaddas *et al.* [17]. Thus, the variance in pH results in a trade-off between THM and HA concentrations [24]. These studies carried out by Pourmoghaddas *et al.* displayed the effect of pH over 6, 48 and 168 hours over three pH values of 5, 7 and 9.4.

1.2.2 Contact Time

As one would expect, as the contact time increases so does the formation of DBPs. This is not the case for the formation of haloacetonitriles and haloketones. These compounds, upon formation, decay due to residual chlorine [2, 23].

1.2.3 Temperature and Season

Due to the kinetics of the formation process, the increase in temperature during the summer months causes an increase in the level of DBPs in water. In addition to this, at this time there exists a larger level of NOM. During the water treatment process, this NOM must be removed if it is to become suitable for human consumption. As a result, higher concentrations of chlorine are added to water [15, 23]. The effect of temperature led to experiments being carried out by Dojlido *et al.* [21] to investigate if boiling of a spiked HA post-treatment sample would cause them to decompose. Their findings concluded that boiling did have an effect and reduced dissolved HAs. Reductions in concentration were up to 72 % for TCA and 31 % for MBA. However, boiling was later found to decompose the HAs to their corresponding THMs [22].

1.2.4 Concentration and Properties of NOM

Formation increases with increasing levels of NOM [20]. However, the composition of NOM is vital for the classification of DBPs. NOM contains a large distribution of hydrophobic and hydrophilic materials due to differences in species and vegetation, thus having an effect on the formation and type of DBP.

1.2.5 Concentration of Chlorine and Residual Chlorine [2]

An increase in the dose of chlorine causes an increase in the level of HAs as opposed to THMs. Moreover, the amount of trichlorinated organics is greater than that of the di- and monochlorinated species with this increase. The quantity of chlorinated organics is greater than that of the brominated category. As stated earlier, an increase in chlorine dose does limit the formation of some species of DBPs by hydrolysis due to residual chlorine. Chlorine dioxide has been used as an alternative method for chlorination and shows that with an increased concentration of ClO_2 there is a reduction in the formation probabilities of THMs and HAs, with little effect from variances in pH [20].

1.2.6 Concentration of Bromide [2, 16, 19]

In water treatment systems hypobromous acid is formed due to reaction of bromide and chlorine [16]. Hypobromous acid reacts roughly 25 times faster than hypochlorous acid and forms DBPs with natural organic matter. The HOBr/HOCl ratio plays an important role in the formation of THMs and HAs. The bromide ion shifts the distribution of DBPs to the more brominated form.

1.3 The Haloacetic Acids (HAs)

The second most abundant form of DBPs next to the THMs is the HAs. Their structure and formation, as already discussed, is primarily due to the chlorination of water intended for human consumption. What follows is a brief outline of their physical and chemical properties and observed effects on laboratory mice and/or humans for the five regulated HAs.

1.3.1 Chlorinated Acetic Acids

1.3.1.1 Physical and Chemical Properties

Chlorinated acetic acids covered by legislation are mono-, di- and trichloroacetic acids. A list of their physical and chemical properties is given in *Table 1.1* below.

Table 1.1. Physical properties of chlorinated acetic acids [27]

Property	MCA	DCA	TCA
Boiling Point (°C)	187.8	194	197.5
Melting Point (°C)	52.5	13.5	-
Density at 20 °C (g/cm ³)	1.58	1.56	1.63 (at 61°C)
Water Solubility (g/L)	Very soluble	86.3	13

1.3.1.2 Effects on Laboratory Animals and/or Humans

Chlorinated acetic acids have been shown to absorb quickly through the walls of the intestine, not to reside in adipose tissue, exist in higher concentrations in the liver and kidney of laboratory mice and are excreted virtually unchanged in urine. World Health Organisation studies [27] have shown that short-term exposure to fixed doses of mono-, di- and trichloroacetic acid had numerous effects on these laboratory mice including increased actual liver and kidney weights in males, decreased absolute and relative heart weights, elevated alanine and aspartate aminotransferases and

decreased lymphocyte and erythrocyte counts. Long-term exposure (0, 15 or 30 mg/kg body weight in drinking water for 2 years) indicated that survival was significantly decreased in both male and female species. Carcinogenicity and mutagenicity studies showed the MCA had no effect on laboratory rats over a two-year bioassay, but DCA and TCA had significant effects and concluded that these two HAs were carcinogenic at a level of 1000 mg/kg of body weight and resulted in the development of tumours in the livers of mice. DCA has shown to decrease total cholesterol count in human serum. Biochemical effects show depressed alanine levels, decreased triglyceride, elevated plasma ketone bodies and elevated serum uric acid levels for diabetic patients. For two hypercholesterolaemia patients, a similar reduction in total cholesterol was observed with additional effect of degradation and weakening of muscles.

1.3.2 Brominated Acetic Acids [28]

1.3.2.1 Physical Properties

Only two brominated HAs are currently covered by legislation by the WHO, MBA and DBA. Their physical and chemical properties are given in *Table 1.2* below.

Table 1.2. Physical and chemical properties of brominated acetic acids

Property	MBA	DBA
Molecular Weight (AMU)	138.9	217.8
Appearance	Hygroscopic crystal	Hygroscopic crystal
Water Solubility	Miscible	Very soluble

1.3.2.2 *Effect on Laboratory Animals and/or Humans*

DBA is rapidly absorbed in the intestinal tract and is metabolised to glyoxylic acid via glutathione-S-transferase (DCA also undergoes this metabolism). However, DBA is not lipophilic in nature and does not reside in adipose tissue, and hence is excreted in urine. There is no evidence of literature pertaining to MBA metabolism or uptake. Exposure of laboratory mice to MBA shows no long-term toxicity, however short term exposure displayed symptoms of diarrhoea, restricted breathing and thirst. Mutagenic and carcinogenic studies show mutagenic effects in *Salmonella typhimurium* and also caused DNA strand breaks in L-1210 mouse leukaemia cells. Dibromoacetic acid has an effect on mouse liver, causing an increase in absolute and relative weights. Its mutagenic effects are similar to MBA causing mutations in *Salmonella typhimurium* cells. DBA also has a large effect on the reproductive organs of laboratory mice and data suggests that DBA is genotoxic. The WHO recommends a total daily intake of less than 20 µg/kg of total body weight to suppress these effects. No carcinogenicity data exist for DBA. However, a study is currently being carried out by the US National Toxicology Program to determine the carcinogenicity of DBA.

1.4 Chromatographic determination of HAs

1.4.1 Introduction to chromatographic theory [31-33]

During the chromatographic process, solutes are retained on a stationary phase through various sorption mechanisms. The strength of these sorption mechanisms is described by the adsorption and partition coefficients for each solute-phase interaction. The length of time a species takes to pass through the stationary phase and reach the detector is called its retention time, t_r . A more convenient method for the measure of retention is retention factor, k'

$$k' = \frac{(t_r - t_0)}{t_0}$$

Equation 1.1

where t_0 is the void volume. A representation of a typical chromatogram is shown below in Fig. 1.4.

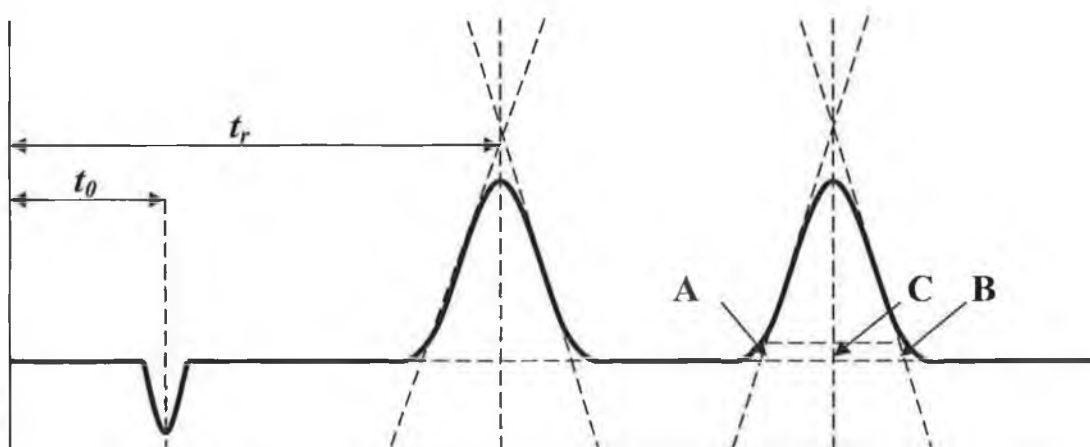


Fig. 1.4 Typical chromatogram for the separation of two species showing retention time and peak asymmetry (A_s).

In ideal circumstances, separated peaks should be Gaussian in shape, but in practice, they can be either tailed or fronted due to various experimental factors in the separation process, for example a poorly packed column, column overload, extra band broadening or secondary retention effects [38]. For peak shapes to be acceptable, peak asymmetry (A_s) must be less than or equal to 1.2 at 10 % of peak height, as in Equation 1.2

$$A_s = \frac{|CB|}{|AC|} \quad \text{Equation 1.2}$$

For evaluating chromatographic efficiency, the concept of theoretical plates is considered. The efficiency of a stationary phase is its ability to produce sharp Gaussian peaks. The plate height, H , is a measure of band broadening that is normalised for column length. As columns are commercially available in a variety of lengths, it is necessary to consider theoretical plate number, N . N is defined as the quotient of the square of the length of the column (L) and the standard deviation of the band in length units. Also, N can be expressed directly from the chromatogram with Equation 1.3.

$$N = 5.54 \left(\frac{t_r}{W_h} \right)^2 \quad \text{Equation 1.3}$$

Both H and N are related using Equation 1.4.

$$H = L / N \quad \text{Equation 1.4}$$

where W_h is the width of the peak at half height.

When two or more species elute close to each other it may be necessary to assess the quantity of resolution. Resolution, R_s , is the degree of separation of

two adjacent peaks and is expressed as a unitless decimal number and shown in Equation 1.5 and Fig. 1.5 below.

$$R_s = \frac{2(t_r^2 - t_r^1)}{W_1 + W_2} \quad \text{Equation 1.5}$$

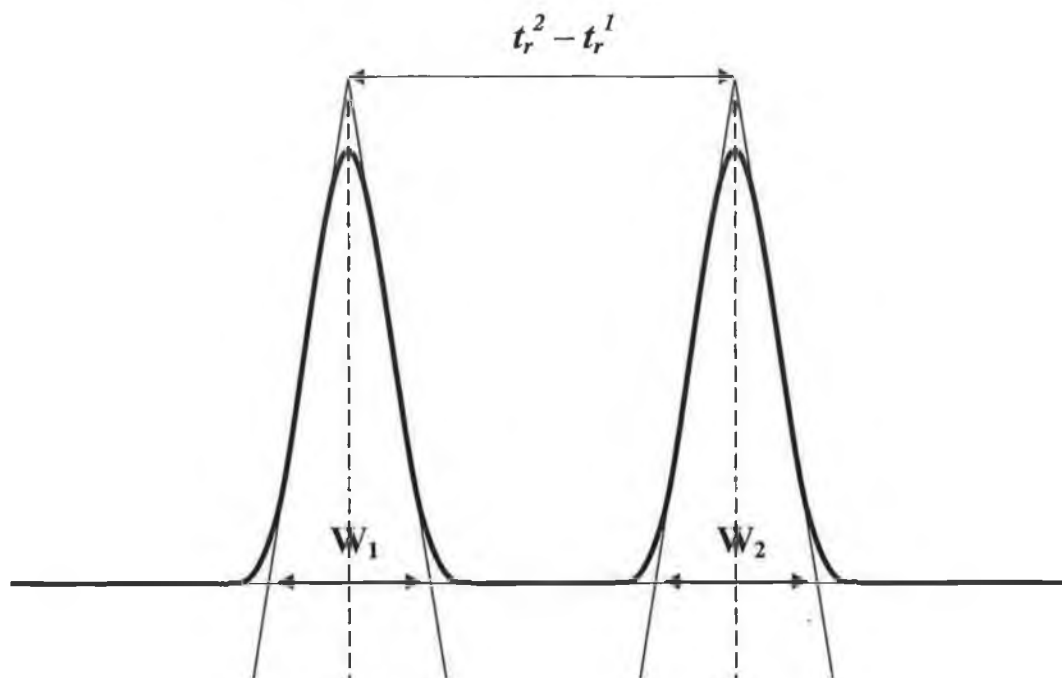


Fig. 1.5 Calculating the resolution of two adjacent peaks, where W and t_r are measured in decimal minutes.

For complete separation to be achieved in liquid chromatography, resolution must be greater than 1.5, which describes separation of two adjacent peaks of similar size with the signal returning to baseline between peaks. In addition to resolution, there exists a separation factor (α), which is a measure of the degree of proximity of two closely eluting bands.

$$\alpha = \frac{k_2}{k_1} \quad \text{Equation 1.6}$$

For liquid chromatographic separations, α values should be in the range of 1.05 – 1.10. Resolution may also be expressed in terms of α and k'_{av} , which represents the average of the retention factor for both bands. The variable, N , in this case represents the product of the number of theoretical plates for both bands.

$$R_s = \frac{\sqrt{N}}{4} \left(\frac{\alpha - 1}{\alpha} \right) \left(\frac{k'_{av}}{1 + k'_{av}} \right) \quad \text{Equation 1.7}$$

1.4.2 Band broadening in chromatography [1-3,7]

Ideally, observed chromatographic peaks should be sharp and totally Gaussian in nature. As a solute band passes through the column, individual molecules within it will experience a combination of factors that will cause the band to spread. The extent of the broadening is primarily governed by three factors;

1. Multiple path lengths for the solute through the column;
2. Molecular Diffusion;
3. Mass transfer between the mobile and stationary phases.

1.4.2.1 Multiple path lengths

As the solute molecule traverses through the stationary phase, it may be carried along through a different route to that of the next solute molecule. The flow of mobile phase is different across the diameter of the column depending on the structure of the packing. Thus, the analyte molecules travel through the column by different routes and at different flow rates, with the result being a broadened peak (see Fig. 1.6). This is also known as eddy diffusion. The magnitude of this effect may be quantified by Equation 1.8.

$$H_P = 2\lambda d_p$$

Equation 1.8

where H_p is the theoretical plate height, d_p the average particle size diameter and λ represents the particle size distribution and generally is close to 1.0. Thus from this equation it can be seen that a decrease in the particle size will increase efficiency, as will a more uniform particle size distribution.

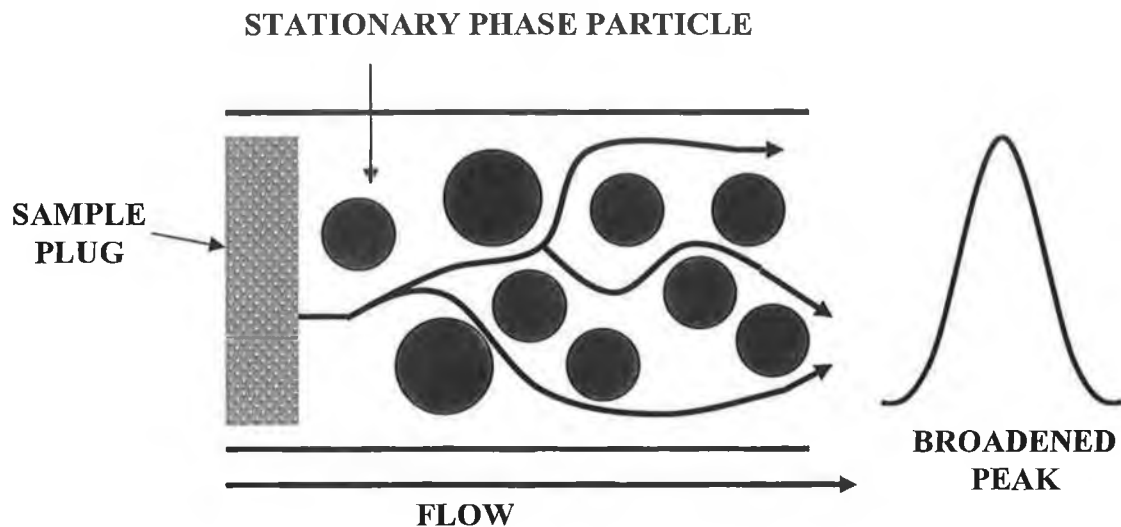


Fig 1.6 Schematic of eddy diffusion of solute molecules causing band broadening in chromatographic separations.

1.4.2.2 Molecular diffusion

Dispersion of the band in the longitudinal direction (along the column axis) is common in chromatographic separations. The magnitude of this is dependent primarily on the flow rate of mobile phase. The lower the flow rate, the higher the ability of the zone to spread behind and ahead of the bulk mass of the analyte band. The degree of zone spreading due to molecular diffusion is given in Equation 1.9.

$$H_d = 2 \frac{\gamma D_m}{u} \quad \text{Equation 1.9}$$

where γ is a constant representing the opposition to zone spreading due to column packing ($\approx 0.5-1.0$), D_m is the diffusion coefficient of the solute and u is the column flow velocity.

1.4.2.3 Mass transfer

This contributor to band broadening is the most insignificant of the three. No pressure driven flow exists within the stationary phase particles themselves. Therefore, solute molecules that travel into these particles do so only by diffusion. The degree of this band broadening increases with increasing flow rate and is given by,

$$H_m = \omega \frac{d_p^2}{D_m} u \quad \text{Equation 1.10}$$

where d_p is the particle diameter, D_m is the diffusion coefficient, ω is the coefficient to describe the pore size and shape of the stationary phase particles and u , again, is the mobile phase flow velocity.

1.4.2.4 The van Deemter equation

The three contributors to band broadening in chromatography are combined and described by the van Deemter equation to determine the optimum flow rate for a specific separation.

$$H = H_p + H_d + H_m \quad \text{Equation 1.11}$$

or rearranged by removing u from Equations 1.8-1.10

$$H = A + \frac{B}{u} + Cu \quad \text{Equation 1.12}$$

This can be represented graphically as in Fig 1.7 as the van Deemter plot.

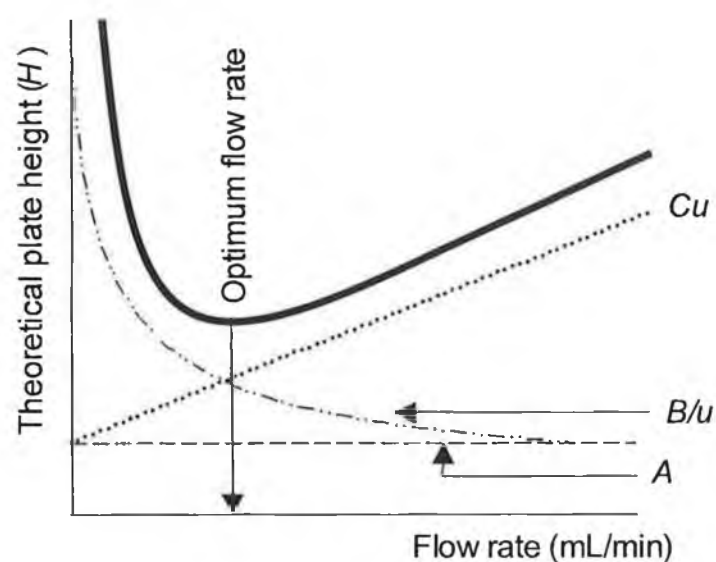


Fig 1.7 Van Deemter Plot to determine the optimum flow rate for a chromatographic system.

1.5 Ion Exchange Chromatography

Ion exchange chromatography (IC) is *the reversible interchange of ions of like charge between a solution and a solid, insoluble material in contact with it* [32].

Electrical neutrality must be maintained at all times, i.e. as one charged species enters the ion exchange model, one must leave. Additional reactions may also occur with hydrogen ions, which combine with the anions of weak

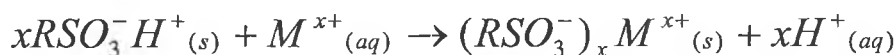
acids. Furthermore, metals may form coordination complexes. The basis on which separation occurs lies in the equilibrium between the analyte ion and the ion exchanger. Differences in solute affinity for the exchange site cause variation in retention times and thus separation.

1.5.1 The Ion Exchange Process [37]

The most common ion exchange sites are sulphonic acid $[-SO_3^-H^+]$ and carboxylic acid groups $[-COO^-H^+]$ for separation of cations, and primary $[-NH_3^+OH^-]$ and quaternary amine groups $[-N(CH_3)_3^+OH^-]$ for anion separations.

1.5.1.1 Cation Exchange

Sulphonic acid is a strong ion exchanger as opposed to weak carboxylic acid groups. The following relationship describes the ion exchange model for a sulphonic acid group and a metal cation (M^{x+}).

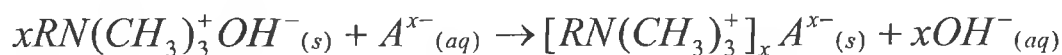


Equation 1.13

where $RSO_3^-H^+$ is one of the sulphonic acid groups attached to a polymer support.

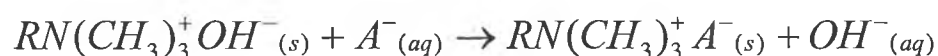
1.5.1.2 Anion Exchange

Similarly, quaternary amines are strong anion exchangers, as opposed to the weaker primary amines. The ion exchange relationship for anions is as follows,



Equation 1.14

In an application of the mass action law to ion exchange equilibria, we will consider an anion, A^- , with a quaternary ammonium functionalised resin packed within a column in the hydroxide form. Retention of A^- occurs at the beginning of the column and distributes between the mobile and stationary phases according to,



Equation 1.15

As these anions traverse down the column length, retention is observed due to a series of these distributions. The equilibrium constant for the exchange is,

$$K_{ex} = \frac{[RN(CH_3)_3^+ A^-]_{(s)} [OH^-]_{(aq)}}{[RN(CH_3)_3^+ OH^-]_{(s)} [A^-]_{(aq)}}$$

Equation 1.16

Rearranging this equation to Equation 1.17 gives

$$\frac{[RN(CH_3)_3^+ A^-]_{(s)}}{[A^-]_{(aq)}} = K_{ex} \frac{[RN(CH_3)_3^+ OH^-]_{(s)}}{[OH^-]_{(aq)}}$$

Equation 1.17

During the elution process, the concentration of hydroxide ions is much greater than the concentration of the solute ion. Additionally, the ion exchanger has significantly more ion exchange sites relative to the number of A^- ions. As a result, the concentrations of $[RN(CH_3)_3^+ OH^-]_{(s)}$ and $[OH^-]_{(aq)}$ are not significantly altered by changes in equilibrium. Therefore, the right hand side of equation becomes constant and we can write,

$$K = \frac{[RN(CH_3)_3^+ A^-]_{(s)}}{[A^-]_{(aq)}} = \frac{c_S}{c_M} \quad \text{Equation 1.18}$$

where K is the *distribution constant*. It should be noted that this equilibrium constant value depends on the selectivity of the stationary phase for either A^- or OH^- . If K is large then the stationary phase will retain A^- quite well and the reverse for when K is small. By taking a common reference ion like OH^- , the distribution constants can be experimentally measured for a wide variety of anions and similarly, H^+ can be used to determine K for cations.

When using a typical cation exchange resin (i.e. a sulphonated functionality), the value of K decreases over the order of $Tl^+ > Ag^+ > Cs^+ > Rb^+ > K^+ > NH_4^+ > Na^+ > H^+$. For divalent cations, the order is $Ba^{2+} > Pb^{2+} > Sr^{2+} > Ca^{2+} > Ni^{2+} > Cd^{2+} > Cu^{2+} > Co^{2+} > Zn^{2+} > Mg^{2+} > UO_2^{2+}$. For anion exchange on a typical anion exchange resin like a quaternary ammonium functionality, the value of K decreases over the order of $SO_4^{2-} > C_2O_4^{2-} > I^- > NO_3^- > Br^- > Cl^- > HCO_2^- > CH_3CO_2^- > OH^- > F^-$.

1.5.2 Ion Exchange Stationary Phases [32,34]

There is a wide range of commercially available stationary phases available to the chromatographer for ion chromatography. The majority of these stationary phases are manufactured by Dionex Corporation, Metrohm AG and Alltech Associates, with some smaller industry players such as Transgenomic Inc. For a solid substrate to exchange with anions or cations it must possess ions that move in and out of the solid phase freely. The actual solid phase structure itself therefore must be permeable and have charged sites attached to it. These are called fixed ions and are electrically balanced by mobile counterions. Counterions are ions that take part in ion exchange and are free to distribute between mobile and stationary phases during the exchange process. Resins such as these are represented in *Fig. 1.8* below.

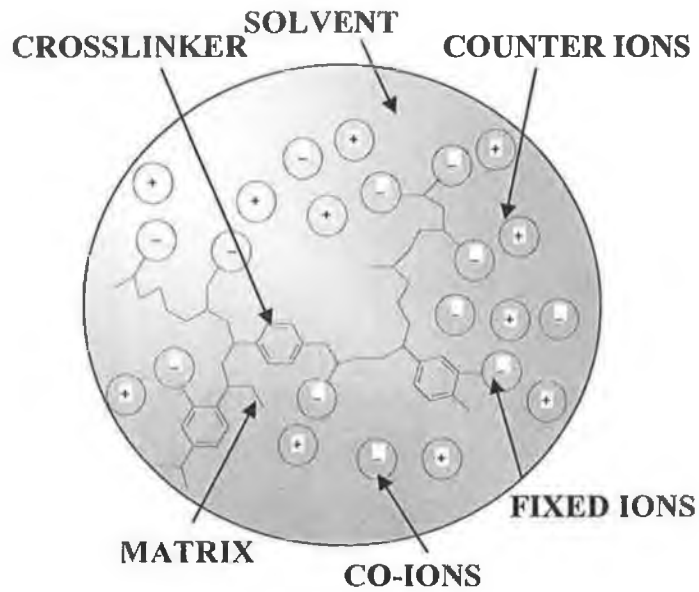


Fig 1.8 Structure of an ion exchange resin

1.5.2.1 Polymeric exchangers

The majority of ion exchangers are based upon polymeric materials such as styrene-divinyl benzene. The chemical structure of polymerised ion exchangers is represented in Fig. 1.9.

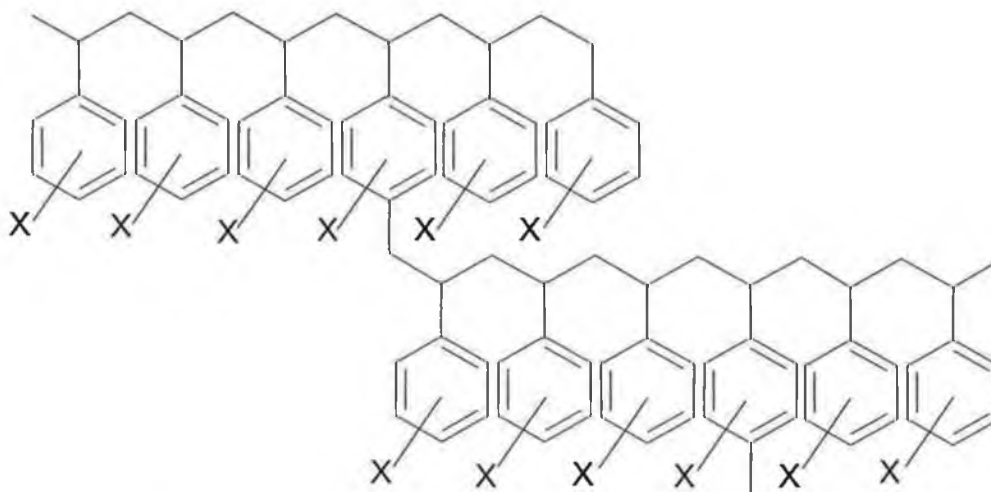


Fig. 1.9 Crosslinked polymeric ion exchanger

where X represents the ionic functional group (i.e. sulphonic acid etc). Sulphonic acid ionic groups can be introduced to the polymer by treating the cross-linked beads with fuming sulphuric acid. Other functionalities mentioned are added in place of X. For example in anion exchange, the group $-\text{CH}_2\text{NR}_3\text{Cl}$ may be employed because the negatively charged chloride ion may be exchanged for an analyte anion. Chloride may be interchanged with hydroxide to give a very strong anion exchanger.

The structure given in *Fig. 1.9* is generally termed as a cross-linked polymer. If one in four polymeric units are joined together with a divinylbenzene (DVB) unit, it can be classed as 25 % cross-linked. The importance of cross-linking lies primarily in maintaining a rigid structure. High cross-linking allows for higher selectivity, capacity, higher rigidity and pressure across the column. Low cross-linked polymers act in the opposite way. These polymers may be very weak under pressure and may collapse. A compromise is used to find an intermediate suitable cross-linked polymer. According to Haddad [32], the most common degree of cross-linking is 8 %, i.e. 8 moles of DVB to 92 moles of styrene. Particle size is also another important factor. Generally, particle sizes in most high performance ion exchange columns are less than 10 μm and this refers to the particle sizes when exposed to water and hence their swollen size.

1.5.2.2 *Dionex micro-bore anion exchangers suited to HA and oxyhalide analysis*

Dionex Corporation manufacture a wide range of ion exchange resins that are predominantly based on ethylvinylbenzene-divinylbenzene (EVB-DVB) with a variety of different structural designs such as agglomerated, surface functionalised and grafted resins. These columns, for the most part, use a strong alkanol quaternary ammonium functionality as a strong ion exchanger, but some weak anion exchangers based on tertiary amine functionalised resins are also available. Variation in resin structure results in a wide range of selectivities and these columns have shown application to the analysis of a variety of ionic species in increasingly more complex matrices. Most of these

columns are available in 4 mm standard bore and 2 mm micro-bore internal diameters, but some are also available in 3 mm format. The use of micro-bore columns is particularly suited to the analysis of ionic species by IC-MS, operating at flow rates of between approximately 0.20 - 0.40 mL/min. The IonPac AS11 is an example of a *hydroxide selective* anion exchange column manufactured by Dionex [96]. Packings for this column employ a core substrate of EVB-DVB (55 % crosslinked) with a coating of 85 nm MicroBead™ latex particles functionalised with the anion exchanger. The EVB-DVB core of the IonPac AS11 is a 9 µm microporous bead (< 10 Å pore size), but is also available as the IonPac AS11-HC, which has a macroporous structure (2000 Å). This column is coated with slightly smaller 70 nm MicroBeads™ giving the resin a higher overall capacity of 72.5 µeq/column. The latex beads are 6 % crosslinked in both types of this column. The IonPac AS11-HC displays medium-low hydrophobicity and can be applied to the separation of HAs and according to the manufacturer, are particularly suited to the analysis of low molecular weight organic acids. Another column possibly suitable for HA analysis is the hydroxide selective micro-bore IonPac AS16 [97], which is based on a similar structure to that of the AS11-HC, but displays ultra-low hydrophobicity and has a capacity of 42.5 µeq/column. This column has been applied to the analysis of polarisable anions such as perchlorate, iodide, thiocyanate and thiosulphate. The high capacity nature of the IonPac AS16 and AS11-HC columns allows for large sample volume injection without overloading. This is particularly suited to the analysis of trace anionic DBPs in the presence of mg/L concentrations of inorganic anions typically associated with drinking water matrices.

Other hydroxide selective anion exchangers currently available from Dionex include the IonPac AS19 column [98]. This stationary phase is based on a hyper-branched anion exchange polymer, which is electrostatically attached to a macroporous 7.5 µm diameter EVB-DVB core and has a capacity of 60 µeq/column. According to the manufacturer, this resin has optimised selectivity for bromide and bromate and is therefore particularly suited to the determination of bromate in drinking water. The IonPac AS15 column utilises a

packing that is unique in structure and is composed of a highly cross-linked macroporous substrate with a grafted anion exchange surface in place of the previously discussed MicroBead™ latex coating [99]. This column has been applied to chlorate determinations along with low molecular weight organic acid determinations in high ionic strength matrices with the 3 mm internal diameter bore format. Flow rates for this column are generally similar to that of the standard bore format and may be too high for IC-MS applications.

1.5.2.3 *Acrylic polymer based phases*

Another widely used stationary phase for ion chromatography is acrylic polymer. Again, these stationary phases have sites to which functionalities may be bound in order to facilitate the ion exchange process. There are many different preparative methods for various types of acrylic polymers suited to hold ion exchange sites. For example, methyl methacrylate can be polymerised along with a divalent cross-linking agent and hydrolysed to give polymethacrylic acid. Sulphonic acids can be added as the cation exchange sites by reaction with sodium dichloroacetate and sodium hydroxide followed by chlorosulphonic acid. For anion exchange, the polymer can be reacted with $\text{ClCH}_2\text{CH}_2\text{NEt}_2\text{HCl}$ and NaOH to produce $\text{C}_2\text{H}_4\text{OC}_2\text{H}_4\text{NEt}_2$. Another type of acrylic polymer stationary phase is Spheron. This involves the copolymerisation of 2-hydroxyethyl methacrylate with ethylene glycol dimethacrylate. The main difference between the PS-DVB stationary phases and these acrylic phases is that they are softer. This means that they are not compatible with systems under high pressure. However, their advantage is that they are more hydrophilic and therefore are particularly suited to the separation of proteins. In addition to this is the fact that being non-aromatic in character, they do not retain small non-ionic analytes like the polystyrenes.

1.6 **Ion Chromatography Instrumentation**

Instrumentation required for ion exchange chromatography generally comprise of eluent reservoirs, a gradient pump, guard and analytical columns,

temperature control oven and some form of detection. A schematic of a typical IC system is shown in *Fig. 1.10*.

1.6.1 Eluent delivery and pumping systems [37]

Requirements for an adequate pumping system are extensive and include the ability to pump against back pressures of ≥ 6000 psi; the ability to deliver a smooth flow without pulsation; depending on the type of chromatography required, the possibility to deliver flow rates over a range of 0.1 – 10 mL/min; reproducible and easily controlled flow and finally, the pump internal plumbing should be composed of non-corrosive material over extended solvent usage. There are three main types of pump: reciprocating, displacement and pneumatic pumps. The reciprocating pump is the most common type of pump and is used in over 90 % of all high performance liquid chromatography (HPLC) instrumentation. Flow is delivered to the column by passing the solvent through a chamber within which a reciprocating piston is housed. Before entering and exiting the pump head, the solvent passes through two check valves, which inhibit reverse flow. A schematic of a reciprocating pump is incorporated into *Fig. 1.10*.

Chromatography when run using a single eluent is termed *isocratic elution* and is sometimes enhanced by the use of *gradient elution*. When a gradient is required, one or more eluent reservoirs may be used simultaneously and each eluent type can be used at constant or at varying proportions over time, either linearly or in a stepwise fashion. Pumping from one or more of these reservoirs is usually aided by using a head pressure of either helium or nitrogen on the eluent caps. As a result, eluent mixing systems are available and often appear as standard on modern HPLC instruments. As solvent mixing is often subject to outgassing, some systems employ a degasser prior to reaching the pump. In addition, eluent lines are usually fitted with filters to remove any suspended solids.

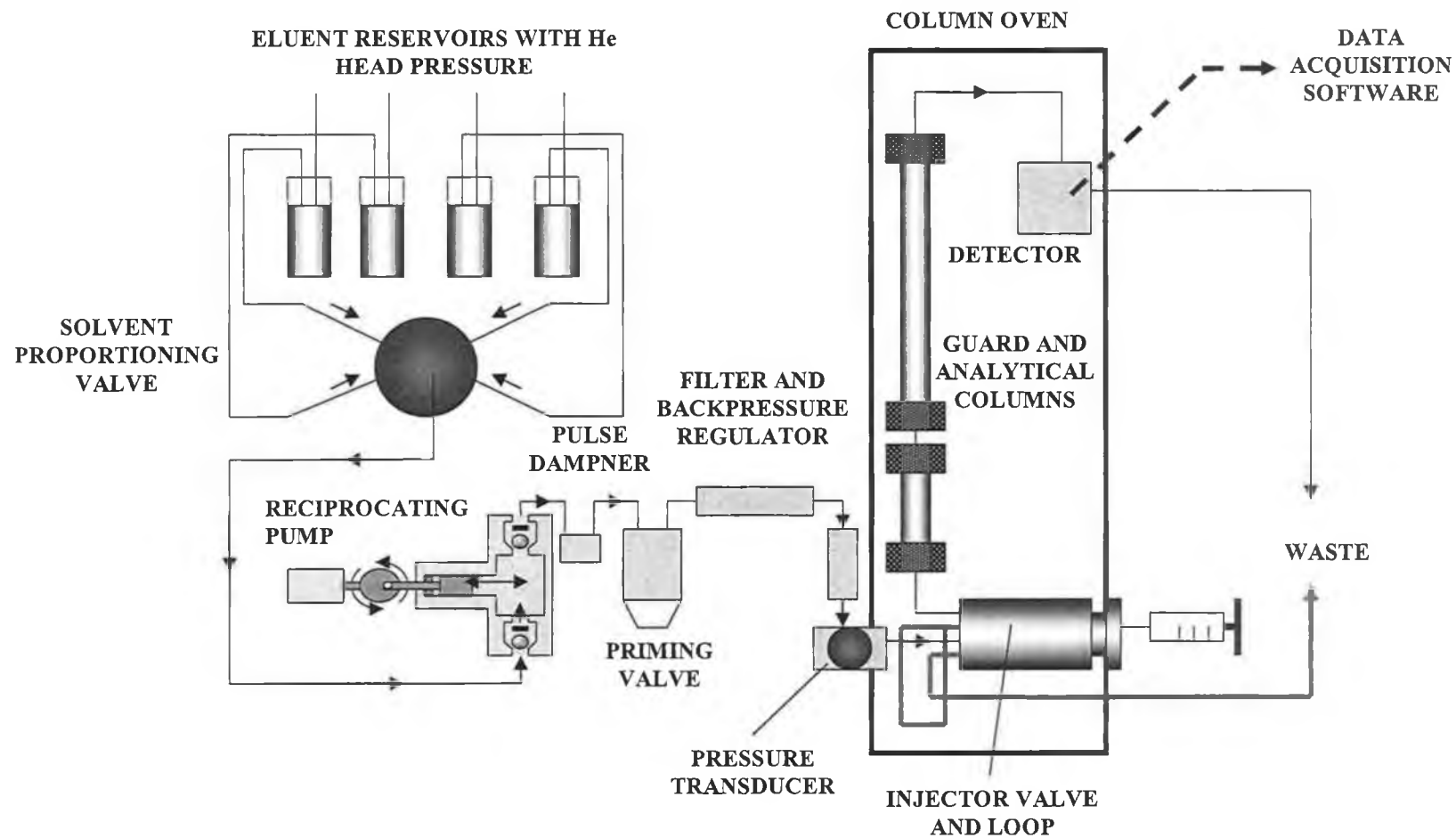


Fig. 1.10 Schematic of an IC system showing reciprocating pump, injector valve, guard and analytical columns and detector. Only conductivity detector cells are located inside the column oven. UV and mass spectrometric detectors lie external to column oven.

1.6.2 Injection systems

The most common type of injection system used in modern day chromatography is by use of a valve injector. These valves utilise fixed loop lengths to accurately deliver often large volumes of sample onto the column. The main advantage of these injector valves is their ability to withstand operating pressures of up to 7000 psi.

1.6.3 Detection Techniques in Ion Chromatography

1.6.3.1. UV detection [37]

UV detectors are commonly used for detection in IC. Operation of these photometric detectors is based on the Beer-Lambert law, which states that the absorbance of a solution in a sample cell depends on the path length of the cell, the concentration and absorptivity of the sample molecule and the wavelength selected,

$$A = \epsilon cl = \log \left(\frac{I_r}{I_s} \right) \quad \text{Equation 1.19}$$

where A is the absorbance (dimensionless), ϵ is the molar absorptivity of the sample (in $\text{Lmol}^{-1}\text{cm}^{-1}$), c is the concentration of the sample (mol/L), l is the path length of the sample cell (cm), I_r is the intensity of the reference solution (AU) and I_s is the intensity of the sample solution (AU).

The variable wavelength detectors (VWD) utilises a deuterium lamp, which emits a wide range of UV wavelengths. When a wavelength is selected, UV light is reflected by two curved mirrors onto a rotating diffraction grating. The subsequent selected wavelength is reflected onto an additional curved mirror, then to a plane mirror, through a quartz lens, through the sample cell and finally focussed by another quartz lens onto the photocell. The use of the

rotating grating allows maximum sensitivity at the selected wavelength, which allows for UV λ_{max} optimisation studies to be carried out for known and unknown samples. The UV absorption spectrum can be obtained for all analytes and can aid to confirm peak identity and peak purity. The added versatility of this detector is its main advantage, but it is not as sensitive as the fixed wavelength detector with maximum sensitivity of approximately 1×10^{-7} g/mL. A schematic of a variable wavelength detector is shown in Fig. 1.11.

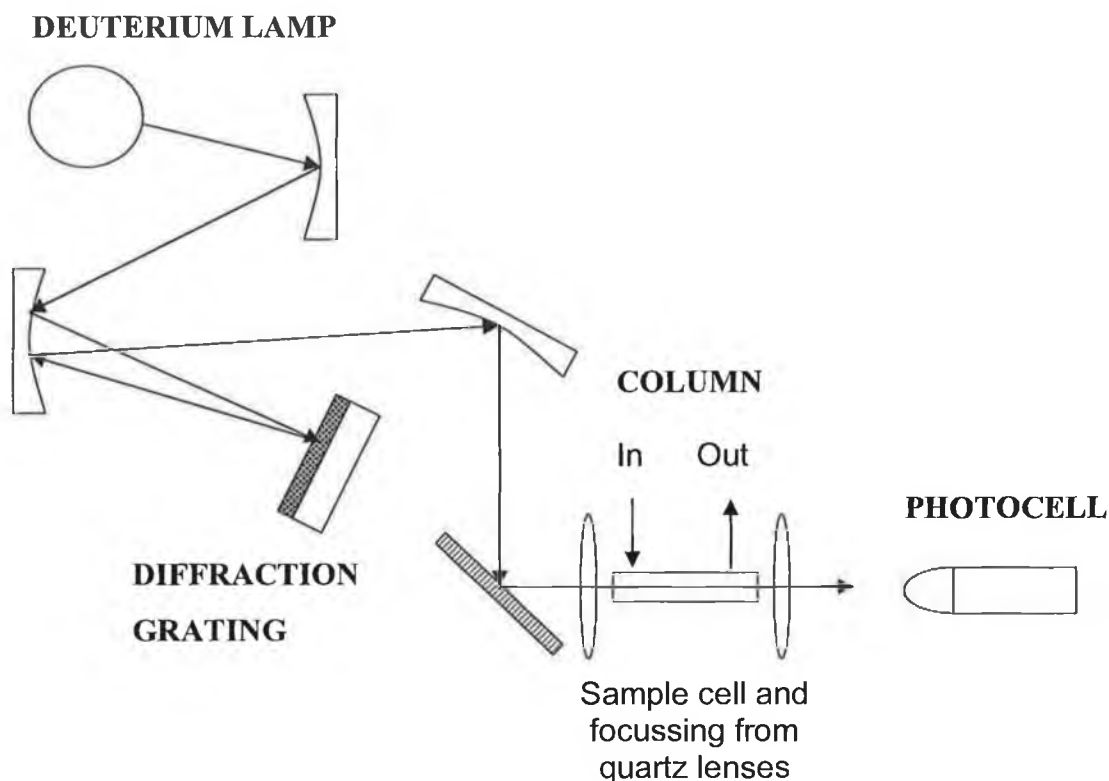


Fig. 1.11 Schematic of a variable wavelength detector with deuterium lamp, diffraction grating, sample cell and photocell.

1.6.3.2. Conductivity Detection [35]

The ionic nature of the solutes in IC means conductivity detection is a very suitable detector option. The ability of a solution to conduct is directly proportional to the salt content and the mobility of the anions and cations. Size of the ion plays a role in conductivity, with larger bulky ions having low ionic conductances in contrast to small mobile ions having high ionic conductances.

Electrolytic conductivity is a measure of the ability of an electrolyte to conduct electricity between two electrodes across which an electrical potential is applied. The magnitude of the current is partly dependent on the potential applied. This system obeys Ohm's Law and the conductance, G , is expressed as a function of the solution electrolytic resistance.

$$G = \frac{1}{R} \quad \text{Equation 1.20}$$

G is measured in reciprocal ohms, mhos, or in the SI unit, Siemens (S). Specific conductance (k) includes the area (A) of the electrodes in cm^2 and the distance (l) between the electrodes, in cm.

$$k = G \left(\frac{l}{A} \right) \quad \text{Equation 1.21}$$

The units of k are S/cm. Also, the cell constant (K) is equal to l/A and has units of cm^{-1} . Another term used to describe the extent to which a particular ion conducts in solution is the *limiting equivalent ionic conductance* (λ) and is specific for each ion extrapolated to infinite dilution. This is given by Equation 1.22, where e is the electronic charge, F is the Faraday constant, z_i is the number of charges on the ion, η is the viscosity and r is the ionic radius. The limiting equivalent ionic conductances of some selected ions are shown in *Table 1.3*.

$$\lambda_i = \frac{eFz_i}{\eta r} \quad \text{Equation 1.22}$$

Equivalent conductance incorporates the concentration of the solution and is defined by,

$$\Lambda = \frac{(1000 k)}{C}$$

Equation 1.23

Where C is the molar concentration of the solution per litre. The units of Λ are $S \text{ cm}^3 \text{ equiv}^{-1}$. Rearranging equations 1.22 and 1.23 shows the relationship of measured conductance to equivalent conductance.

$$G = \frac{\Lambda C}{1000 K}$$

Equation 1.24

An electric field is applied to the solution in a conductivity cell. The ions migrate at a certain velocity towards the electrode of opposite charge and a signal is obtained. The conductivity of the solution under analysis depends on the total velocities of all the ions and these, in turn, depend on their individual mobilities and the strength of the applied field. The individual mobilities of the ions depend on their size, charge, the temperature and type of solution matrix and the ionic concentration. As one increases the applied field, detector response increases proportionately. Applied fields can be kept constant or take form in that of a square or sinusoidal oscillation. Cell current can be easily measured, but the conductance depends on the ionic behaviour of the solution, as it can decrease the effective potential applied to the cell as a higher set potential is applied. In addition, Faradaic electrolysis may cause double layer capacitance at the electrodes. It is the formation of this double layer capacitance that causes a decrease in the effective potential applied to the solution. In order to overcome this, certain measures have been taken to eliminate the double layer. Reversing the polarity causes the ions to move in the opposite direction. If the frequency of polarity change is increased, the electrolysis is lessened, as is the capacitance formation. When the frequency is increased to an upper limit of about 1 MHz, the ion flow is ceased, but dipole reorientation still takes place. Undesirable capacitance effects are reduced by matching the cell capacitance in the circuitry, or by measuring instantaneous

current. This instantaneous current is measured as the applied field is initially applied and before the double layer has a chance to form.

Sinusoidal wave potentials are used at 100 to 10,000 Hz. 1 kHz is the typical frequency value of most conductivity detectors employing these potential types. Very little or no electrolysis occurs up to a potential of 20 V at this frequency. The measured current is only measured instantaneously at the moment where current matches applied potential frequency. This is known as synchronous detection. In addition to sinusoidal potential conductivity detectors, pulse potentials may also be utilised. These consist of two short pulses of potential to the cell. The two pulses are equal, but opposite in magnitude and are of identical duration. At the end of the second pulse, the cell current and resistance is measured and the measurement is instantaneous. Therefore, any capacitance effects do not interfere with the measurement.

Eluents suitable for direct conductivity detection are chosen for their low background conductance, low interference and background noise. For example, *p*-hydroxybenzoate and other aromatic acid anions may be used with unsuppressed detection. Modes of detection for most anion separations utilise suppressed conductivity for its simplicity and low background noise and thus, better sensitivity and detection limits. Conductivity of the eluent is not a consideration here as with unsuppressed detection.

Table 1.3 Limiting equivalent ionic conductances in aqueous solution at 25°C

Anion	λ^- (ohm ⁻¹ cm ² equiv ⁻¹)	Anion	λ^- (ohm ⁻¹ cm ² equiv ⁻¹)	Cation	λ^+ (ohm ⁻¹ cm ² equiv ⁻¹)	Cation	λ^+ (ohm ⁻¹ cm ² equiv ⁻¹)
OH ⁻	198	Propionate	36	H ⁺	350	Hg ²⁺	53
F ⁻	54	Benzoate	32	Li ⁺	39	Cu ²⁺	55
Cl ⁻	76	SCN ⁻	66	Na ⁺	50	Pb ²⁺	71
Br ⁻	78	SO ₄ ²⁻	80	K ⁺	74	Co ²⁺	53
I ⁻	77	CO ₃ ²⁻	72	NH ₄ ⁺	73	Fe ³⁺	68
NO ₃ ⁻	71	C ₂ O ₄ ²⁻	74	Mg ²⁺	53	La ³⁺	70
HCO ₃ ⁻	45	CrO ₄ ²⁻	85	Ca ²⁺	60	Ce ³⁺	70
Formate	55	PO ₄ ³⁻	69	Sr ²⁺	59	CH ₃ NH ₃ ⁺	58
Acetate	41	Fe(CN) ₆ ³⁻	101	Ba ²⁺	64	N(Et) ₄ ⁺	33
		Fe(CN) ₆ ⁴⁻	111	Zn ²⁺	53		

1.6.3.2.1 Suppressed conductivity detection in anion exchange chromatography

The use of highly conducting eluents in anion exchange chromatography (like hydroxide or carbonate/bicarbonate) generally requires some form of suppression for sensitive conductivity measurements. Efficient suppression results in a poorly conducting electrolyte such as water or carbonic acid prior to detection. This also makes it compatible with detectors like mass spectrometry.

Originally suppression was carried out using suppressor columns applied post-column. For anion analysis, the suppressor column would have been packed with a strong acid, high-capacity cation-exchange resin in its hydrogen form. An eluted salt such as NaCl was converted to its corresponding acid, i.e. HCl, and carbonate/bicarbonate or hydroxide in the eluent was converted to carbonic acid or water, which has a very low conductivity. Companies such as Alltech Associates, Metrohm and Sequant currently manufacture suppressor columns. These packed bed suppressors can be regenerated continuously and minimise band broadening.

Dionex Corporation membrane suppressors are an alternative to the use of suppressor columns. These electrolytic devices such as the ASRS Ultra II suppressor are compatible with both standard and micro-bore ion chromatography. There are three modes of membrane suppression with the Dionex ASRS Ultra II suppressor. Firstly, and most common, is auto-recycle suppression, then external water mode suppression and finally chemical suppression [36]. Auto-recycle suppression and external water mode suppression are both electrolytic methods. A current is passed through the electrodes on either side of the suppressor separated by a series of membranes through which solute ions may pass. The overall result is a solution of a poorly conducting electrolyte reaching the detector. As analytes pass through the conductivity cell, they are detected with minimal background interference resulting in lower detection limits. For example, when using sodium hydroxide as an eluent, sodium ions pass through the membrane to

the cathode chamber once a potential is applied. The regenerant water in this chamber is electrolysed to form hydrogen gas and hydroxide, which electrostatically neutralise the incoming sodium ions. Hydronium ions are formed upon electrolysis of regenerant water in the anode chamber and pass through the membrane into the eluent chamber combining with hydroxide ions and results in a solution of analytes in pure water. Conversely, chemical suppression utilises no current, as the regenerant is generally a strong acid. For chemical suppression of hydroxide eluents, 25-100 mM H_2SO_4 is generally used. Figs. 1.12 and 1.13 illustrate the three modes of membrane suppression.

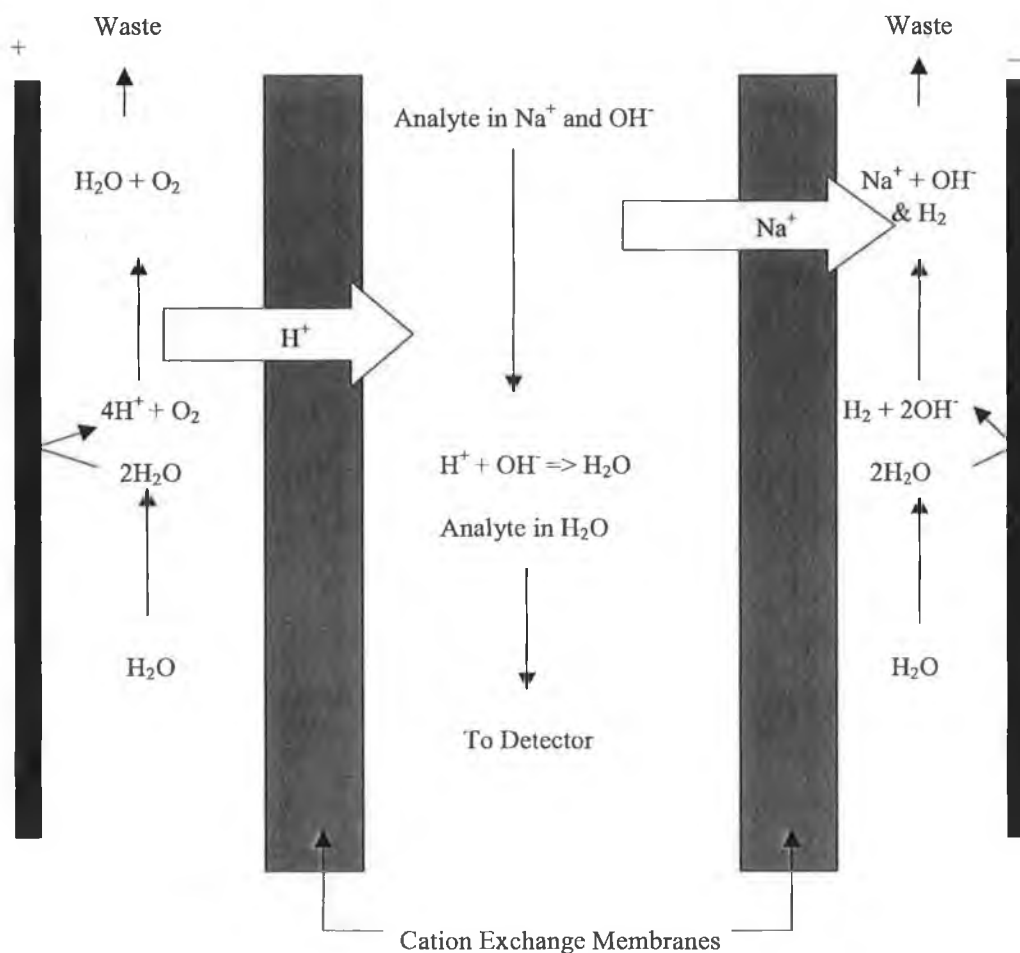


Fig. 1.12 Suppressed ion chromatography in auto suppression and external water modes [36].

The main difference between auto-recycle suppression and external water mode is that water eluent exiting the detector in auto-recycle suppression can be rerouted to the regenerant chambers to further suppress incoming eluent. In external water mode, the flow of regenerant is separate to the flow of eluent and requires a secondary pump system [36].

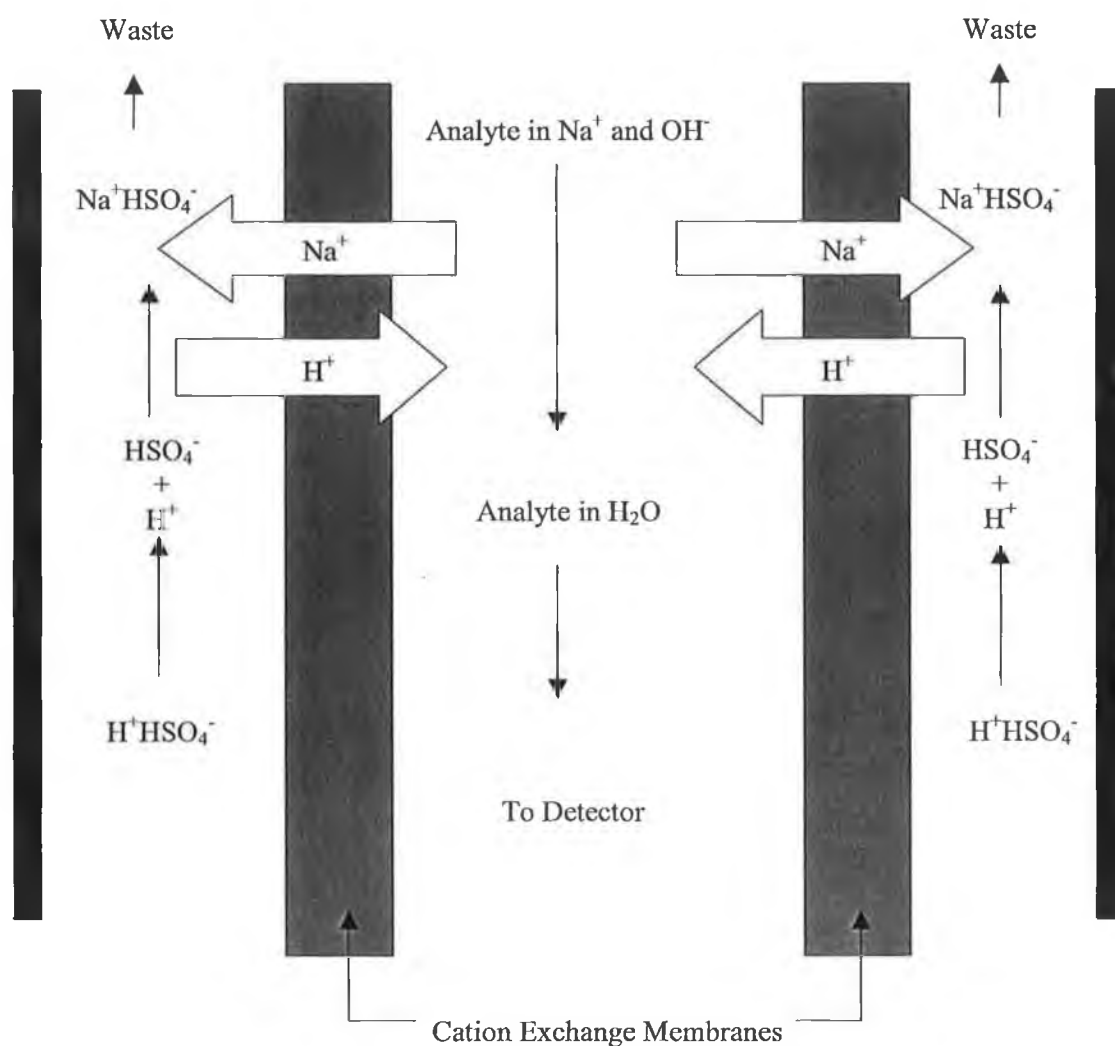


Fig. 1.13 Chemical suppression of hydroxide eluent with sulphuric acid. No electrical potential is required in this mode. All hydroxide is neutralised by hydronium ions to form water. Sodium ions cross membrane to the regenerant chamber to waste [36].

1.6.3.3. *Electrospray Ionisation-Mass Spectrometric Detection (ESI-MS)*

1.6.3.3.1 *Principles of Electrospray Ionisation (ESI)*

Electrospray ionisation sources are one of the interfaces to couple liquid chromatographic techniques to mass spectrometric detectors. The technique is used for the determination of polar analytes and ionic compounds at atmospheric pressure. Unlike other chromatographic techniques like gas chromatography (GC), the flow of mobile phase and sample is in liquid form, which gives rise to the requirement for suitable desolvation and ionisation procedures. The following is a brief summary of the main principles behind electrospray generation [39].

The sample enters the spray chamber via a grounded needle, which is concentrically surrounded by an outer tube, through which nebulizer gas flows. The combined effect of the electrostatic forces within the spray chamber and the physical shear force of the nebulizer gas causes the flow of sample to break down into droplets. As the droplets disperse, the ions of opposite polarity within the droplets move to the surface of the droplet attracted by the electrostatic field. As a result, the sample is simultaneously charged and converted to a fine spray upon nebulization, giving rise to the term *electrospray*. During nebulization, no heat is supplied to the needle, so there exists no thermal decomposition of the sample. The aerosol droplet contains the pseudo-molecular analyte ion (in the form $[M-H]^-$ in negative mode and in positive mode in the form of $[M+H]^+$), the solvent and both positive and negative ions.

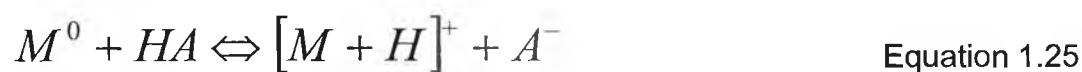
The next step in the ion generation process is desolvation. As the electrospray is produced, a flow of drying gas, typically nitrogen, is used to evaporate the solvent. As the size of the droplet reduces in size, the repulsion between the ions on the surface of the droplet increases and overcomes the forces associated with surface tension (the Rayleigh Limit). As a result, a Coulombic explosion occurs causing fragmentation of the droplet to smaller charged daughter droplets of approximately 10 % of its original size. This process continues until extremely small droplets with high

surface-charge density are formed. When the charge density reaches approximately 10^8 V/cm², the ions within the droplets begin to evaporate. It should be noted that the choice of solvent greatly affects the ionisation process. Solvents with low heat capacity, surface tension and dielectric constant, result in better nebulization and desolvation.

Ion evaporation (or ion desorption) has been described by Fenn *et al.* [44] and originally developed by Iribarne and Thomson [45]. Essentially, once the charge density overcomes the surface tension, the solvent droplets and the charged ions 'separate' and analyte ions are evaporated into the gas phase. Generally, the more hydrophobic the analyte is in the sample solution, the better it desorbs into the gas phase.

1.6.3.3.2. *Negative ion, positive ion and neutral modes*

There are two basic modes of electrospray ionisation. The choice of one over the other depends mostly on the analyte and its solution chemistry. Analytes can be determined in the anionic and cationic form as well as neutral molecules. By and large with analytes that ionise directly in solution, forming electrospray is indeed simple and highly sensitive. If the analyte is cationic in solution, positive mode is chosen and conversely, when the species is anionic, negative ion mode is more suitable. For analytes that do not readily dissociate, addition of a polar solvent, such as acid or base may cause the analyte to ionise or take on a dipole moment. The ionisation process for analytes, which display a strong dipole moment but do not ionise, is carried out utilising the electrostatic field in the spray chamber, which introduces a charge on the droplet surface. Addition of special chemicals may also induce ionisation with the formation of adduct ions.



When used in the positive ion mode, the analyte acquires a proton from solution as in Equation 1.25. An increase in concentration of hydronium

ions present in solution results in more effective ionisation of polar analytes. Solutions of formic, acetic or propionic acid perform best. Unlike strong acids, the weak acid anions do not pair with analyte cations resulting in higher ion abundance. Usually analytes with basic nitrogen functionalities achieve higher sensitivity in slightly acidic solutions. However, hydrocarbons show poor response in positive ion mode.



Conversely, when negative ion mode is used, the analyte anion loses a proton to the solution as in Equation 1.26. Again, the more basic the solution, the more effective ionisation becomes. Analytes with acidic functionalities like the HAs are best monitored in negative ion mode. Finally, neutral molecules which do not ionise in strong electric fields are analysed by the formation of adduct ions. For example, sugars can be adducted by addition of low concentrations of alkali metals in the form of sodium acetate or potassium acetate.

1.6.3.3.3. *Considerations for practical hyphenation to ion chromatography*

Coupling ion chromatography to electrospray sources brings its own considerations for successful application. Unlike other liquid-based separation techniques such as capillary electrophoresis-mass spectrometry (CE-MS), interfaces are generally a lot simpler for IC and outflow lines can be directly attached to electrospray needles using conventional fittings. However, there are several different factors to take into account such as column choice, eluent composition, flow rate, as well as volatility and hydrophobicity of the analyte.

Firstly, composition of the eluent is of critical importance. It not only must consist of a solvent that is easily evaporated from the analyte, but any added buffers or ion pair reagents must be volatile to ensure the mass

spectrometer does not become contaminated. For instance, eluents containing conventional ion pair reagents such as involatile tetrabutylammonium salts can seriously contaminate a mass spectrometer leading to a significant background peak at m/z 242. As a result, the mass spectrometer often requires an extensive cleaning procedure of steam wash (50:50 IPA/H₂O, 0.1 % formic acid) for up to 48 hours. Another disadvantage of tetraalkylammonium salts is their tendency to form cluster ions with anionic analytes, which can reduce sensitivity of IC-MS applications when using single ion monitoring (SIM). These ion pairs are not separated and detected by MS and give rise to the term *ion suppression*, which is the observed reduction in sensitivity and is based on eluent composition. As a result, more volatile ion pair reagents are required such as triethylamine. The requirement of less conventional and more volatile ion pair reagents for the analysis of polar disinfectant byproducts was shown recently by Takino *et al.* in which three types of ion pair reagent were investigated and will be discussed later [40]. Buffers are traditionally used in eluents for a variety of reasons such as improvement in peak shape or assuring ion formation occurs in solution prior to electrospray formation. Where pH buffering is required, it is important to choose a suitable reagent that will not hinder the electrospray process. For example, when using positive ion mode for the analysis of polar materials such as peptides and proteins, the pH of the eluent should be within the range of 2 – 5 pH units. Generally acetic acid or formic acid are acceptable buffers of choice for this application. It should also be noted that when electrospray ionisation is in the positive mode, the formation of adduct ions generally occurs leading to both sodiated $[M+Na]^+$ and potassiated $[M+K]^+$ forms of the molecular ion, along with the traditional pseudo molecular ion $[M+H]^+$.

The solvent itself plays a major role in high sensitivity measurements. For electrospray to be successful, polar solvents are the best choice. Non-polar solvents such as toluene should be modified with some polar solvent (e.g. 15 % IPA). Pure water, although very polar, does not allow for effective electrospray generation when used in concentrations above 80 % and generally requires secondary organic solvent addition. Appropriate solvents

are methanol, ethanol, *n*-propanol, isopropanol, *t*-butanol and acetonitrile. This is mainly due to their volatility. Pure water has a higher boiling point of 100°C and all the solvents listed above generally perform better simply due to the fact that their boiling points are lower. It is also important to note that very polar analytes will desorb better from less polar solvents. For example, the HAs and oxyhalides are extremely involatile polar analytes and do not desorb well from aqueous solvents. Addition of more than 20 % of an organic solvent like methanol to the eluent will significantly enhance sensitivity for polar solutes. Where an organic component becomes an issue, for example when using electrolytic auto-recycle or external-water mode suppression, solvent may be added via a T-piece post column prior to the electrospray needle to achieve the same result.

A feature of ESI is its sensitivity to changes in concentration and not only to the total quantity of sample injected into the ion source. Sensitivity is reduced when sample is injected at higher flow rates. Generally, for direct infusion, sample injection flow rates should be as low as possible (e.g. 15 $\mu\text{L}/\text{min}$) to maximise sensitivity to trace concentrations of analyte. Unfortunately, when IC separations are necessary, flow rates are required to be higher than that of direct infusion (approximately 400 $\mu\text{L}/\text{min}$), due to chromatographic band broadening effects. To overcome this problem and to successfully couple IC to ESI-MS, the internal diameter of column must be reduced, otherwise the aforementioned addition of a flow splitter before the electrospray needle is necessary. Replacing the standard bore IC column with micro-bore columns requires lower flow rates, a lower volume of IC eluate and increased band concentration of the solute. When flow rates above 500 $\mu\text{L}/\text{min}$ are used, sensitivity is compromised. In addition to this, there have been developments into the design and positioning of the electrospray needle with respect to the capillary face. In a paper by Hiraoka *et al.* the proposed alignment of the needle orthogonal to the ion optic direction offered increased sensitivity at higher flow rates (up to 4 mL/min were reported) by reducing the level of contamination on the face of the sample orifice [41]. Previous designs directed the needle off centre or directly into the sample orifice and thus caused unwanted waste to build up, requiring

regular cleaning and maintenance. Hewlett-Packard (Agilent)/Bruker Daltonics have introduced a design similar to that described by Hiraoka *et al.* and offers an extremely attractive package of LC-UV-MS to the analytical chemist. This design also boasts the option for both atmospheric pressure chemical ionisation (APCI) and ESI as ion sources with in interchangeable chamber on the face of the instrument. This instrument also uses an octopolar lens and an ion trap for mass analysis. A schematic for introduction of sample into this chamber is shown in *Fig. 1.14*.

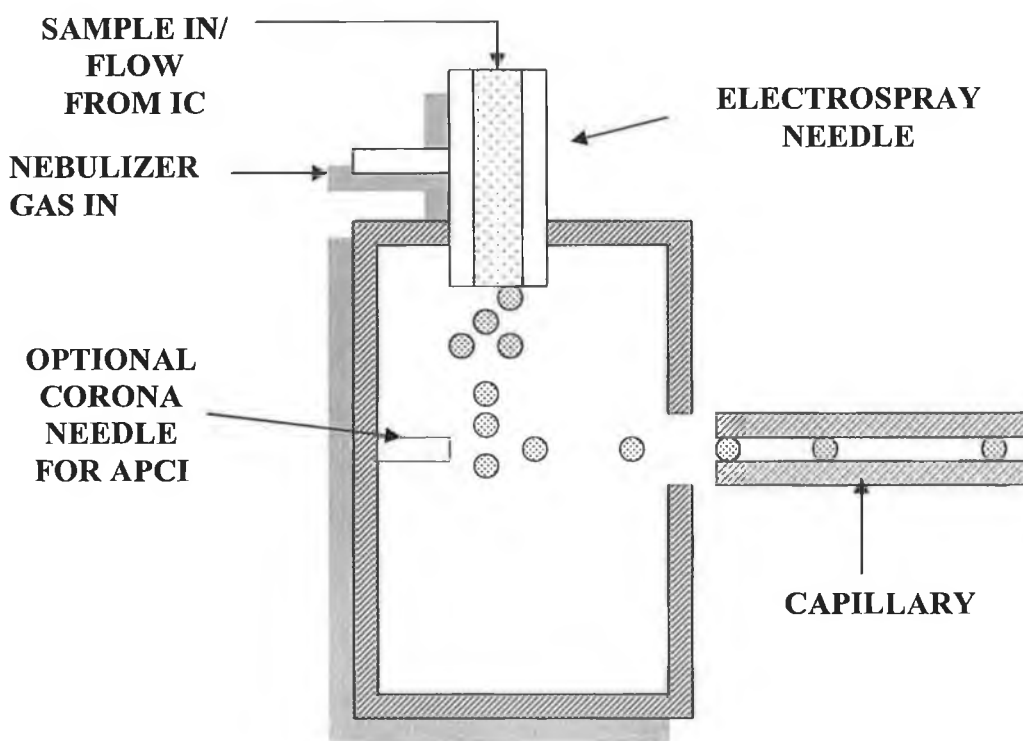


Fig 1.14 Hiraoka and Hewlett-Packard/Bruker Daltonics design schematic for orthogonal sample introduction into ion source [39, 41].

If the separation step involves anion exchange chromatography, generally suppressors are used. Commercially available suppressors such as the Dionex AEES Atlas or ASRS Ultra II offer the best possibilities in

coupling the IC to MS interfaces. As discussed earlier, for hydroxide eluents, the suppressed eluate from the IC is simply a solution of analytes in pure water and more suited to MS detectors. Where carbonate/bicarbonate eluents are used, the highly conducting electrolyte is converted to carbonic acid. These suppressors should be configured in the external water mode as described earlier. In principle, this should lead to increased sensitivity in conductivity detector measurements if also connected in series. The regenerative flow is now a pure solution of water as opposed to a redirected eluate flow of analytes in water, which conducts slightly. Resulting baselines should be quieter from improved suppression.

1.6.3.3.4. The Ion trap mass analyser

Ion trap instruments comprise of a ring electrode surrounded by grounded end-cap electrodes. The overall shape of the ion trap has a hyperbolic structure. This conformation is used for its ability to produce a quadrupolar electric field within which the ions move. A high radio frequency potential ($\Omega = 781$ kHz) is applied to the ring electrode. This RF voltage is the deciding factor on what mass range of ions are retained in the trap. Sample ions enter through an aperture in the centre of the first end-cap and oscillate in the x , y and z planes. However, these ions move within the field in cylindrical symmetry ($x^2 + y^2 = r^2$) and so the overall motion can be described by axial (z) and radial (r) motion. Since the direction of entry is in the axial direction, this is the most significant oscillation. The quadrupolar electric field acts as a pseudo-potential well for analyte ions of a specified mass range and the total oscillation is governed by the RF drive level and the mass to charge ratio on the ion [42].

Movement of ions in the ion trap is governed by the solutions to the second-order linear differential Mathieu equation and is shown in its simplest form in equation 1.27 below, where u is represents the x , y and z coordinate axes, ξ is a dimensionless parameter equivalent to $\Omega t/2$, such that Ω is a frequency and t is time and a_u and q_u represent additional dimensionless parameters, called trapping parameters.

$$\frac{d^2 u}{d\xi^2} + (a_u - 2q_u \cos 2\xi)u = 0$$

Equation 1.27

Moreover, the overall motion of the ions, controlled by the applied RF voltage with angular velocity $\omega=2\pi\nu$, is harmonic oscillation and they do not oscillate at the fundamental frequency (ν) due to their inertia, but at a frequency f lower than ν , called the secular frequency (f_z) given by Equation 1.28 below, where β is a term derived directly from the trapping parameters. It should be noted at this point that a_u and q_u , and thus β , are inversely proportional to the m/z value. Therefore, a lower m/z value results in a higher secular frequency. Furthermore, a gas stream of helium is required to dampen the ion motion, enabling the ions to be trapped more easily [43].

$$f_z = \frac{\beta_z \nu}{2}$$

Equation 1.28

The range of masses that can be simultaneously retained in the ion trap has a lower cut-off limit. It is determined by the RF voltage on the ring electrode and is defined by the mass whose secular frequency is close to one half of that of the RF drive frequency. Theoretically, there should not be an upper cut-off limit, but for thermal and practical purposes there exists a cut off level, which is approximately 20 or 30 times the lower cut off mass value. Ejection from ion trap involves an alteration of the RF amplitude, called an *analytical scan* or *ramp*, over a period of 3-85 ms. Ejection occurs axially through the end-cap electrode in order of increasing m/z ratio.

1.7 Applications of IC to DBP Analysis

We can define IC to include all modes of liquid chromatography (LC) that utilise a charged stationary phase (permanent or dynamic) for the separation of ionic analytes. In recent years, there has been an increased interest in the development of IC to determine trace levels of charged disinfectant by-products in drinking waters. To date, USEPA methods 552.0 and 552.2 have been the standard methods for regulatory analysis of HAs, which both involve a tedious liquid-liquid extraction to methyl tertbutyl ether, followed by esterification with diazomethane and gas chromatographic analysis coupled with either electron capture detection (ECD) [46] or mass spectrometry [47]. Even though these methods require a great deal of sample preparation, they are compensated by low detection limits. An alternative approach, considering that HAs and some other DBPs are ionic in nature, is to separate and detect them by IC, without the requirement for analyte derivitisation. The following is a report of studies carried out on various types of charged DBP using ion chromatographic techniques.

1.7.1 Chloral Hydrate

According to USEPA regulations, the maximum contamination goal and maximum contamination level for chloral hydrate in drinking waters are 40 µg/L and 60 µg/L respectively. Bruzzoniti *et al.* investigated the use of ion chromatography to separate and detect chloral hydrate in drinking waters [48]. Both ion interaction chromatography and ion exchange chromatography were considered and both methods included a derivitisation step. For ion-interaction separations, dansylhydrazine and *o*-(4-nitrobenzyl)hydroxylamine were investigated as possible derivatization reagents, but it was found that 1,2-benzenedithiol with UV detection at 220 nm achieved the best results with a mobile phase of acetonitrile-water (40:60 v/v) and 9 mM NaCl, 6 mM sodium dodecylsulphate, 19 mM HCOOH at pH 3. However, this method offered poor detection limits (>20 mg/L) and so IC was considered as a possible alternative. This method involved derivitisation with sodium hydroxide to form sodium formate, which was separated with an eluent of 2.5

mM NaOH and detected by suppressed conductivity. Results showed that the second method offered lower limits of detection (LODs) and quantitation (0.2 µg/L), well below the regulation limit.

1.7.2 *Oxyhalides of Chloride and Bromide*

Extensive research has been carried out on the oxyhalides of chloride and bromide as disinfectant by-products and new and improved methods for their determination are constantly being developed. As discussed earlier, these DBPs result from ozonation and the addition of chlorine dioxide as an alternative type of disinfection to chlorination. The maximum contamination limits for chlorite and bromate, as proposed by the World Health Organisation (WHO) are 200 µg/L and 0.5 µg/L respectively [49]. The USEPA regulate chlorite less stringently at 1000 µg/L. There is currently no regulation for maximum contamination limits for chlorate as little is known of its toxicity. Such is the concern that bromate causes significant renal tumour counts per capita, that the WHO revised their MCLs from 25 µg/L to the aforementioned 0.5 µg/L at a lifetime risk of 1 in 10⁵. The USEPA regulate bromate in a similar manner, stating that exposure to drinking waters with contaminated levels of bromate at a concentration of 5 µg/L results in a potential cancer risk of 1 in 10⁴ [50]. More recently, the Drinking Water Commission of the European Union (DWCEU) proposed a parametric value of 10 µg/L, connected with a method detection limit of 2.5 µg/L [51]. As a result, the application of new and diverse methods to detect these carcinogens became more abundant in recent years. The most widely used technique for analysis of oxyhalides is IC using various modes of detection. The USEPA first released Method 300.0, which utilised an IC method for determination of bromate in drinking water [52], but achieved inadequate limits of detection (20 µg/L) for regulation monitoring. Drinking water matrices pose a problem for trace DBP determinations by IC using non-analyte specific detection modes like UV and suppressed conductivity. High mg/L concentrations of interferent ions such as chloride, sulphate, carbonate and nitrate often coelute with trace oxyhalides impeding their accurate determination. For example, matrix

chloride in drinking water often coelutes with bromate using eluents of sodium hydroxide with some Dionex IonPac anion exchange columns. Borate eluents aid separation and are employed in earlier methods by Nowack *et al.* and Valsecchi *et al.* [53, 54]. Sensitivities of these methods were increased in two ways. Improvements in column technology allowed the separation of 1.3 µg/L bromate from mg/L concentrations of these commonly interfering anions [55]. Secondly, sample pre-treatment with ISO Method 15061 allowed removal of these anions by solid phase extraction cartridges in the silver, barium and acid forms to achieve a detection limit of 0.5 µg/L [56].

From the literature, it seems best sensitivity for detection of ultra trace levels of bromate using IC is often with some form of post column reaction (PCR), often achieving limits of detection in the sub-µg/L range. In a paper by Achilli *et al.* a carbonate/bicarbonate eluent was allowed to react with a solution of SO_2^- reduced fuchsin and then with dilute HCl at 65°C [57]. The resultant solution was then determined spectrophotometrically at 530 nm for bromate in a drinking water sample. The method boasted detection limits of 0.1 µg/L and was virtually free from interference from other higher concentration anions. The use of 3,3-dimethoxybenzidine (ODA, *o*-dianisidine) has been used quite effectively by Divjak *et al.* [58] and Wagner *et al.* [59, 60] for the analysis of bromate in sub-µg/L levels when used with UV detection and has been used as a standard method for determination of bromate in USEPA Method 300.1 [55]. Wagner *et al.* showed that this PCR method showed similar detection limits to another complex *selective anion concentration* (SAC) method and was much simpler to carry out. However, in water disinfected with chlorine dioxide, interference resulting from high levels of chlorite using UV detection was observed. They further went on to successfully determine bromate using this technique by selectively removing this interference by addition of an Fe(II) solution to the sample, converting chlorite to the free chloride ion and converting a quantity of the added Fe(II) to $\text{Fe}(\text{OH})_3$, which could be analysed by argon-plasma atomic emission spectroscopy to determine chlorite levels in the original sample. As a result, bromate, chlorite and chlorate, as well as inorganic bromide could be determined simultaneously and maximum detectable limits (MDLs) of 0.120

$\mu\text{g/L}$ were achieved for bromate [60]. However, although the method is indeed sensitive, the use of a human carcinogen, ODA, may require extra disposal costs once the analysis is completed. In another PCR method utilising ion exchange chromatography with carbonate/bicarbonate eluents, Salhi and von Gunten showed that a PCR with $10\ \mu\text{M}$ ammonium molybdate, $50\ \text{mM H}_2\text{SO}_4$ and $0.26\ \text{M}$ potassium iodide led to lower detection limits than the USEPA method at $0.1\ \mu\text{g/L}$ [61]. The method involved measuring a triiodide species at $352\ \text{nm}$. This method also was applied to the determination of nitrite at $0.5\ \mu\text{g/L}$ and bromide at $3\ \mu\text{g/L}$. Other PCR methods include those carried out by Delcomyn and Weinberg *et al.* in which bromate was determined by formation of a tribromide ion by PCR with nitrous acid and sodium bromide and detected using UV at $267\ \text{nm}$ [62]. Detection limits for this method were surprisingly low at $10\ \text{ng/L}$ and also offered excellent independence from interferent species such as sulphate, chloride, phosphate and nitrate. In a study by Echigo *et al.* the works of Weinberg, Salhi and Wagner were compared and contrasted [63]. In their study, the results agreed with the order of sensitivity of the three methods, i.e. the NaBr- NaNO_2 method (BrO_3^- MDL: $0.17\ \mu\text{g/L}$) was more sensitive than the $\text{KI}-(\text{NH}_4)_7\text{Mo}_7\text{O}_{24}$ method (BrO_3^- MDL: $0.19\ \mu\text{g/L}$), which in turn was more sensitive than the *o*-dianisidine method (BrO_3^- MDL: $0.24\ \mu\text{g/L}$). However, even though the reported MDLs differed very little from each other, they did differ from the results reported by each individual researcher, especially the Delcomyn and Weinberg method, which differed by roughly a factor of 20. The results reported by Echigo *et al.* suggest that each of the three methods was capable of detecting bromate at a level of $0.5\ \mu\text{g/L}$, the $1\ \text{in}\ 10^5$ cancer risk level proposed by both the WHO and the USEPA. Echigo and co-workers concluded that the *o*-dianisidine method was to be their method of choice for its simplicity. They reported that the NaBr- NaNO_2 was subject to interference when analysing real samples at the lower wavelength and was too complicated to set up. The method also utilised a suppressor to convert the NaNO_2 to nitrous acid.

Conductivity detection has long been the choice of many analysts due to its simplicity and cost effectiveness compared with other detection

techniques. Jackson *et al.* showed the use of direct conductivity detection with no sample pre-treatment or use of PCR for the determination of oxyhalides [64]. The separations carried out used standard-bore Dionex AS-9SC and AS9-HC analytical columns and their respective guard columns at a flow rate of 1.0 mL/min. Suppression was carried out in the external water mode with a Dionex ASRS Ultra II suppressor at 100 mA and 8 mL/min regenerant flow rate. Limits of detection for the method were quite good for direct injection. For regulated oxyhalides chlorite and bromate, their MDLs were 2.38 and 1.73 $\mu\text{g/L}$ respectively. In a recent paper by Bose *et al.*, the application of new suppressor technology reduced detection limits much further [65]. This disposable suppressor cartridge achieved suppression of carbonate/bicarbonate eluents and also boasted removal of carbonate from the eluent, similar to that of the Dionex continuously regenerating anion trap column (CR-ATC). This suppressor, however, had no regenerant flow and was connected in series with the flow of eluent and expired quite quickly (from 4 – 16 hours lifetime) and as a result, long-term unattended analysis was not possible. Detection limits for chlorite and bromate were 1.36 and 0.59 $\mu\text{g/L}$ without any sample pre-treatment or chloride and sulphate removal. It should be noted that these two conductivity detection methods used a 200 μL loop for detection limit studies. Even with all the PCR methods, high loop volumes seem to be of crucial importance to the sensitivity of the method, often using up to 1.5 mL injection volumes [54]. In a more recent paper, Liu *et al.* displayed such large volume loop injection [66]. The use of a 500 μL loop for the determination of bromate and HAs in bottled water meant that trace levels of bromate at 60 ng/L could be determined. However, this method did involve a ten-fold preconcentration step, so the reported direct injection detection limits were at a similar level to that of Bose *et al.* taking into account the % recovery for bromate as 93 % in the preconcentration step. In a previous paper by Liu *et al.*, the same procedure was applied to the determination of oxyhalides in drinking water samples [67]. In this method, the researchers used a twenty-fold preconcentration step and the suppressor was an ASRS Ultra II suppressor with a hydroxide eluent. The detection limits for bromate, perchlorate, iodate and chlorate were 0.1, 0.2, 0.1 and 0.2 $\mu\text{g/L}$, respectively, which, when preconcentration factors are taken into account, was not as

sensitive as the other method which used a Dionex Atlas suppressor. Liu later went on to show the superiority of the monolithic-type Atlas suppressor to the membrane-based Ultra II suppressor in the determination of trace HAs in drinking water [68].

Alongside the development of these PCR and conductimetric methods, researchers assessed the possibility of coupling IC systems to mass spectrometry as an unambiguous method for determination of oxyhalides. Interferences due to inorganic anions present in drinking water were reduced with the possibility for *single ion monitoring* (SIM). However, as discussed earlier, problems arose with eluent composition, as mass spectrometers are extremely sensitive to strong eluents, especially if they comprise of sodium salts. Ammonium carbonate eluents were employed to allow detection of oxyhalides without significant interference [58]. In a study by Charles *et al.*, the assessment of eluent type concluded that ammonium nitrate in methanol:water (9:1) showed adequate separation to allow electrospray mass spectrometric detection of bromate, chlorite, chlorate and iodate [69]. Ions were visible as their molecular ions $[M]^-$ and subsequent fragments consisting of $[M-nO]^-$, where n represents the number of oxygen atoms removed as part of the fragment. The chromatograms were not acquired in SIM mode, but as mass intervals to include all isotopic masses present. The method showed excellent sensitivity for bromate and chlorate at 50 ng/L, measured over a mass to charge range 111-127 and 67-83 m/z units respectively. Sensitivities for chlorite and iodate were slightly less at 1.0 and 0.5 $\mu\text{g/L}$ over mass intervals of 51-67 and 159-175 m/z units respectively. Hydroxide eluents were also used in conjunction with suppressors to convert the IC eluate to water as well as removing sodium ions. The suitability of hydroxide as an eluent combined with suppression allowed the use of up to 100 mM hydroxide without fear of contamination of the mass spectrometer. However, these methods were not as sensitive as others and detection limits were in the 0.1 – 0.2 μM range [70,71]. The probable reason for this was the pure aqueous nature of the eluent as opposed to the method proposed by Charles *et al.* which showed an almost 100 % increase in sensitivity for all species when increasing proportions of methanol were used in the eluent. Electrolytic

suppressors utilising applied currents are generally not compatible with organic solvents and can only be added via post-column T-pieces as discussed earlier. As a result however, overall flow rate to the MS increases and sensitivity reaches a plateau, then decreases once it exceeds approximately 0.5 mL/min. However, Seubert *et al.* demonstrated the use of a Metrohm MSM 753 suppressor with a carbonate eluent containing 10 % acetonitrile at pH 11.3 [72]. The researchers later went on to compare IC with atmospheric pressure ionisation-mass spectrometry (API-MS) or inductively coupled plasma-mass spectrometry (ICP-MS), the latter requiring no suppressor. The comparison of the two methods was based on (1) accuracy and precision, (2) chromatographic requirements and (3) limit of detection. The eluent used with the IC-ICP-MS method was similar to that of Charles *et al.* It was found that both detectors showed acceptable agreement with each other on the measurement of a series of standards from 2-10 µg/L, with a tendency for the ICP-MS to measure slightly higher values than the API-MS detector. The standard deviations for the API-MS detector were far better than for the ICP-MS and the researchers assumed the reason for this being the plasma source causing high levels of noise. On the other hand, the limits of detection with the ICP-MS were roughly a factor of ten better at 60 ng/L for bromate. The ICP-MS also showed that the throughput using their IC-ICP-MS system was double that of the IC-API-MS method. In a recent paper by Eickhorst *et al.* IC-ICP-MS was used as the detection mode for the analysis of bromate and iodate [73]. The use of germanium dioxide as an internal standard improved external calibration and also lent application to semiquantitative analysis of bromate, bromide, iodide and iodate without any calibration procedure. According to Eickhorst *et al.*, the criteria for a suitable internal standard for ICP-MS included no interaction with IC stationary phases, a mass similar to that of the analytes (i.e. first ionisation energy) and at least one interference free peak in the mass spectrum that could be continuously monitored. By adding it to the eluent, a constant signal was produced and currents could be read at any point in the chromatogram, which was applied to internal standard correction, real time calibration and monitoring system performance. Baseline drift, pump failure, spray chamber drainage problems, electronic spikes and problems associated with clogging,

nebulizer stoppage and MS overheating could be monitored in real time. In addition, impressive detection limits of 66 and 45 ng/L were achieved for bromate and iodate respectively.

Many researchers have carried out comparisons between all these various approaches to oxyhalide analysis. Seubert *et al.* furthered their research from that just discussed to compare IC-PCR, IC with conductivity detection and IC-ICP-MS techniques for the analysis of oxyhalides [74]. They concluded that IC with conductivity detection was not a suitable method compared with PCR and ICP-MS, as its sensitivity was poorer, as well as the fact that all samples required some form of sample pre-treatment for removal of chloride and sulphate. The other two showed very little interference from these anions. The IC-ICP-MS method showed the best ruggedness and sensitivity, but the IC-PCR offered the most information. Yamanaka *et al.* also compared the use of PCR and ICP-MS [75]. Using an eluent of ammonium carbonate, they allowed it to react in a similar way to the method proposed by Delcomyn and Weinberg *et al.* and was passed through a UV detector at 268 nm. For ICP-MS detection, the detection limits were 0.45 and 0.034 µg/L for bromate and iodate respectively. When applied to three ozonised water samples, both methods showed excellent agreement with each other and levels of bromate were quantified from 1.87 µg/L to 13.0 µg/L. More recently in work published by Ingrand *et al.*, laboratory methods were developed using a wide spectrum of techniques for the analysis of bromate [76]. They first assessed the problems associated with conductimetric detection. Many methods, as previously described, utilise some form of cleanup procedure. In order to tackle the cumbersome nature of these methods, this group automated the cleanup step using two injector valves and managed to better the existing automated USEPA method. However, the LODs were similar to samples that were manually cleaned using solid phase extraction cartridges and injected subsequently onto the IC. This group went on further to investigate other methods for bromate determination in detail. These include IC-ICP-MS, IC-PCR with chlorpromazine, flow injection-ICP-MS and ion pair-fluorescence (IP-Fluo). In the case of the IP-Fluo method, detection limits for bromate were similar to the conductimetric method (1.6

µg/L), but all others achieved better sensitivity with detection limits between 0.1-0.3 µg/L. Most interestingly, this group went on further to develop a field method for bromate analysis. This method involved allowing a sample to react with methylene blue under acidic conditions with indirect spectrophotometric detection. Remarkably, this field method allowed bromate determinations in the range 4- 50 µg/L.

In a paper by Biesaga *et al.*, the merits of IC and CE were applied to the determination of chlorinated oxyhalides [77]. In the case of chlorite and chlorate, the detection limits were lower than that of CE at 0.18 and 0.15 µg/L. However, for the analysis of perchlorate, the detection limits for CE were twice as sensitive as the ion chromatographic method at 0.6 µg/L. Perchlorate is not an oxyhalide associated with disinfection of drinking water, but used in solid rocket motors and is a known endocrine disruptor. The ion chromatographic method here utilised a phthalate eluent with indirect UV detection at 254 nm. In a similar study using phthalate eluents and indirect UV detection at 279 nm, Connolly *et al.* tackled the time consuming nature of these separations and achieved a separation of nine common inorganic anions, including bromate, in under 160 seconds using a didodecyldimethylammonium bromide (DDAB) coated octadecyl silica (ODS) analytical column [78]. However, detection limits were in the mid µg/L range and in a European context, was not sensitive to the 2.5 µg/L detection limit stipulation.

So to date, IC with ICP-MS or IC-PCR offer the most promising results for bromate analysis in particular. As it has the lower regulation limit, one would expect to set a target MDL of 0.5 µg/L for bromate as the benchmark expectation for sensitivity of the detector of choice with new IC based methods. Only with improvements in sensitivity, combining new suppressor and column technology, can the relatively simple and cost effective conductimetric methods offer themselves to the routine analysis of bromate in drinking water.

1.7.3 Application of IC to the determination of HAs

It is possible to separate and detect HAs by various forms of IC, and this section will detail work involving ion exchange chromatography, ion interaction chromatography and ion exclusion chromatography. Detection with each of the above is generally either based on direct UV/Vis absorbance or suppressed conductivity. More recently ESI-MS and ICP-MS have been successfully applied to the detection of HAs following IC separation and these will be dealt with separately.

1.7.3.1 Ion-interaction chromatography

Certain HAs show retention on reversed-phase columns without the use of an ion-interaction reagent (IIR) [79]. However, to obtain acceptable resolution of each HA and common matrix anions, the use of a suitable IIR is essential. Early work in this area was carried out by Vichot and Furton [80], who developed an ion-interaction method coupled with indirect UV detection. More recently, Sarzanini *et al.* [81] developed and compared two ion-interaction methods for the separation of HAs. The first method involved the use of tetrabutylammonium chloride (TBACl) as the ion-interaction reagent used within a MeOH/water mobile phase. The second method developed used cetyltrimethylammonium chloride (CTACl) as the IIR, this time within a MeCN/water mobile phase. Both methods used a 25 cm ODS column and direct UV absorbance at 210 nm. With the CTACl method, the concentration of the IIR required was < 10 times that of the TBACl method, due to a much higher degree of hydrophobicity of the IIR. Both methods, under optimal conditions were able to separate MBA, DCA, DBA and TCA in under 20 mins (MCA not shown). However, when the above HAs were spiked into tap water (at high levels of between 25 and 30 mg/L), NO₃⁻ interfered with MBA and overall detector sensitivity was insufficient making the methods on their own unsuitable for real sample analysis.

Takino *et al.* [40] investigated the use of a number of volatile aliphatic amines as IIRs for the separation of HAs. The volatile nature of the IIR was necessary to allow ESI-MS be used for detection, as discussed below. The IIRs investigated were dimethylbutylamine (DMBA), dibutylamine (DBuA) and tributylamine (TBuA). Gradient elution methods were developed by Takino *et al.* for each of the above IIRs, with the mobile phase containing 5 mM of IIR and increasing from 10 % to 50 % MeCN over 20 min. The separations were carried out on a 15 cm micro-bore ODS column, with the DBuA method resulting in the baseline separation of all nine HAs in under 14 min. In a more recent study, Loos and Barcelo [82] used triethylamine (TEA) as an IIR, again at 5 mM concentration, with a MeCN gradient of 15-50 % over 12 min. On a standard 250 x 4 mm ODS column, only partial separation of the HAs was achieved using this method, although the use of ESI-MS detection in single ion monitoring (SIM) mode allowed the quantification of individual HAs.

1.7.3.2 Ion exchange chromatography

Nair *et al.* [83] were among the first to highlight the potential of IC, using anion exchange in combination with suppressed conductivity detection for the monitoring of HAs in drinking water. Although detection limits using a $\text{Na}_2\text{CO}_3/\text{NaHCO}_3$ eluent were less than those obtainable using the standard GC-ECD method, reasonable separations were possible. However, in this work, MCA and MBA were found to co-elute and tribromoacetic acid (TBA) was not shown.

A much more complex (and much more sensitive) IC based method was developed later by Lopez-Avila *et al.* [84]. This method combined a multi-step solvent micro-extraction procedure (mentioned earlier), an on-line anion concentrator column, upon which the total extract from the micro-extraction was loaded, and a 12 stage gradient elution program over 60 min. The method employed a 25 cm micro-bore Dionex AS11 separator column with a NaOH eluent and suppression using a 2 mm anion self-regenerating suppressor module (ASRS, Dionex). Perhaps not surprisingly, the multi-step gradient resulted in impressive resolution of the 9 HAs and common anions

and detection limits for the 9 HAs, based upon 60 mL sample volumes, were between 0.05 and 1.1 µg/L.

Sarzanini *et al.* [81] evaluated and compared two anion exchange columns and various eluents for the isocratic separation of HAs and common anions, specifically Dionex AS9 and AS11 columns with NaOH or Na₂CO₃/NaHCO₃ eluents. Using both of the above eluents in turn, Sarzanini *et al.* found resolution of MBA and Cl⁻ and DCA and NO₃⁻ was poor with the AS11 column. With the AS9 column resolution of the above species was somewhat improved. Using a 0.3 mM carbonate/bicarbonate (3:1) eluent the separation of 5 HAs, Cl⁻ and NO₃⁻ in spiked (500 µg/L each) and preconcentrated (10 fold) tap water was shown (SO₄²⁻ peak not included in chromatogram shown).

Most recently, Liu *et al.* [85] has attempted to improve detection limits of a suppressed anion exchange method (Na₂CO₃/NaHCO₃ gradient) through the use of a high capacity column (AS9-HC) and the direct injection of up to 500 µL of sample. In standard solutions detection limits for all 9 HAs were in the range 0.4 to 32 µg/L. In the analysis of real samples, matrix anions caused problems with the quantification of several HAs and the samples required a clean-up stage using On-Guard Ag cartridges to lower chloride, bromide and phosphate levels prior to sample analysis. This study showed the results from the analysis of several treated water samples, within which traces of DCA, BCA, DBA and TCA could be identified.

1.7.3.3 Ion-exclusion chromatography

Ion-exclusion chromatography has long since been a popular choice for the separation of weak hydrophilic carboxylic acids. Stationary phases of highly sulphonated PS-DVB in the H⁺ form are commonly used with dilute solutions of sulphuric acid and hydrochloric acid as eluents. Such conditions often result in peak tailing for hydrophobic carboxylic acids, but hydrophilic acid peak shapes are relatively sharp [86, 87]. However, the use of strong

acid eluents reduces the sensitivity of conductimetric detection for weak acid analytes, including HAs.

In an attempt to solve this problem, Tanaka *et al.* proposed a novel method called vacancy ion-exclusion chromatography [88, 89] and applied it to the separation and detection of HAs [90]. Vacancy ion-exclusion uses a solution of the analyte anions or the sample itself as the eluent. Injections of pure water result in 'vacancy' peaks at retention times matching those of the acids contained within the mobile phase solution or sample. Although the exact retention mechanism for this vacancy ion chromatographic method is not completely explained within these papers, the actual separations achieved (for standard solutions) were impressive. However, it was not clear how such a technique could be applied to real samples and so more work is required for this technique to be practical.

1.7.3.4 IC-ESI-MS

The development of ESI-MS has meant an alternative sensitive and selective method of detecting HAs is now available. The simplicity of ion chromatography as a separation step for the HAs, (requiring no sample derivitisation), combined with the selectivity and sensitivity of ESI-MS detection potentially makes IC-MS an ideal approach to the determination of trace HAs in drinking water. For IC-ESI-MS work, low flow rates must be used, with eluents consisting of only volatile species. Therefore, conventional standard bore IC columns cannot be used due to excessive band broadening. Micro-bore IC columns are now available from most IC manufacturers and can be run at flow rates of less than 0.5 mL/min, which approximately corresponds to the maximum flow rate for ESI-MS before sensitivity is compromised.

As mentioned above, ion-interaction chromatography has been used with ESI-MS by a number of groups and has shown some promising results. Takino *et al.*, who work with DMBA, DBuA and TBuA as IIRs [40], showed that an increase in chain length offered longer retention but also more

importantly reduced contamination of the mass spectrometer and hence proposed TBUA as an ideal IIR for this type of detection. Loos *et al.* supported this hypothesis and suggested the use of the TEA as the IIR [82]. Using negative ESI mode and a mobile phase flow rate of 0.5 mL/min, optimised detector conditions for the HAs were as follows; Drying gas flow – 11 L/min; Drying gas temp – 350 °C; Nebuliser pressure – 55 p.s.i.; Vaporiser temperature – 400 °C; Capillary potential – 5000 V; Fragmentation potential – 40 V. HAs were observed in ESI-MS under the above conditions as their pseudo molecular ions $[M - H]^-$, their decarboxylated form $[M - COOH]^-$ and in a dimer form $[2M - H]^-$. A list of m/z values for these ions is shown in *Table 1.4*.

Table 1.4 Observed/measured ions (m/z) for HAs using ESI-MS. Most abundant ions for each HA are highlighted in bold.

HA	$[M - H]^-$	$[M - COOH]^-$	$[2M - H]^-$
MCA	93		187
DCA	127, 129		257
TCA	163	117	
MBA	137, 139		277
DBA	217	173	435
TBA	295	251, 253	
BCA	173		345
CDBA	251	207	
DCBA	207	163	

Roehl *et al.* [71] proposed a method using anion exchange chromatography (Dionex AS16, 2 mm I.D. column) with a gradient of 5 – 70 mM NaOH at a flow rate of 0.25 mL/min with eluent suppression. It is important to note that HAs are non-volatile organic compounds. After suppression, the eluate comprises of a very dilute solution of HAs in water. This solution does not allow complete volatilisation of the analyte ions at the electrospray nozzle and results in a poor signal from the MS. To overcome this problem a secondary pump is required that delivers a volatile organic

solvent such as methanol through a T-junction before the MS that acts to improve sample volatilisation and subsequent sensitivity. Post separation introduction of an organic solvent was also shown to improve sensitivity by Takino *et al.* [40].

1.7.3.5 IC-ICP-MS

In the very latest application of IC to the determination of HAs, Liu *et al.* [92] have utilised ICP-MS as a highly sensitive and selective detection system. The study used suppressed IC with a hydrophilic anion exchange column and a steep gradient of NaOH (flow rate = 1 mL/min), coupled on-line with the ICP-MS. The detector was used to selectively monitor ^{35}ClO ions for chlorinated HAs and ^{79}Br for brominated species (dominant ions formed within the plasma). Detection limits between 16 and 24 $\mu\text{g/L}$ for the chlorinated acids and 0.3 and 1 $\mu\text{g/L}$ for the brominated acids were quoted based upon an injection volume of 150 μL . For application to actual drinking water samples reduction of chloride was required and carried out using Dionex OnGuard Ag cartridges prior to injection.

Table 1.5 summarises how the above IC-ESI-MS and IC-ICP-MS based methods compare with the other IC methods discussed within this review. The table shows the type of separation method, eluent conditions, mode of detection and detection limits with preconcentration details if used.

Table 1.5 Ion chromatographic methods for HAs, separation and detection conditions and detection limits.

Separation mode (column)	Eluent	Detection mode	Detection limits (conditions)	Ref.
Anion exchange (IonPac AS11)	NaOH gradient	Suppressed conductivity	0.45 – 1.10 µg/L (60 mL preconcentrated to 6 mL by microextraction, followed by 5 mL injection onto anion trap column IonPac TAC-LP)	84
Anion exchange (IonPac AS9HC)	Na ₂ CO ₃ isocratic	Suppressed conductivity	0.06 – 0.85 µg/L (10 fold preconcentrated using microwave evaporation, 500 µL injection volume)	66
Anion exchange (IonPac AS9)	Na ₂ CO ₃ /NaHCO ₃ isocratic	Suppressed conductivity	25 – 207 µg/L (100 µL injection volume)	81
Anion exchange (Alltech Universal Anion 300)	Na ₂ CO ₃ /NaHCO ₃ isocratic	Suppressed conductivity	8 – 80 µg/L (100 µL injection volume)	83
Anion exchange (IonPac AS16)	NaOH gradient	Eluent suppression / ICP-MS	0.34 – 24 µg/L (150 µL injection volume)	92
Ion interaction (LiChrospher RP-18)	50 % MeOH, 50 mM TBACl, pH 5.0	UV absorbance at 210 nm	1.5 – 30 mg/L (100 µL injection volume)	81
Ion interaction (LiChrospher RP-18)	MeCN gradient, 5 mM TEA, 5 mM acetic acid	ESI-MS	0.2 – 1.6 µg/L (166 fold enrichment by SPE)	82
Ion interaction (Inertsil ODS3)	MeCN gradient, 5 mM DBA	ESI-MS	0.02 – 0.12 µg/L (500 µL injection volume)	40
Vacancy exclusion (TSKgel OApak-A)	500 µM DCA, MCA and TCA, pH 3.17, 1 % butanol	Conductivity	0.15 – 3.4 µM (500 µL injection volume)	90

1.7.4 Preconcentration methods for HAs

In order to analyse trace levels of HAs in drinking and potable waters by most current methods, including IC, it is necessary to employ a preconcentration step and therefore the preconcentration of HAs is also briefly discussed here. A number of preconcentration techniques have been investigated for the HAs and current USEPA method 552 incorporates solvent extraction using MTBE and an acidified sample solution. Method 552.2 also uses MTBE solvent extraction but includes a back extraction procedure into sodium hydrogen carbonate solution following a derivitisation step. Both these extraction methods were developed with analysis using GC in mind.

Some efforts have been made to modify solvent extraction methods for improved compatibility with IC. Lopez-Avila *et al.* [84] modified a micro-extraction procedure specified within Standard Method 6233B of the American Public Health Association. The modified procedure was based upon the extraction of aqueous samples (acidified to pH <0.5 and amended with copper sulphate pentahydrate and sodium sulphate) with MTBE, and subsequent back extraction into reagent water. However, this modified procedure gave highly variable % recoveries from spiked drinking water samples, particularly recoveries for spikes within the low µg/L range (<30 % in several cases). In addition, the whole extraction procedure was rather complex and convoluted, including long periods of mixing and centrifugation, in total, well over 1 hour preparation time per sample was required. In more recent work by Liu *et al.* [66, 93], a microwave evaporation preconcentration method was developed. From initial observations of this work recoveries appear excellent at >90 % for MCA, DCA and TCA. However, upon closer inspection it becomes clear that these data were obtained for spiked samples at relatively high concentrations, up to 0.2 mg/L, approximately 100 times greater than the spikes used by Avila *et al.* to calculate their recovery data [84]. In addition, this method resulted in no reduction in the concentration of residual inorganic anions, meaning high chloride, nitrate and sulphate levels caused problems in the subsequent separation step. The degradation of certain HAs at high temperatures suggested by Dojlido *et al.* [21] was said to

be overcome through adjustment of the sample to >pH 10, although the exact reasons for this are unclear. Without such adjustment, recoveries for DCA and TCA at pH 8 were as low as 30 to 40 %.

1.7.4.1 *Solid phase extraction (SPE)*

Solid phase extraction (SPE) has continuously gained in popularity since commercially available silica-based chemically bonded phases appeared somewhere around the mid 1970s. These silica-based sorbents have dominated SPE and have proven very successful. More recently, polymeric phases have gained in popularity due to their greater compatibility to highly acidic or basic solutions. For reasons of cost, practicality, safety and the inability to be used 'on-line', traditional solvent extraction methods are, where possible, being replaced with SPE. An obvious example of this is the USEPA method 552.1, which replaces solvent extraction with SPE using anion-exchange phases for the extraction and preconcentration of HAs.

1.7.4.1.1 *Problems with SPE*

There are several fundamental problems associated with SPE as a preconcentration technique, a number of which are particularly pertinent to the extraction and preconcentration of HAs from drinking water. Firstly, SPE in most instances can be regarded as, at best, a 'semi-selective' technique. This means sample matrix will always affect analyte recoveries to some extent, as components of the sample will have some degree of affinity, however small, for the stationary phase used. For example, using ion-exchange resins will see matrix ions competing for stationary phase sites and when using reversed-phase substrates, neutral species within the sample will also compete for retention. Secondly, by its very nature SPE is capacity dependant. Cartridges used will have a finite capacity for analytes under specific sample conditions. This often means that recoveries vary with sample load volume, analyte concentration and also sample load rate (details of which are often missing from papers discussing sample preparation using SPE). Finally, there exists the problem of analyte recovery. It is clear that the

higher the affinity of the analyte for a particular stationary phase, the more difficult it will be to obtain quantitative recovery of that analyte from that phase. Further to the above, there exist the physical problems associated with SPE such as contamination, blocking, channelling and dissolution.

The first of the above fundamental problems is ideally illustrated by USEPA method 552.1, which by using anion exchange based SPE sees the sample matrix play a role in analyte recoveries, as relatively high concentrations of matrix anions, such as chloride, nitrate and sulphate, compete for ion exchange sites within the stationary phase.

1.7.4.1.2 Comparison of stationary phases

Martinez *et al.* carried out a study on four commercially available SPE cartridges for the extraction and preconcentration of HAs [94]. The four sorbents investigated were a strong quaternary ammonium anion exchanger (LC-SAX), a hyper cross-linked polymer of polystyrene-divinylbenzene (EVB-DVB) (LiChrolut EN), a graphitised carbon black (Envi-Carb) and a macroporous poly(divinylbenzene-co-N-vinylpyrrolidone) copolymer (Oasis HLB). With the latter three phases, samples were adjusted to pH 0.5 to ensure HAs were extracted in protonated form (see Table 1.6 for pK_a values). The work proved to be a useful comparison of these phases, but unfortunately was carried out on simple standard solutions and not actual drinking water samples, limiting its applicability. The study showed that the hyper-cross-linked EVB-DVB phase (LiChrolut EN) resulted in the highest % recoveries, between 91 and 104 % for MCA, DCA and TCA, and 64 and 84 % for MBA and DBA respectively (25 mL sample volume). Increasing sample volume further saw substantial reductions in these recovery data.

Table 1.6 Haloacetic acids (HAs) and known pK_a values

HA	Abbreviation	Chemical formula	pK_a [Ref]	Boiling point
Monochloro-acetic acid	MCA	$ClCH_2CO_2H$	2.86 ^[91]	187.8
Dichloro-acetic acid	DCA	Cl_2CHCO_2H	1.25 ^[90] 1.29 ^[91] 1.30 ^[81]	194
Trichloro-acetic acid	TCA	Cl_3CCO_2H	0.63 ^[90] 0.65 ^[91] 0.7 ^[81]	197.5
Monobromo-acetic acid	MBA	$BrCH_2CO_2H$	2.87 ^[81] 2.86 ^[82] 2.7 ^[91]	208
Dibromo-acetic acid	DBA	Br_2CHCO_2H	1.47 ^[95]	195
Tribromo-acetic acid	TBA	Br_3CCO_2H	0.66 ^[91]	245
Bromochloro-acetic acid	BCA	$BrClCHCO_2H$	1.39 ^[95]	103.5
Dibromochloro-acetic acid	CDBA	Br_2ClCCO_2H	1.09 ^[95]	—
Dichlorobromo-acetic acid	DCBA	Cl_2BrCCO_2H	1.09 ^[95]	—

The above LiChrolut EN phase has also been applied to HA extraction in two similar studies carried out by Loos and Barcelo [82] and Sarzanini *et al.* [81]. The variability in the recovery data reported for HAs in these three studies is summarised in *Table 1.7*. It is clear from *Table 1.7* that substantial differences in recovery data can be obtained dependent upon the exact conditions used. Sarzanini *et al.* [81] also briefly investigated preconcentration of HAs on activated carbon. However, under the conditions used, recoveries were insufficient and evidence was presented of incomplete elution of DBA, TCA and TBA using MeOH.

1.7.4.1.3 Interference elimination

As mentioned briefly above, the use of various preconcentration methods for HAs often produces a concentrated sample that contains a high

concentration of matrix anions, which may interfere with the determination of target HAs in the following IC analysis. This may be a result of these anions being present in high concentrations in the original sample and they have not been eliminated during the preconcentration procedure, or they may result from a sample pre-treatment step such as sample acidification. With drinking water samples, these matrix anions are generally chloride and sulphate (and to a lesser extent nitrate). The reduction/removal of these anions from the concentrated sample can be achieved using treatment with cation exchange SPE cartridges in the Ag form, for the selective removal of chloride [81, 85], or in the Ba form, for the removal of excess sulphate. However, it is recommended that following the use of a Ag cartridge clean-up step, a cation exchange SPE cartridge in the acid form (H^+) be used to remove any Ag ions which may have bled from the Ag SPE cartridge into the sample extract, and which could form precipitates in the sample solution and eventually foul the analytical column.

Table 1.7 Variation in recovery data for HAs on LiChrolut EN SPE cartridges

HA	Sample matrix	Sample pH ^a	HA concentration (mg/L)	Sample volume (mL)	Number of replicates (n)	% Recovery (± %RSD)	Ref.
MCA	Standard	0.5	0.2	25	4	91(<12)	94
MCA	Ground water	1.8	0.3	50	4	26(3)	82
MCA	Groundwater	1.8	0.03	50	4	35(8)	82
MBA	Standard	0.5	0.2	25	4	65(<12)	94
MBA	Groundwater	1.8	0.2	50	4	42(6)	82
MBA	Groundwater	1.8	0.02	50	4	51(9)	82
MBA	Tap water	1.0	0.05	100	3	80.3(8.4)	81
DCA	Standard	0.5	0.2	25	4	104(<12)	94
DCA	Groundwater	1.8	0.3	50	4	55(5)	82
DCA	Groundwater	1.8	0.03	50	4	45(12)	82
DCA	Tap water	1.0	0.05	100	3	83.7(13)	81
DBA	Standard	0.5	0.2	25	4	85(<12)	94
DBA	Groundwater	1.8	0.1	50	4	56(7)	82
DBA	Groundwater	1.8	0.01	50	4	48(9)	82
DBA	Tap water	1.0	0.05	100	3	73.1(13)	81
TCA	Standard	0.5	0.2	25	4	101(<12)	94
TCA	Groundwater	1.8	0.1	50	4	75(5)	82
TCA	Groundwater	1.8	0.01	50	4	69(8)	82
TCA	Tap water	1.0	0.05	100	3	81.8(11)	81
TBA	Groundwater	1.8	1.0	50	4	33(2)	82
TBA	Groundwater	1.8	0.1	50	4	39(8)	82
TBA	Tap water	1.0	0.05	100	3	77.7(3)	81

^a Adjusted using sulphuric acid

From compiling this section, a number of trends have become clear. It has been shown in almost every case that currently most IC methods developed require some form of sample preconcentration, combined in many cases with removal/reduction of matrix anions. So far the results obtained show this aspect of the work to be lacking, with recovery data being highly irreproducible. The use of automation and on-line technologies to carryout such sample pre-treatment may provide some progress in this area, although there has been few attempts made in this area to-date. The use of ESI-MS detection appears to be a very promising development. However, there are still only a few papers investigating this approach. With the large number of variables affecting sensitivity with ESI-MS and the incompatibility of ESI-MS with many common IC eluents, it is clear much more work in this area is still required.

1.8 References

1. R. F. Christman, D. L. Norwood, D. S. Millington and J. D. Johnson, *Environmental Science and Technology*, 1983, 17, 625-628.
2. A. D. Nikolau, S. K. Golfinopoulos and T. D. Lekkas, *Journal of Environmental Monitoring*, 2002, 4, 910-916.
3. C.M. Villanueva, M. Kogevinas, J.O. Grimalt, *Water Research*, 2003, 37, 953-958.
4. L. A. Rossman, R. A. Brown, P. C. Singer and J. R. Nuckols, *Water Research*, 2001, 35, No. 4, 3483-3489.
5. A. Ghani, I. Dalvi, R. Al-Rashid and M.A. Javeed, *Desalination*, 2000, 129, 261-271.
6. Stage 1 Disinfectants and Disinfection Byproducts Rule 63 FR 69390 – 69476, December 16, 1998, Vol. 63, No. 241.
7. V. Camel and A Bermond, *Water Research*, 1998, 32, No. 11, 3208-3222.
8. W.R. Hag and J. Hoigné, *Environmental Science and Technology*, 1983, 17, 261-267.
9. W.R. Hag, J. Hoigné and H. Bader, *Water Research*, 1984, 18, 1125-1128.
10. Y. Kurokawa, A. Maekawa, M. Takahashi and Y. Hayashi, *Environ. Hlth. Persp.*, 1990, 87, 309-335.
11. M.J. Kirisits, V. N. Snoeyink, J.C. Kruithof, *Water Research*, 34, (2000), 4250-4260.
12. J.E. Cavanagh, H.S. Weinberg, A. Gold, R. Sangaiah, D. Marbury, W.H. Glaze, T.W. Collette, S.D. Richardson and A.D. Thurston, *Environmental Science and Technology*, 1992, 26, 1658-1662.
13. American Water Works Association, *Chlorine for Water Disinfection*, May 1995.
14. D. A. Reckow, P. C. Singer and R. L. Malcolm, *Environmental Science and Technology*, 1990, 24, No. 11, 1655-1664.
15. D.T. Williams, G.L. LaBel and F. Benoit, *Chemosphere*, 1997, 34, No.2, 299-316.

16. E.E. Chang, Y.P. Lin and P.C. Chiang,
Chemosphere, 2001, 43, 1029-1034.
17. H. Pourmoghaddas and A.A. Stevens,
Water Research, 1995, 29, No. 9, 2059-2062.
18. M.S. Siddiqui, G.L. Amy and B.D. Murphy,
Water Research, 1997, 31, No. 12, 3098-3106.
19. A.A. Kampioti and E.G., Stephanau,
Water Research, 2002, 36, 2596-2606.
20. C.Y. Chang, Journal of Hazardous Materials, 2000, B79, 89-102.
21. J. Dojlido, E. Zbieć and R. Świetlik,
Water Research, 1999, 33, No. 14, 3111-3118.
22. X. Zhang, R. A. Minear, Water Research, 2002, 36, 3665-3673.
23. J. B. Sérodes, M. J. Rodriguez, H. Li, Christian Bouchard,
Chemosphere, 2003, 51, 253-263.
24. J. Kim, Y. Chung, D. Shin, M. Kim, Y. Lee, Y. Lim and D. Lee,
Desalination, 2002, 151, 1-9.
25. D. E. Kimbrough and I.H. Suffet, Water Research, 2002, 36, 4902-4906.
26. A.D. Nickolau, M.N. Kostopoulo and T.D. Lekkas,
Global Nest: the International Journal, 1999, 1, No. 3, 143-156.
27. World Health Organisation, Guidelines for drinking water quality, 1996,
2nd edition, Volume 2, 873-884.
28. World Health Organisation, Guidelines for drinking water quality, 1996,
3rd edition.
www.who.int/docstore/water_sanitation_health/GDWQ/draftchemicals/brominatedaceticacids2003.pdf
29. H. Weinberg, Analytical Chemistry - News and Features, Dec 1, 1999.
30. B. Legube, B. Parinet, K. Gelinet, F. Berne, J.P. Croue, Water Research,
38 (2004), 2185-2195.
31. Journal of Chromatography Library – Volume 51A, 1992.
Chromatography 5th Edition, Part A, "Fundamentals and Applications of
Chromatography and Related Differential Migration Methods".
32. P.R. Haddad and P.E. Jackson, "Ion Chromatography – Principles and
Applications". Journal of Chromatography Library Series– Volume 46,
1990.

33. Chromatographic Science Series – Volume 78, “Handbook of HPLC”, 1998. Edited by E. Klatz, R. Eksteen, P. Schoenmakers and N. Miller.
34. Chromatographic Science Series – Volume 47, “Packings and Stationary Phases in Chromatographic Techniques”, 1990. Edited by K.K. Unger.
35. Ion Chromatography – J.S. Fritz and D. T. Gjerde, 3rd Edition, 1999.
36. Product Manual, “Anion Self-Regenerating Suppressor Ultra”, Document No. 031367, Revision 09, 18th February 2003, Dionex Corporation, Sunnyvale, CA, USA.
37. D.A. Skoog, F.J. Holler, T.A Nieman, “Principles of Instrumental Analysis”, 5th Edition, 1998.
38. N. Penner, P. Nesterenko, Journal of Chromatography A, 884 (2000), 41-51.
39. Bruker – HP Esquire-LC Operations Manual, Version 3.1.
40. M. Takino, S. Daishima, K. Yamaguchi, The Analyst, (2001), 125, 1097-1102.
41. K. Hiroaka and I. Kudaka, Rapid Communications in Mass Spectrometry, 4, No. 12 (1990), 519-526.
42. E. de Hoffmann, Mass Spectrometry: principles and applications, 2nd Edition, Wiley, 2001.
43. R.E. March, Journal of Mass Spectrometry, 32 (1997) 351-369.
44. J.B. Fenn, M. Mann, C.K. Meng, S.F. Wong and C.M. Whitehouse, Science, 246 (1989), 64-71.
45. J.V. Iribarne and B.A. Thompson, Journal of Chem. Phys., 64 (1976), 2237-2294.
46. J.W. Hodgeson, J. Collins, R.E. Barth, EPA Method 552.0, Revision 1.0, Methods for Determination of Organic Compounds, Supplement II, EPA document no. 600-4-88-039, GPO, Washington, DC, 1990.
47. D.J. Munch, J.W. Munch, A.M. Pawlecki, EPA Method 552.2, Revision 1.0, Methods for Determination of Organic Compounds, Supplement III, EPA document no. 600-R-95-131, GPO, Washington, DC, 1995.
48. M.C. Bruzzoniti, E. Mentasti, C. Sarzanini, E Tarasco, Journal of Chromatography A, 920 (2001), 283-289.
49. WHO, Guidelines for drinking water quality, 1996. 2(2): p. 813.

50. USEPA, Disinfectant and disinfection by-products rule: proposed rule. Fed Reg 38709, 1994. 59(145).
51. Council Directive 98/83/EC. Official Journal of the European Communities Legislation, 1998: p. 32.
52. Method 300.0, U.S.E.P.A., EPA/600/R93/100, 1991.
53. B. Nowack, U.v.G., Journal of Chromatography A, 1999. 849: p. 209-215.
54. S. Valsecchi, A.I., S. Polesello, S. Cavelli, Journal of Chromatography A, 1999. 864: p. 263-270.
55. Method 300.1, U.S.E.P.A., EPA/600/R98/188, 1997.
56. ISO, DIS 15061, 1998.
57. M. Achilli, L.R., Journal of Chromatography A, 1999. 847: p. 271-277.
58. B. Divjak, M.N., W. Goessler, Journal of Chromatography A, 1999. 862: p. 39-47.
59. H.P. Wagner, Journal of Chromatography A, 1999. 850(1-2): p. 119-129.
60. H.P. Wagner, B.V.P., D.P. Hautman, D.J. Munch, Journal of Chromatography A, 2000. 882: p. 309-319.
61. E. Salhi, and U. von Gunten, Water Research, 1999. 33(15): p. 3239-3244.
62. C.A. Delcomyn, H.S. Weinberg, and P.C. Singer, Journal of Chromatography A, 2001. 920(1-2): p. 213-219.
63. S. Echigo, R.A. Minear, H. Yamada, P.E. Jackson, Journal of Chromatography A, 2001. 920: p. 205-211.
64. L.K. Jackson, R.J. Joyce, M. Laikhtman, P.E. Jackson, Journal of Chromatography A, 1998. 829(1-2): p. 187-192.
65. R. Bose, R. Saari-Nordhaus, A. Sonaike, D.S. Sethi, Journal of Chromatography A, 2004. 1039(1-2): p. 45-49.
66. Y. Liu and S. Mou, Chemosphere, 2004. 55(9): p. 1253-1258.
67. Y. Liu, S. Mou, and S. Heberling, Journal of Chromatography A, 2002. 956(1-2): p. 85-91.
68. Y. Liu and S. Mou, Journal of Chromatography A, 2003. 997(1-2): p. 225-235.

69. L. Charles, and D. Pepin, *Journal of Chromatography A*, 1998. 804(1-2): p. 105-111.
70. J.T. Creed, M.L. Magnuson, J.D. Pfaff, C. Brockhoff, *Journal of Chromatography A*, 1996. 753: p. 261-267.
71. R. Roehl, R.S., N. Avdalovic, P.E. Jackson, *Journal of Chromatography A*, 2002. 956: p. 245-254.
72. A. Seubert, G. Schminke, M. Nowack, W. Ahrer, W. Buchberger, *Journal of Chromatography A*, 2000. 884: p. 191-199.
73. T. Eickhorst, A. Seubert, *Journal of Chromatography A*, 2004. 1050: p. 103-109.
74. G. Schminke and A. Seubert, *Fresenius Journal of Analytical Chemistry*, 2000. 366(4): p. 387-391.
75. M. Yamanaka, T. Sakai, H. Kumagai, Y. Inoue, *Journal of Chromatography A*, 1997. 789: p. 259-265.
76. V. Ingrand, J.L. Guinamant, A. Bruchet, C. Brosse, T.H.M. Noij, A. Brandt, F. Sacher, C. McLeod, A.R. Elwaer, J.P. Croué, Ph. Quevauviller, *Trends in Analytical Chemistry*, 2002. 21(1): p. 1-12.
77. M. Biesaga, M. Kwiatkowska, and M. Trojanowicz, *Journal of Chromatography A*, 1997. 777(2): p. 375-381.
78. D. Connolly, B. Paull, *Journal of Chromatography A*, 2002. 953: p. 299-303.
79. H. Carrero and J.F. Rusling, *Talanta*, 48 (1999) 711.
80. R. Vichot, K.G. Furton, *J. Liq. Chromatogr.*, 17 (1994) 4405.
81. C. Sarzanini, M.C. Bruzzoniti and E. Mentasti, *J. Chrom. A*, 850 (1999) 197.
82. R. Loos and D. Barceló, *Journal of Chromatography A*, 938 (2001) 45.
83. L.M. Nair, R. Saari-Nordhaus and J.M. Anderson Jr., *J. Chrom. A*, 671 (1994) 309.
84. V. Lopez-Avila, Y. Liu and C. Charan, *J. AOAC Intl.* 82 (1999) 689.
85. Y. Liu and S. Mou, *J. Chrom. A*, 997 (2003) 225.
86. K. Ohta, A. Toweta and M. Ohashi, *J. Chrom. A*, 997 (2003) 95.
87. L. Yang, L. Liu, B.A. Olsen and M.A. Nussbaum, *J. Pharm. Biomed. Anal.* 22 (2000) 487.

88. K. Tanaka, M-Y Ding, H. Takahashi, M.I.H. Helaleh, H. Taoda, W. Hu, K. Hasebe, P.R. Haddad, M. Mori, J.S. Fritz and C. Sarzanini, *Anal. Chim. Acta*, 474 (2002) 31.
89. K. Tanaka, M-Y Ding, H. Takahashi, M.I.H. Helaleh, H. Taoda, W. Hu, K. Hasebe, P.R. Haddad, J.S. Fritz and C. Sarzanini, *J. Chrom. A*, 956 (2002) 209.
90. M.I.H. Helaleh, K. Tanaka, M. Mori, Q. Xu, H. Taoda, M-Y. Ding, W. Hu, K. Hasebe and P.R. Haddad, *J. Chrom. A*, 997 (2003) 133.
91. J.F.J. Dippy, S.R.C. Hughes, and A. Rozanski, *J. Chem. Soc.*, (1959) 2492.
92. Y. Liu, S. Mou and D. Chen, *J. Chrom. A*, 1039 (2004) 89.
93. Y. Liu and S. Mou, *Microchem. J.* 75 (2003) 79.
94. D. Martínez, F. Borrull, and M. Calull, *J. Chrom. A*, 827 (1998) 105.
95. D. Kou, X. Wang, S. Mitra, *Journal of Chromatography A*, 1055 (2004) 63-69.
96. Dionex Corp., Draft Product Note, IonPac AS11 and AS11-HC anion exchange columns, 2004.
97. Dionex Corp., Draft Product Note, IonPac AS16 anion exchange columns, 2004.
98. Dionex Corp., Draft Product Note, IonPac AS19 anion exchange columns, 2004.
99. Dionex Corp., Draft Product Note, IonPac AS15 anion exchange columns, 2004.

Chapter 2.0

Anion Exchange Chromatography of Haloacetates

"They say that God is everywhere, and yet we always think of Him as somewhat of a recluse"
Emily Dickinson (1830-1886)

2.1 Introduction

The analysis of disinfectant by-products has been the focus of some liquid chromatography researchers in the past few years. As outlined previously in Chapter 1.0, ion exchange chromatography has shown particular use in the determination of the ionic DBPs, namely the oxyhalides chlorate [1] and bromate [2,3], chloral hydrate [4] and the HAs [5-7]. Separation of carboxylic acids has traditionally been carried out using ion exclusion chromatography [8,9]. Therefore as anion exchange chromatography offers high sensitivity and reproducibility, its further application to HA determinations was of interest here. There is currently no other standard method for determination of HAs in drinking waters except for GC-ECD or GC-MS [10,11], which, as stated previously, involves tedious extraction derivitization procedures. In this preliminary chapter, an anion exchange method for the separation of seven HAs is presented. For haloacetic acids, it is proposed by the USEPA [12,13] that the MCL for five commonly occurring HAs, namely, MCA, MBA, DCA, DBA and TCA should not exceed 60 µg/L in total. Within this regulation, DCA should never be present and TCA concentrations should not amount to more than 30 µg/L. The upcoming Stage 2 DBP negotiations will propose the lowering of this total 60 µg/L limit to 30 µg/L for all HAs. Taking this into account, the principal aim of the development of this method was to achieve detection limits in the µg/L range to qualitatively and quantitatively determine the HAs in drinking water samples. The column of choice was a high capacity hydrophilic anion exchange stationary phase of EVB-DVB, thus lending itself to the quite hydrophilic nature of the HAs, which are generally ionised at drinking waters pH, due to their low pK_a values. Problems with the separation, such as interference from other naturally occurring inorganic anions are included for presentation here as well gradient elutions as a possible means to reduce overall run times. Anion exchange chromatography is generally carried out using suppressed conductivity detection. As this chromatography is carried out in conjunction with a membrane suppressor in the auto-recycling mode, the standard operating procedures allow no addition of organic solvent to the eluent. An alternate parameter, temperature, is investigated and results showing a variation in selectivity and even retention order are presented and

lends itself as a useful parameter for resolution of HAs from inorganic anions. Finally, analytical performance characteristics of linearity, reproducibility and limits of detection were performed and the application of the method to spiked HA drinking water samples shown.

2.2 Experimental

2.2.1 Instrumentation

All separations were carried out on a Dionex Model DX500 ion chromatograph (Sunnyvale, CA, USA) comprising of a GP50 gradient pump, CD20 conductivity detector, AD20 UV Detector at 230 nm and an LC25 chromatography oven. The oven temperature was optimised at 40°C. The analytical column employed was a Dionex AS11-HC (250 x 2 mm). Eluent suppression was carried out on a Dionex ASRS-ULTRA I (2 mm) suppressor run in the auto recycle mode at an operating current of 50 mA. Injection volume was 25 µL, unless specified, and all chromatography loops and tubing were micro-bore polyether ether ketone (PEEK). Instrument control, data acquisition and analysis were carried out with a Dell personal computer with Dionex Peak Net version 6.0 software installed. A concentration gradient of sodium hydroxide was used to elute HAs in a minimum timeframe without compromising resolution between matrix inorganic anions. Optimum gradient parameters were 10 mM NaOH for the first 15 minutes of separation and then linearly ramped to 100 mM NaOH over a time period of 15 minutes where it remained constant for further 10 minutes leading to a total run-time of 40 minutes. Between runs, the column was re-equilibrated to 10 mM NaOH over a period of 10 minutes.

2.2.2 Reagents

All chemicals were of analytical grade purity and were ordered from Aldrich (Milwaukee, WI, USA). Stock haloacetic acid solutions of MCA, DCA, TCA, TFA, CDFA, MBA and DBA were prepared to a concentration of 10 mM and were stable for approximately one fortnight when stored at 4°C in the dark.

Working standards were prepared fresh daily using water from a Milli-Q water purification system (Millipore, Bedford, MA, USA). Two eluent reservoirs each of 10 and 100 mM NaOH were prepared daily from a 50 % solution of sodium hydroxide. Where drinking water samples were used, samples were collected in a 1L bottle by allowing the tap to flow for approximately 3 minutes prior to sampling. Samples were analysed within 24 hours and stored in the dark and at 4°C when not in use.

2.3 Results and Discussion

2.3.1 Isocratic separations

Ion exchange chromatography was considered as a suitable method to separate small anions such as the HAs. As could be seen from *Table 1.6* in Chapter 1.0, the pK_a of all HAs are all well below pH 7. Therefore, it is important to note, that HAs, in this sense, were ionised in solution at all times. Taking into account the polarity of the analytes, a micro-bore Dionex IonPac AS11-HC micro-bore column was ordered from Dionex (UK) Ltd. A mixed solution of 0.1 mM of the seven HAs was prepared in Milli-Q water and 25 μ L was injected and run at a pump flow of 0.38 mL/min and with an isocratic eluent of 30 mM sodium hydroxide. The resulting chromatogram displayed 7 distinct peaks for each of the HAs. It was noticed that for such a large concentration of standard, that the baseline displayed excessive levels of noise (1.5 μ S sampled over 10 minutes). Seven individual standards, each of 0.1 mM concentration, were also prepared to determine elution order.

Elution order for the seven HAs is shown in *Fig. 2.1* and in *Table 2.1*. MCA, being the first to elute, was obviously the smallest of the HAs. Considering that the charge was similar in the case of all HAs, it was expected that the separation be based predominantly on molecular size, though some hydrophobic interactions were expected to occur. Results showed that retention for all homogeneously halogenated HAs occurred in the order of mono- < di- < trisubstituted HAs (in order of increasing retention). In the case of CDFA, which is not a molecule containing one type of halogen species, the existence of two fluorine molecules makes this elute before DBA because its spatial distribution is dissimilar to HAs with one halogen type.

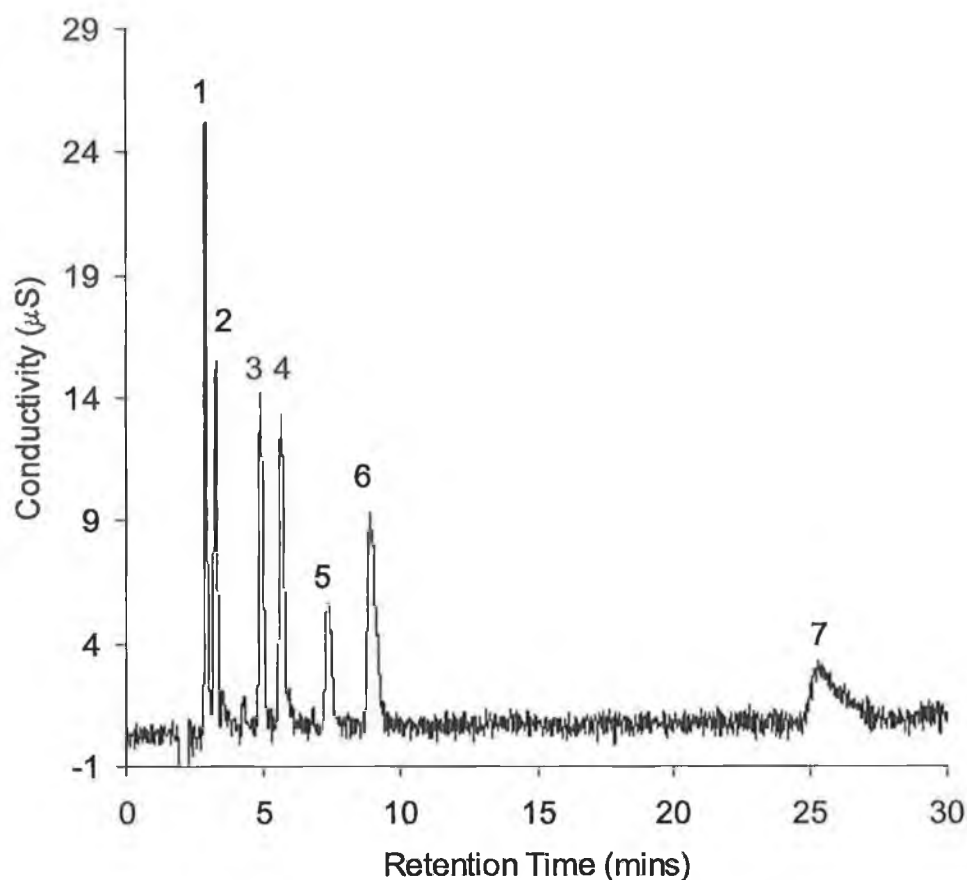


Fig. 2.1 Initial isocratic separation of 25 μL of 0.1 mM of the seven HAs at 0.38 mL/min, and 30 mM NaOH eluent. Elution order: 1 = MCA, 2 = MBA, 3 = TFA, 4 = DCA, 5 = CDFA, 6 = DBA, 7 = TCA.

Table 2.1. Elution order, retention time and resolution of HAs

HA	Retention Time (minutes)	Resolution
MCA	2.91	MCA/MBA - 1.98
MBA	3.29	MBA/TFA - 6.73
TFA	4.93	TFA/DCA - 2.63
DCA	5.67	DCA/CDFA - 4.86
CDFA	7.39	CDFA/DBA - 3.34
DBA	8.91	DBA/TCA - 15.72
TCA	25.28	N.A.

As can be seen from the data in *Table 2.1*, the retention times are relatively low compared to that of TCA, which elutes much later than the other six at 25.28 minutes and is obviously much more hydrophobic than the other HAs. It should also be noted that resolution between MCA and MBA is just above complete baseline resolution. This will be more relevant later when interferent anions are introduced to the separation mixture. From this point, it was necessary to optimise other chromatographic parameters to develop and validate an optimum method for HA analysis by IC.

2.3.2 Gradient separations

In order to reduce run time without changing eluent flow rate, a higher concentration of NaOH eluent was required in order to elute TCA in a minimum time frame without affecting resolution between the MCA/MBA pair. As a result, a gradient of sodium hydroxide eluent was considered. At first, a gradient of sodium hydroxide linearly ramped from time zero from 30 to 100 mM NaOH was considered. This separation worked well by reducing run time by roughly 8 minutes. However, it must be noted that with gradient separations a re-equilibration time between successive runs was necessary in order to completely equilibrate the column stationary phase at the initial eluent concentration of the gradient program. Consequently, an equilibration time of 10 minutes was used, which meant that though separation time was shorter, in fact, the overall run time increased by 2 minutes using gradients. Nevertheless, the gradient was necessary to improve the peak shape of late eluters such as DBA and TCA. Another drawback associated with these gradient separations was an increase in baseline and noise levels with respect to eluent concentration. This can be observed in *Fig. 2.2* as a linear increase in signal over the course of the run. Weak solutions of hydroxide prepared in ultra-pure Milli-Q water absorb carbonate readily from air. As a result, care was taken to ensure that the sodium hydroxide was added just before pump priming commenced.

Peak asymmetries for these two peaks in the isocratic methods are 2.43 and 5.24 respectively. For peaks to have acceptable asymmetry, peaks should have a value of 1.2 or less at 10 % peak height. The gradient separation highlighted its advantage when the asymmetry values for each peak were compared to isocratically run chromatography of HAs. Peak asymmetry for the gradient program was comparable to the isocratic run for the early eluting HAs, but improved to 2.22 and 3.45 for DBA and TCA. This was still not acceptable asymmetry for peaks, but gradients were observed to improve and sharpen peaks. Resolution for this gradient method showed values of above 1.8 for all adjacent peaks. The sample concentration injected was 0.1 mM MCA, MBA, TFA, DCA, CDFA and 0.2 mM DBA and TCA (see Fig. 2.2).

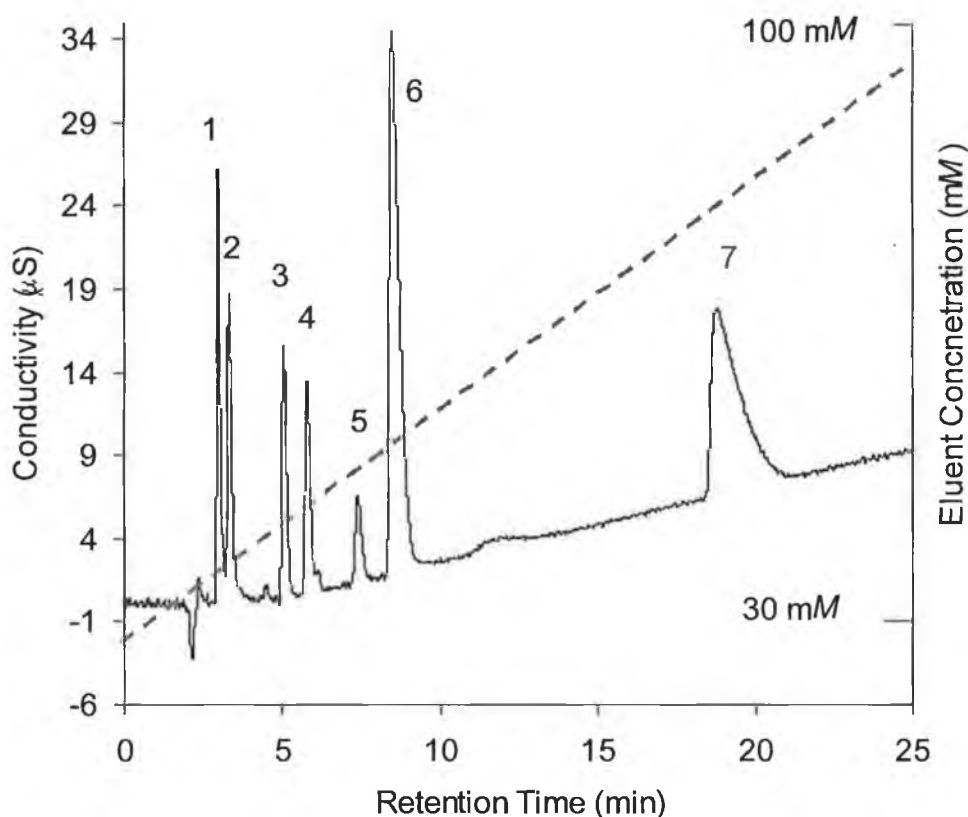


Fig. 2.2. Linear gradient of 30-100 mM NaOH eluent showing separation and improved peak shape for the HAs. Elution order: 1 = MCA, 2 = MBA, 3 = TFA, 4 = DCA, 5 = CDFA, 6 = DBA, 7 = TCA.

Table 2.2 Resolution of seven HAs using linear gradient from 30-100 mM NaOH.

HA Peaks	Resolution
MCA/MBA	2.74
MBA/TFA	9.07
TFA/DCA	2.7
DCA/C DFA	5.52
C DFA/DBA	2.32
DBA/TCA	9.77

2.3.3 Inorganic anions

In order to apply the gradient parameters to real sample analysis, it was necessary to assess interference from other commonly occurring anions in drinking water. A 0.05 mM standard of the seven HAs was prepared in Milli-Q and spiked with 0.06 mM chloride, bromate, nitrite, nitrate, sulphate and 0.1 mM phosphate and run using a gradient of 30 – 100 mM NaOH after 10 minutes with a linear ramp duration time of 20 minutes. The gradient was not carried out at time zero like the previous gradient experiment, as it was expected that these small inorganic anions like fluoride and chloride would elute early and may have coelutes with the HAs, providing inconclusive data. Therefore, the gradient was not initiated until DBA had eluted from the column. From this short study it was shown that chloride coeluted with MBA, bromate coelute with MCA and sulphate with C DFA. As a result of this, it was decided to reduce the initial concentration of eluent to 10 mM NaOH to try and compensate for this. Bromate only occurs in significant detectable quantities in ozonated drinking water. All samples were taken from water supplies where chlorination was used as the disinfectant. However, drinking waters were expected to contain significant mg/L concentrations of chloride, so bromate was not included in further development of the method. In this analysis, the effluent from the conductivity detector was redirected through a UV detector for positive

identification of nitrite and nitrate at 230 nm (Fig. 2.4). This UV wavelength was not optimised, but showed adequate sensitivity for HAs, which absorb closer to 200 nm, as well as nitrite and nitrate, which absorb best at 214 nm. When 214 nm was chosen, interference was observed from chloride and other anions that began to absorb in the low UV region. In order to use UV as a detection technique, high levels of chloride would have to be selectively removed first. As a result, an arbitrary wavelength was chosen until the separation was fully optimised, using conductivity as the main means of detection.

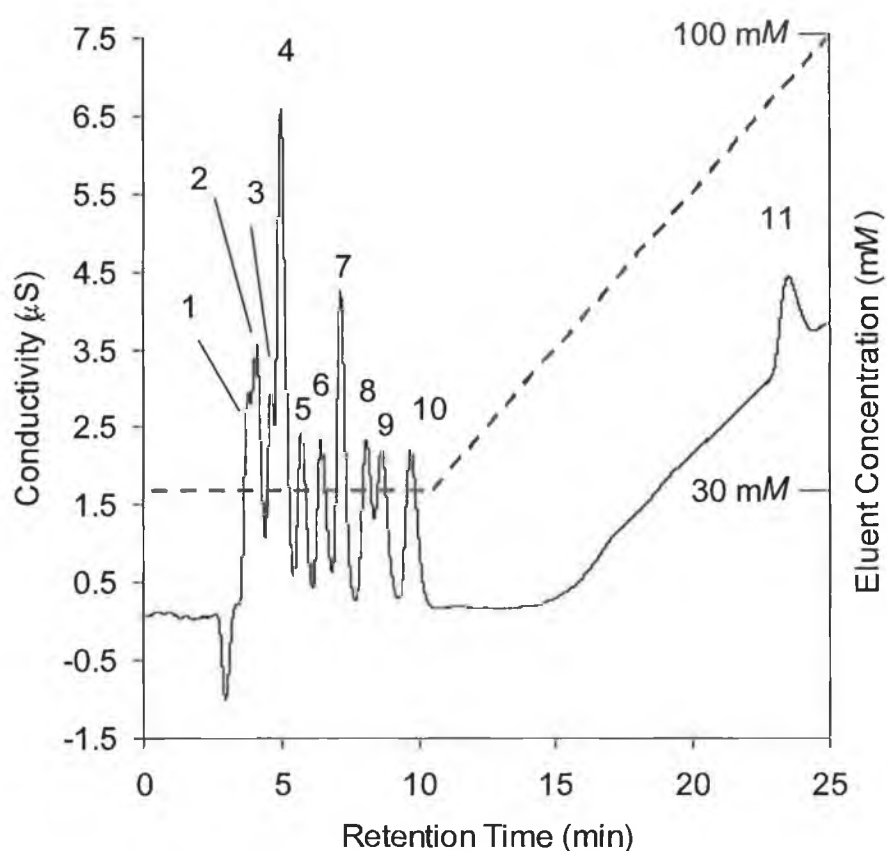


Fig. 2.3. Conductivity trace of 0.05 μM of seven HAs with 0.06 μM spike of Cl^- , BrO_3^- , NO_2^- , NO_3^- , SO_4^{2-} and 0.1 μM PO_4^{3-} . Elution order: 1 = MCA, 2 = BrO_3^- and Cl^- , 3 = NO_2^- , 4 = PO_4^{3-} , 5 = TFA, 6 = DCA, 7 = NO_3^- , 8 = CDFA, 9 = SO_4^{2-} , 10 = DBA, 11 = TCA. Flow rate: 0.38 mL/min; Loop size: 25 μL .

The suppressor used for the first two separations displayed significant noise levels. In an attempt to reduce noise levels, the Dionex ASRS Ultra suppressor was replaced with a SeQuant Continuous Anion Regeneration System (CARS) suppressor. It can be seen in *Fig. 2.3* that noise levels decreased and was measured as 0.281 μS over a baseline range of 5 minutes. However, this system was more cumbersome than the ASRS Ultra format and not ideal for the analysis of these species (it did not physically fit into the LC25 oven and large unwanted lengths of tubing were required to connect this suppressor to the system). Hence, a new ASRS Ultra was acquired to ensure the determined performance characteristics of the Dionex suppressor were accurate.

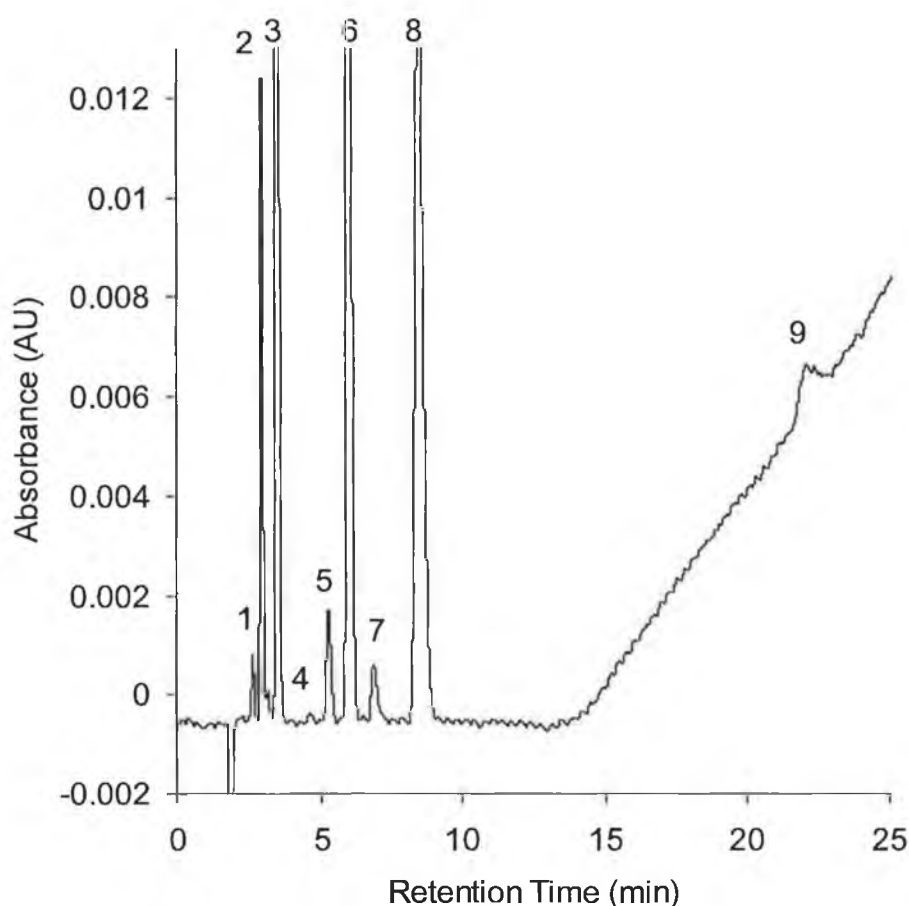


Fig. 2.4. UV trace of HAs and interfering inorganic anions at 230 nm. Elution Order: 1 = MCA, 2 = MBA, 3 = NO_2^- , 4 = TFA, 5 = DCA, 6 = NO_3^- , 7 = CDFA, 8 = DBA, 9 = TCA.

In an attempt to improve peak tailing and asymmetry further, the gradient was ramped linearly at 10 minutes from 10 mM to 100 mM NaOH for 25 minutes. The post-run equilibration time was again 10 minutes (Fig. 2.5). The sample concentration injected was the same as the previous gradient trial.

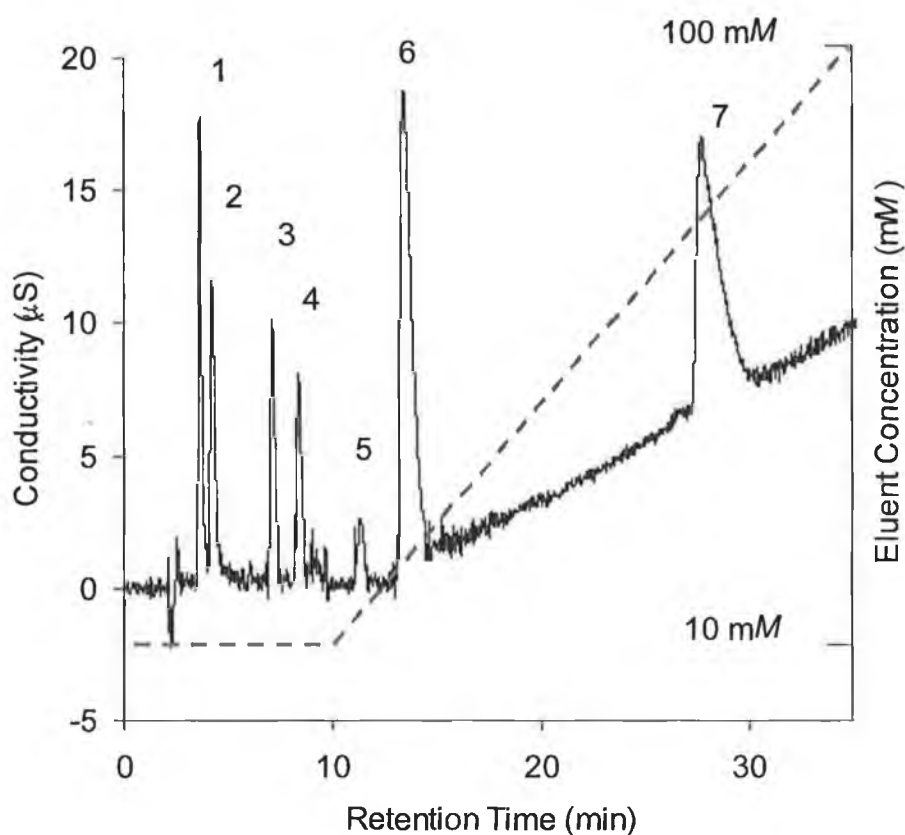


Fig. 2.5. Gradient of 10-100 mM NaOH after 10 minutes. Elution order: 1 = MCA, 2 = MBA, 3 = TFA, 4 = DCA, 5 = CDFA, 6 = DBA, 7 = TCA.

Table 2.3. Resolution of seven HAs using a gradient of 10 – 100 mM NaOH after 10 minutes

HA Peaks	Resolution
MCA/MBA	1.68
MBA/TFA	7.22
TFA/DCA	3.12
DCA/C DFA	4.57
C DFA/DBA	2.21
DBA/TCA	9.84

As can be seen from *Fig 2.5*, the overall separation was better, but the sensitivity was very poor. Resolution was slightly poorer with this gradient type than with the 30 – 100 mM NaOH method. This could be due to band broadening at this low eluent concentration and thus affected early eluters MCA and MBA. Nevertheless, to this point, gradients showed the best results and investigation of gradient slope and type were examined further once the next parameter was optimised.

2.3.4 Flow rate

The new ASRS Ultra suppressor was installed in the system and to optimise the system further, the column flow rate was addressed. One of the prerequisites for the analysis of HAs in this study was the compatibility of the ion chromatographic technique with mass spectrometry. For this, the optimum flow rates for electrospray devices are not more than 0.50 mL/min. As discussed in Chapter 1.0, electrolytic suppressors generally are not compatible with organic solvent. It was decided that if, at a later stage, a secondary pump flow of organic solvent was required to boost MS sensitivity, that a lower flow rate was required than 0.50 mL/min. Taking this into account, the flow rate was set arbitrarily at 0.30 mL/min. Similar chromatographic conditions were used as the last experiment, with a gradient of 10 – 100 mM NaOH, but at a flow rate of

0.30 mL/min. Fig. 2.6 shows the separation achieved for injection of 25 μ L of a standard of 0.1 mM of each of the seven HAs.

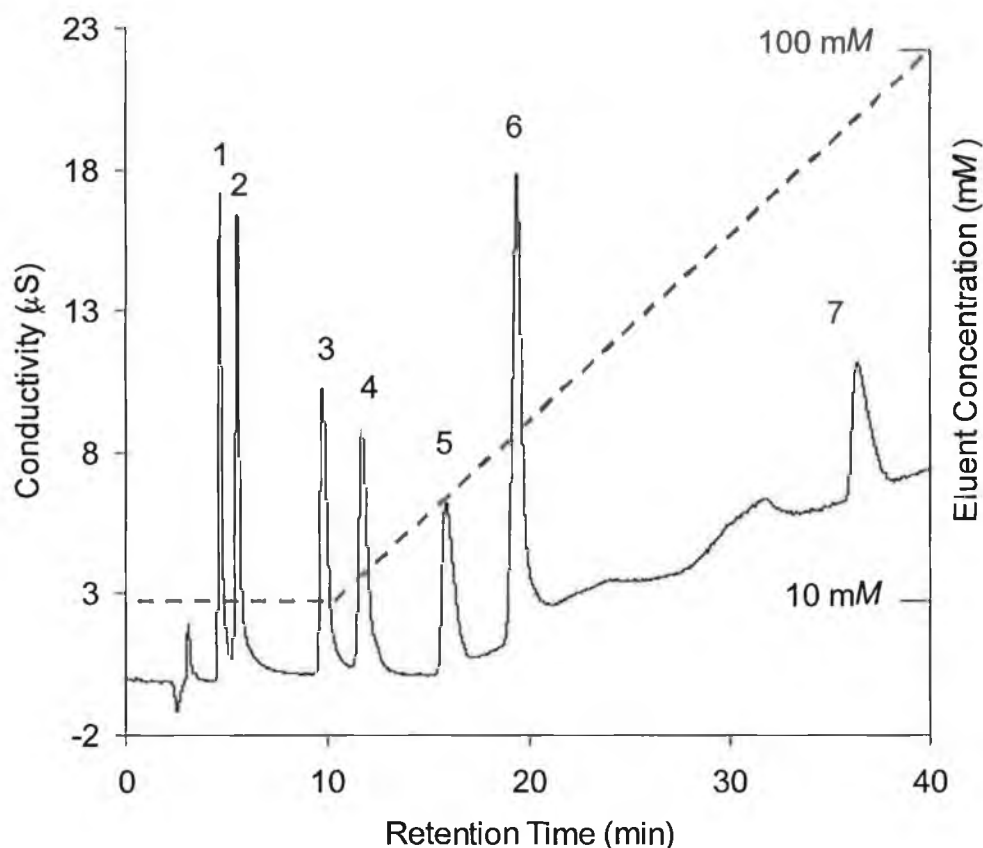


Fig. 2.6. Gradient separation of the seven HAs using 10 – 100 mM NaOH at a flow rate of 0.30 mL/min. Elution Order: 1 = MCA, 2 = MBA, 3 = TFA, 4 = DCA, 5 = CDFA, 6 = DBA, 7 = TCA.

The noise was measured over a time frame of 10 minutes using this new suppressor and it was found that noise levels decreased further to 0.109 μ S showing a clear fault with the original suppressor. The only drawback with using low flow rates was increased run time. Here, a reduction of 0.08 mL/min caused an increase in retention time for TCA of roughly ten minutes. This was not acceptable, as run-times were already excessively long. It was attempted to carry out a gradient where the concentration of eluent was ramped linearly over a period of fifteen minutes and then kept constant at 100 mM NaOH until

the strongly retained HAs eluted. In this analysis, low levels of inorganic ions were spiked into the Milli-Q water standards as markers of fluoride (2 mg/L), chloride (2 mg/L), nitrite (0.5 mg/L), nitrate (1 mg/L) and sulphate (2 mg/L). These inorganic anions naturally exist in excess of the HAs in drinking water sources. The reason why low levels of these ions were added for optimisation of the separation, as opposed to excess amounts, was due to the cleaning effect of the preconcentration method (discussed in Chapter 3.0), where these anions were not well retained on a EVB-DVB preconcentration cartridge, unlike the HAs, and only residual amounts were present in chromatograms. *Fig. 2.7* shows the optimum gradient parameters for the separation of HAs in Milli-Q water from this study.

The resolution between the HAs was excellent with all values above 2.0 (*Table 2.4*), but all of the inorganic anions, with the exception of fluoride, coeluted with one of the HAs. Sulphate coeluted directly with DBA showing no resolution at all and chloride was similar with no resolution from MBA. The largely tailed coeluting peaks of MBA and chloride also masked the small nitrite peak. Nitrate was seen as a shoulder on the tail of the DCA peak with incalculable resolution. Overall, separation was poor with respect to the seven HAs and the commonly occurring inorganic ions. In order to assess the viability of IC with this column as a practical method for HA determinations, these inorganic anions may need to be selectively removed from solution. For example, as discussed in Chapter 1.0, chloride and sulphate may be removed by passing the solution through a series of solid phase extraction cartridges in the silver, barium and acid forms prior to HA determination by IC.

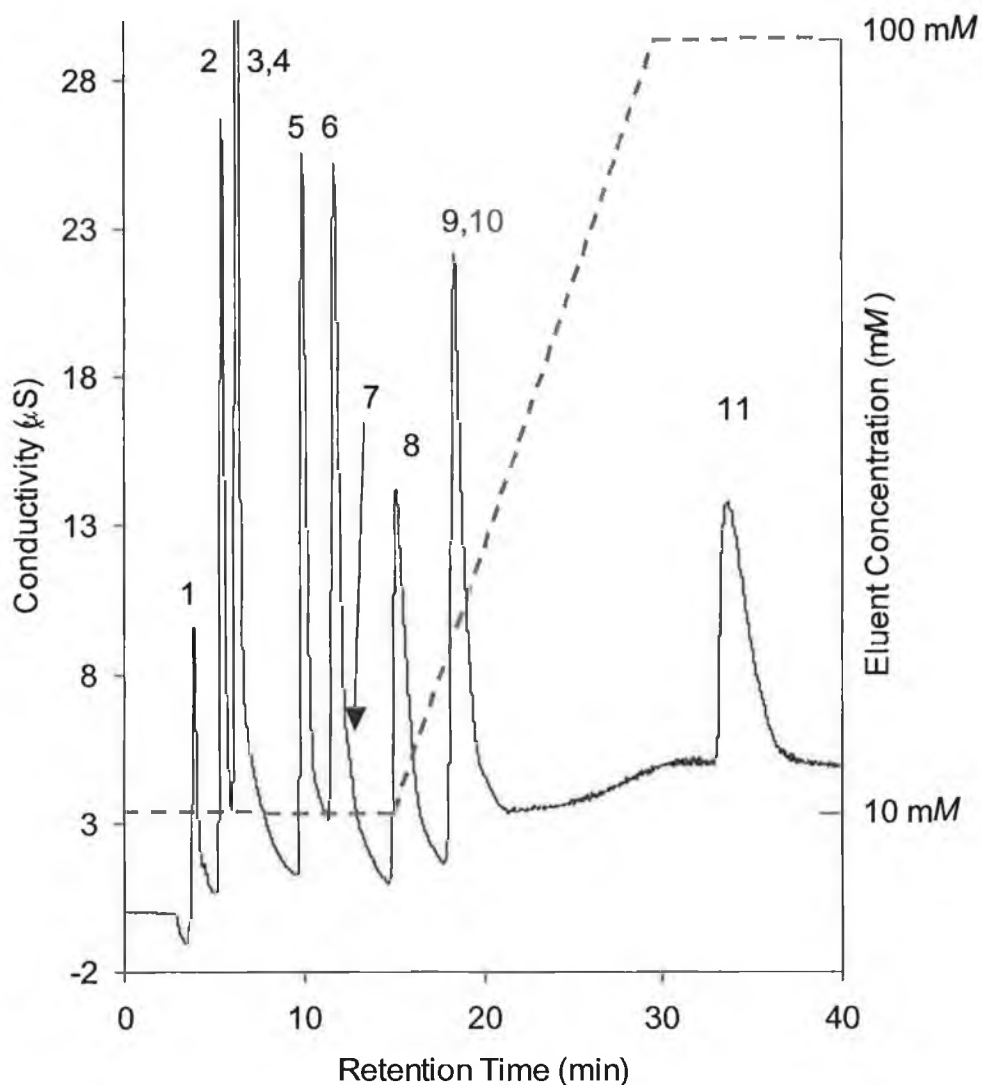


Fig 2.7. Gradient separation of 0.1 mM of seven HAs in Milli-Q water spiked with commonly occurring inorganic anions. Elution order: 1 = F (2 mg/L), 2 = MCA, 3 + 4 = Cl⁻ (2 mg/L) and MBA, 5 = TFA, 6 = DCA, 7 = NO₃⁻ (1 mg/L), 8 = CDFA, 9 + 10 = SO₄²⁻ (2 mg/L) and DBA, 11 = TCA. Flow rate: 0.30 mL/min; Injection volume: 25 µL. Gradient Parameters: 10 mM NaOH for 15 minutes; 10-100 mM NaOH over 15 minutes; 100 mM NaOH for a further 10 minutes. Post-acquisition parameters and equilibration: 100-10 mM NaOH for 5 minutes; 10 mM NaOH for a further 5 minutes. Detection: Suppressed conductivity at 50 mA.

Table 2.4. Collected data for observed peaks in Fig 2.7 above.

Peak	Ret.Time (min)	Height (μ S)	Width (min)	Resolution	Asymmetry	Plates
F ⁻	3.89	8.75	0.37	3.91	1.36	1756
MCA	5.44	24.92	0.43	2.21	1.42	2620
MBA, Cl ⁻ , NO ₂ ⁻	6.29	51.93	0.35	7.56	1.67	5402
TFA	9.93	23.77	0.62	2.64	2.65	4040
DCA	11.73	21.88	0.76	3.41	2.39	4041
NO ₃ ⁻	12.34	-	-	-	-	-
CDFA	15.19	13.07	1.30	2.63	3.27	2186
DBA, SO ₄ ²⁻	18.38	20.13	1.03	7.92	2.80	4221
TCA	33.66	8.60	4.57	N.A.	2.69	2422

Peak symmetries have improved for TCA at 2.69. However, symmetries overall have worsened, possibly due to the effect of the inorganic coeluters. Accordingly, the peak asymmetries assigned to impure HA peaks are not true representations of chromatographic performance.

2.3.5 The effect of temperature

Chromatographic retention at elevated temperatures is best shown by the van't Hoff plot, which is a plot of $\ln k$ versus reciprocal temperature. Equation 2.1 is the general thermodynamic equation for retention of a species.

$$\frac{d \ln k}{dT} = \frac{\Delta H^{\circ}}{RT^2} \quad \text{Equation 2.1}$$

where k is the retention factor, T is the temperature in Kelvin, R is the universal gas constant and ΔH° is the enthalpy of exchange. If the separation is carried

out under isocratic conditions and ΔH° is independent of temperature, then Equation 4.2 can be integrated to

$$\ln k = A - \frac{B}{T} \quad \text{Equation 2.2}$$

A and B are constants pertaining to the particular species and if $\ln k$ is plotted versus reciprocal temperature, a linear relationship should result. According to Hatsis *et al.*, the slope of the van't Hoff plot may be either positive or negative with increasing temperature [14]. In other words, some analytes experience a decrease in retention (exothermic) and some may be more strongly retained (endothermic) with increasing temperature. For optimum selectivity, it was necessary to determine the effects of temperature on the retention of HAs as well as the interfering inorganic anions. For the van't Hoff plot to be successful, the separation was carried out under isocratic conditions, as eluent strength, as we have seen, also played a role in the retention characteristics of a particular analyte. The DX500 system was equipped with an LC25 oven, which houses the analytical column, the conductivity cell, the injector valve and the ASRS Ultra suppressor. This allowed the complete control of temperature throughout the separation process as well as precisely matching and regulating the conductivity cell temperature. Initial eluent strength was 10 mM in the optimum developed method to this point, but it was felt that the analysis for this particular experiment would be excessively long at this eluent strength, so an isocratic method of 30 mM NaOH was applied with a flow rate of 0.30 mL/min and injection volume of 25 μ L to study primarily the retention behaviour of the inorganic anions. As TCA was strongly retained on the column, gradient separations alone were adequate to improve peak shape, reduce retention and overall run time. So, as a result TCA was not considered in this preliminary study. Moreover, CDFA and TFA did not coelute with any anion in the mixture. The aim of this temperature work was to optimise the separation between those haloacetic acid ions, which coeluted with an inorganic anion, so TFA and CDFA were also omitted. The effect of temperature for the full seven HAs and all inorganic anions will be included in the gradient separations. The temperature

of each run was increased from ambient (measured at 21°C on that day) in steps of 5°C to 45°C. It should be noted that ion exchange columns are not stable above 60°C, so column temperature was kept to the working range of the LC25 chromatography oven ($\leq 45^\circ\text{C}$). A standard of 0.1 mM MCA, MBA, DCA and DBA was prepared in drinking water containing levels of fluoride, chloride, nitrate, and sulphate and run according to the conditions outlined above. The data was collected and van't Hoff plots were graphed and the results were linear for the analytes under investigation, see *Fig. 2.8*.

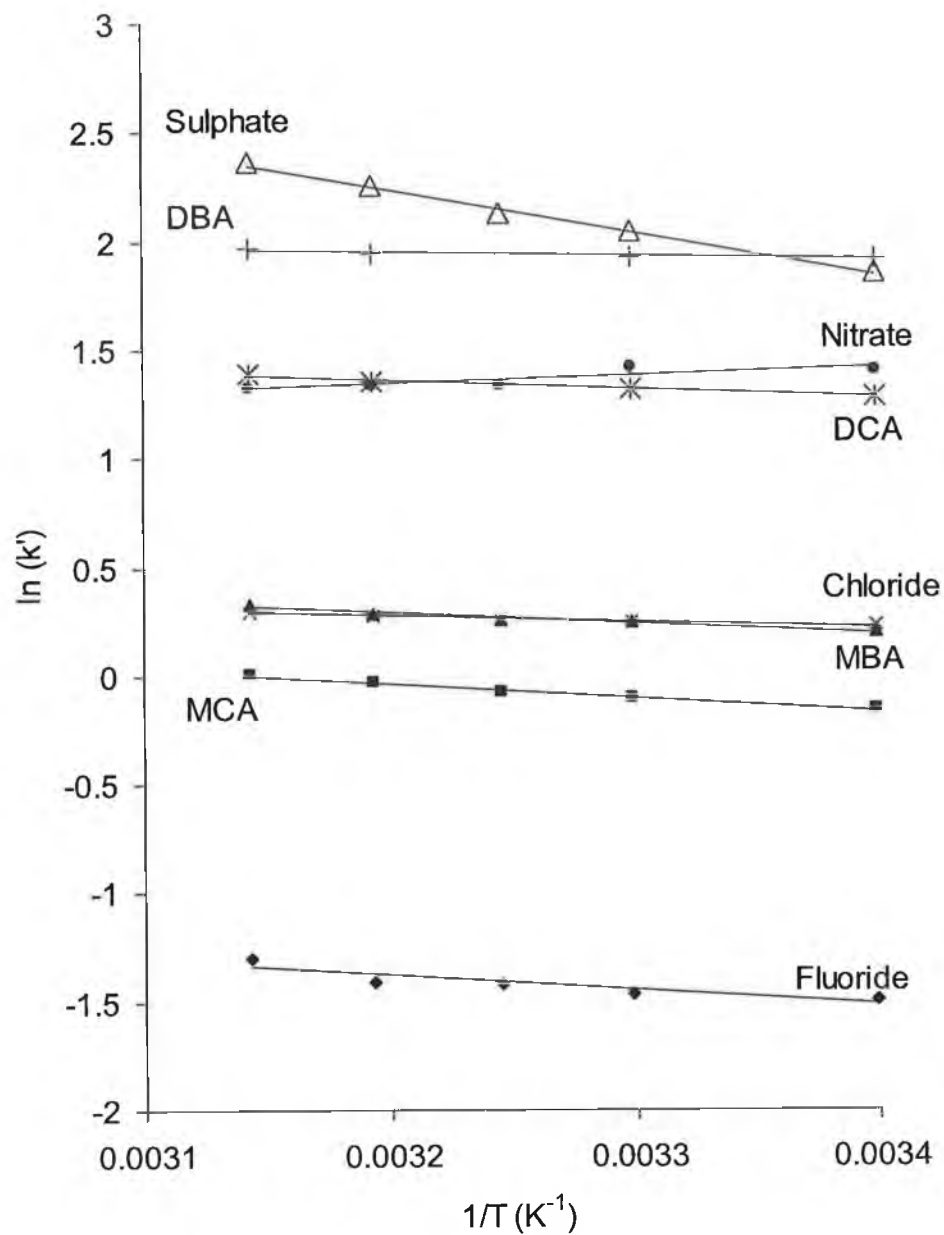


Fig. 2.8. Van't Hoff Plots for fluoride ($R^2 = 0.8399$; $m = -669.25$), MCA ($R^2 = 0.9825$; $m = -646.53$), chloride ($R^2 = 0.9419$; $m = -257.17$), MBA ($R^2 = 0.9520$; $m = -481.32$), DCA ($R^2 = 0.9755$; $m = -393.18$), nitrate ($R^2 = 0.6974$; $m = 351.77$), DBA ($R^2 = 0.9035$; $m = -190.95$) and sulphate ($R^2 = 0.9948$; $m = -2000.10$) using a 30 mM NaOH isocratic gradient at a flow rate of 0.30 mLmin^{-1} over a temperature range of 21-45 °C.

From this study it was possible to deduce two very distinct points. The retention behaviour of nitrate and sulphate were opposite with increasing temperature. Sulphate especially, had a significant shift in retention with variance in temperature with a van't Hoff plot slope of -2000 and R^2 of 0.9948 . This meant that sulphate retention could be selectively shifted with temperature so as not to coelute with DBA. Furthermore, nitrate retention decreased with increasing temperature, though less than sulphate (van't Hoff slope of 352). Similar outcomes have been found by Rey *et al.* in cation separations and report a change in divalent/monovalent selectivities with increase in temperature [15]. This could be so in the case of sulphate being divalent as opposed to the HAs and could explain the greater shift in retention time per unit temperature. Unfortunately, chloride/MBA resolution was not improved by a temperature variance. The general trend for the four HAs in this study was an increase in retention with an increase in temperature, but to a lesser extent than that of the inorganic anions. MCA was included here to investigate if fluoride retention would increase significantly so as to interfere, but no coelution occurred and both were baseline resolved at all temperatures. An optimum temperature for the developed gradient method was required to balance resolution of DCA from nitrate and sulphate from DBA. The separation was carried out using the optimum methodology highlighted in *Fig. 4.7* above, again at 5 different temperatures, ambient, 30°C , 35°C , 40°C and 45°C . The retention properties of the HAs, as well as the inorganic anions were monitored in an attempt to further improve their separation. A 0.1 mM standard of all seven HAs was prepared in Milli-Q water and spiked with 2 mg/L fluoride, 2 mg/L chloride, 1 mg/L nitrate and 2 mg/L sulphate.

Results showed again that for the HAs there appeared to be a slight increase in retention time with increasing temperature. It was found that both nitrate and sulphate were significantly affected by the increase in temperature, even with the steep gradient of sodium hydroxide, but in opposite ways. Retention decreased for nitrate from 12.34 minutes to 11.02 minutes with increasing temperature. Sulphate was significantly affected yet again by temperature variance, stressing the requirement for, at least, temperature regulation within the laboratory environment. Sulphate retention increased from 18.38 minutes

at ambient temperature (measured as 23°C on that day) to 22.09 minutes at 45°C. Resolution between the DBA/sulphate pair improved from 0 to 3.71 and was totally resolved from DBA. At 45°C however, nitrate began to coelute with TFA and appeared as a shoulder on the tail of the peak. The optimum temperature was found to be 40°C. At this temperature resolution between DBA and sulphate was 3.07. For nitrate, resolution values were 1.56 for TFA/nitrate and 1.51 for nitrate/DCA. Unfortunately, chloride was not affected by column temperature to a significant extent to allow any separation from MBA. The trends in retention for each of the HAs for an increase in temperature were plotted. It was noticed that retention did not increase dramatically for the temperature window of 23-30°C and once higher temperatures were investigated, retention increased linearly, except in the case of TCA, in which retention decreased from 33.49 to 33.42 minutes at 40 and 45°C respectively. Plotted data can be seen in *Fig. 2.9* and an overlay of all chromatograms at each temperature in *Fig. 2.10* with special attention to nitrate in *Fig. 2.11*.

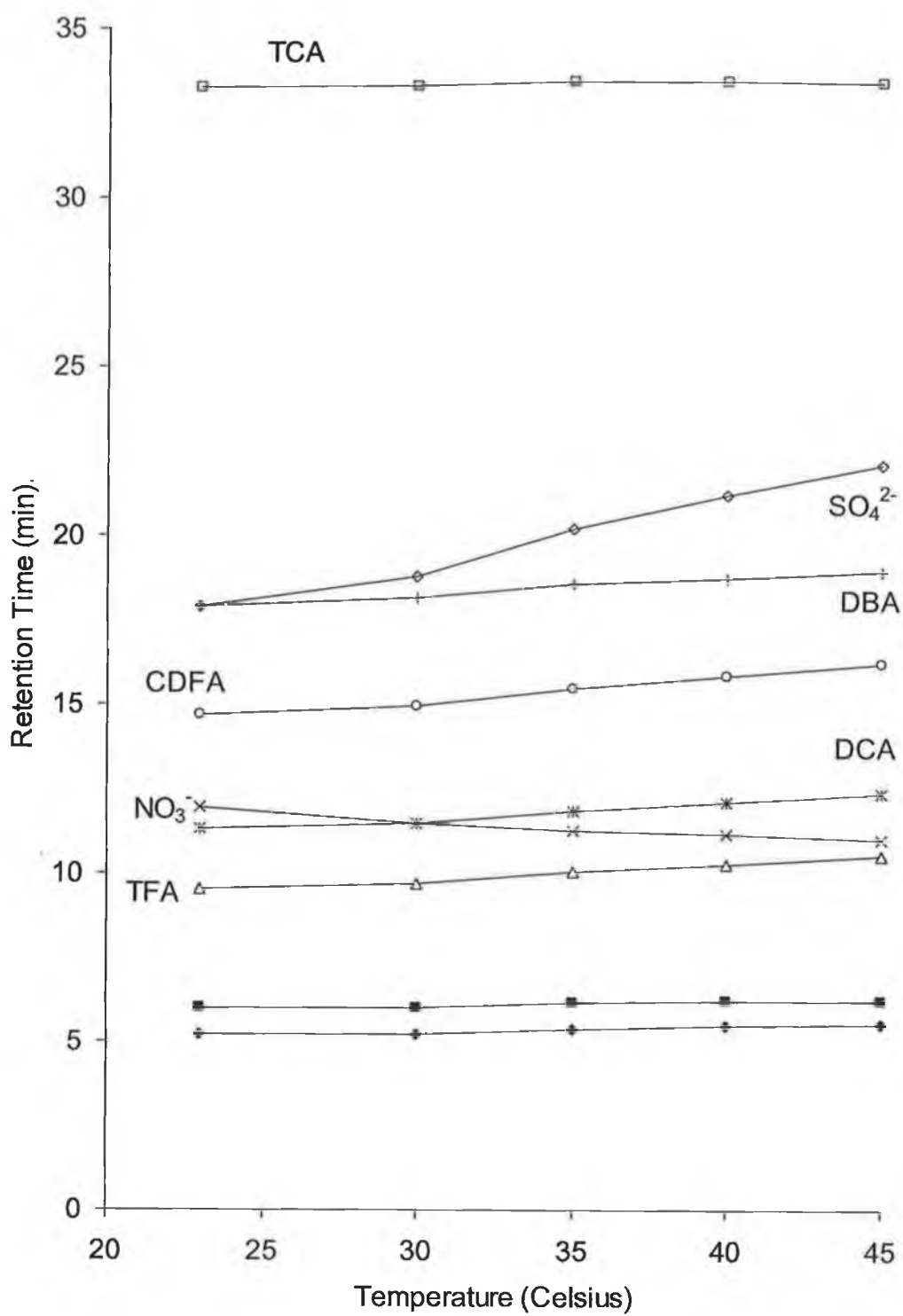


Fig 2.9 The effect of temperature on the retention of the seven HAs and two inorganic anions in eluent gradient of 10-100 mM NaOH.

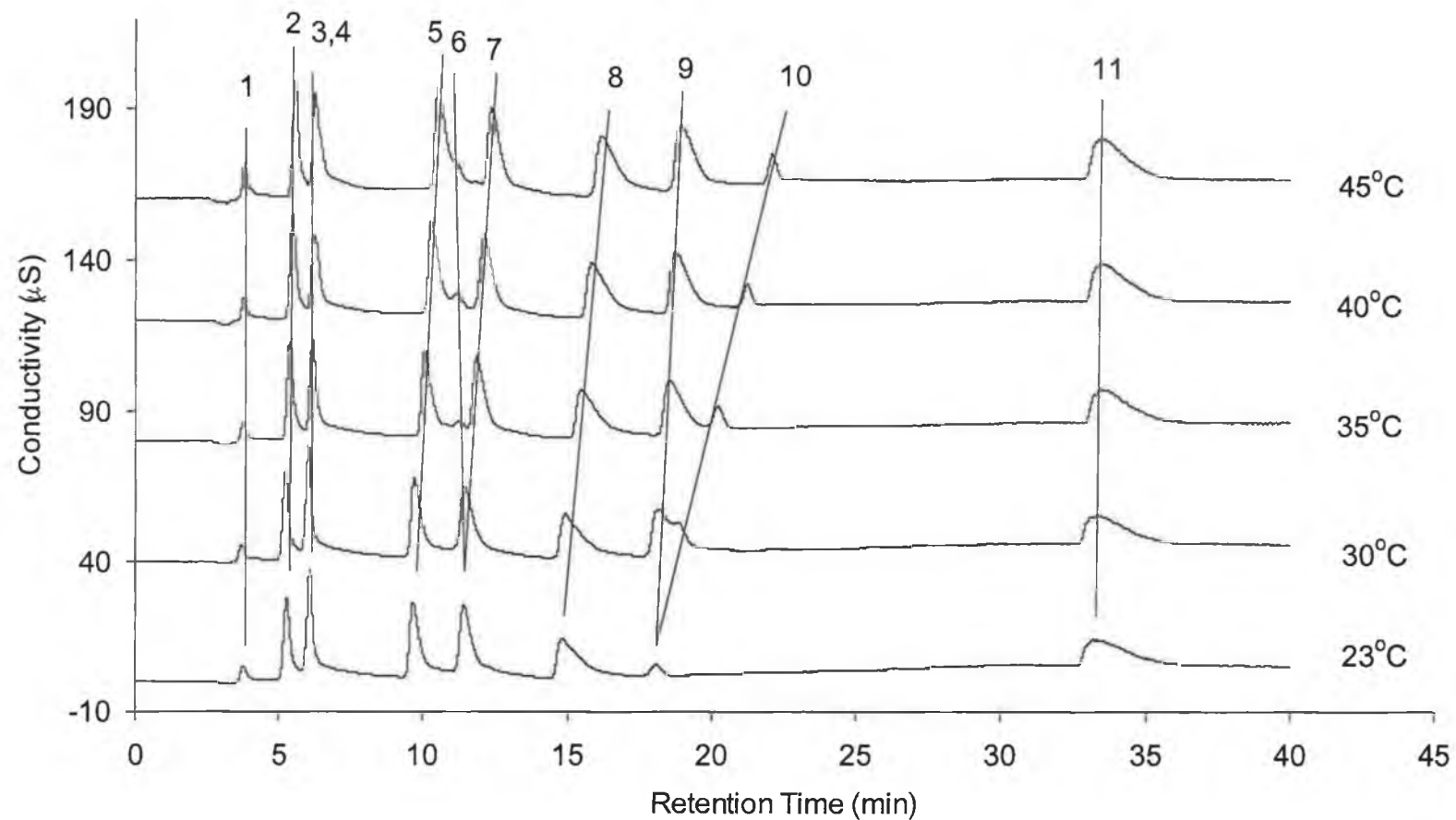


Fig. 2.10. The effect of temperature on the retention behaviour of seven HAs and 5 inorganic anions. Elution Order: 1 = fluoride, 2 = MCA, 3 = chloride/MBA, 4 = TFA, 5 = nitrate, 6 = DCA, 7 = CDFA, 8 = DBA, 9 = sulphate, 10 = TCA. [HA] = 0.1 mM. Note: 23°C trace does not contain DBA, to illustrate the retention of sulphate.

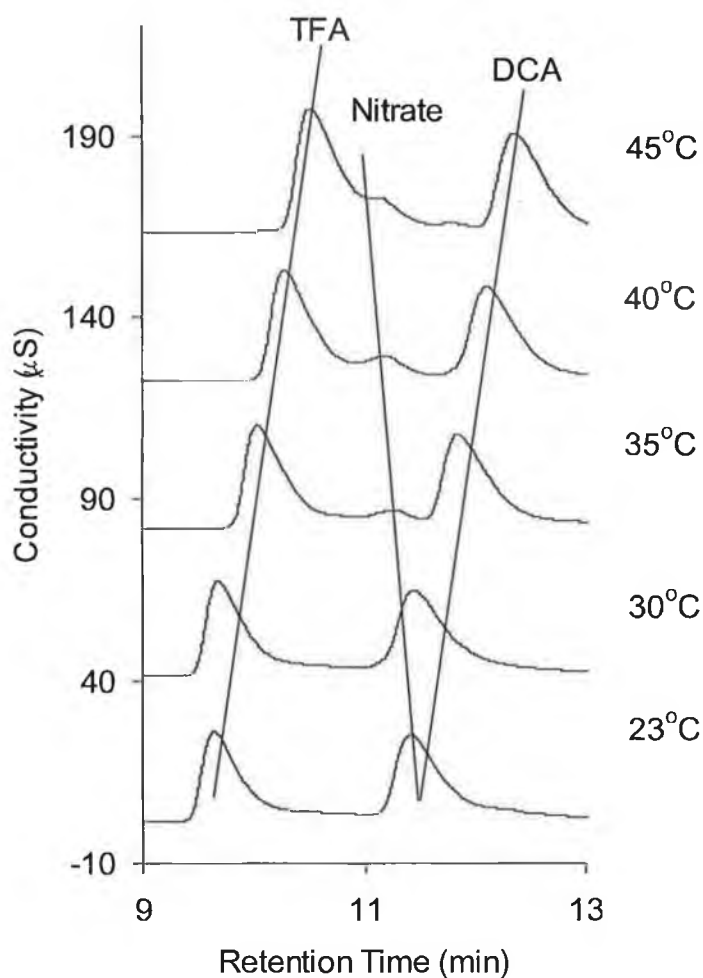


Fig. 2.11. The effect of temperature on nitrate retention.
 1 = TFA, 2 = nitrate, 3 = DCA.

2.3.6 Optimum separation parameters

From these studies, the optimum separation conditions were derived. The optimum separation consisted of a flow rate of 0.30 mL/min. The gradient applied was 10 mM NaOH eluent for 15 minutes, 10-100 mM NaOH over 15 minutes and 100 mM NaOH for a further 10 minutes. Column temperature optimum was found to be 40°C. Post-acquisition parameters and equilibration steps were 100-10 mM NaOH for 5 minutes and 10 mM NaOH for a further 5 minutes. Detection was carried out by suppressed conductivity at 50 mA.

Where necessary, UV detection was carried out using a wavelength of 230 nm. Fig. 2.12 shows the optimum separation of the seven HAs and all of the inorganic anions discussed above. Unfortunately, chloride was still unresolved from MBA.

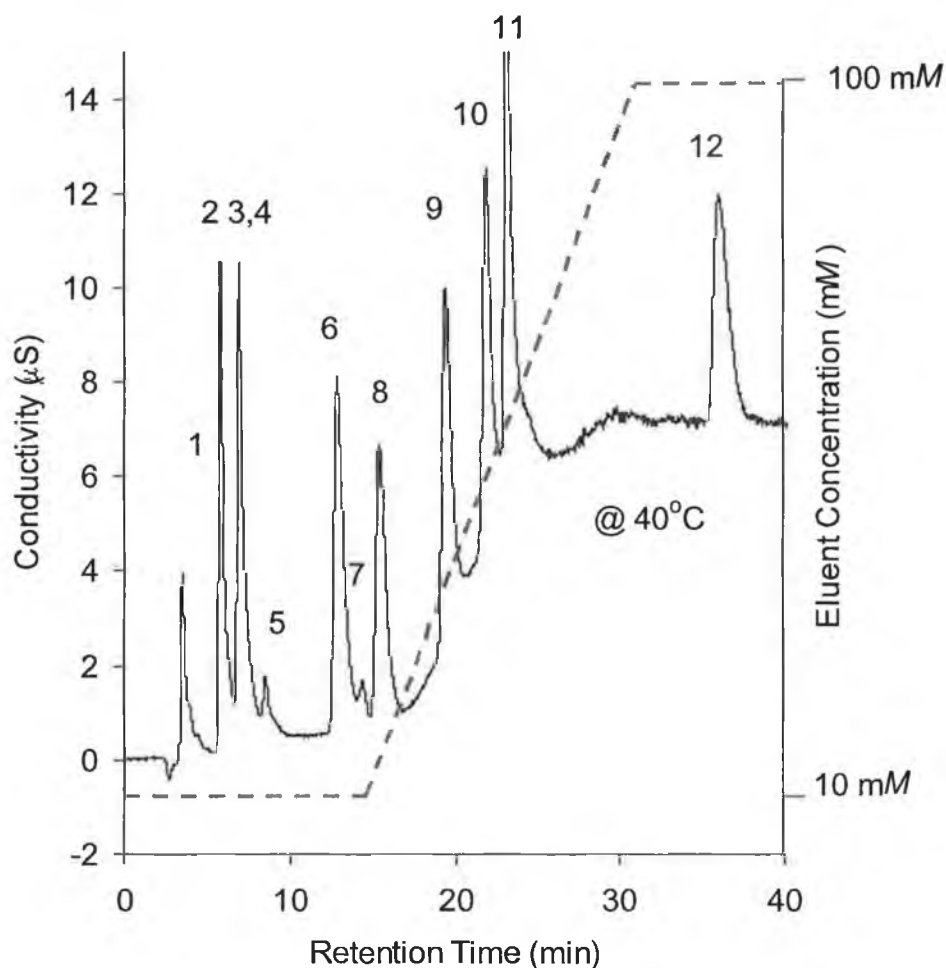


Fig. 2.12. Optimum separation of 50 μM of seven HAs and five inorganic anions at an oven temperature of 40°C. Elution order: 1 = fluoride (2 mg/L), 2 = MCA, 3 + 4 = MBA/chloride (0.5 mg/L), 5 = nitrite (1 mg/L), 6 = TFA, 7 = nitrate (1 mg/L), 8 = DCA, 9 = CDFA, 10 = DBA, 11 = sulphate (5 mg/L), 12 = TCA.

2.3.7 Analytical performance characteristics

For the optimised method to be validated, the method was put through a standard series of tests to ensure the method is suitable for the analytes under investigation. Studies of linearity and reproducibility were carried out, as well as determination of the limits of detection.

2.3.7.1 Linearity

Standards were prepared in Milli-Q water to a concentration of 200, 100, 80, 40, 20, 10 μM of the seven HAs and run in triplicate using the optimum methodology in section 5.4.6 above. It was found that all HAs displayed R^2 values of 0.99 or greater with the exception of DBA and MCA. This could possibly be due to the fact that the Milli-Q water contained trace levels of chloride and sulphate, thus affecting the linearity at low levels. R^2 values are listed in *Table 2.5* below, as well as standard deviations for the triplicate runs. All linearity calibration curves can be found in *Appendix A.1 (Fig. A.1-1 (a)-(g))*.

Table 2.5 Correlation coefficients, slopes, intercepts and standard deviations for $n = 3$ replicate linearity standard runs of the seven HAs

HA	R^2	Slope (S/M)	Intercept (μS)	Standard deviation (μM) ($n = 3$) ^a
MCA	0.9944	0.0265	0.1153	0.24
MBA	0.9879	0.0265	-0.0898	0.57
TFA	0.9995	0.0400	-0.0183	0.46
DCA	0.9992	0.0352	-0.0597	0.39
CDFA	0.9974	0.0397	0.0078	0.43
DBA	0.9793	0.0284	0.2053	0.61
TCA	0.9955	0.0438	0.2277	0.30

^a Refers to the maximum standard deviation of all points run in triplicate for the linearity curve

2.3.7.2 Reproducibility

Reproducibility studies for seven repeat injections of a standard at 10 µM of HA show little variance in retention times with the exception of TCA, which varied, to an RSD of 2.53 % (Table 2.6).

Table 2.6. Reproducibility of optimum ion exchange methodology for the seven HAs where n = 7.

HA	Average Retention Time (n = 7) (min)	% RSD t_r (min)	% RSD Peak Area (µS.min)	% RSD Peak Height (µS)
MCA	5.83 ± 0.03	1.00	4.15	3.40
MBA	6.98 ± 0.03	0.89	3.43	2.96
TFA	12.88 ± 0.04	0.65	4.08	4.08
DCA	15.47 ± 0.05	0.69	3.71	5.00
CDFA	19.45 ± 0.06	0.60	4.54	4.43
DBA	21.88 ± 0.08	0.73	4.49	3.78
TCA	35.66 ± 0.45	2.53	4.86	2.19

Upon inspection of peak area and peak height % RSD values, all were below 5 % for the seven repeat injections.

2.3.7.3 Limits of Detection (LOD)

2.3.7.3.1 LOD in Milli-Q Water

For the regulatory determination of HAs in drinking water, this method must have detection limits in the low µg/L range. Remembering that the maximum total concentrations of each of MCA, DCA, TCA, MBA and DBA must be less than or equal to 60 µg/L, according to the USEPA Stage 1 Disinfectant and Disinfectant By-Product Rule, the aim of this experiment

was to determine whether this IC method could successfully observe and quantify these HAs at such a low level and to ensure the sensitivity of the instrument to minor changes in concentration. To this point, all injection volumes were 25 μL , which was taken as the upper limit for micro-bore columns and to maximise sensitivity. However, when preliminary LOD studies were carried out, it was found that even whilst using this micro-bore column, 25 μL injection volumes were insufficient in all cases to meet the USEPA limit of $\leq 60 \mu\text{g/L}$ for all HAs. Limits of detection were in the 4 – 35 μM range for all HAs using this injection volume. Although technically not ideal in validation procedures, the effect of injection volume was studied here considering that sensitivity was so poor. Loops of 25, 50, 75 and 100 μL were investigated. It was found that even with an injection volume of 100 μL , peak shape did not distort sufficiently and consequently, showed little evidence of column overloading. It was assumed that the high capacity of the AS11-HC allowed for these extra large injection volumes. Thus, all of the LOD experiments were carried out using a 100 μL loop in place of the traditional 25 μL loop using the predetermined IC conditions. Sequential dilution standards were prepared of the seven HAs from stock concentrations of 100 μM until the LOD signal-to-noise (S:N) limit of 3:1 was almost reached. The noise levels were calculated between 7.5 and 10 minutes for the section corresponding to 10 mM NaOH eluent and between 25 and 35 minutes corresponding to the 100 mM eluent. The noise over the baseline rise representing a mixture of the two eluent concentrations was calculated as 0.299 μS in an interval of 14-17 minutes to calculate DBA and CDFA signal-to-noise ratios. As stated earlier, low concentration eluents of sodium hydroxide absorb carbonate from the air. Efforts to try and prevent this were included in instrument design, via sealed reservoirs with head pressures of high purity helium or nitrogen, but unfortunately exposure to air is inevitable in preparation of eluents. Therefore, the noise levels in 100 mM hydroxide gradients will be much more significant than lower NaOH concentrations depending on the degree of carbonate absorbed. So, two noise readings were taken as per the time intervals outlined above and it was found that the 7.5-10 minute noise levels were roughly one half that of

the 25-35 minute interval at 0.152 μ S, as opposed to 0.309 μ S. From these noise levels the peak heights were used from the chromatogram close to LOD value to calculate the LOD for a signal-to-noise ratio of 3:1. LOD concentrations of HAs for this method are listed in *Table 2.7* below.

Table 2.7. LOD (S:N = 3) values for the developed ion exchange methodology.

HA	[HA] for which S:N = 3 (μ M)	[HA] (μ g/L)
MCA	1.34	130
MBA	Not available	Not available
TFA	0.86	90
DCA	1.64	210
CDFA	4.60	1010
DBA	10.59	2290
TCA	6.46	1050

As can be seen, the limit of detection was not sufficiently low as to detect the 60 μ g/L MCL for the five regulated HAs, even with the 100 μ L loop. As an undesired consequence, it was necessary to investigate preconcentration techniques, as well as baseline noise reduction, in order to achieve this goal. As previously stated, MBA coelutes with chloride. The Milli-Q water obtained did contain trace levels of chloride (from reagent used for disinfection) and thus LOD values were not available for MBA. The chromatogram for the minimum detectable limit (roughly one third of the LOD) is shown in *Fig. 2.13* below overlaid with a standard of four times its concentration and just above LOD for each HA.

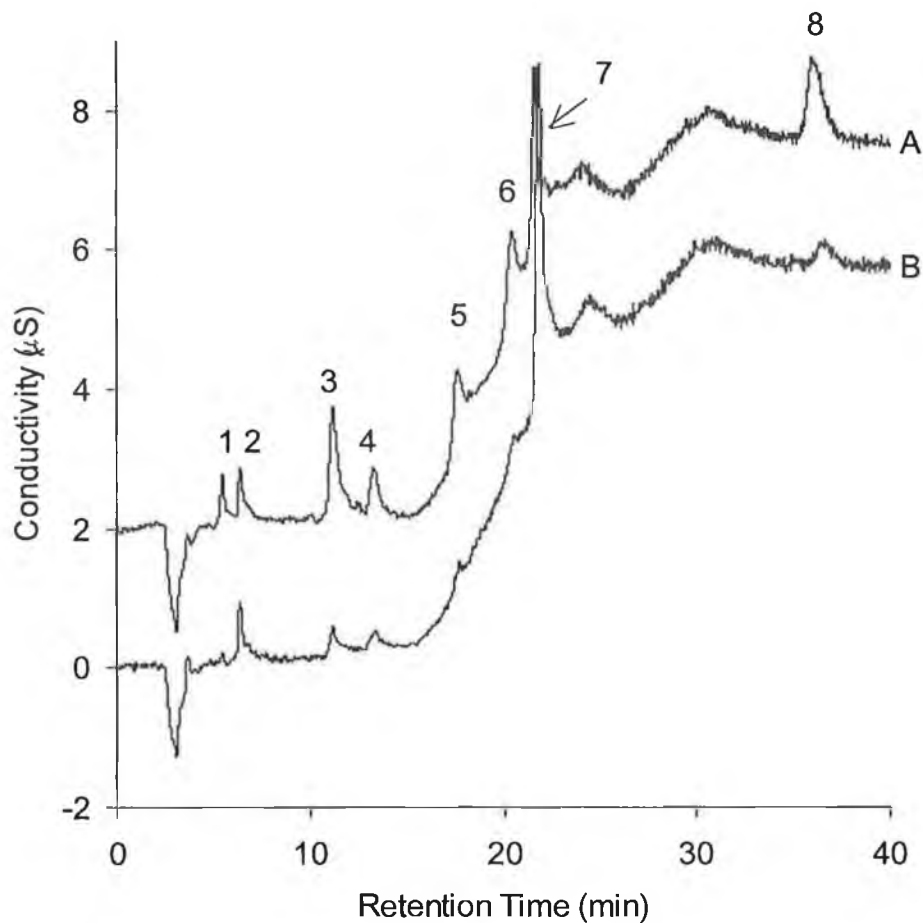


Fig 2.13. A: Standard of 5, 5, 7.5, 7.5, 15, 15, and 25 μM of the seven HAs respectively of elution order and just above LOD of S:N of 3:1. B: One-tenth concentration of A representing the MDL for the seven HAs. Elution Order: 1 = MCA, 2 = MBA/chloride, 3 = TFA, 4 = DCA, 5 = CDFAA, 6 = DBA, 7 = sulphate, 8 = TCA.

2.3.7.3.2 Separation in Drinking Waters and LOD.

This method was applied to the analysis of laboratory drinking water. LOD determination was achieved in two parts. The first six HAs were analysed first and TCA was analysed on the following day and in a different drinking water sample. Samples in the first mixture were spiked with 20, 20, 30, 30, 60 and 60 μM of each of MCA, MBA, TFA, DCA, CDFA and DBA. The samples were then sequentially diluted until close to the LOD limit as before

and the LOD value calculated from the noise levels. Similarly, TCA was spiked into a drinking water sample the following day at 0.1 mM concentration and LOD values calculated from signal-to-noise ratios. A separation was achieved, similar to the matrix-matched standards in the previous section. Nitrate concentration in the drinking water was significantly larger and separation was slightly compromised. No dissolved analytes seemed to interfere with TCA. Only four of the seven HAs were observed in the spiked drinking water sample, i.e. MCA, TFA, DBA and TCA. The resulting LOD values are listed below in *Table 2.8*. The intervals for noise calculation were from 8-10 minutes at 0.056 μ S and for TCA, noise was calculated over the timeframe 37-40 minutes at 0.304 μ S.

Table 2.8. LOD values for 4 detected HAs in a spiked water sample.

HA	[HA] for which S:N = 3:1 (μ M)	[HA] (μ g/L)
MCA	1.07	95
TFA	2.22	250
DBA	2.67	578
TCA	15.38	2505

Comparison to the LODs observed in Milli-Q show a large improvement in the LOD for DBA and a slight improvement for MCA, but LOD worsened for the other two observed HAs. *Figs. 2.14 & 2.15* show separations and LOD traces in drinking water.

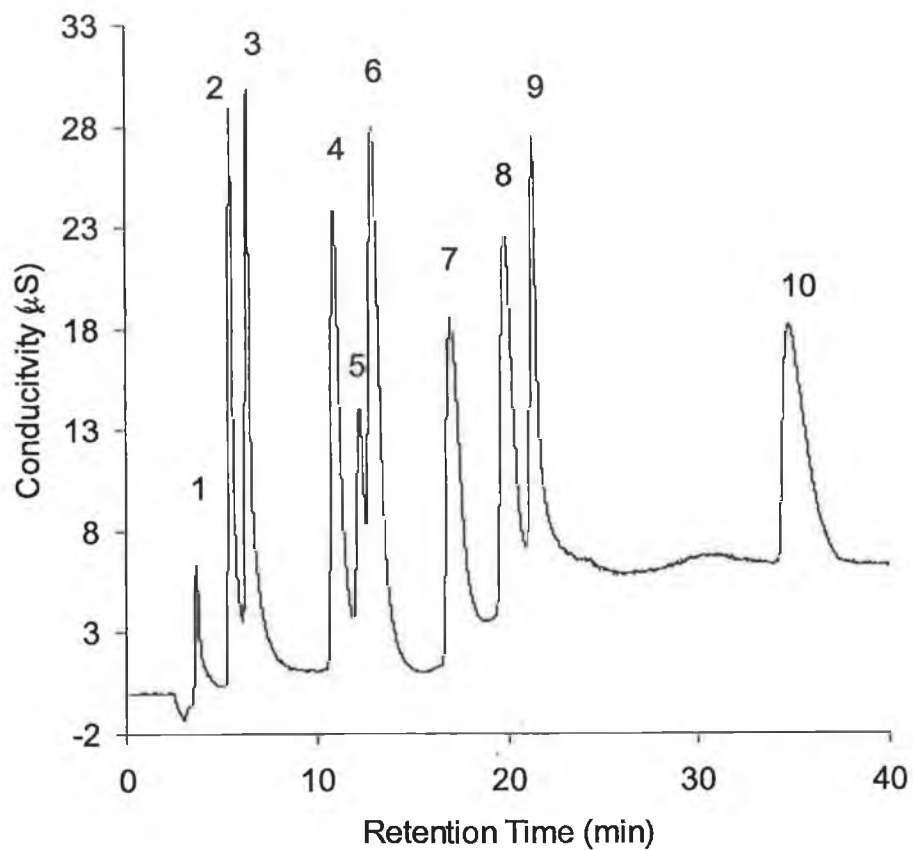


Fig. 2.14. Separation of 0.1 mM of seven HAs in drinking water using the optimum methodology. Elution Order: 1 = fluoride, 2 = MCA, 3 = MBA/chloride, 4 = TFA, 5 = nitrate, 6 = DCA, 7 = CDFA, 8 = DBA, 9 = sulphate, 10 = TCA. Loop: 25 μL .

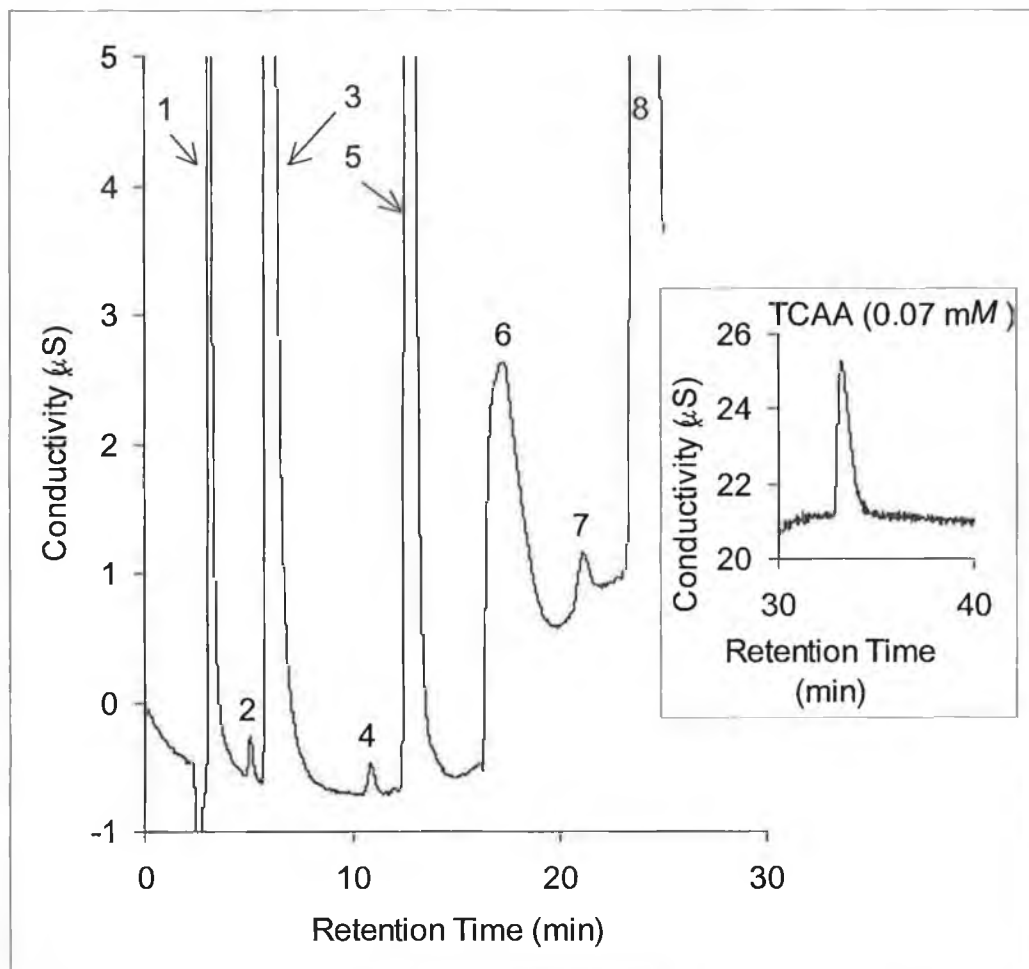


Fig. 2.15. Near LOD trace for four of the seven HAs. Elution Order: 1 = fluoride, 2 = MCA (2 µM), 3 = chloride/MBA (2 µM), 4 = TFA (3 µM), 5 = nitrate, 6 = carbonate, 7 = CDFA (6 µM), 8 = sulphate. Inset: TCAA near LOD peak (70 µM).

2.4 Conclusions

A method was developed for the separation and detection of HAs in Milli-Q and drinking water. The optimum separation involved a gradient of sodium hydroxide from 10 – 100 mM at $t = 15$ minutes for a duration of 15 minutes. The eluent concentration was kept constant for a further 10 minutes and equilibrated post acquisition for a further 10 minutes. The suppressor

current used for background noise reduction was 50 mA and displayed good suppression capability with noise readings at LOD at approximately 0.152 μ S at 10 mM NaOH concentration and twice this value at 100 mM NaOH. In Milli-Q, all HAs were well separated from each other, but when inorganic anions of chloride, sulphate, nitrate, fluoride and nitrite were added to the solution, MBA was not resolved from chloride, which was the main shortcoming of this method along with poor sensitivity. Efforts to try and separate these two peaks were unsuccessful. However, the other inorganic anions were not resolved from the HAs until column temperature was investigated. When the column temperature was raised to 40 °C, the other inorganic anions separated from their coeluting HAs, but sulphate not to baseline resolution. Van't Hoff plots show that sulphate can be selectively retained depending on column temperature. Retention of HAs increase with increasing temperature, but not to the same extent as the inorganic anions. All HAs displayed linearity ($R^2 > 0.99$), except MBA and DBA, which had slight interference from residual Milli-Q chloride and sulphate. Reproducibility studies show that for seven repeat injections, retention time varied by less than 1 % RSD for all HAs, except TCA with an RSD of 2.54 %. Peak area and peak height variations were all less than 5 %. Unfortunately, limits of detection were not as sensitive as were required with the lowest LOD value being for TFA in Milli-Q at 90 μ g/L. In drinking water samples, only four of the seven HAs were observable due to high levels of inorganic anions. In order for this method to be useful, sample pre-treatment and/or preconcentration is required to remove interference as well as boost detection limits.

2.5 References

1. B. Nowack and U. van Gunten,
Journal of Chromatography A, 849, (1999), 209-215.
2. S. Valsecchi, A. Isernia, S. Polesello and S. Cavalli,
Journal of Chromatography A, 864, (1999), 263-270.
3. J. Creed, M.L. Magnuson, J.D. Pfaff and C. Brockhoff,
Journal of Chromatography A, 753, (1996), 261-267.
4. M. Bruzzonitl, E. Mentasi, C. Sarzanini and E. Tarasco,
Journal of Chromatography A, 920, (2001), 283-289.
5. C. Sarzanini, M.C. Bruzzoniti, E. Mentasti,
Journal of Chromatography A, 1999, 850, 197-211.
6. P. Akhtar, C.O. Too, G.G. Wallace,
Journal of Chromatography, 341, (1997), 141-153.
7. V. Lopez-Avila, Y. Liu and C. Charan,
Journal of AOAC International 1999, 82, No. 3, 689-704.
8. K. Ohta, A. Towata and M. Ohashi,
Journal of Chromatography A, 2003, 997, 95-106.
9. L. Yang, L. Liu, B.A. Olsen and M.A. Nussbaum,
Journal of Pharmaceutical and Biomedical Analysis, 2000, 22, 487-493.
10. J. Hodgeson, J. Collins, R.E. Barth, Determination of Haloacetic Acids in Drinking Water by Liquid-Liquid Extraction, Derivatisation and Gas Chromatography with Electron Capture Detection, EPA Method 552.0, Revision 1.0, National Exposure Research Laboratory, Office of Research and Development, U.S. Environmental Protection Agency, Cincinnati, Ohio, USA, 1990.
11. D.J. Munch, J.W. Munch, A.M. Pawlecki, Determination of Haloacetic Acids and Dalapon in Drinking Water by Liquid-Liquid Extraction, Derivatisation and Gas Chromatography with Electron Capture Detection, EPA Method 552.2, Revision 1.0, National Exposure Research Laboratory, Office of Research and Development, U.S. Environmental Protection Agency, Cincinnati, Ohio, USA, 1995.

12. USEPA, Stage 1 Disinfectants and Disinfection By-Products Rule, May 2001. Drinking Water Regulations and Health Advisories, USEPA, Office of Ground Water and Drinking Water, Cincinnati, OH, 1996.
13. Off. J. Eur. Communities, Legis., Council Directive 98/83/EC, L330/32, 3rd November 1998.
14. P. Hatsis and C. Lucy,
Journal of Chromatography A, 920, (2001), 3-11.
15. M.A. Rey and C.A. Pohl,
Journal of Chromatography A, 739, (1996), 87-97.

Chapter 3.0

Preconcentration of HAs by solid phase extraction

"You should listen to him, he's a man of science and you can barely read"
-Lisa Simpson from the TV series, 'The Simpsons'

3.1 Introduction

Limitations with sensitivity of conventional IC detection techniques thus far has led to the development of pre-separation preconcentration procedures. Preconcentration techniques have been widely researched for analytes such as the HAs and efforts have been made to modify the USEPA liquid-liquid extraction method for use with IC. Back extractions from methyl *tert*-butyl ether (MTBE) into aqueous phases have been reported by Lopez-Avila *et al.* [1] giving high percent recoveries, but these still constitute tedious and time-consuming extraction procedures. In recent work by Liu *et al.* [2], a microwave evaporation preconcentration method has proven very successful with percent recoveries all above 96 % for nine HAs. However, no reduction in residual inorganic anions was observed and chloride had to be selectively removed by use of a Dionex On Guard II Ag cartridge (Dionex, Sunnyvale, CA, USA) prior to separation. Martinez *et al.* investigated the analysis of HAs by capillary electrophoresis with indirect UV detection [3,4] and demonstrated preconcentration of HAs in latter work by solid phase extraction using four commercially available cartridges [5]. The preconcentrated HAs were injected and separated by CE and method boasted high percent recoveries and reductions in the residual levels of inorganic anions after preconcentration. Application of solid phase extraction of HAs and separation by IC has been similarly successful. Loos *et al.* investigated four commercially available SPE cartridges [6] and concurred with results found by Martinez *et al.*, that the Merck LiChrolut EN (Merck, Darmstadt, Germany) was most applicable to the preconcentration of HAs for use with IC.

In the following study the use of SPE combined with IC and suppressed conductivity detection was developed in more detail. Merck LiChrolut EN, a polymeric ethyl vinyl benzene-divinyl benzene SPE cartridge, was identified in earlier studies as being the most suitable for HA extraction [5,6]. A full evaluation of extraction and elution conditions was carried out and optimal extraction conditions identified with real drinking

water samples containing trace levels of HAs. Elution of extracted HAs was investigated using dilute NaOH for compatibility with the IC method used. Wash conditions were determined which allowed selective removal of much of the residual chloride, nitrate and sulphate (the removal of the remainder where necessary was investigated using IC-Ba and IC-Ag clean-up cartridges). The analytical performance of this extraction method was fully evaluated, including percentage recoveries and extraction reproducibility, once again in real samples. The combination of the optimised extraction and separation conditions were then applied to drinking water samples collected and analysed over summer and winter periods.

3.2 Experimental

3.2.1. Reagents

All chemicals were of analytical grade purity and were obtained from Aldrich (Milwaukee, WI, USA). Stock HA solutions of MCA, DCA, TCA, TFA, CDFA, MBA and DBA were prepared to a concentration of 10 mM and were stable for approximately 2 weeks when stored at 4 °C in the dark. Working standards were prepared fresh daily using water from a Milli-Q water purification system (Millipore, Bedford, MA, USA). Sulphuric acid (99 % purity) was used for acidification of samples to be preconcentrated. All standards and samples were prepared in ultra pure water delivered from a Milli-Q water purification system (Millipore, Bedford, MA, USA) and working standards were prepared daily.

3.2.2 Instrumentation

All separations were carried out on a Dionex DX500 system (Dionex, Sunnyvale, CA, USA) comprising of a GP50 pump, a CD20 conductivity detector complete with Dionex ASRS Ultra (2 mm) suppressor at 50 mA and an LC25 chromatography oven at 40°C. Separations were carried out with a Dionex IonPac AS11-HC ion exchange column at an eluent flow rate of 0.30

mL/min. The injector loop volume was 100 μ L. Instrument control, data acquisition and analysis were carried out with a Dell personal computer with Dionex Peak Net Version 6.0 software installed. All IC conditions were similar to that optimised in Chapter 2.0, with a hydroxide gradient of 10-100 mM NaOH after 15 minutes for a duration of 15 minutes and kept constant for a further 10 minutes at 100 mM NaOH. Post separation re-equilibration time was 10 minutes. For preconcentration, Merck LiChrolut EN cartridges were employed (Merck, Darmstadt, Germany) which comprise of a 3 mL internal volume cartridge housing 200 mg of the EVB-DVB copolymer. Automated preconcentration was not carried out under vacuum, as highly regulated low flow rates were required and was achieved using a Gilson Minipuls 3 peristaltic pump (Gilson, Middleton, WI, USA).

3.2.3 Procedures

Cartridges were conditioned prior to use using two rinse steps of 3 mL methanol, followed by 3 mL of 200 mM sulphuric acid. Acidification of samples was carried out by taking a 4.5 mL aliquot of sulphuric acid and adding to 50 mL of sample solution. This corresponded to a theoretical pH of -0.48 . The total 54.5 mL acidified samples were pumped through the preconditioned LiChrolut EN cartridges at a flow rate of 2 mL/min. After the acidified sample/standard was preconcentrated, the cartridge was washed with 1 mL of Milli-Q water to remove any excess unbound sulphate. The optimum eluent was found to be 2 mL of 10 mM NaOH. Thus, the overall preconcentration procedure resulted in a 25-fold preconcentration factor for all analytes involved. It should be noted that percent recovery in this work is defined as the percentage of the quotient of the peak height of an HA extracted from a spiked, preconcentrated solution in Milli-Q water and the peak height of a freshly prepared standard that is 25 times the concentration of the sample spike, also in Milli-Q water.

3.3 Results and Discussion

3.3.1 Extraction and elution of HAs using LiChrolut EN SPE cartridges

The aim of this work was to develop a practical and reliable means of preconcentration HAs prior to quantitation using IC. The use of anion exchange cartridges for this purpose was deemed unsuitable, as common matrix anions would also be preconcentrated making the subsequent IC separation more complex. In addition to this, high levels of matrix anions would inevitably affect recovery of HAs due to 'self elution' effects, as mentioned by Lopez-Avila *et al.* in relation to EPA Method 552.1 [14]. Therefore, preconcentration of protonated HAs on polymeric reversed-phase materials was seen as the most promising approach. For the successful preconcentration of HAs it was deemed necessary to acidify sample/standard solutions to below pH 0.3. The pK_a values for the HAs are all in the range 0.65 to 2.90 (with the exception of TFA with a pK_a of 0.30). From previous research by Martinez *et al.* [5], Loos *et al.* [6] and Sarzanini *et al.* [7], the hyper-crosslinked EVB-DVB LiChrolut EN SPE cartridges (Merck, Darmstadt, Germany) appeared to provide the most acceptable % recovery values for the HAs, in some cases up to 10 times the capacity of other available sorbents. However, in each of the above studies HA sample/standard solutions were adjusted to different pH values prior to preconcentration, ranging from pH 0.5 to 1.8, and so large variations in recovery data were reported. On closer inspection, the results of the three above studies are not entirely unexpected, as work on similar hypercrosslinked PS-DVB phases by Penner and Nesterenko have shown greater affinity for hydrophilic species than seen with normal PS-DVB phases. In fact, Penner and Nesterenko showed that using only hyper crosslinked PS-DVB resin, actual separations of inorganic anions could be obtained, illustrating that under acidic conditions the material exhibited some degree of surface charge.

3.3.2 Determination of the eluting agent

In a preconcentration procedure developed by Sarzanini and co-workers, the bound HAs were eluted from the SPE cartridge with methanol [7]. It was found in our preliminary experiments that methanol caused a notable disturbance in chromatography baselines shortly after the void volume and was deemed unfit for use. HAs are highly soluble in aquatic solvents, but Milli-Q water yielded surprisingly poor percent recoveries at less than 20 % for all HAs. However, it was suggested that weak hydroxide solutions be used, both for IC eluent compatibility and to deprotonate bound HAs by increasing alkalinity. Such an increase in alkalinity was expected to lead to an increase in polar character and should cause desorption of HAs from the cartridge stationary phase into the eluent. Two concentrations were investigated to match the eluent hydroxide concentration of 10 and 100 mM NaOH used in the IC gradient elution. It was found that the percent recoveries for CDFA and DCA using 100 mM hydroxide as the eluting agent were marginally better than when 10 mM NaOH solution (*Table 3.1.*) was used. Considering that 100 μ L of 100 mM NaOH was such a large concentration to be injected onto this micro-bore column, it was not surprising that a very large interferent peak was observed eluting immediately after the void volume dip. As a result, obscured peaks were observed for MCA, MBA and TFA and did not allow accurate calculation of % recoveries at this hydroxide concentration. Conversely, the 10 mM NaOH eluting agent offered minimal interference and only with marginally poorer % recoveries. In addition, % recoveries were easily calculated for the early eluting HAs. From this, it was decided that 10 mM NaOH would be assigned as the eluting agent.

Table 3.1 Effect of NaOH concentration on % recovery.

HA	10 mM NaOH % Recovery	100 mM NaOH % Recovery
MCA	37	27
MBA	59	165
TFA	11	7
DCA	100	106
CDFA	46	70
DBA	Coelutes with sulphate	Coelutes with sulphate

It should be noted that TCA percent recoveries were not included here as the percent recovery of TCA remained high, even with increasing volume preconcentrated and will be illustrated later. It should be noted that percent recoveries for TFA were very poor at 11 %. This was due to the low pK_a of this acid. Considering that a theoretical pH of -0.48 was used, it was felt that any further reduction in pH may have adversely affected the EVB-DVB stationary phase.

3.3.3. Sample load rate and recoveries

As part of optimisation of the preconcentration step it was necessary to assess the effect of sample loading rate upon HA recoveries. Martinez *et al.*, [5] prescribed the use of sample load rates of 15 mL/min. When these rates were attempted in this study, HA recoveries were very poor, in most cases < 10 %. Hence, lower load rates of 1, 2 and 3 mL/min were investigated here. At the same time, the minimum volume of 10 mM NaOH required to elute the HAs was also determined. Standards of 5 μ M MCA, MBA, TFA and DCA and 10 μ M CDFA and DBA were converted to their

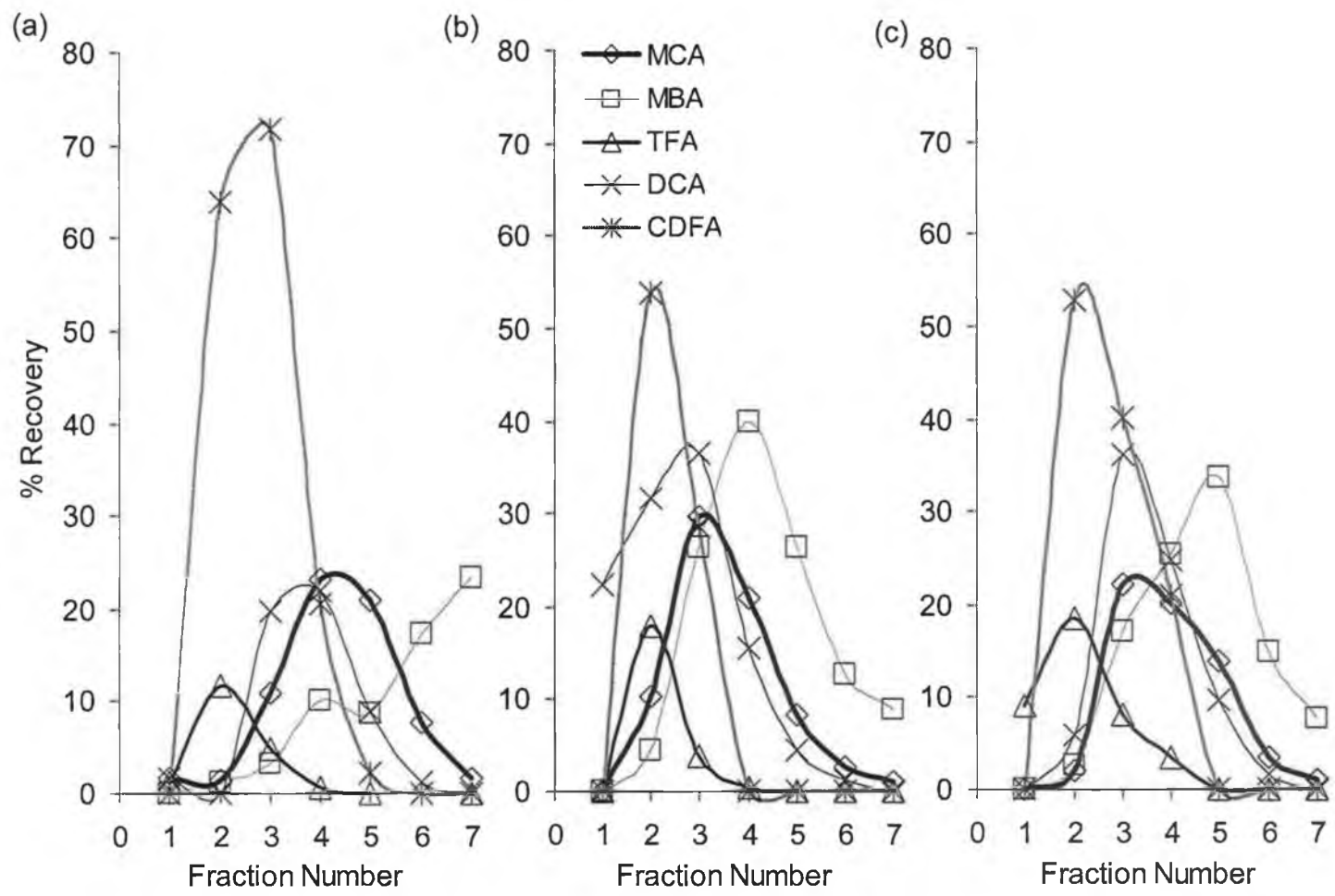


Fig. 3.1 Percent recoveries and elution profiles for HAs within each 0.5 mL fraction of eluate at three preconcentration flow rates on LiChrolut EN SPE cartridges. Eluent = 10 mM NaOH; (a) eluent = 1 mL/min; (b) eluent = 2 mL/min; (c) eluent = 3 mL/min sample loading flow rate.

respective acids and pre-concentrated at each of the above flow rates. After pre-concentration, 0.5 mL of Milli-Q water, followed by seven individual fractions of 0.5 mL of 10 mM NaOH were passed through the SPE cartridge, individually collected and analysed using IC.

As expected, the results showed that percent recoveries were much improved at lower flow rates. *Fig. 3.1* shows the elution profiles at varying sample load rates for 5 HAs (chosen to cover large range in pK_a values) obtained during the above experiment.

Percent recovery for the HAs and elution profiles for the three loading rates were relatively similar, although a number of clear trends were evident. For example, TFA showed the lowest affinity for the phase under the conditions used, clearly due to its very low pK_a . Alternatively, the recoveries for CDFA were very high, although interestingly the elution of CDFA was similar to TFA, as both acids could be quantitatively eluted from the SPE cartridge in <2.5 mL of 10 mM NaOH. Recoveries for MCA, DCA and MBA were found to be the highest at a load rate of 2 mL/min, with a total of 3.0 mL of 10 mM NaOH required to quantitatively elute the acids from the cartridge. For all of the acids investigated, the results showed that, in the initial 0.5 mL of Milli-Q water passed through the cartridge, there was very little elution of the pre-concentrated acids. This was very significant, as it allowed the selective elution of sample matrix anions, particularly excess sulphate (later this wash step was increased to 1.0 mL again without any significant further elution of retained HAs). To determine precision, the above study was repeated in triplicate (using fresh SPE cartridges for each pre-concentration) at 2 mL/min, this time with the inclusion of TCA. The pre-concentrated acids were then eluted with 2.0 mL of 10 mM NaOH and recoveries calculated. From analysis of the results shown in *Fig. 3.1* it is clear that the use of 2.0 mL of NaOH to elute the acids results does not result in quantitative elution of all acids. However, close analysis of the elution curves, illustrates how using larger elution volumes would produce a more dilute extract, (albeit with higher % recoveries). This study of elution profiles highlights the deficiencies in many studies that quote % recovery

data without investigating the effects of elution volume. Table 3.2 shows the average % recoveries obtained for the above HAs, together with the % RSD of these recovery data, based upon triplicate results. Table 3.2 shows acceptable recoveries for all but TFA under the conditions used. Recovery data for DBA is not shown due to close elution of DBA with sulphate on the AS11-HC column. However, the elution profile of DBA was found to be similar to MBA. Precision of the preconcentration procedure was found to range from approximately 10 to 30 % (average RSD of 17 % for 6 HAs).

3.3.4 *Durability of the LiChrolut EN cartridge*

Due to the use of low pH, the stationary phase may become unstable with successive preconcentrations on the same cartridge. In this short study, the durability of the LiChrolut EN cartridge after six successive preconcentrations was assessed. Fresh working standards of 5 μM MCA, MBA, TFA and DCA and 10 μM CDFA, DBA and TCA were prepared and preconcentrated on the same cartridge in order to compare directly to the calculated % recoveries obtained for replicate preconcentrations carried out on separate SPE cartridges. After six successive preconcentrations, the repeatability of % recovery values was comparable to that of the repeatability study on fresh cartridges, indicating little or no effect of low pH on the cartridge stationary phase. Further preconcentrations were carried out using one cartridge and it was found that repeat preconcentrations could be carried out on the cartridge for much more than six repeats as long as sufficient methanol cleaning was carried out between each successive preconcentration procedure. Repeatability data can be observed in Table 3.2.

Table 3.2 Recovery and precision data for preconcentration of HAs on LiChrolut EN SPE cartridges.

HA	Standard concentration (μM) ^a	Eluent volume (10 mM NaOH) ^b (mL)	Average % recovery between SPE cartridges ($n=3$) ^c	% RSD ($n=3$) ^c	Average % recovery with single SPE cartridge ($n=6$) ^d	% RSD ($n=6$) ^d
MCA	5	2.0	65	10	66	15
DCA	5	2.0	84	10	82	12
TCA	10	2.0	58	13	62	11
MBA	5	2.0	63	28	66	16
CDFA	10	2.0	87	15	88	13
TFA	5	2.0	17	23	16	29

^aAdjusted using sulphuric acid.

^bFollowing 1.0 mL wash using Milli-Q.

^cEach repeat preconcentration carried out using fresh SPE cartridges.

^dSix repeat preconcentrations carried out on single SPE cartridge.

3.3.5 Capacity of LiChrolut EN cartridge

For application to drinking water analysis any developed method must be capable of detection of HAs at levels well below 60.0 µg/L, this being the EPA regulated MCL for the sum total of MCA, MBA, DCA, DBA and TCA. As yet, there are no MCLs for fluorinated carboxylic acids included in the drinking water quality regulations. To achieve such low limits of detection it was important to evaluate the maximum sample preconcentration volumes possible (maximum preconcentration volume determined as volume of sample resulting in highest average % recovery). As before, a standard solution containing 5 µM MCA, DCA, MBA, TFA and 10 µM CDFA, DBA and TCA was prepared and volumes of 10, 20, 50 and 250 mL were preconcentrated on the LiChrolut EN cartridge at optimal conditions and % recoveries calculated. It was noticed that maximum percentage recoveries corresponded to the 50 mL sample volume (25-fold preconcentration factor) for all but TFA and MCA, and hence this volume was used for all subsequent studies. This data is shown in *Fig. 3.2*. The figure shows the significant effect sample volume has upon analyte recovery, with small sample volumes resulting in significantly poorer recoveries. The reason for this low recovery data for small sample volumes initially seemed unusual. However, as mentioned above, it is clear from Penner and Nesterenko's study [8] that a dual retention mechanism exists with hyper-crosslinked PS-DVB resins, which indicates both reversed-phase and anion exchange interactions contribute to retention. Therefore, it may be the case that some minor portion of the analytes are filling these anion exchange sites and are not being removed with the NaOH eluent. This effect would obviously be most significant at lower sample volumes and result in the type of recovery trend show in *Fig. 3.2*. Further evidence of this dual retention mechanism perhaps lies in the fact that recovery of TCA was the lowest of all the analytes investigated at low sample volume, and that TCA also exhibits the highest affinity for alternative standard anion exchange resins of all the analytes shown. In addition, the recovery data for MCA and MBA was the highest at low sample volume, with these analytes exhibiting least retention on standard anion exchange resins. At the higher sample volumes it is clear the overall

capacity of the cartridge is being exceeded and analyte breakthrough is occurring. These recovery versus sample volume results are very significant for future users of hyper-crossed linked EVB-DVB resins for preconcentration of polar analytes, as they illustrate that on such materials, an understanding of the exact retention mechanism is required if suitable elution procedures are to be identified and acceptable recoveries obtained.

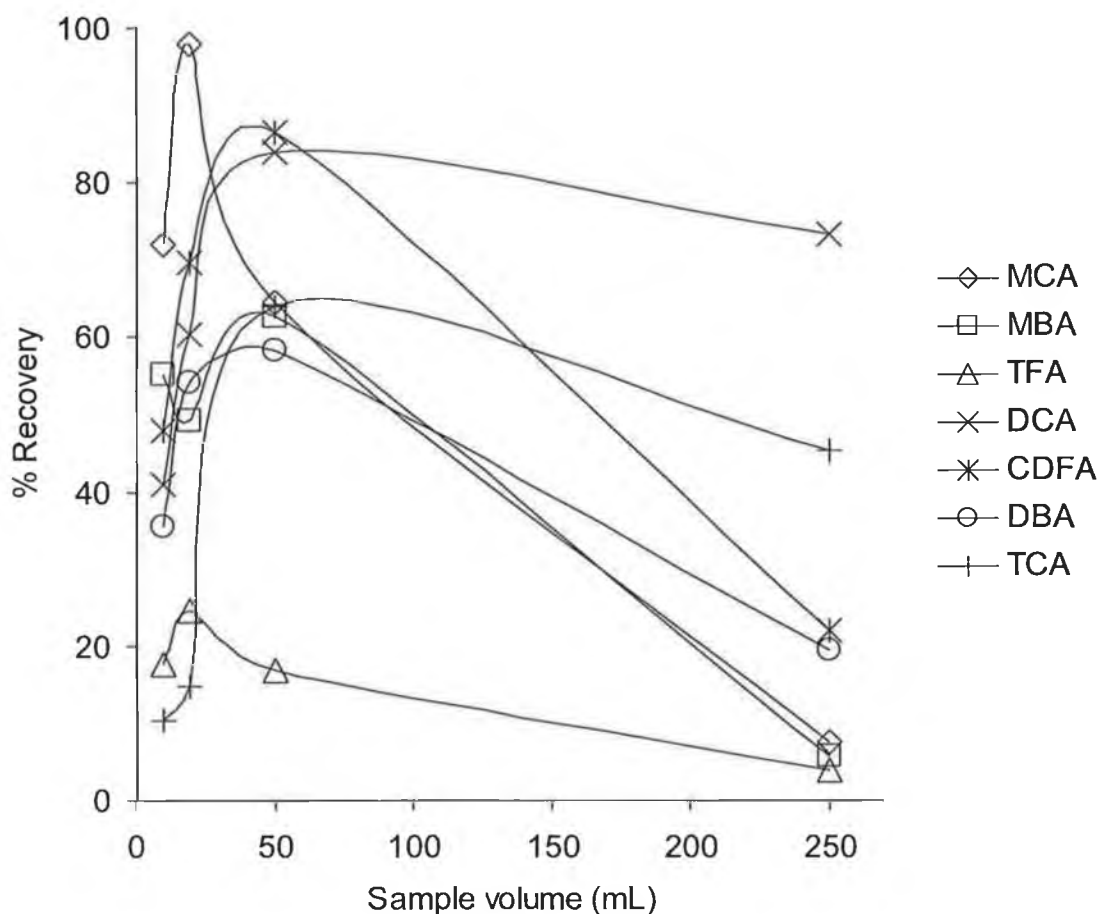


Fig. 3.2 Capacity study for LiChrolut EN cartridge. Volumes of 10, 20, 50 and 250 mL of 5 μ M MCA, MBA, TFA and DCA and 10 μ M CDFA, DBA and TCA pre-concentrated to 2 mL NaOH with LiChrolut EN cartridge.

3.3.6 Analysis of real samples

The preconcentration methodology was applied to real samples collected from three sources within Dublin City and one in Celbridge, Co. Kildare and run at optimum conditions on the IC. Standards containing 1, 2, 3, 4 and 8 μM of the identified HAs were prepared in Milli-Q and run in duplicate. Calibration curves using peak area were plotted and all R^2 values were greater than 0.98 at this concentration range. Samples from the four sources were acidified to below pH 0.3 to convert them to their respective acids and preconcentrated on fresh LiChrolut EN cartridges in duplicate. HA determinations by IC are listed in *Table 3.3* and all calibration curves can be found in *Appendix A.2 (Fig. A.2-1)*.

Table 3.3 Identification and quantification of HAs from four sources in Dublin City and Co. Kildare.

Source	HAs identified	Concentration ($\mu\text{g/L}$) ^a	Error ($\mu\text{g/L}$) ^b
Dublin City University, North Dublin City, Ireland	MCA	2 (± 0.1)	± 0.2
	DCA	7 (± 0.3)	± 0.7
	TCA	20 (± 0.8)	± 2.6
Drumcondra, Inner Dublin City, Ireland	MCA	0.34 ($\pm < 0.1$)	$\pm < 0.1$
	DCA	45 (± 2.0)	± 4.5
Ballsbridge, South Dublin City, Ireland.	DCA	40 (± 1.8)	± 4.0
Celbridge, Co. Kildare, Ireland.	DCA	10 (± 0.1)	± 0.1

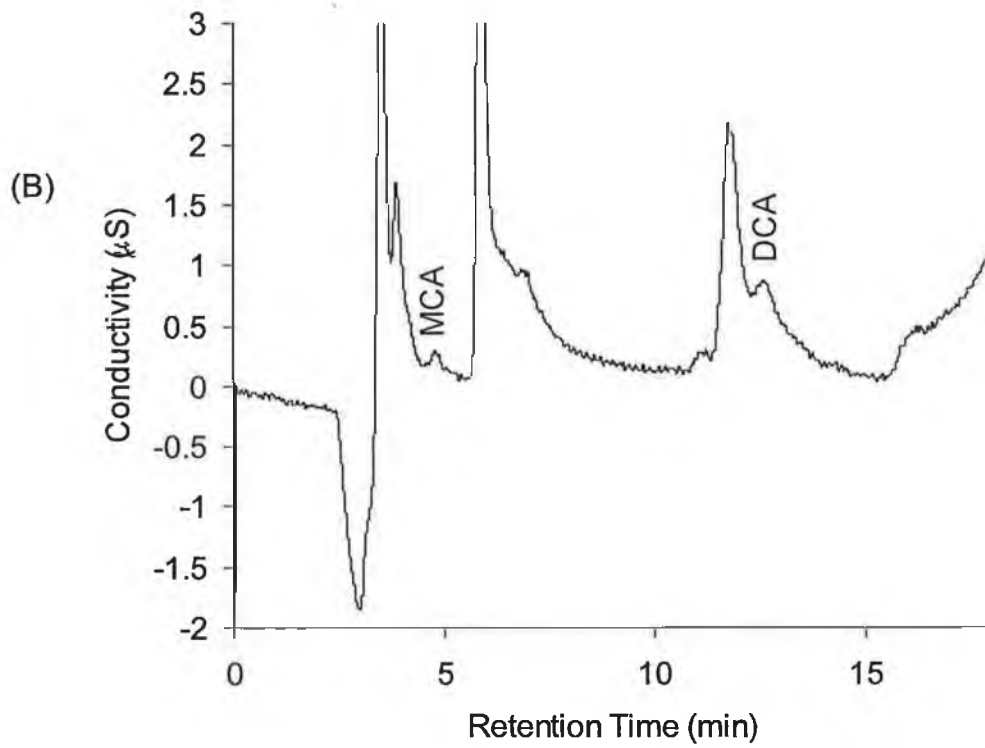
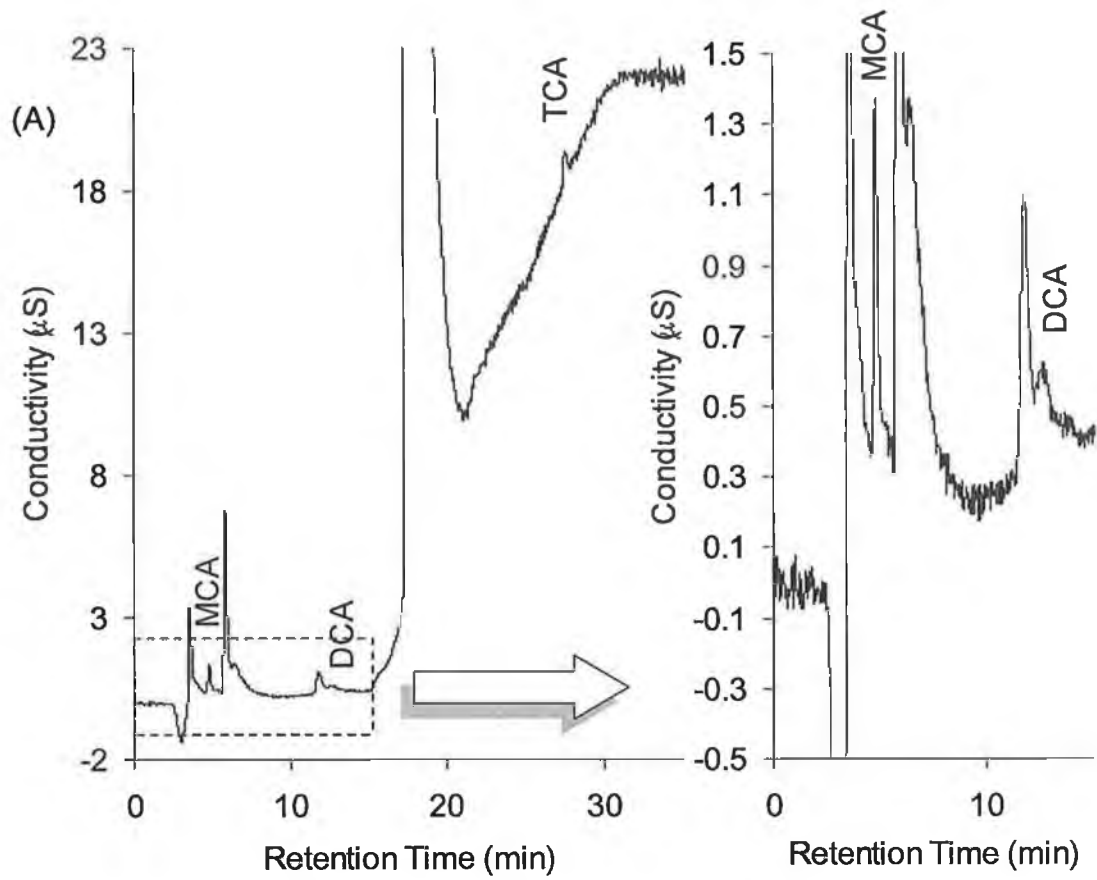
^a Errors calculated based on variations in peak height from duplicate runs of each preconcentrated sample

^b Errors calculated in accordance with Table 3.2

In all cases, levels of DCA were observed (see *Fig. 3.3*). With the exception of the university drinking water source, DCA levels on that day in the other two urban Dublin drinking water sources were almost four times that of the nearest satellite town of Celbridge in Co. Kildare. Sum totals of HAs were 29 $\mu\text{g/L}$ (Dublin City University), 45 $\mu\text{g/L}$ (Drumcondra), 40 $\mu\text{g/L}$

(Ballsbridge) and 10 µg/L (Celbridge) and were all within the USEPA regulations of 60 µg/L for the total of MCA, MBA, DCA, DBA and TCA. However, DCA is regulated never to be present, but in the resulting ion chromatograms DCA appeared repeatedly in all cases, suggesting it forms readily within water chlorination systems. Results from this study also show that fluorination of water causes no formation of TFA or CDFA at this detection level.

Another observed improvement when using preconcentration briefly mentioned earlier was the reduction of interferent inorganic anion concentrations in the samples. The method gave rise to an inherent *self-cleaning effect*. This was no doubt due to the fact that nitrate would not have preconcentrated at the adjusted pH due to the extreme pK_a of nitric acid. However, some levels of nitrate were still present in the samples and as discussed earlier, may have been due to some reversed phase interactions, since the LiChrolut EN cartridge was a hypercrosslinked polymer. It was both expected and observed that levels of nitrite were present and the anion preconcentrated quite readily and was observed as a peak directly after the chloride/MBA pair and fortunately did not pose any further interference. In addition to nitrate, there was a significant reduction in sulphate levels in the samples, and although still in excess of all other anions present due to the acidification step, was not present in sufficient concentration to overload the analytical column. Moreover, chloride concentration decreased markedly, but unfortunately not enough to allow resolution from any MBA present.



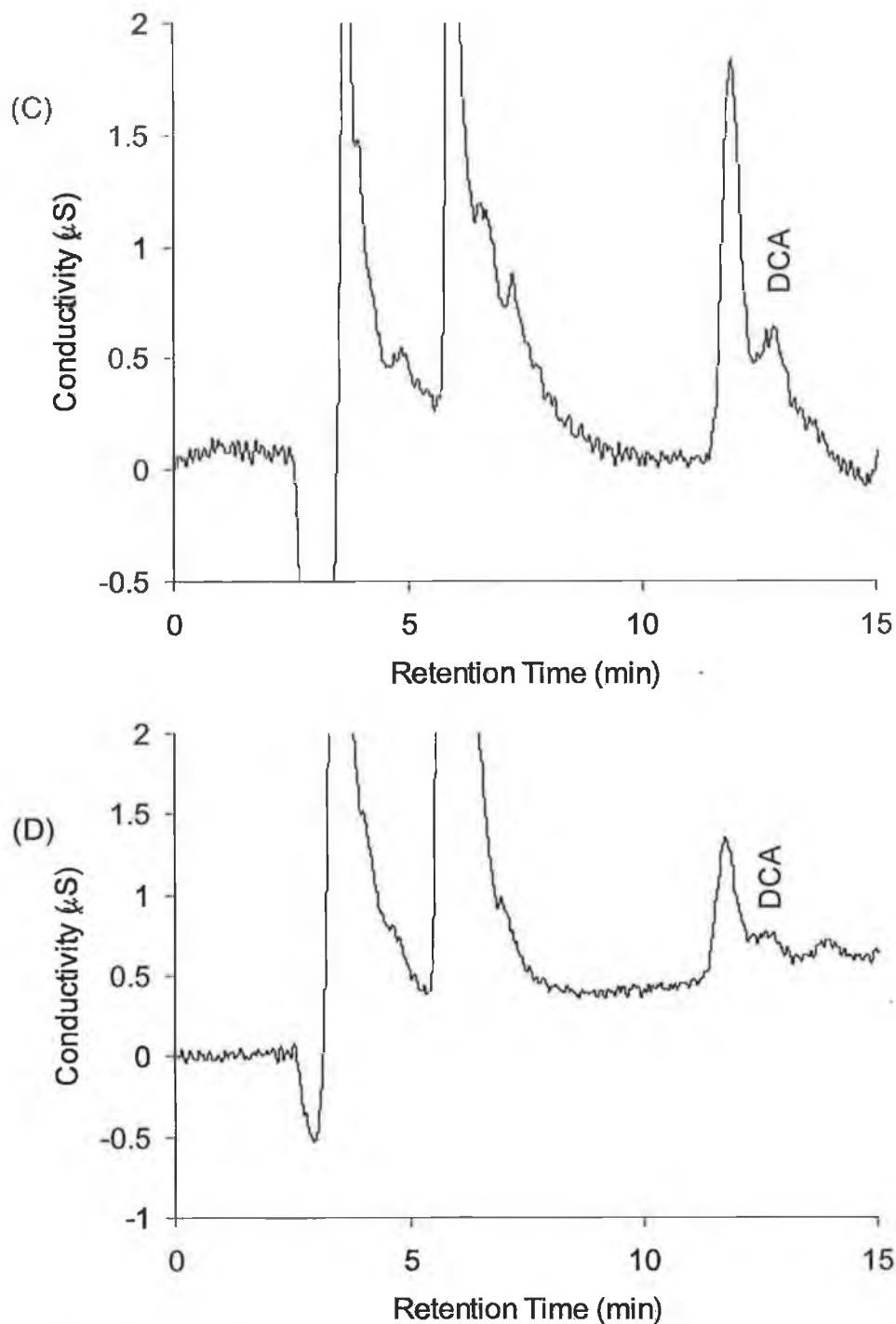


Fig. 3.3 Chromatograms of preconcentration of drinking water using LiChrolut EN solid phase extraction cartridges from (A) Dublin City University showing MCA, DCA and TCA with inset enlarged to the right (B) Drumcondra showing MCA and DCA (C) Ballsbridge showing DCA and (D) Celbridge Co. Kildare showing levels of DCA.

3.3.7 Standard Addition

It was necessary to more accurately represent the sample matrix for quantification purposes, so a standard addition experiment was carried out for determination of any of the seven HAs present in a drinking water sample. A 1 L drinking water sample was collected from our laboratory using the sampling procedure outlined above and preconcentrated in the usual manner. After separation by IC it was observed that the only HA present was DCA. As a result, four further 50 mL aliquots of the same sample were spiked with DCA at concentrations of 0.2, 0.4, 0.8 and 1.0 μM . Following the usual acidification to below pH 0.3, the spiked samples were preconcentrated on the LiChrolut EN cartridge and run on the IC. Peak heights were collected for DCA and plotted versus concentration of DCA spike. From the standard addition curve in *Fig. 3.4*, it can be observed that the corresponding concentration of DCA found in the drinking water samples on that day was 0.27 μM or 34 $\mu\text{g/L}$ (*Fig. 3.5*) which also lies in the concentration range of the calibration curve experiment above and is below the USEPA limit of 60 $\mu\text{g/L}$. Another point to note was the correlation of the linearity data collected for DCA. An R^2 value of 0.98 displays acceptable linearity, though not ideal. It was expected that linearity would be poorer than that found for the IC method in Chapter 2, as there were many sources of error in the preconcentration procedure. Linearity is shown in later work for all HAs using this LiChrolut EN preconcentration technique.

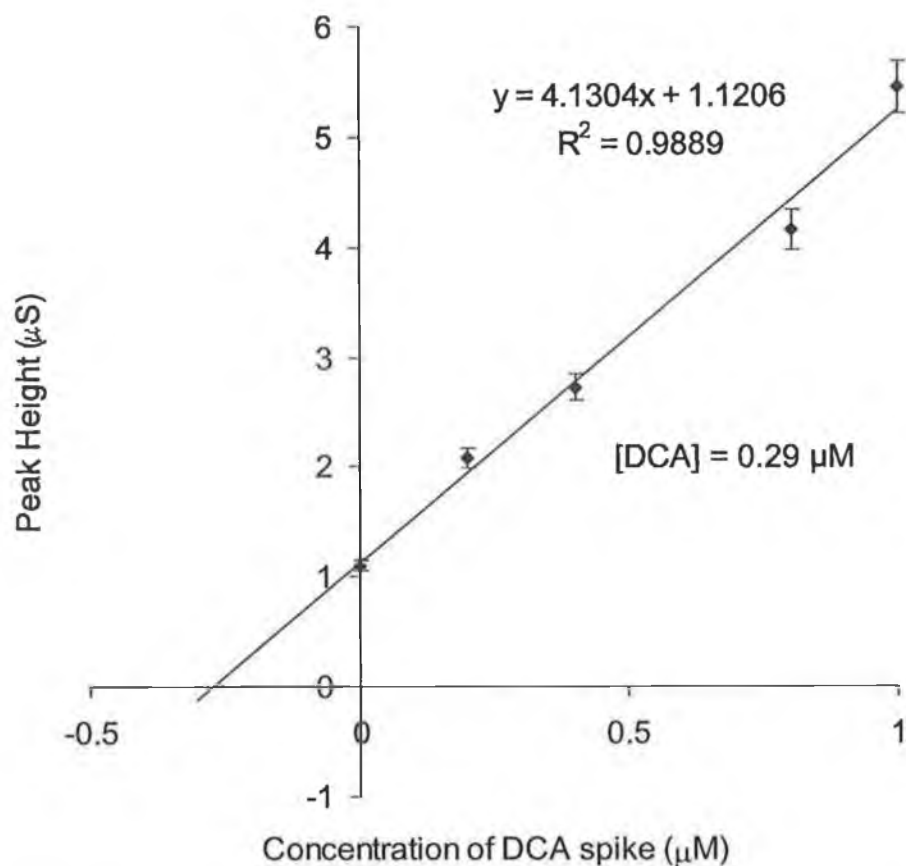


Fig. 3.4 Standard addition curve for DCA found in Dublin City University drinking water source. $[\text{DCA}] = 0.29 \mu\text{M}$ or $34 \mu\text{g/L}$.

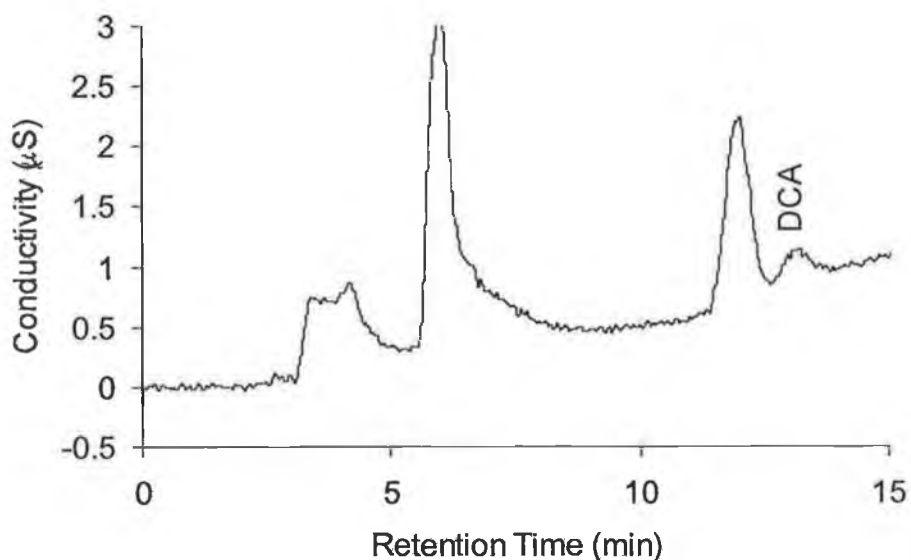


Fig. 3.5 Preconcentrated unspiked sample of Dublin City University drinking water source. Standard addition shows that DCA was present at a concentration of $34 \mu\text{g/L}$ on that date.

3.4 Conclusion

This work demonstrated further applicability of IC to the analysis of HAs with separation and detection of seven HAs now in the $\mu\text{g/L}$ range. Preconcentration of trace levels of HAs below previously reported LOD levels in Chapter 2.0 was achieved and was found that percent recoveries were above 58 % for all HAs except TFA, which with a very low $\text{p}K_a$ value of 0.30, was difficult to protonate successfully without damaging the cartridge stationary phase. The maximum preconcentration capability for the Merck LiChrolut EN cartridge showed that the majority of bound HAs on the stationary phase could be unbound with a minimum of 2 mL of 10 mM NaOH from an overall original sample volume of 50 mL resulting in a 25-fold preconcentration factor. Washing the cartridge with 1 mL of water reduced overall residual nitrate to negligible levels and sulphate due to acidification is dramatically reduced. As a result, drinking water samples with mg/L concentrations of nitrate could easily be resolved from $\mu\text{g/L}$ DCA concentrations. Repeatability studies for six preconcentrations on fresh cartridges demonstrated that percent recoveries vary with a standard deviation of less than 9 % for all HAs. For six successive injections on the same cartridge, the LiChrolut EN cartridge maintained its ability to preconcentrate with similar percent recoveries within the standard deviation quoted in experiments carried out on fresh cartridges. The capacity of the cartridge was assessed and it was found that DCA and TCA had a greater affinity for the EVB-DVB stationary phase than the MCA and all brominated forms. Real samples were successfully preconcentrated and levels of MCA, DCA and TCA were observed and quantified successfully by both standard calibration and standard addition methodologies. Standard addition curves show that when a real sample was spiked with increasing DCA concentrations, that linear increases in peak height were observed when the preconcentration technique was employed.

3.5 References

1. V. Lopez-Avila, Yan Liu and Chatan Charan,
Journal of AOAC International 1999, 82, No. 3, 689-704.
2. Yongjian Liu and Shifen Mou, Microchemical Journal, 2003, In Press.
3. D. Martínez, J. Farré, F. Borrull, M. Calull,
Journal of Chromatography A, 1999, 835, 187-196.
4. D. Martínez, J. Farré, F. Borrull, M. Calull, J. Ruana, A. Colom,
Journal of Chromatography A, 1998, 808, 229-236.
5. D. Martínez, F. Borrull, and M. Calull,
Journal of Chromatography A, 1998, 827, 105-112.
6. R. Loos, D. Barceló,
Journal of Chromatography A, 2001, 938, 45-55.
7. C. Sarzanini, M.C. Bruzzoniti, E. Mentasti,
Journal of Chromatography A, 1999, 850, 197-211.
8. N.A. Penner, P.N. Nesterenko, Journal of Chromatography A, 884
(2001), 41.

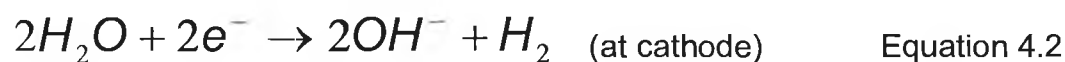
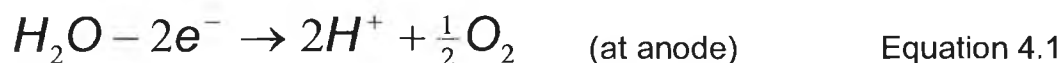
Chapter 4.0

Reagentless ion exchange chromatography of haloacetates and separations with an AS16 column

"In science the credit goes to the man who convinces the world, not the man to whom the idea first occurs", Sir Francis Darwin (1848 - 1925), -Eugenics Review, April 1914

4.1 Introduction

Electrolytic Eluent Generation (EG) is a relatively new technology introduced to further automate the IC process. Its main advantage is the production of high purity eluents with only the addition of deionised water. Furthermore, the interference due to carbon dioxide dissolution in low concentration hydroxide eluents is almost fully removed due to a combination of the air-sealed generation process and the use of an anion trap column prior to the separation step. At the heart of the generation process, is the generator cartridge. For the anion separations carried out here, only hydroxide eluent generators will be discussed. The cartridge consists of a high pressure KOH generation chamber and a low pressure K^+ reservoir. A platinum cathode is placed in the K^+ reservoir to generate K^+ ions and a similar anode in the KOH generation chamber. To generate a hydroxide eluent, deionised water is pumped through the KOH generation chamber and a DC current is applied across the electrodes. Electrolysis of water occurs at the anode and cathode. At the anode H^+ ions and oxygen gas are created and displace the K^+ ions from the electrolyte, see Equation 4.1. The KOH generation chamber is connected to the K^+ reservoir by a cation exchange membrane connector and only cations can migrate across it. At the cathode, OH^- ions combine with migrating K^+ ions to form the KOH solution, see Equation 4.3.



The concentration of this solution is inversely related to the flow rate of the deionised water through the KOH generation chamber and directly related to the DC current applied across the electrodes. A schematic of this process

can be seen in *Fig. 4.1*. Control of the device is by simple on screen manipulation of the desired concentration. This conception offers the possibility to carry out complex gradient separations without the need for extensive eluent preparation for optimisation.

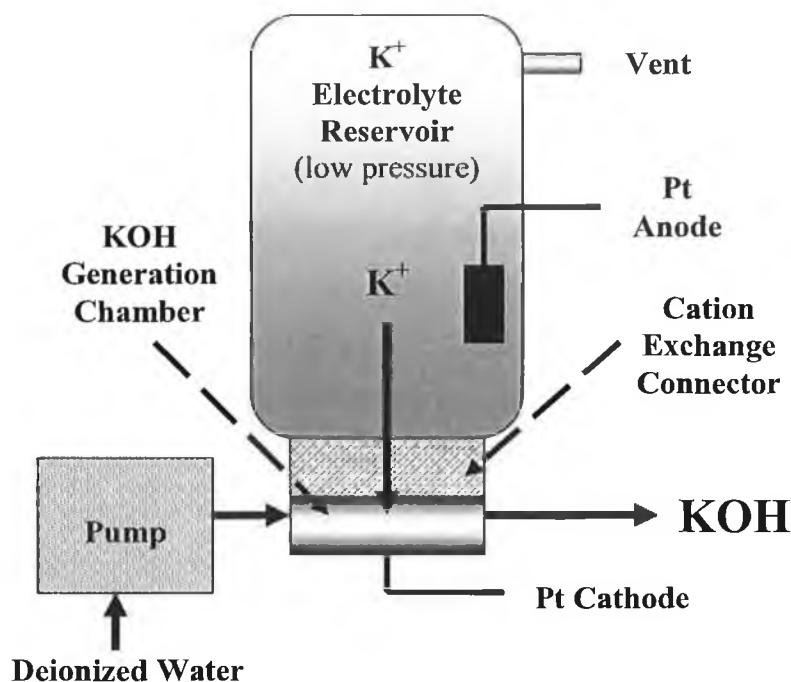


Fig 4.1. Schematic of the eluent generation process [1].

The continuously regenerated anion trap column CR-ATC is another useful device for the further purification of eluent. To remove any trace levels of inorganic anions, namely sulphate, carbonate and chloride, from the deionised water, the flow from the eluent generator module is directed through the CR-ATC prior to the injector valve and separator column. The CR-ATC column consists of two chambers. The chamber carrying the eluent flowing to the separator column contains a cathode at which electrolysis of water occurs, generating OH⁻ ions. Suppressed eluate from the conductivity detector flows through the other chamber which contains the anode and where generation of H⁺ ions occurs. Once a current is applied, any anionic

impurities in the eluent are transported across an ion exchange membrane to the anode. The OH⁻ ions at the cathode also pass across this membrane and serve to continuously regenerate the anion exchange bed and the hydronium ions combine with the removed anionic impurities to form acids. Thus, the solution leaving the CR-ATC is a purely alkaline solution of KOH. A schematic of this process is illustrated in Fig. 4.2.

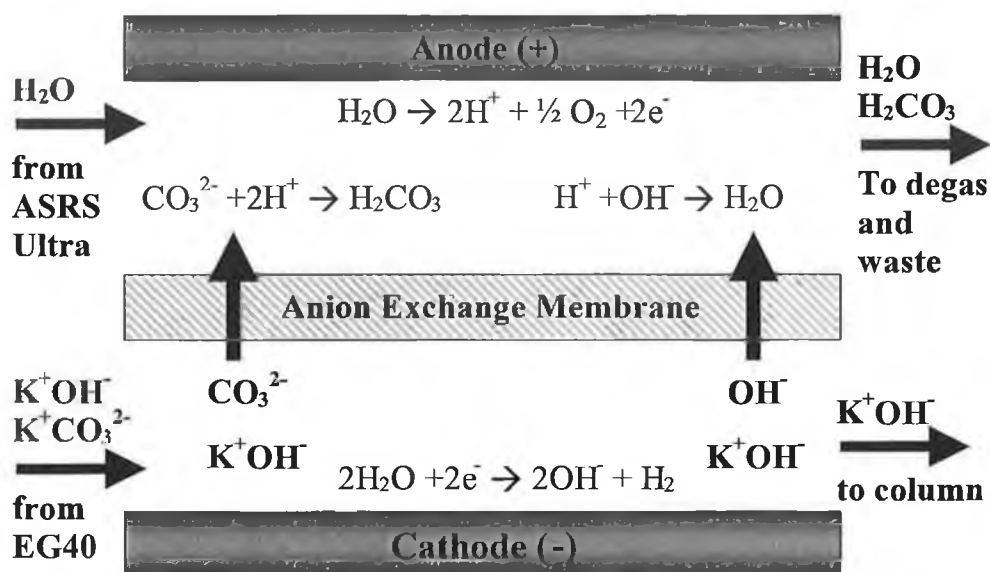


Fig. 4.2. Schematic of the continuously regenerated anion trap column (CR-ATC) [2].

The aim of this experiment was to assess the suitability of this system for the analysis of HAs. In addition to this, factors such as reproducibility, limit of detection and direct application of the optimised method were investigated. Up to this stage, separation of chloride from MBA had not been successful. Separation of chloride from MBA was attempted here using a new anion exchange column of lower capacity than the IonPac AS11-HC. The separation was carried out in conjunction with the eluent generator system to optimise gradient parameters. The optimum preconcentration of some standards was also investigated with this new column and any improvements in limits of detection determined.

4.2 Experimental

4.2.3 Instrumentation

The ion chromatograph was similar to that found in Chapter 2.0 with an extra EG40 eluent generator module equipped with a CR-ATC column installed. The oven temperature was optimised at 45°C for this system with the Dionex AS11-HC (250 x 2 mm). An automatic eluent generator concentration gradient of potassium hydroxide was used to elute HAs. Optimum gradient parameters were 10 mM KOH for the first 15 minutes of separation and then linearly ramped to 100 mM KOH over a time period of 15 minutes where it remained constant for further 5 minutes leading to a total run-time of 30 minutes. Between runs, the column was re-equilibrated to 10 mM KOH over a period of 10 minutes. Separations were also carried out on a Dionex AG16 (50 x 2 mm) guard and AS16 (250 x 2 mm) analytical column. The AS16 is an alkanol quaternary ammonium based column of lower capacity (42.5 µeq/column) to that of the AS11-HC (72.5 µeq/column). Optimum AS16 column ion chromatography conditions were 2.5 mM KOH for 10 minutes, then ramped linearly to 20 mM for 5 minutes and kept at 20 mM KOH for a further 20 minutes (eluent flow rate = 0.3 mL/min). All preconcentrations were carried out on the Merck LiChrolut EN solid phase extraction cartridges (Merck, Darmstadt, Germany).

4.2.4 Reagents

All chemicals were of analytical grade purity and were ordered from Aldrich (Milwaukee, WI, USA). As before, stock haloacetic acid solutions of MCA, DCA, TCA, TFA, CDFA, MBA and DBA were prepared to a concentration of 10 mM and were stable for approximately one fortnight when stored at 4°C in the dark. Working standards were prepared fresh daily using water from a Milli-Q water purification system (Millipore, Bedford, MA, USA). Sulphuric acid used for acidification of preconcentration samples and standards was of 99 % purity and ordered from Sigma-Aldrich (Milwaukee, WI, USA).

4.3 Results and Discussion

4.3.1 Initial Separations and Comparison of EG40 to Manually Prepared Eluents

In order to assess and validate the use of an eluent generator for this analysis, it must be capable of reproducing a similar separation to those obtained in Chapters 2.0 and 3.0. As manual eluent preparation was now eliminated, the expected result was the elimination of carbonate from the eluent, due to the fact that the generated eluent has no contact with air. Theoretically, this was expected to improve detection limits by reducing background noise levels, as well as remove any baseline inclines due to hydroxide gradient separations. Moreover, the addition of the CR-ATC eliminated further interference from trace anions in the Milli-Q water, such as sulphate, nitrate, carbonate and chloride. In order to compare the two systems, a standard of the seven HAs was prepared containing 0.5 μM MCA, 0.5 μM MBA, 0.75 μM TFA, 0.75 μM DCA, 1.5 μM CDFA, 1.5 μM DBA and 2.5 μM TCA. This standard was a near limit of detection HA concentration for the optimum method outlined in Chapter 2.0. The aim was to determine any improvement in limits of detection and also to observe baseline stability. An injection volume of 100 μL of this standard was run at the optimum flow rate of 0.30 mL/min on the AS11-HC analytical column using suppressed conductivity at 50 mA and an oven temperature of 40°C. Gradient separations were carried out using both electrolytically generated and manually prepared eluents from 10 – 100 mM hydroxide.

Samples of noise levels were taken from 7.5 – 10 minutes (represented in section A of *Fig. 4.3*) and from 30 – 35 minutes (represented in section B of *Fig. 4.3*) in both eluent type chromatograms. The reason for two separate noise ranges being sampled was to accurately calculate noise levels directly corresponding to hydroxide concentrations at the beginning and end of the gradient run. It was noted that noise levels had roughly decreased by one third with the eluent generator. For the generated 10 mM hydroxide eluent, noise levels were 0.042 μS as opposed to 0.152 μS with manually

prepared eluents. Similarly, the section of the chromatogram representing the generated 100 mM hydroxide, noise levels were reduced to 0.083 μS , in contrast to 0.302 μS for the traditional approach. Secondly, the rise in baseline, due to gradient separations with different concentrations of hydroxide and with varying degrees of carbonate contamination, was virtually eliminated. Baselines were observed as almost completely flat over the course of the gradient and the result affirmed the effective removal of carbonate from the generated eluents. Noise comparisons and baseline improvements can be seen in Fig 4.3.

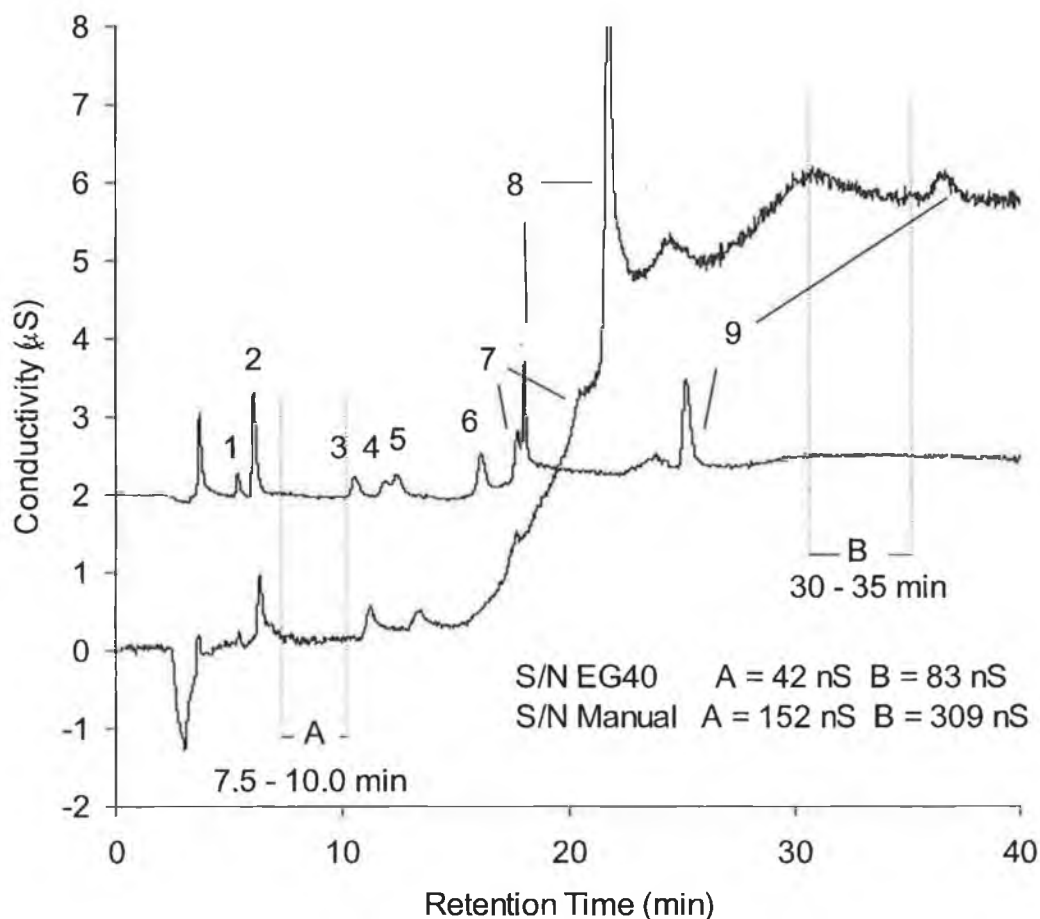


Fig. 4.3 Comparison of electrolytically generated eluents with manually prepared hydroxide eluents with respect to baseline stability, retention matching and noise level. Elution Order: 1 = MCA ($0.5 \mu\text{M}$), 2 = MBA ($0.5 \mu\text{M}$)/Chloride, 3 = TFA ($0.75 \mu\text{M}$), 4 = Nitrate, 5 = DCA ($0.75 \mu\text{M}$), 6 = CDFA ($1.5 \mu\text{M}$), 7 = DBA ($1.5 \mu\text{M}$), 8 = sulphate, 9 = TCA ($3.0 \mu\text{M}$).

A third and final observation from this short experiment was the mismatch of retention times between the two systems. It seemed that for the EG40 driven system, that there was a reduction in the overall runtime with retention of all analytes being lower in all cases. Furthermore, as a result of this, the separation between sulphate and DBA was compromised. There was no additional polyether ether ketone (PEEK) tubing required for either of the two systems, which would account for this and no explanation was found except for a variance in the eluent concentrations. The only possible explanation for the variance was that the eluent concentrations did not match. To further investigate this possibility, a 50 mL volume of electrolytically generated potassium hydroxide at a concentration of 50 mM was collected in a beaker, of which 2 mL aliquots were titrated using 0.0487 M HCl as a primary standard. Eight replicate microscale titrations were carried out in this manner, the results from the first and second of which were discarded. The final titre was 1.025 ± 0.012 mL HCl corresponding to a hydroxide concentration of 47.5 ± 0.6 mM hydroxide ($n=6$), which was slightly lower than that of the set 50 mM concentration set by the eluent generator. In a similar manner, a 500 mL solution of sodium hydroxide was prepared in a volumetric flask by adding 1.325 mL of the 50 % w/v solution used for eluent preparation in previous experiments. Again, eight successive microscale titrations of 2 mL aliquots of this solution were carried out, of which, the results of the first two titrations were discarded. The final titre was 1.027 ± 0.008 mL of the 0.0487 M HCl primary standard. Results for six replicate runs show a concentration corresponding to 47.43 ± 0.38 mM NaOH. Therefore, it could be concluded from this that even though concentrations were slightly inaccurate at lower than 50 mM OH⁻, both prepared and manual eluent preparation show similar precision. Therefore the concentration of eluent was not a factor in the observed reduction in retention time for EG40 driven separations. The only explanation for a reduction in retention times for all HAs in the EG40 driven separations was that some component of the eluent which was non-ionic hindered interaction of the HAs with the stationary phase. This will be discussed in more detail in Chapter 6.0, Section 6.3.4.1.

As was shown in Chapter 2.0, the retention of sulphate can be selectively altered with slight variances in column temperature to increase resolution from DBA. Moreover, when using an EG40, it should be noted that nitrate appeared as an unresolved shoulder on the leading edge of the DCA peak, which may have caused significant interference in real sample analysis. When temperature was increased to 45°C, the retention of nitrate decreased slightly and sulphate increased slightly with respect to these two HAs. It was concluded that the oven temperature required was 45°C when electrolytically generated eluents were employed.

4.3.2 Reproducibility of retention time with electrolytically generated eluents

In order for this system to replace the manual preparation of eluents, the reproducibility of the system was investigated via 25 repeat injections of a 10 µM standard of all seven HAs. The data was processed, with means, standard deviations and percent relative standard deviations listed in *Table 4.1*. In addition to these figures, it was investigated if there were any predictable variances in retention, so the data was plotted. Retention times for all HAs displayed excellent reproducibility at less than 0.2 % RSD over the 25 repeat runs. Also, considering that the time between successive injections was 40 minutes, the reproducibility data represented here shows remarkable stability over a 17 hour period. When the data was examined, all retention times seemed randomly distributed around the mean with no trends (*Fig 4.4 B*). As TCA was the most hydrophobic and strongly retained analyte, its retention time data was an adequate measure of system reproducibility when gradients were applied. It was noticed that even though the %RSD for TCA retention times were less than 0.2 %, there existed a slight trend towards an increase in retention time throughout the experiment (*Fig. 4.4 C*). However, this was taken as negligible considering the low %RSD, along with the considerable time period over which the sequence was run, and as a result the method was considered valid with regard to reproducibility. In a similar manner, peak heights were plotted to determine any detector flaws (*Fig. 4.4*

A). Peak heights for all seven HAs varied less than 4 % with the exception of DBA at roughly 8 %, still due to interference from sulphate.

Table 4.1. Reproducibility of Eluent Generation Methodology where n = 25.

HA	Standard Deviation	Average Retention Time (min)	% RSD for Retention Time	% RSD for Peak Height
MCA	0.01	5.29	0.19	3.17
MBA	0.01	6.13	0.18	3.34
TFA	0.01	10.22	0.14	3.25
DCA	0.02	12.05	0.18	3.43
CDFA	0.01	15.80	0.08	3.48
DBA	0.02	17.57	0.09	7.93
TCA	0.03	25.00	0.11	3.18

In comparison to reproducibility data derived from Chapter 2.0, there was a significant improvement in both retention time and peak height reproducibility and in the case of TCA there was a 25-fold increase in retention time reproducibility.

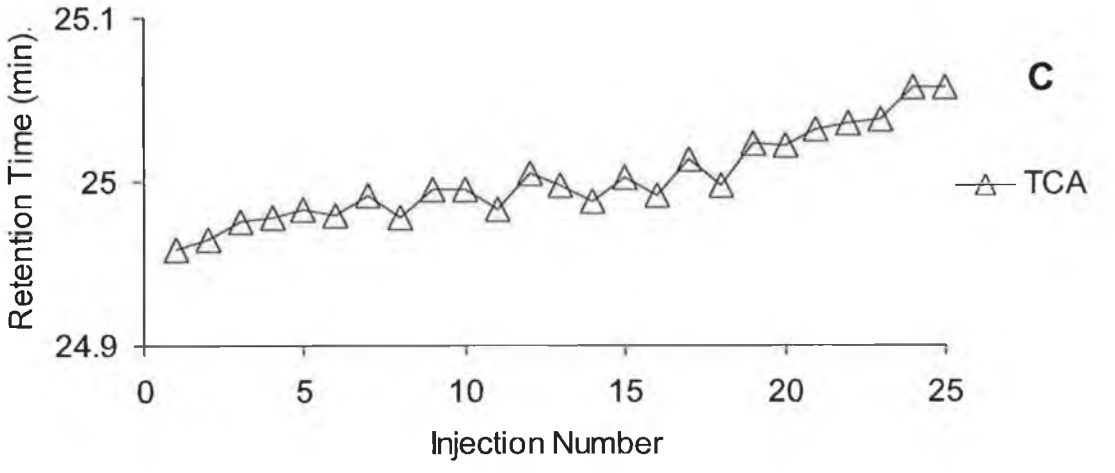
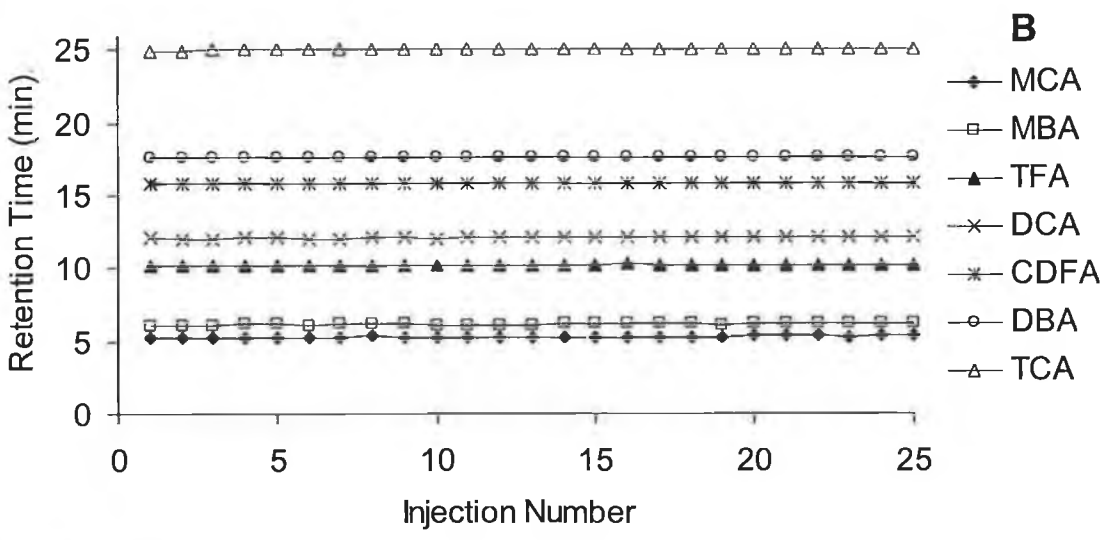
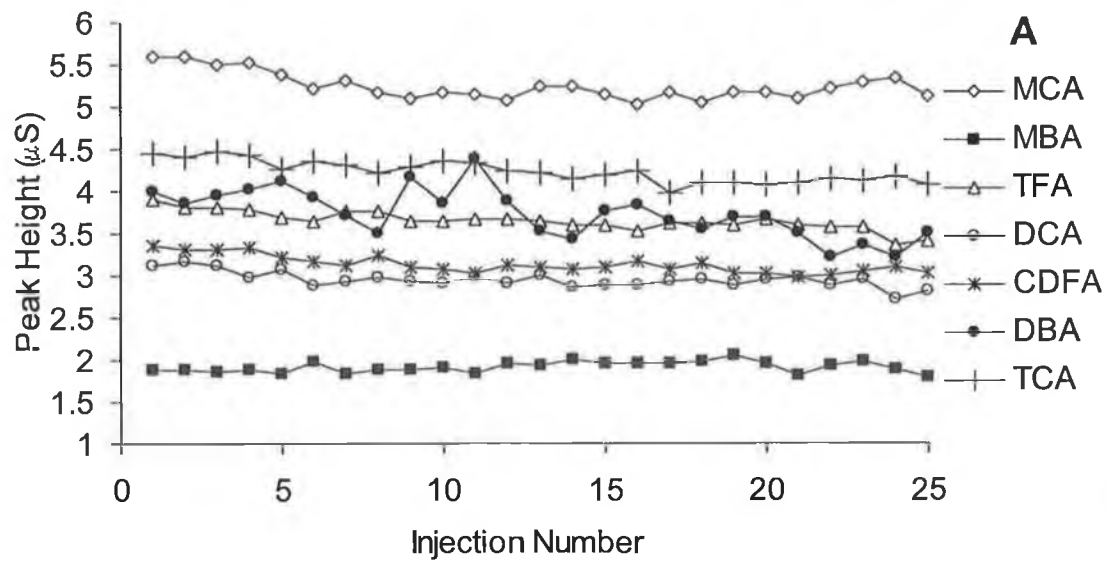


Fig. 4.4 Reproducibility of A: peak height; B: t_r and C: t_r for TCA in particular. $[\text{HA}] = 10 \mu\text{M}$ with electrolytic eluent generation system ($n = 25$).

4.3.3 Limits of Detection

Similarly to previous LOD experiments, sequential dilutions of a 100 μM standard of the seven HAs in Milli-Q were carried out until a signal-to-noise ratio of close to 3:1 was obtained. From this, the true LOD was calculated using samples of noise levels in around the peak of interest. It was noticed that LODs have improved in all cases and most notably for CDFA, DBA and TCA. A comparison of the eluent generation system LOD values to the manually prepared eluent system is shown in *Table 4.2*.

Table 4.2. Comparison of Absolute LOD values for both EG40 and manually prepared eluent systems

HA	Absolute LOD for EG40 system (ng)	[HA] ($\mu\text{g/L}$)	[HA] (μM)
MCA	2	20	0.215
MBA	not available	not available	not available
TFA	6	60	0.53
DCA	7	70	0.55
CDFA	13	130	1.007
DBA	7	70	0.323
TCA	14	140	0.864
HA	Absolute LOD for Manually Prepared Eluent System (ng)	[HA] ($\mu\text{g/L}$)	[HA] (μM)
MCA	12.5	130	1.34
MBA	not available	not available	not available
TFA	9.67	90	0.86
DCA	20.8	210	1.64
CDFA	100.91	1010	4.6
DBA	229.9	2290	10.59
TCA	104.6	1050	6.46

Unfortunately, LODs could not be calculated for MBA as residual chloride originating from reagents used for disinfection of the Milli-Q system still interfered with the MBA peak. The results suggested that manually prepared

eluent suffered from significant carbonate absorption and reduced limits of detection by a factor of ten in some cases. The combination of the CR-ATC and the enclosed EG40 system clearly had a remarkable effect on both baseline noise and stability. The baseline rise over the gradient due to carbonate was just 0.4 μS as opposed to 6 μS in the manually prepared eluent system and was very stable, even at near-LOD concentration levels (Fig. 4.5).

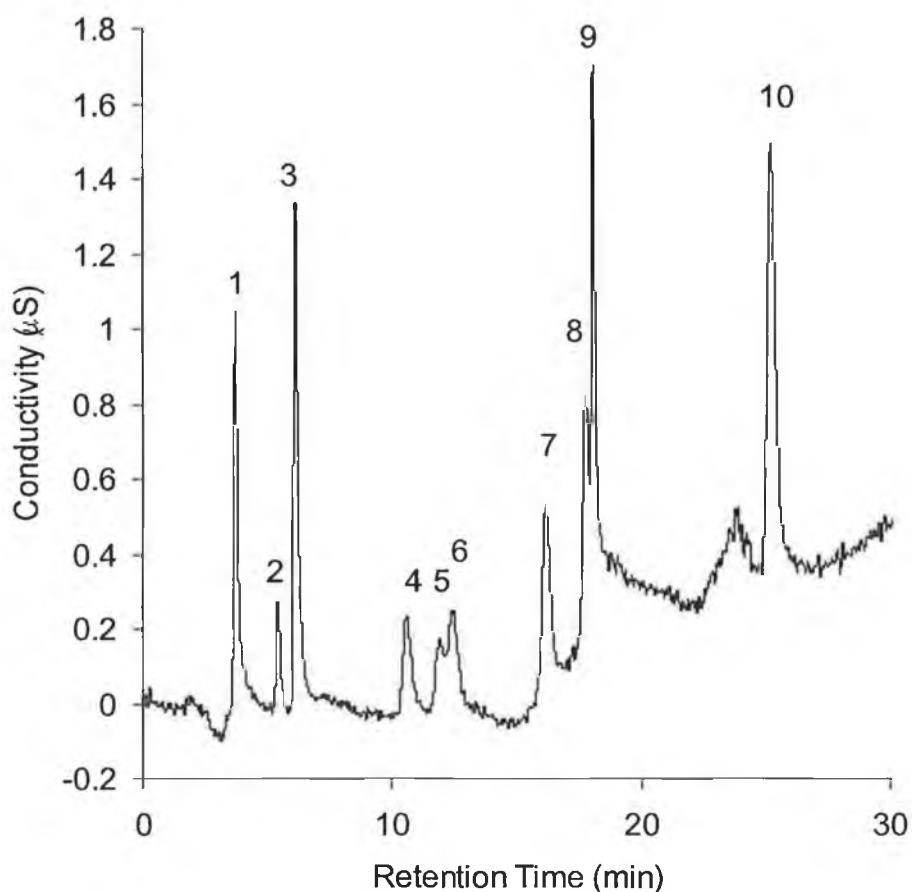


Fig. 4.5. Near LOD trace of seven HAs. 1 = Fluoride, 2 = MCA (0.5 μM), 3 = Chloride/MBA (0.5 μM), 4 = TFA (0.8 μM), 5 = Nitrate, 6 = DCA (0.8 μM), 7 = CDFA (1.5 μM), 8 = DBA (1.5 μM), 9 = sulphate, 10 = TCA (3 μM).

4.3.4 Analysis of Real Samples with Preconcentration and EG40 System Separation

Application of the EG40 system to the analysis of real samples was investigated using the preconcentration methodology outlined in Chapter 3.0. Samples of the laboratory water supply were taken on four successive days (1st - 4th September 2003), as well as one from Drumcondra in inner city Dublin on the 1st September 2003. A calibration curve was constructed of 10, 15, 25, 40, 75 and 100 μM of the seven HAs and run in triplicate on the IC fitted with the EG40 system at optimum parameters (see *Appendix A.3, Fig. A.3-1*). Aliquots of 25 mL of each sample were acidified to below pH 0.3 and preconcentrated to 2 mL of 10 mM NaOH. The cartridge was washed with 1 mL of Milli-Q water and then eluted with hydroxide.

Samples showed varying levels of MCA, DCA, TCA, CDFA and in one case TFA. When peaks were integrated, all peak heights fell within the range of the calibration curve and concentrations for each detectable HA calculated accordingly. Three of the four samples taken from the laboratory were within USEPA regulations, but the sample taken on the 1st September 2003 displayed concentrations of MCA, which were almost double (112 $\mu\text{g/L}$) the USEPA limit of 60 $\mu\text{g/L}$ for the five HAs (*Fig. 4.6*). At first, this was considered to be an erroneous result, so the preconcentration was repeated. Great care was taken in ensuring there was no carry over from previous runs and the 100 μL loop was rinsed with Milli-Q water prior to analysis. Fresh SPE cartridges were used in all preconcentration experiments here and were washed with 3 mL MeOH prior to use. The results concurred that for that day there were unacceptable levels of HAs in the laboratory water supply. In addition to this, TFA existed in 35 $\mu\text{g/L}$ quantities on that day.

As stated earlier, fluorinated acetic acids are not governed by the USEPA. However, the two fluorinated forms included here repeatedly occur in drinking water. The sample taken from Drumcondra on that day was also preconcentrated, but levels did not agree. This sample contained only a sum total of 24 $\mu\text{g/L}$ for the five governed HAs and an additional concentration of

CDFA of 18 µg/L which when summed remained within acceptable limits (see Fig. 4.7).

The other three samples taken on the 2nd, 3rd and 4th of September all displayed levels of at least one of the seven HAs and all were within the 60 µg/L limit, even when the fluorinated acetic acids were included. Again, CDFA occurred regularly and was quantified along with any of the HAs present. See Table 4.3 for a list of all the HAs observed and their concentrations. Figs 4.8, 4.9 and 4.10 show the chromatograms of the samples taken on the 2nd, 3rd and 4th of September.

Table 4.3 HAs observed in 5 drinking water samples and their concentrations (µg/L). Errors calculated from Table 3.2.

HA (µg/L)	Drumcondra (1/09/03)	DCU (1/09/03)	DCU (2/09/03)	DCU (3/09/03)	DCU (4/09/03)
MCA	-	113 ± 11.3	-	<LOQ	-
MBA	-	-	-	-	-
TFA	-	35 ± 8.1	-	-	-
DCA	25 ± 2.5	-	17 ± 1.7	31 ± 3.1	20 ± 2.0
CDFA	18 ± 2.7	-	-	21 ± 3.2	-
DBA	-	-	-	-	-
TCA	<LOQ	<LOQ	-	<LOQ	<LOQ

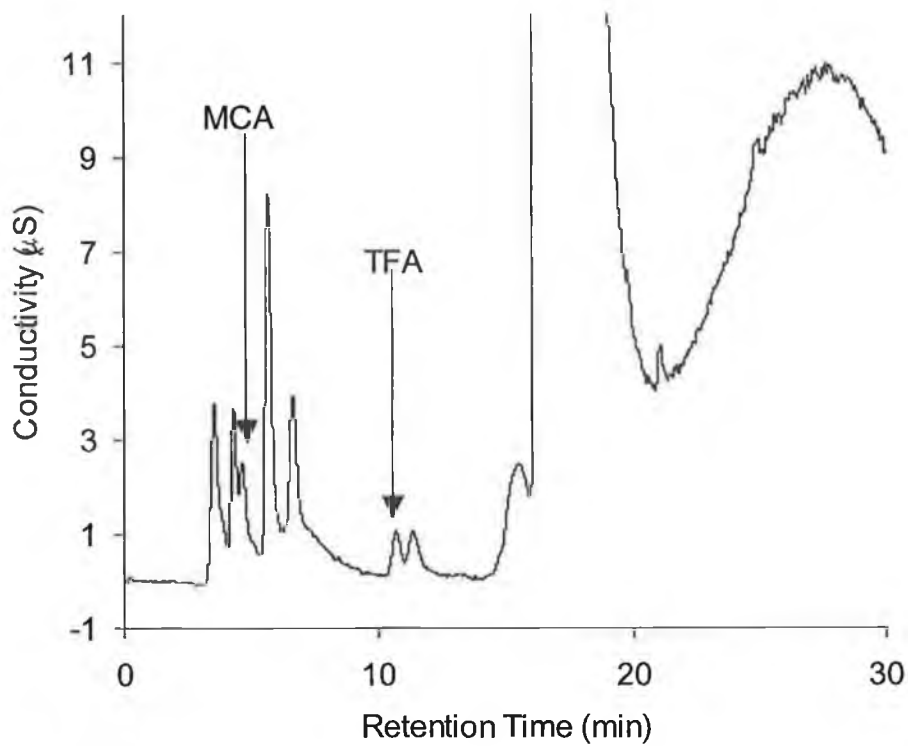


Fig. 4.6. Sample taken 1st September 2003 from laboratory water supply showing out of specification levels for MCA (113 µg/L) and TFA (35 µg/L).

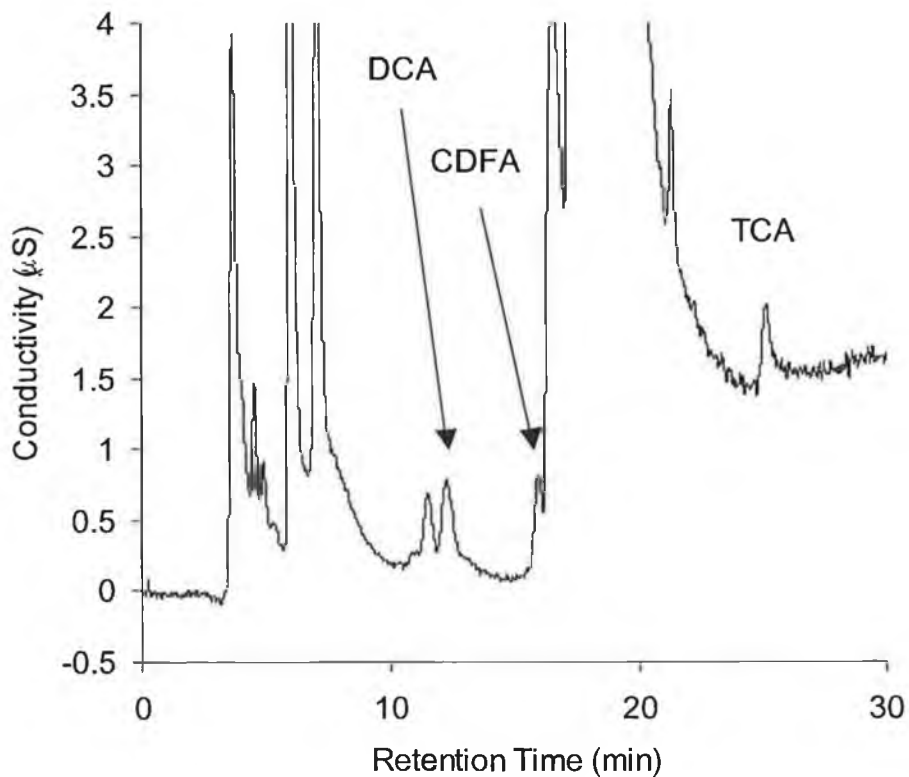


Fig 4.7. Preconcentration of Drumcondra sample taken on 1st September 2003 showing levels of DCA (25 µg/L), CDFA (18 µg/L) and TCA (<LOD).

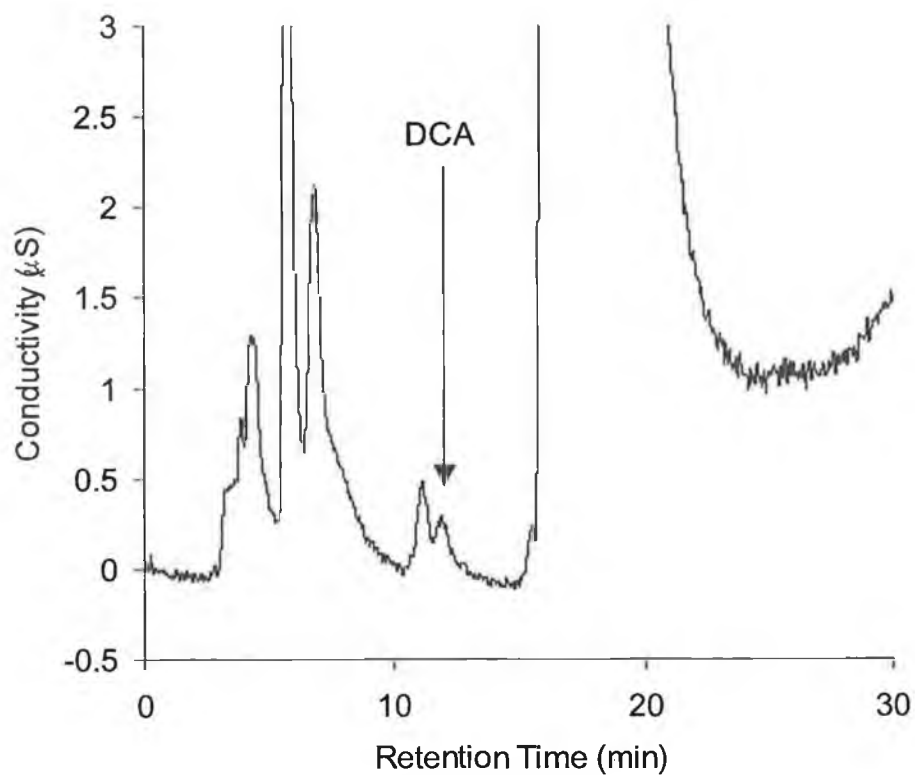


Fig 4.8. Sample of drinking water taken on the 2nd September 2003 showing levels of DCA (17 µg/L).

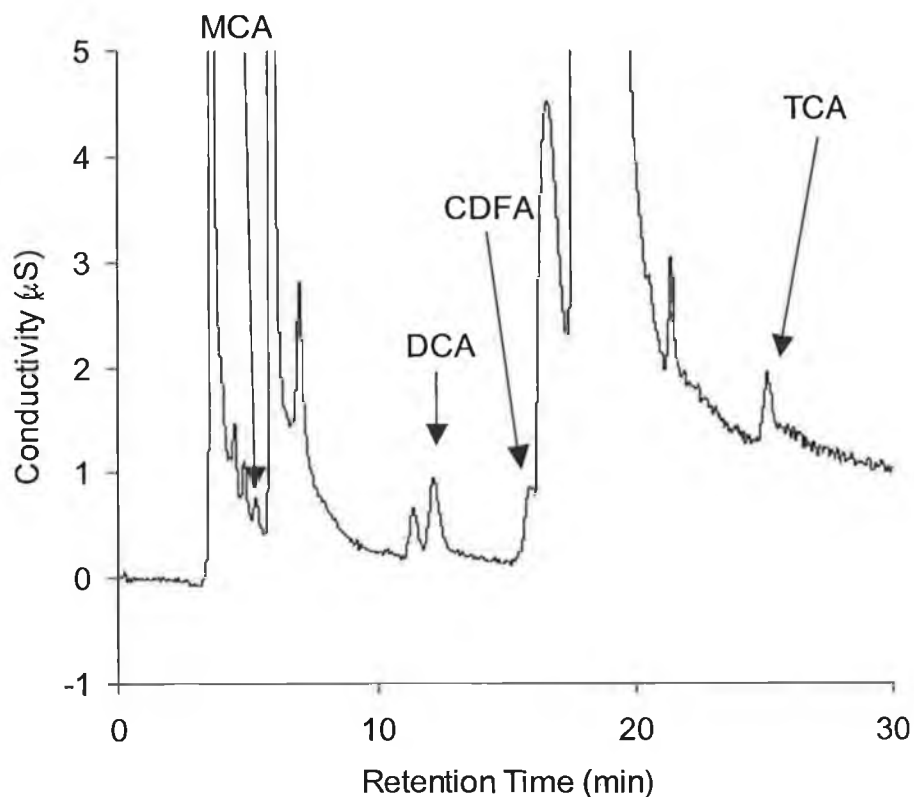


Fig. 4.9 Sample taken on the 3rd September 2003 showing levels of MCA (<LOD), DCA (31 µg/L), CDFA (20 µg/L) and TCA (<LOD).

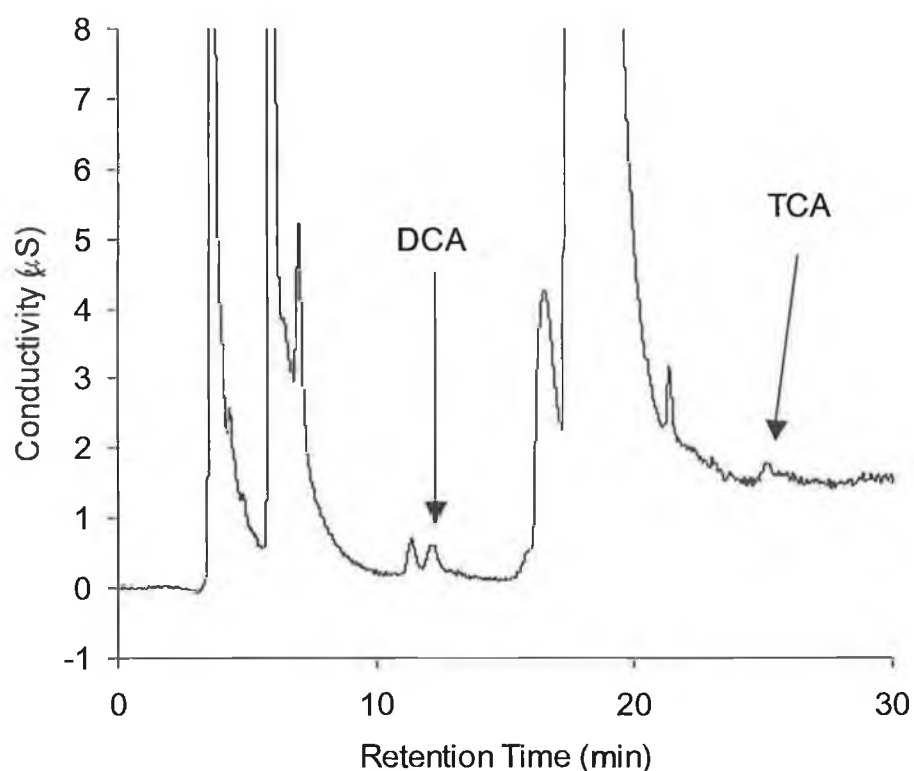


Fig. 4.10. Sample taken on 4th September 2003 showing levels of DCA (20 µg/L) and TCA (<LOD).

4.3.5 Separation of inorganic chloride and MBA

To this point, separation of chloride and MBA was unsuccessful. The addition of chloride removal steps to the analysis was not considered until all chromatographic possibilities to separate the two were investigated. For this reason, an AS16 micro-bore column was chosen as a possible solution to the problem. This column was similar to the AS11-HC column in that it comprised of an alkanol quaternary ammonium based exchanger on a bonded phase of EVB-DVB polymer and was stable at pH ranges from 0 – 14 units. The capacity of this column was lower than that of the AS11-HC and comparison of the packing specifications of the two columns are given in *Table 4.4* below. The degree of hydrophobicity is lower than that of the AS11-HC also, which suits the high level of hydrophilicity of the HAs.

Table 4.4. Comparison of AS11-HC and AS16 column packing specifications [3,4].

Column	Particle Size (μm)	% Crosslinking	Capacity ($\mu\text{eq}/\text{column}$)	Hydrophobicity
AS11-HC	9	70	72.5	Medium-Low
AS16	9	55	42.5	Ultra Low

The optimum method parameters for the AS11-HC were taken as the starting point of the optimisation procedure for the AS16 separations. A standard of all seven HAs at a concentration of 15 μM was run using these parameters and it was found that there existed a very crude separation of MCA, chloride and MBA. The initial eluent concentration of 10 mM KOH was too strong for adequate separation so both 5 and 2.5 mM were investigated. It was found that 2.5 mM gave the best resolution between MCA/chloride at 1.66 and chloride/MBA at 1.43. Any lower concentration of KOH would have caused the peaks to become excessively broad and increase analysis time. The elution order of the separation was identical to the AS11-HC separations with the order of elution being fluoride, MCA, chloride, MBA, TFA, nitrate DCA, CDFA, DBA, sulphate and TCA. Chromatograms of the three separations corresponding to 2.5, 5 and 10 mM KOH for the seven HAs is given in *Fig. 4.11* and retention data and resolution values in *Table 4.5*.

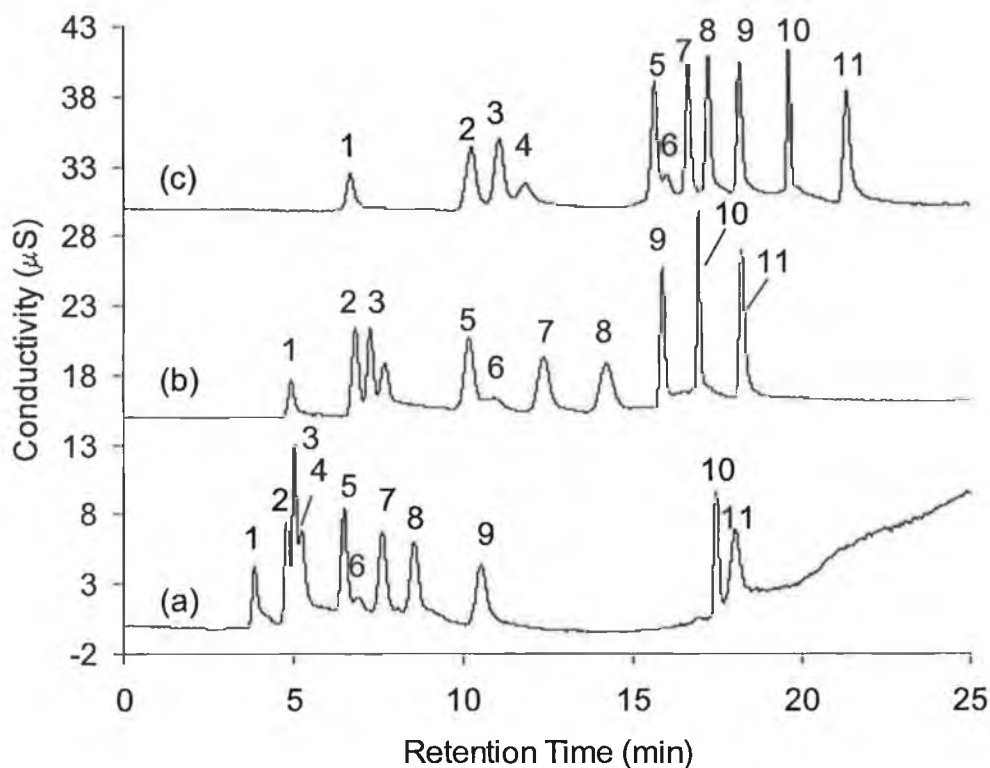


Fig. 4.11 (a) Gradient of 10 – 100 mM KOH at 15 minutes for a duration of 15 minutes at 45°C (b) Gradient of 5 – 100 mM KOH at 15 minutes for a duration of 15 minutes at 45°C (c) Gradient of 2.5 – 100 mM KOH at 10 minutes for a duration of 5 minutes at 45°C. Elution Order: 1 = fluoride, 2 = MBA, 3 = chloride, 4 = MBA, 5 = TFA, 6 = nitrate, 7 = DCA, 8 = CDFA, 9 = DBA, 10 = sulphate, 11 = TCA. [HA] = 15 µM.

As can be seen from Fig. 4.11 above, the retentions of sulphate and TCA could have caused problems when excess sulphate was in solution from the acidification step. As a consequence, it was decided to reduce the final concentration of the gradient to 20 mM KOH and to observe the effect on run time and their separation. Overall run time did not increase dramatically with the weaker eluent and TCA eluted at roughly 25 minutes. Fig. 4.12. shows the separation of 15 µM of the seven HAs with a gradient of 2.5 – 20 mM KOH from 10-15 minutes and an overall acquisition time of 30 minutes. Post acquisition equilibration was carried out again with eluent concentration reset to the original 2.5 mM over 5 minutes and equilibration for a further 5 minutes.

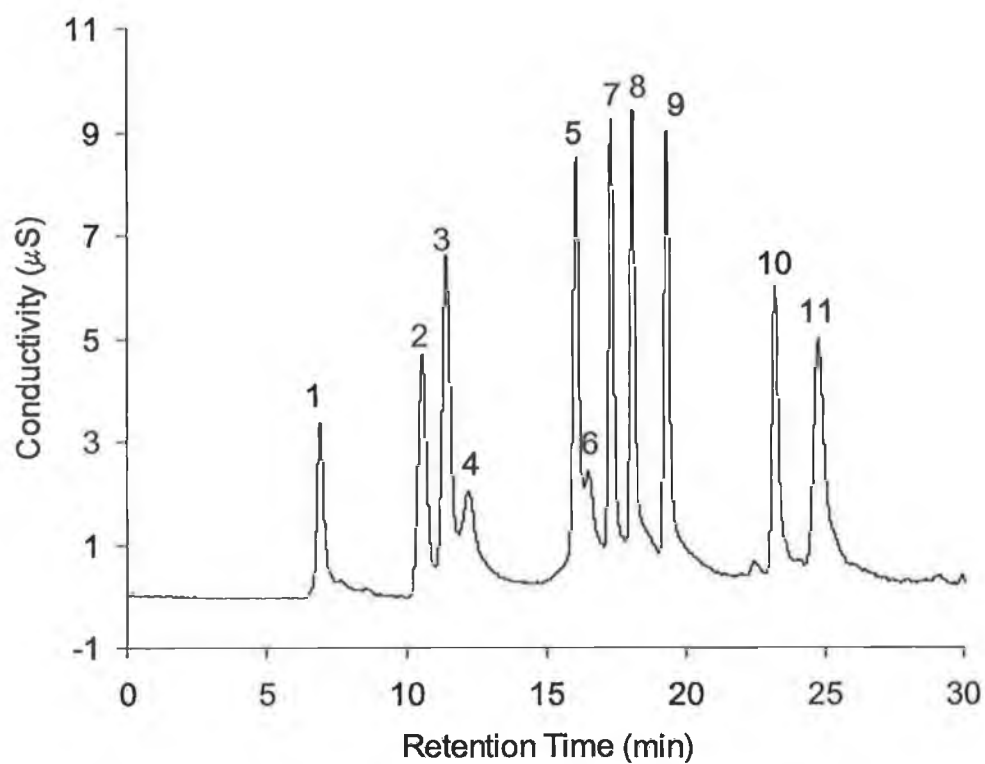


Fig. 4.12. Gradient separation of 2.5 mM – 20 mM KOH at 10 minutes over a duration of 5 minutes of 15 μ M of the seven HAs at 45°C. Elution order: 1 = fluoride, 2 = MCA, 3 = chloride, 4 = MBA, 5 = TFA, 6 = nitrate, 7 = DCA, 8 = CDFA, 9 = DBA, 10 = sulphate, 11 = TCA.

Table 4.5. Retention and resolution data for three AS16 gradient separations.

10-100 mM KOH gradient			5-100 mM KOH gradient			2.5-100 mM KOH gradient		
HA	Retention Time (min)	R _s	HA	Retention Time (min)	R _s	HA	Retention Time (min)	R _s
MCA	4.80	1.11	MCA	6.83	1.35	MCA	10.24	1.60
chloride	5.03	1.11	chloride	7.27	1.18	chloride	11.06	1.44
MBA	5.23	4.98	MBA	7.67	5.67	MBA	11.85	8.39
TFA	6.49	3.15	TFA	10.16	3.92	TFA	15.67	1.16
DCA	7.60	2.26	DCA	12.36	2.78	nitrate	16.02	2.23
CDFA	8.54	3.86	CDFA	14.22	3.46	DCA	16.66	2.20
DBA	10.52	16.43	DBA	15.90	5.03	CDFA	17.25	3.39
sulphate	17.47	1.49	sulphate	16.97	5.44	DBA	18.18	5.98
TCA	18.03	n.a.	TCA	18.23	n.a.	sulphate	19.63	6.01
						TCA	21.35	n.a.

4.3.6 Effect of Temperature

Similarly to the AS11-HC experiments, the effect of temperature was investigated for full optimisation of the method on the AS16 column. Again, a mixed standard of 15 μM of the HAs was prepared and injected onto the column at ambient (measured as 23°C on that day), 30, 35, 40 and 45°C oven temperature. A larger concentration of chloride was used in this standard to ensure optimum separation from MBA even at higher concentrations, so 2 mg/L chloride was added to the standard. The chloride peak did interfere at lower temperatures but was resolution improved as temperature reached 45°C. Sulphate on the other hand eluted quite close to TCA and it was thought that it would interfere significantly at higher concentrations. As a result, 40°C was taken as the optimum temperature for the separation. As was observed in the AS11-HC experiments, the inorganic anion retention was yet again affected more than that of the HAs, with sulphate similarly being affected more than any other anion. The previously noted decrease in nitrate retention was observed here again and the separation of nitrate from DCA and TFA was at optimum at 40°C. The effect of temperature here can be seen in the overlay of each trace at each temperature in *Fig 4.14* and the optimum separation overleaf in *Fig 4.15*.

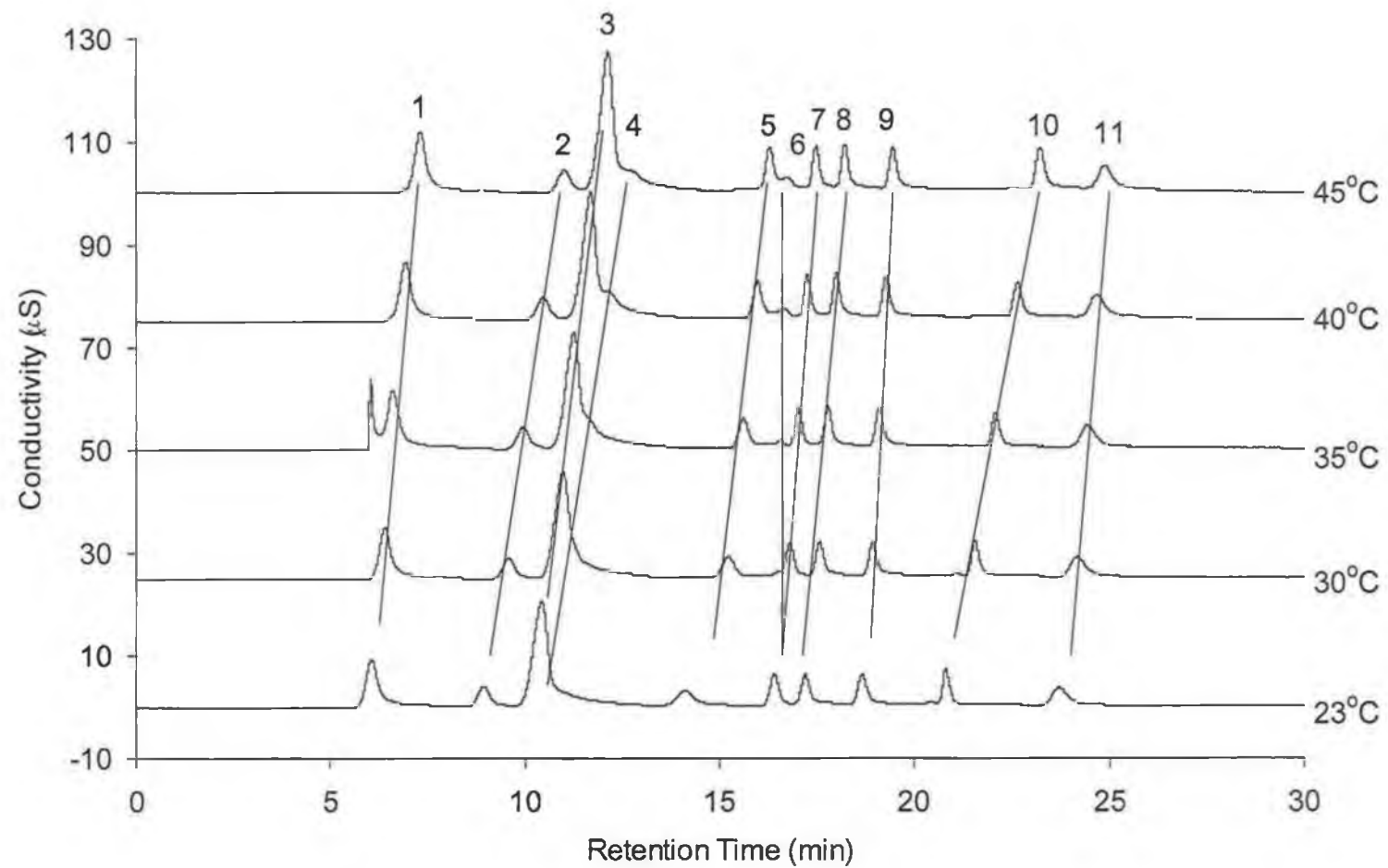


Fig. 4.13. The effect of temperature on AS16 HA separations. Elution order: 1 = fluoride, 2 = MCA, 3 = chloride (2 mg/L), 4 = MBA, 5 = TFA, 6 = nitrate, 7 = DCA, 8 = CDFA, 9 = DBA, 10 = sulphate, 11 = TCA. $[\text{HA}] = 15 \mu\text{M}$.

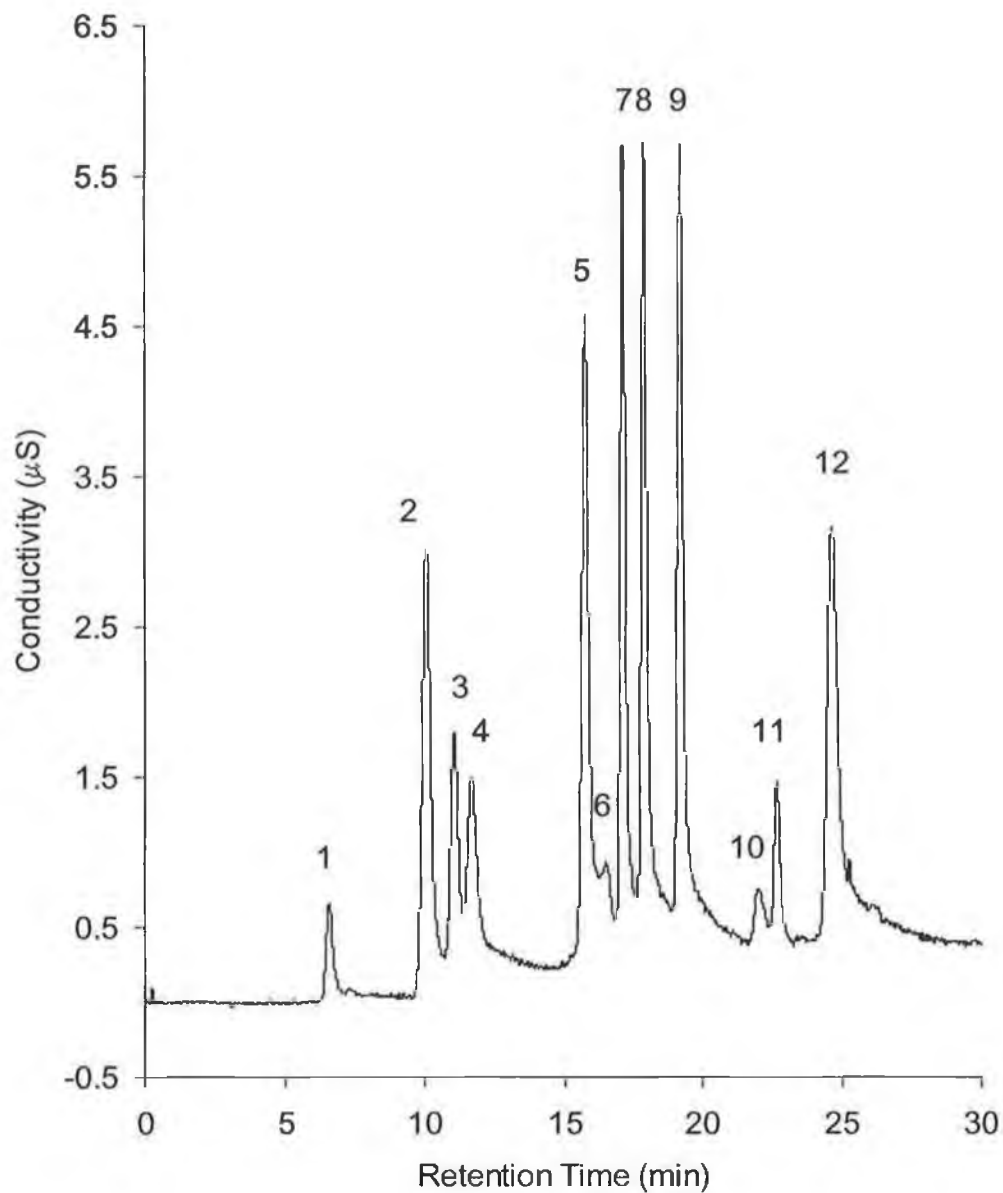


Fig 4.14. Optimised separation of HAs and inorganic anions on AS16 column. Flow rate: 0.30 mL/min; loop size: 100 μ L; gradient: 2.5 – 20 mM KOH at 10 minutes for a duration of 5 minutes; suppressor current: 50 mA. Elution Order: 1= fluoride, 2 = MCA, 3 = chloride, 4 = MBA, 5 = TFA, 6 = nitrate, 7 = DCA, 8 = CDFA, 9 = DBA, 10 = carbonate, 11 = sulphate, 12 = TCA. [HA] = 15 μ M.

4.3.7 Comparison of Limits of Detection of AS16 and AS11-HC column methods

Separations with the AS16 column were visibly improved over the AS11-HC method, but the most obvious drawbacks in this analysis were the limits of detection. It was crucial that these limits, coupled with the SPE procedure, would be low enough to fall within the range of 0 – 60 µg/L HA. Sequential dilutions were carried out as before by diluting a 100 µM standard of the seven HAs and the LOD for the AS16 method determined when signal-to-noise ratios came close to 3:1. The results are listed in *Table 4.6* and a chromatogram of a near limit of detection standard is shown in *Fig 4.15*. Unfortunately, accurate MBA LODs were not calculated due to the residual chloride in the Milli-Q, which still posed a problem.

Table 4.6. Comparison of LODs for AS16 and AS11-HC methods

HA	Absolute LOD for AS16 method with EG40 system (ng)	[HA] (µg/L)	[HA] (µM)
MCA	7	65.5	0.7
MBA	not available	not available	not available
TFA	9	84.3	0.7
DCA	6	73.3	0.6
CDFFA	6	72.1	0.6
DBA	6	123.5	0.6
TCA	32	519.6	3.2

HA	Absolute LOD for AS11-HC method with EG40 system (ng)	[HA] (µg/L)	[HA] (µM)
MCA	2	20	0.2
MBA	not available	not available	not available
TFA	6	60	0.5
DCA	7	70	0.6
CDFFA	13	130	1.0
DBA	7	70	0.3
TCA	14	140	0.9

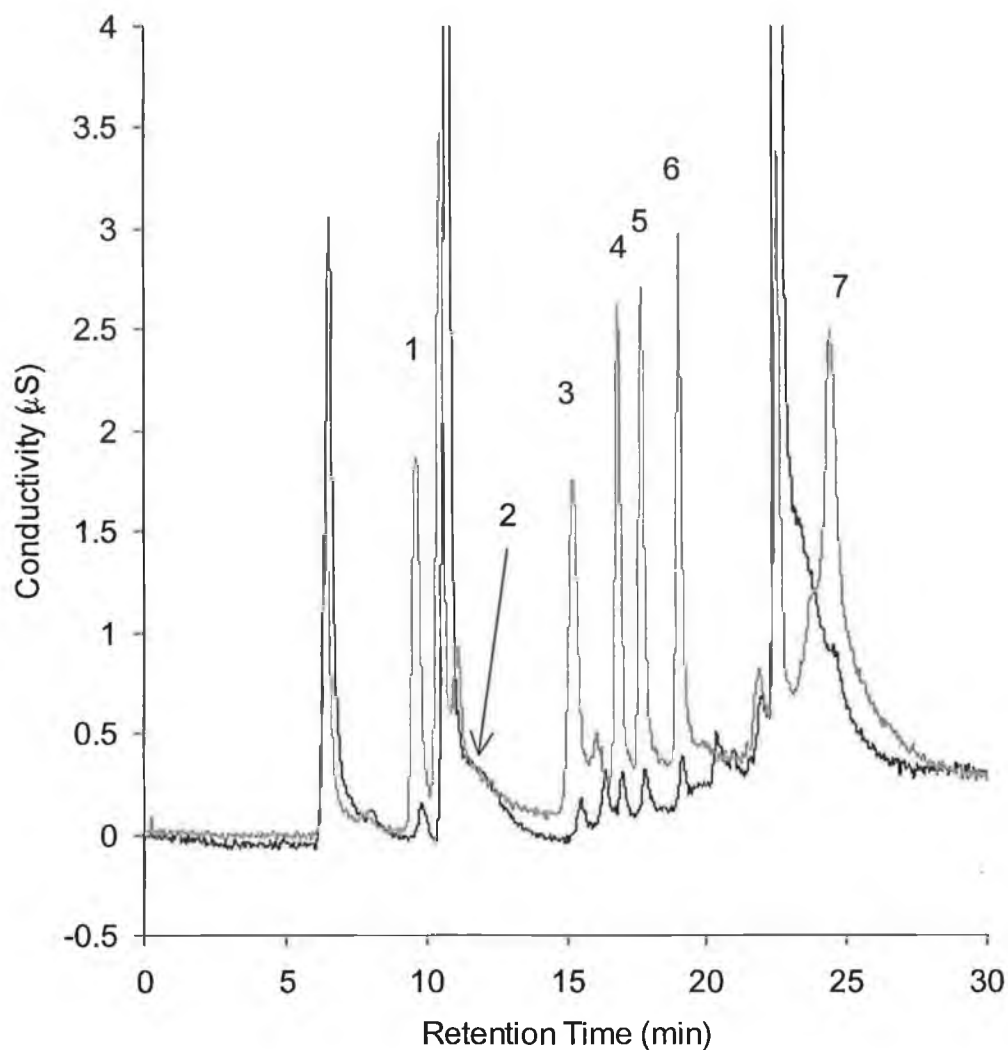


Fig. 4.15. Black Trace: Near LOD trace of 0.5 μM of seven HAs with the optimum method. Grey Trace: 5 μM standard of seven HAs with optimum AS16 method. Elution order: 1 = MCA, 2 = MBA, 3 = TFA, 4 = DCA, 5 = CDFA, 6 = DBA, 7 = TCA.

From these results it was observed that when the AS16 column was used sensitivity was reduced, albeit with a better separation. In order to assess its suitability to the analysis of these DBPs, an analysis of a preconcentrated standard was carried out. A sample of laboratory water was taken and spiked with 1 μM of each of the seven HAs using the optimised 25-fold SPE method in Chapter 3.0 and run together with a standard of 25 μM of the seven HAs. Although MBA was not baseline resolved from the inorganic chloride, the method served to identify the compound quite well at this level.

The reduction in the quantity of the inorganic anions due to the preconcentration procedure was again observed, with levels quite similar to that of the Milli-Q standard. The overlay of these two chromatograms can be found in Fig 4.16. From this it was determined that the developed AS16 column method was suitable for the analysis of HAs. Two more HAs are now visible (MBA and DBA) and CDFA is well resolved from the sulphate peak in this method. The only drawback with this method is the fact that TCA appears on the tail of the large sulphate peak.

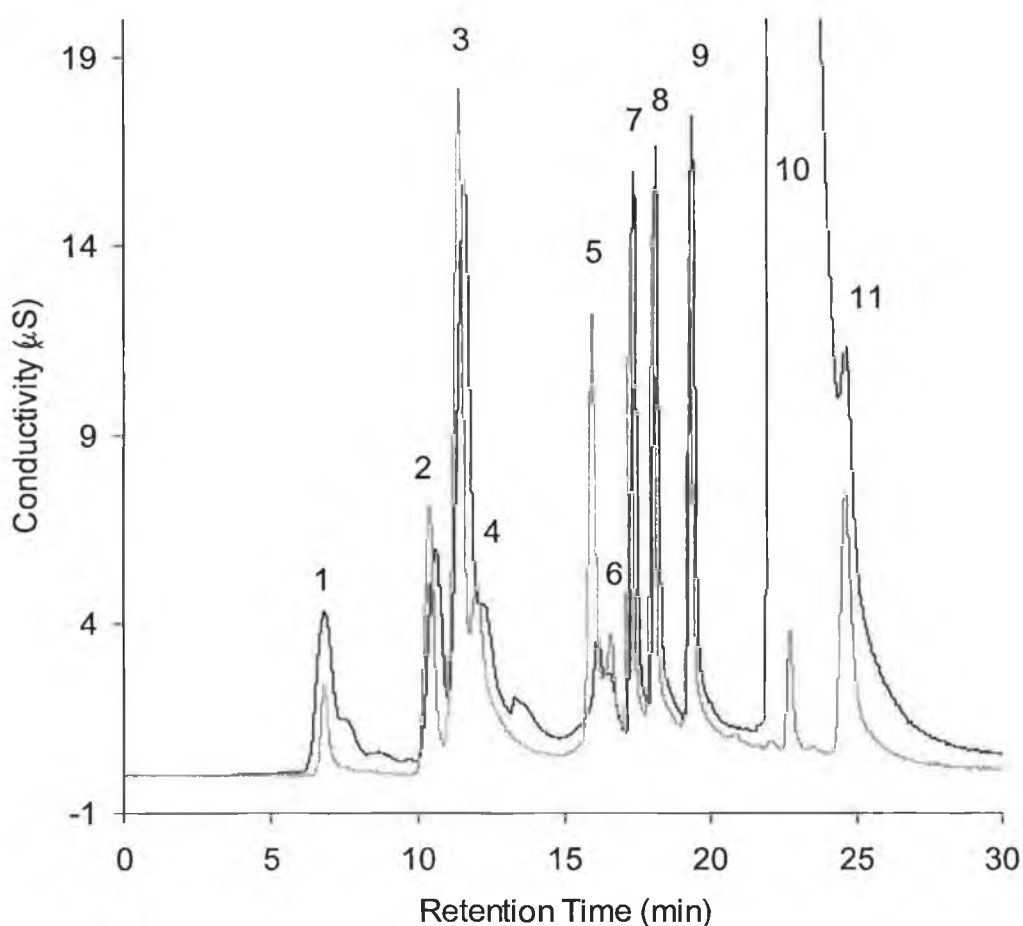


Fig 4.16. Overlay of preconcentrated drinking water sample (black trace) spiked with 1 μM of seven HAs and expected 100 % 25 μM standard in Milli-Q (grey trace). Elution order and % recoveries: 1 = fluoride, 2 = MCA (102 %), 3 = chloride, 4 = MBA (71 %), 5 = TFA (13 %), 6 = nitrate, 7 = DCA (110 %), 8 = CDFA (111 %), 9 = DBA (123 %), 10 = sulphate, 11 = TCA (104 %).

4.3.8 Repeatability of AS16 Method

For completion, the repeatability of the AS16 column method was determined over 20 successive injections to further examine the EG40 system, as well as validate the method. A peristaltic pump (Gilson, Middleton, WI, USA) was connected to the injector port on the injector valve supplying the 100 μL loop with a constant flow of a 10 μM mixed standard of the seven HAs and injected 20 times. Repeatability data for peak height and retention time was determined and is listed in *Table 4.7*. Studies showed that the retention time for each HA varied less than 1 % RSD in all cases and peak height RSD was less than 3 % in all cases. This again highlighted the stability of the EG40 system (see *Fig 4.17*).

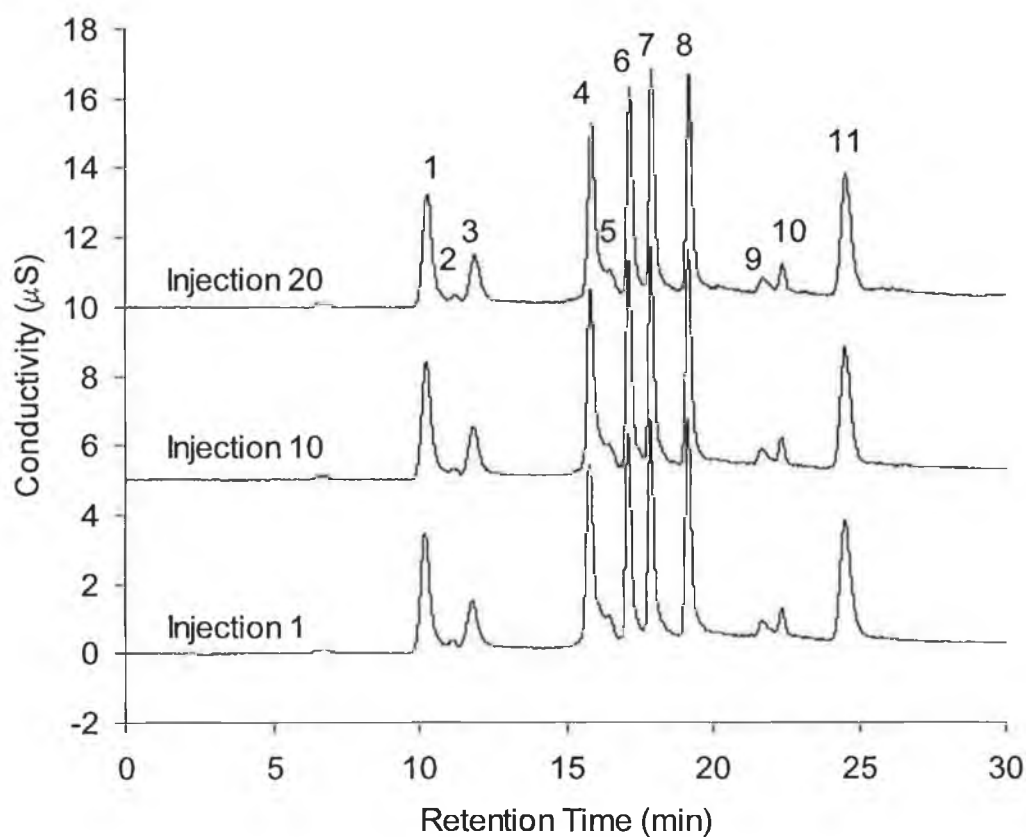


Fig 4.17 Overlay of 1st, 10th and 20th repeat injection of 10 μM of seven HAs with AS16 and EG40 methods. Elution Order: 1 = MCA, 2 = chloride, 3 = MBA, 4 = TFA, 5 = nitrate, 6 = DCA, 7 = CDFA, 8 = DBA, 9 = carbonate, 10 = sulphate, 11 = TCA.

Table 4.7. Repeatability of AS16 method for 20 successive injections

HA	% RSD for Peak Height	% RSD for Retention Time
MCA	3.0	0.6
MBA	3.0	0.6
TFA	2.2	0.3
DCA	1.4	0.2
CDFA	2.0	0.1
DBA	1.7	0.1
TCA	2.1	0.1

4.3.9 Linearity of AS16 method

In order to assess the linearity of the method a series of standards were prepared to concentrations of 5, 10, 15, 25, 40, 50, 75 μM of each of the HAs and were run in triplicate. All HAs showed excellent linearity with all R^2 values above 0.99, with the exception of MBA and TFA at 0.9868 and 0.9829. Linearity calibration curves and summarised linearity data can be found in *Appendix A.3, Fig. A.3-2 and Table 4.8* respectively.

Table 4.8 Linearity data for AS16 column method

HA	R^2	Intercept	Slope
MCA	0.9990	0.62	0.27
MBA	0.9868	-0.28	0.12
TFA	0.9829	-0.72	0.37
DCA	0.9935	-1.23	0.60
CDFA	0.9949	-1.18	0.66
DBA	0.9981	-0.65	0.61
TCA	0.9984	0.12	0.32

4.4 Conclusions

From this work, it was possible to conclude that the electrolytic generation of hydroxide eluents for the separation of anions was very robust with respect to retention times, varying less than 1 % in both AS16 and AS11-HC column methods. Furthermore, baselines were significantly less noisy and background was reduced by half in most cases. The interference from carbonate dissolved in manually prepared hydroxide eluents was reduced to a minimum with most baselines remaining flat for the duration of the gradient runs carried out. The application of the EG40 system to the quantification of HAs in drinking water samples proved successful and five drinking water samples were successfully determined for HA content. LODs improved markedly, such as that for TCA with improvements of a factor of ten.

A second anion exchange method for the analysis of the haloacetates was successfully optimised using an IonPac AS16 alkanol quaternary ammonium based anion exchanger with lower capacity than that of the AS11-HC column of similar stationary phase. Factors such as eluent strength and the effect of temperature were investigated and optimised. The optimised method consisted of a gradient of 2.5 – 20 mM KOH from 10-15 minutes at 40°C oven temperature and with an overall runtime of 30 minutes with a post acquisition equilibration time of 10 minutes. With this column it was possible to separate chloride from MBA to a certain degree, but in high concentration chloride solutions, chloride still masked the MBA peak when at low levels. It was possible to observe two more HAs in drinking water preconcentration samples, namely DBA and CDFA, without any interference from residual inorganic anion content. Limits of detection for this method were not as sensitive as those found for the AS11-HC column, but still lay in the preconcentration range of the solid phase extraction method. The repeatability of the method showed that peak heights varied less than 3 % in all cases and 1 % for retention times and was comparable to the AS11-HC column method.

4.5 References

1. Operators Manual, EG40 Eluent Generator System, Document Number 031373, Revision 6.0, 8th July 2002, Dionex Corporation, Sunnyvale, CA, USA.
2. Product Manual, Continuously Regenerating-Anion Trap Column (CR-ATC), Document Number 031910, Revision 1.0, 4th February 2003, Dionex Corporation, Sunnyvale, CA, USA.
3. Product Manual, IonPac AS11-HC Analytical Column, Document Number 031333, Revision 3.0, 7th November 2002, Dionex Corporation, Sunnyvale, CA, USA.
4. Product Manual, IonPac AS16 Analytical Column, Document Number 031475, Revision 2.0, 3rd November 1998, Dionex Corporation, Sunnyvale, CA, USA.

Chapter 5.0

Trace detection of HAs with monolithic cation exchange type suppressor and investigation into the effect of LiChrolut EN sorbent mass

"Glaube heißt nicht wissen wollen, was wahr ist", Friedrich Nietzsche

5.1 Introduction

The main obstacles to overcome for routine HA analysis by IC are reproducible and very sensitive detection measurements in the low $\mu\text{g/L}$ range. Unfortunately, conductivity measurements from the results presented in the previous chapters shows an inability to achieve this. Although separations with the AS16 column displayed improved resolution of HAs from inorganic anions, including chloride, sensitivity seemed to be poorer with the eluent gradient of choice. As a result, the requirement for a further investigation into suppression types was required. If suppression is efficient, then analytes should be present in a solution of pure water before reaching the detector allowing lower detection limits to be achieved.

Improvements in HA detection limits have recently been reported through the use of the new Dionex AEES Atlas suppressor with carbonate/bicarbonate eluents [1]. The suppressor itself has been specifically designed for use with carbonate/bicarbonate eluents, and is of too low a capacity to be used with hydroxide eluents run with standard bore IC (suppression capacity up to 25 mN at 1.0 mL/min compared to 200 mN at 1.0 mL/min for the ASRS Ultra suppressor (Dionex)). However, the work detailed in this chapter outlines the possibility of using the Atlas suppressor with electrolytically generated hydroxide eluents for a micro-bore IC method. The large reduction seen in baseline noise resulting from this combination results in a large reduction in detection limits compared to those obtained using the ASRS Ultra suppressor. A schematic of the AEES Atlas suppressor is shown in *Fig. 5.1*. It consists of an anodic and a cathodic chamber separated by ion exchange membranes. Within the suppression bed the Atlas comprises of a series of monolithic cation exchange discs, which are separated by flow distributors. These flow distributors serve to alter the flow of eluent through the suppressor to a serpentine pattern allowing increased time in the suppressor to improve current efficiency and dynamic suppression capacity. This flow path is achieved via the use of small exchange membranes at alternate ends of the flow distributor. It should also be noted that the internal

diameter of the Atlas suppressor is only available in standard 4 mm bore. Similar to the traditional ASRS Ultra suppressor, aqueous eluent undergoes electrolysis under the applied current, to form hydroxide and hydrogen gas in the cathode chamber while hydronium ions and oxygen gas are formed in the anodic chamber. Hydronium ions in the Atlas pass through the membrane and neutralise any carbonate or hydroxide (to a lesser extent) eluent ions. All anions present are converted to their acid form. Sodium or potassium cations in the eluent stoichiometrically migrate towards the cathode and combine with hydroxide ions before exiting the suppressor. The porous polyethylene monolithic discs within the suppression chamber are grafted with sulphonated functionalities.

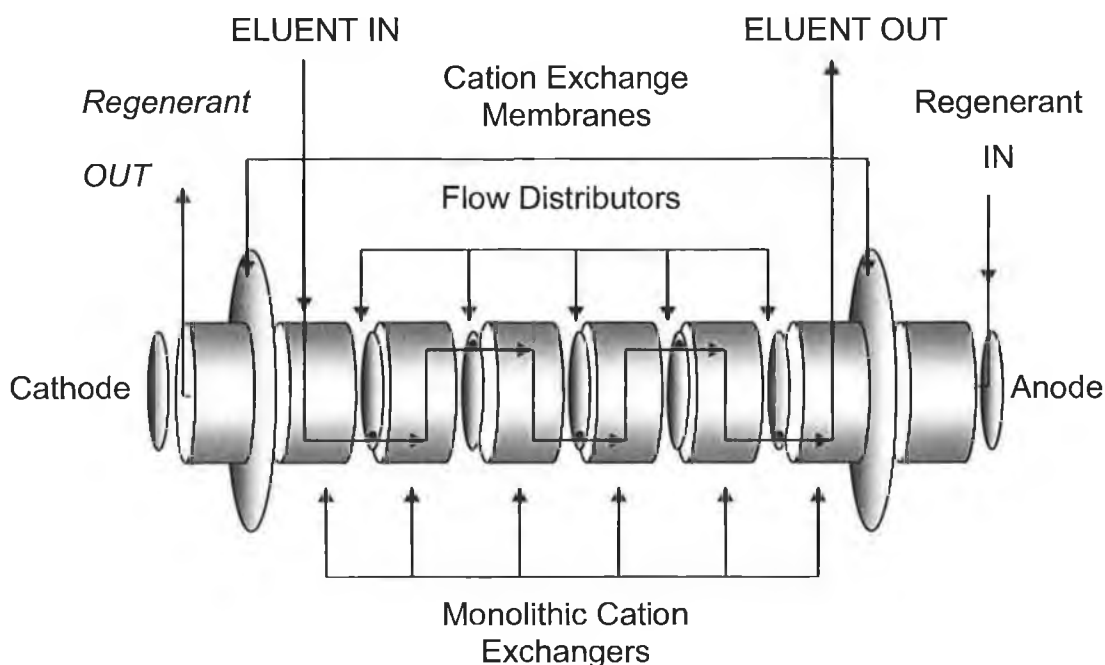


Fig 5.1 Schematic of the Dionex AEES Atlas suppressor [2]

Samples of treated water were collected and the possibility of direct micro-bore IC analysis without preconcentration was investigated. Additionally, to reduce detection limits to sub- $\mu\text{g/L}$ concentrations, samples

were also preconcentrated 25-fold using a hyper-crosslinked EVB-DVB sorbent [3-5] and analysed using the above method.

5.2 Experimental

5.2.1 Instrumentation

The ion chromatograph and instrument conditions were similar to those used in Chapter 4.0, Section 4.2.1 using the Dionex IonPac AG16 and AS16 columns. For comparison, suppression was carried out with either a 2 mm Dionex ASRS Ultra suppressor (at 50 mA) or a 4 mm AEES Atlas electrolytic suppressor (at 19 mA), in the auto-recycle mode. Current was supplied to the Atlas suppressor with a Dionex SC20 suppressor controller. Injection was carried out using a 100 μ L sample loop. Optimum ion chromatography conditions were 2.5 mM KOH for 10 minutes, then ramped linearly to 20 mM for 5 minutes and kept at 20 mM KOH for a further 20 minutes (eluent flow rate = 0.3 mL/min). Preconcentration was carried out as in Chapter 3.0, Section 3.2.1. For chloride and sulphate removal, Alltech Maxi-Clean IC-Ba, IC-Ag and IC-H cleanup cartridges were used (Alltech Associates, Deerfield, IL, USA).

5.2.2 Chemicals

All reagents used were of analytical reagent grade purity. Sodium chloroacetate (98 %), bromoacetic acid (99 %+), sodium trifluoroacetate (98 %), sodium dichloroacetate (98 %), chlorodifluoroacetic acid (98 %), dibromoacetic acid (97 %), trichloroacetic acid (99 %+), neat bromodichloroacetic acid (DCBA) and neat dibromochloroacetic acid (CDBA) were all ordered from Aldrich (Milwaukee, WI, USA) along with all inorganic anions and carboxylates prepared from their respective sodium salts. Stock HA solutions were prepared to a concentration of 10 mM and stored in the

refrigerator for a maximum of 2 weeks at 4 °C in the dark. Stock inorganic anion and carboxylate standards were prepared to a concentration of 1000 mg/L. All working standards were freshly prepared daily using diluent water from a Milli-Q purification system (Millipore, Bedford, MA, USA) with a specific resistance of 18.3 MΩcm. Sulphuric acid used for acidification of preconcentration samples and standards was 99 % purity and also ordered from Aldrich along with analytical grade potassium hydrogen phthalate (with ortho isomer) used for use as an internal standard. This standard was initially prepared to a concentration of 10 mM and was prepared along with the stock HA solutions. Drinking water samples (50 mL) for HA determinations were collected from the Dublin City University laboratory water supply, as well as two others from New Ross, Co. Wexford, and Drogheda, Co. Louth.

5.2.3 Sample collection and treatment

Samples of drinking water were collected from domestic taps by allowing the tap to run for approximately 3 minutes. The sample bottle (1000 mL) was then rinsed three times with drinking water before sampling. Samples were immediately chilled in a refrigerator at 4°C and kept in the dark to minimise degradation of HAs. Samples were kept in a refrigerator until analysis or transportation to the laboratory. During transportation, sample bottles were stored in an insulated container containing an ice pack for analysis on the same day. All the samples collected and analysed in this work originated from chlorinated sources. In all, one sample from three locations was taken in this way and all samples were analysed the following day. In the USEPA method 552.2, ammonium chloride is added to water samples to ensure the conversion of free chlorine to combined chlorine [2]. However, it was feared that the addition of such levels of chloride and subsequent IC separation might have caused overloading of the anion exchange column, even after cleanup with SPE chloride removal cartridges. Fresh working standards were prepared daily from the stock solutions outlined in Section 2.2 for analytical performance determinations and made to the mark with Milli-Q water. All solutions pertaining to a particular sample HA determination were prepared from that sample of drinking water. When

fortifications were made a volume of the stock standard was transferred to a 50 mL volumetric flask and made to the mark with sample. The dilution factor was then taken into account. This dilution factor was small with the largest standard addition spike concentration of 10 μM corresponding to a dilution factor of 1/1000. The phthalate internal standard was used as a retention time marker and to assess its separation from TCA. Phthalate was added to the samples at a concentration of 1 μM , which corresponded to a 1/10,000 dilution factor and as a result was deemed negligible for accurate HA determination (5 μL phthalate in 50 mL of sample).

Volumes of 50 mL of sample were acidified to $< \text{pH } 0.3$ by addition of a 4.5 mL aliquot of concentrated sulphuric acid. LiChrolut EN SPE cartridges were preconditioned with 3 mL MeOH, followed by 3 mL 200 mM sulphuric acid. Samples were loaded onto the solid phase extraction cartridge at a flow rate of 2 mL/min. After preconcentration, the cartridge was washed with 1 mL of Milli-Q water and eluted finally with 2 mL of 10 mM NaOH. This solution was then passed through a series of Alltech Maxi Clean cartridges at a flow rate of 1 mL/min, which were preconditioned with 10 mL Milli-Q water prior to the cleaning step. This series consisted of two IC-Ba, one IC-Ag and one IC-H cartridge. The first 1 mL of the eluate was discarded and the remaining solution was passed through a 0.45 μm filter prior to injection onto the IC.

5.3 Results and Discussion

5.3.1 Improvements in sensitivity with Atlas suppressor

Previously, separations were carried out using a Dionex ASRS Ultra (2 mm) operated at 50 mA, but limits of detection were not low enough to allow direct determination of HAs in drinking water supplies and required 25-fold preconcentration using a solid phase extraction technique (detailed in Section 5.2.3). The Atlas suppressor was considered, even though it was designed for

carbonate eluents, due to the low overall capacity to hydroxide eluents used at micro-bore flow rates (0.3 mL/min). Upon investigation, it was found that the Atlas suppressor offered far superior suppression capabilities to that of the ASRS Ultra under these eluent conditions. A standard solution in Milli-Q water of each of the HAs (concentration 2 μM for all HAs along with trace levels of fluoride, formate, chloride, chlorite, nitrate, carbonate, sulphate and phthalate, was run with both suppressors and the noise levels were compared.

From inspection of the standard chromatograms, the noise levels at the beginning of the gradient run were 15 - 20 times less when the Atlas suppressor was employed, and approximately 5 - 10 times less at the higher 20 mM hydroxide concentration at the end of the run. Typical chromatograms using each suppressor are overlaid and are shown in *Fig. 5.2(a)*, together with expanded sections (*Fig. 5.2(b)*) of the baseline noise to illustrate clearly the improvements obtained (the overlaid chromatogram in *Fig. 5.2(a)* obtained using the ULTRA suppressor has been offset by + 1 μS for clarity). As a result of these improvements, an assessment of limits of detection was carried out. To do this, a standard of the nine HAs was prepared in Milli-Q water to a concentration of 10 μM and serial dilutions were carried out until a signal to noise ratio of just above 3:1 was achieved for each HA. Limits of detection for the chromatographic method are listed in *Table 5.1* and show that once the Atlas suppressor was used, detection limits improved and in some cases, up to 45 times lower (MCA) than when the ASRS Ultra suppressor was used.

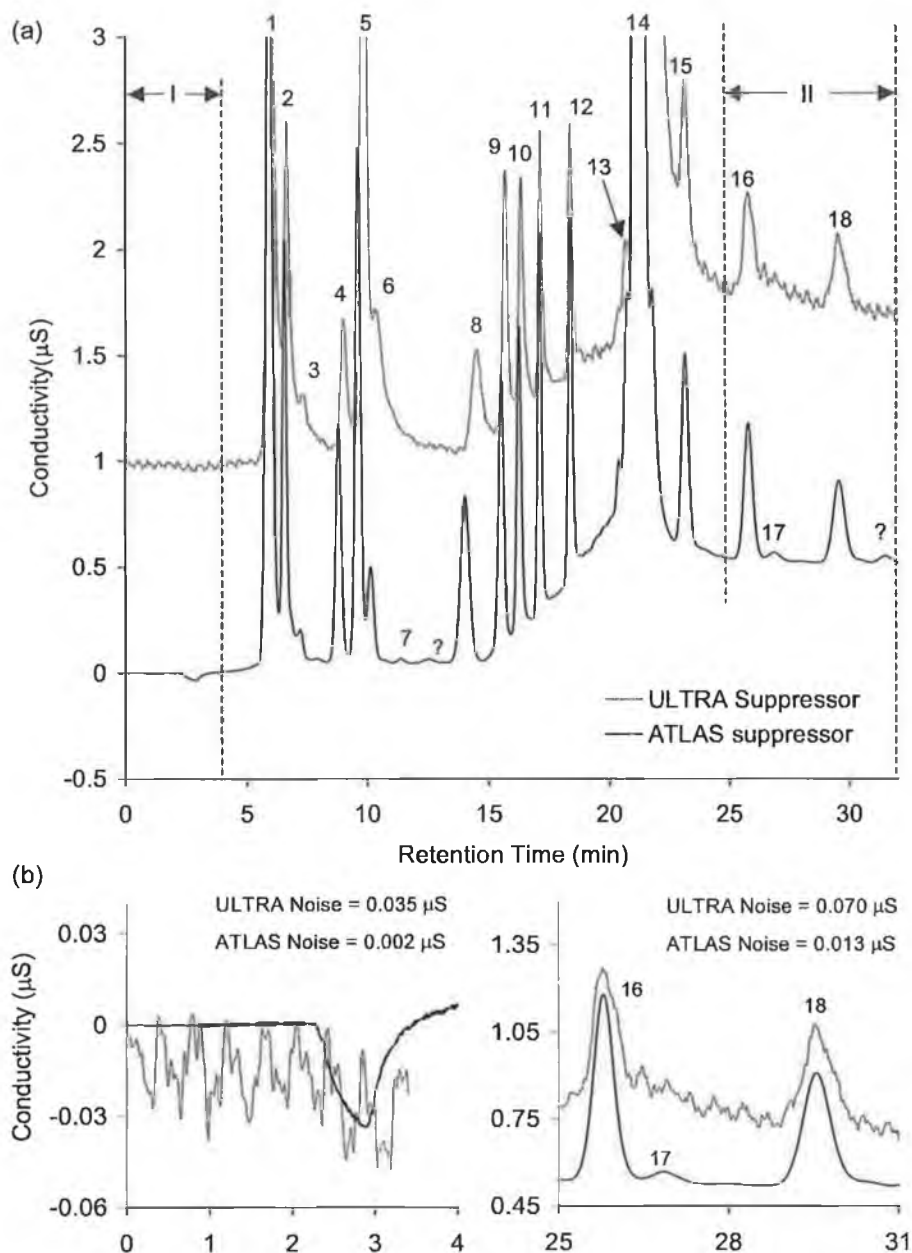


Fig. 5.2. Comparisons of HA separations with both Atlas and ASRS Ultra suppressors. 5.2(a) Elution Order: 1 = fluoride, 2 = formate, 3 = chlorite, 4 = MCA, 5 = chloride, 6 = MBA, 7 = nitrite, 8 = TFA, 9 = nitrate, 10 = DCA, 11 = CDFA, 12 = DBA, 13 = carbonate, 14 = sulphate, 15 = TCA, 16 = DCBA, 17 = phthalate, 18 = CDBA, $[HA] = 2 \mu M$. 5.2(b) Enlargement of region I and II. Other conditions; 2.5 mM KOH for 10 minutes, then ramped linearly to 20 mM for 5 minutes and kept at 20 mM KOH for a further 20 minutes (eluent flow rate = 0.3 mL/min).

5.3.2 Inclusion of DCBA and CDBA

Two more HAs were included in the separation mixture, DCBA and CDBA. Fortunately, these two HAs eluted after TCA and were completely resolved from each other and free from any interference and required no further alteration to the method outlined in Chapter 4.0 except an increase in the final run time. System performance data outlined in *Table 5.1* lists the retention times for these extra HAs along with reproducibility, limits of detection using both suppressors and linearity data.

5.3.3 Sample pre-treatment and removal of interferent ions

Despite these significant improvements in detection limits, to obtain sub- $\mu\text{g/L}$ detection limits (if required), it was necessary to apply developed preconcentration and sample cleanup techniques, or increase the loop size to 500 μL , as carried out by Liu et al. [1, 6, 7]. However, as this was a micro-bore IC method the use of large injection volumes was not investigated due to overloading of the micro-bore column with the excess matrix inorganic anions. To this point efforts to try to completely separate chloride and sulphate from trace level HAs were unsuccessful with HA peaks being entirely masked or appearing on the tail of mg/L concentration inorganic anion peaks. Furthermore, the acidification step outlined in Chapter 2.0 required excessive concentrations of sulphate to be added to the sample in order for it to successfully preconcentrate low level analytes. Although undesired, the possibility of combining the preconcentration method with a further method to selectively remove other high level inorganic anions was considered. Prior to this it was thought that two SPE methods as sample preparation steps would increase analysis time significantly and thus was not investigated without first wholly assessing the possibility of chromatographic separation. Therefore, when developing these two SPE methods, extra care was taken to try to reduce overall analysis time as much as possible, ideally to within one complete run cycle timeframe. If successful, this would allow one sample to be prepared and preconcentrated, while a previous sample was separating on the IC. The inherent self-cleaning effect of the preconcentration procedure

meant that nitrate could be selectively removed and coupled with a suitable solid phase ion exchange cartridge would open the possibility of removal of the other interfering anions. So far, the main interferences to the AS16 column method were sulphate and chloride. Tailoring of the chromatographic method meant that other interfering anions such as carbonate and bromide coeluted with sulphate and nitrate respectively. Other pre-concentrated species such as nitrite and organic acid anions did not interfere significantly as to pose a hindrance to trace level analysis. As a result, the addition of solid phase extraction cartridges in the silver, barium and acid forms in series with the pre-concentration method allowed to removal of the three most significantly interfering anions, chloride, sulphate and nitrate from the pre-concentration method eluate. The silver based cartridge required a further SPE cartridge in the acid form to remove any leached silver ions during the process that may have fouled the analytical column. The cartridges chosen for this procedure were Alltech Maxi Clean IC-Ba, IC-Ag and IC-H cartridges, which worked very effectively. The sorbent bed was 0.5 mL and the internal volume was 0.3 mL with a maximum operating flow rate of 1 mL/min. The use of these cartridges is outlined in Section 5.2.3.

In order to evaluate the performance of these cartridges a working 5 μ M standard of the HAs was prepared in Milli-Q water. Also included in this experiment were DCBA and CDBA. A 30 mL aliquot of this standard was then subjected to the pre-treatment sulphate and chloride removal procedure. The remaining solution, which did not undergo cleanup, was injected in triplicate on the IC and peak heights were recorded. Once the 30 mL aliquot had been cleaned, 100 μ L volumes were injected in triplicate onto the IC. The aim of this short experiment was to evaluate the removal efficiency as well as the effect of the procedure on HA peak heights in order to determine whether the HAs had any affinity for the stationary phase. Percent recoveries for all seven HAs were calculated based on the quotient of unclean standard and pretreated standard peak heights. Overall time required for sample pre-concentration was approximately 30 minutes, which was acceptable within the timeframe of the separation step as discussed earlier.

Trace determinations, as before, were carried out using a 25-fold SPE preconcentration technique outlined in Section 5.2.3. Results from the investigations into the effectiveness of the IC-Ba cartridge suggested that two IC-Ba cartridges in series were required and were successful in removing approximately 90 % of all the residual sulphate (used for acidification) in the eluate. Only one IC-Ag and one IC-H Maxi Clean cartridge was required for chloride removal and this was successful in removing approximately 98 % of total chloride from drinking water samples. Percent recovery data for the Maxi Clean cartridge series are listed in *Table 5.2*, with eight out of nine % recoveries ranging between 93 % and 103 %. Also listed, for completion, are the % recoveries from the preconcentration procedure, which now included DCBA and BDCA % recovery data. Percent recovery for MBA with these cartridges was slightly less at 84 %. This was possibly due to the coelution with residual chloride making integration of peak heights more inaccurate rather than a slight specificity of the cleanup cartridges for MBA. As mentioned in Chapter 3.0, TFA displayed very poor recoveries from the preconcentration procedure at 17 % (pK_a 0.3). It was thought that if lower pH values were used the sorbent would have become unstable. Furthermore, CDBA and DCBA showed very poor % recoveries at 13 % and 30 % respectively. The use of a larger elution volume from the SPE cartridges (from 2 mL to 4 mL NaOH) could be used to improve recovery data %, but this led to a more dilute sample extract and in fact did not improve overall detection limit.

Table 5.1 Analytical performance data for KOH gradient IC method for HAs and LODs with Atlas and ASRS Ultra suppressors and overall method LOD including preconcentration.

	MCA	MBA	TFA	DCA	CDFA	DBA	TCA	DCBA	CDBA
<i>Average t_r (min)</i>	9.2	10.6	14.8	16.5	17.2	18.5	23.3	25.9	29.7
<i>Average Peak Height (μS)</i>	3.5	1.4	4.7	5.9	6.2	6.2	3.5	3.4	2.1
<i>Average Peak Area (μS.min)</i>	1.2	0.5	1.4	1.4	1.4	1.5	1.5	1.3	1.2
Repeatability (% RSD, n=20, [HA] = 10 μM)									
<i>Retention time</i>	0.6	0.6	0.3	0.2	0.1	0.1	0.1	0.2	0.3
<i>Peak Area</i>	1.9	4.9	4.3	1.3	2.3	2.7	3.2	4.4	3.3
<i>Peak height</i>	3.0	3.0	2.2	1.4	2.0	1.7	2.1	3.4	2.2
Peak height linearity (5-75 μM HA, n=7 in triplicate)									
<i>R²</i>	0.999	0.987	0.983	0.994	0.995	0.998	0.998	0.995	0.992
<i>Slope</i>	0.267	0.120	0.370	0.604	0.661	0.606	0.315	0.120	0.067
<i>Intercept</i>	0.622	-0.280	-0.717	-1.232	-1.178	-0.649	0.122	-0.065	-0.054
^aDetection limits (μg/L)									
<i>AEES Ultra</i>	65.1	N/A	79.1	5.6	77.4	129.6	521.6	442.8	379.1
<i>AEES Atlas</i>	1.4	5.4	2.9	8.2	7.3	12.5	16.3	42.6	73.5
<i>With SPE and Atlas</i>	0.1	0.3	0.7	0.4	0.3	0.8	1.1	4.0	21.5

^a Based upon 3 X baseline noise (measured from 0.0 – 2.2 minutes for 2.5 mM KOH and 25-32 minutes for 20 mM KOH eluents), 100 μL injection vol.

Standard errors above the 15 μM calibration standard concentration were all less than 10 % RSD and all lower calibration standard concentration errors were less than 20 % for triplicate injections.

N/A Not calculated due to residual chloride interference

Table 5.2 Recovery and precision data for Maxi Clean cartridge series for nine HAs including SPE preconcentration data for DCBA and CDBA.

HA	Standard conc. (μM)	% Recovery of Maxi Clean cartridge series ($n=3$) ^{a,b}	% RSD ($n=3$) ^a	Average % Recovery of LiChrolut EN SPE preconcentration procedure ($n=3$) ^c	% RSD ($n=3$) ^c
MCA	5	98	0.3	65	10
DCA	5	103	2.4	84	10
TCA	10	98	0.6	58	13
MBA	5	84	3.7	63	28
DBA	0.2	100	1.0	66 ^d	18 ^d
DCBA	0.2	96	0.5	30 ^d	5 ^d
CDBA	0.2	93	2.3	13 ^d	8 ^d
CDFA	10	100	1.5	87	12
TFA	5	94	1.5	17	23

^a Carried out on 3 separate cartridge series of IC-Ba, IC-Ba, IC-Ag, IC-H preconditioned with 10 mL Milli-Q water prior to use.

^b Based on quotient of peak height of a cleaned standard of nine HAs versus an aliquot of the same standard without chloride or sulphate removal.

^c From Table 3.2 except for d.

^d IC separations for calculation of % recovery and % RSD for DBA, DCBA and CDBA carried out on optimised method with AS16 column outlined in Section 5.3.2.

5.3.4 Analysis of drinking water samples

5.3.4.1 HAs in drinking water without using preconcentration procedure

In an attempt to observe HAs directly (no preconcentration stage) a sample of drinking water was collected from our laboratory water supply in Dublin City University, Dublin, Ireland and kept in the refrigerator at 4 °C in the dark and analysed within 48 hours. It was expected from our optimisation procedure that excess chloride present in the sample would interfere significantly with weakly retained MCA and MBA and, furthermore, sulphate was also expected to interfere with trace DBA and TCA. In order to minimise this, approximately 20 mL aliquots of this sample were collected and passed through cleanup IC-Ba, IC-Ag and IC-H cartridges at a flow rate of 1 mL/min using the calibrated peristaltic pump. Prior to the cleanup step, cartridges were preconditioned with approximately 10 mL of Milli-Q water. After removal of excess chloride and sulphate and following filtering, 100 µL of the resulting solution was injected onto the IC using the optimum chromatographic conditions. Upon examination of the chromatograms, trace levels of MCA, CDFA and DBA were observed (see *Fig. 5.3(b)*). For quantification purposes, a standard addition curve was carried out by preparing HAs in the pre-treated water sample over a concentration range of 0.5 – 10 µM. The resulting standard addition curves yielded concentrations of 3.0 µg/L MCA and 43.5 µg/L DBA. Levels of CDFA were below detection limit and so could not be quantified accurately. All correlation coefficients were above 0.99 and demonstrated excellent linearity.

A second sample of drinking water was collected from New Ross, Co. Wexford, Ireland and a similar experiment was carried out. In this case, HA levels were much higher and could be directly quantified without the use of preconcentration. Trace levels of MCA, CDFA, DBA, TCA and DCBA were observed (See *Fig. 5.3(a)*). Similarly, a standard addition curve was constructed over a concentration range of 0.2 – 1.0 µM of each of the HAs and concentrations of each of the HAs found is listed in *Table 5.3*. Some of the HA peaks observed had signal to noise ratios of less than 3:1 and so

were not quantified, although DBA was quantified at a concentration of 22 $\mu\text{g/L}$ and TCA was quantified at a concentration of 18 $\mu\text{g/L}$. It should be noted that nitrate caused significant interference at the level present in the sample when using direct injection and completely masked any DCA that was present in the drinking water supply. In order for this method to be successful for drinking water quality control, DCA needed to be resolved from nitrate, as regulations stipulate that DCA should never be present in domestic drinking water supplies. For standard addition curves, please refer to *Appendix A.4, Figs. A.4-1 and A.4-2.*

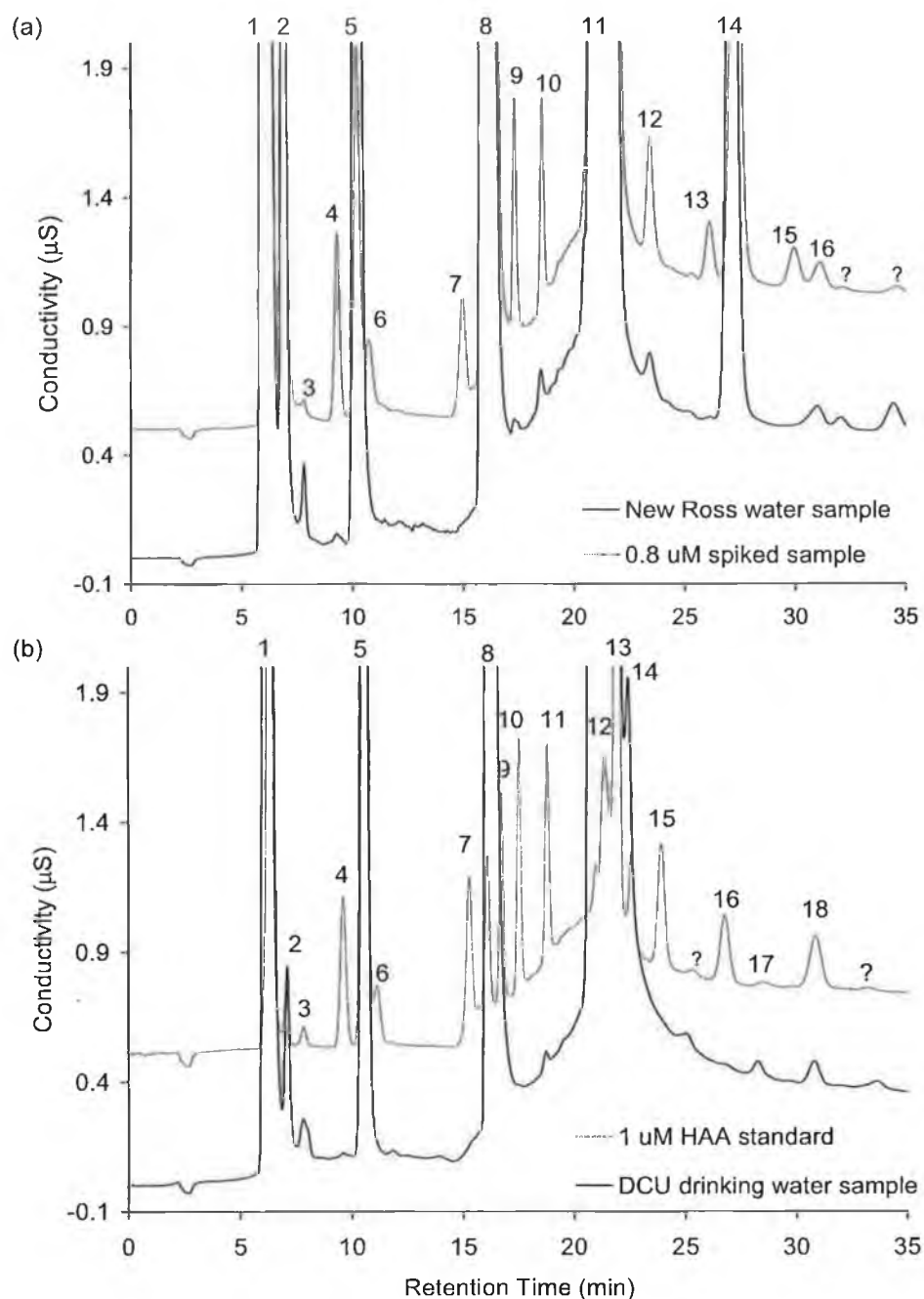


Fig. 5.3(a). Non-preconcentrated sample of New Ross drinking water supply passed through chloride and sulphate removal cartridges and run on IC with overlay of $0.8 \mu\text{M}$ HA spiked water sample. Elution Order: 1 = fluoride, 2 = formate, 3 = chlorite, 4 = MCA, 5 = chloride, 6 = MBA, 7 = TFA, 8 = nitrate, 9 = CDFA, 10 = DBA, 11 = sulphate, 12 = TCA, 13 = DCBA, 14 = phthalate (int. std), 15 = CDBA, 16 = phosphate. Other conditions as Fig. 5.1. Fig. 5.3(b). Non-preconcentrated Dublin City University drinking water sample passed through chloride and sulphate removal cartridges and run on IC overlaid with $1 \mu\text{M}$ standard solution prepared in Milli-Q water. Elution Order: 1 = fluoride, 2 = formate, 3 = chlorite, 4 = MCA, 5 = chloride, 6 = MBA, 7 = TFA, 8 = nitrate, 9 = DCAA, 10 = CDFA, 11 = DBA, 12 = carbonate, 13 = sulphate, 14 = thiosulphate, 15 = TCAA, 16 = DCBA, 17 = phthalate, 18 = CDBA. Other conditions as Fig. 5.1.

5.3.4.2 Preconcentration and HA determination in drinking water supplies

In order to accurately determine HA concentrations, including DCA, preconcentration was carried out on two drinking water samples. These water samples were preconcentrated and pretreated as outlined in Section 5.2.3 above and extracts subsequently injected onto the IC (100 μ L). The first sample was, once again, drinking water from New Ross, Co. Wexford and the second was a sample taken from Drogheda, Co. Louth. As was seen previously, levels of MCA, CDFA, DBA, TCA and DCBA were observed in the New Ross water supply. Furthermore, due to the fact that nitrate was not retained on the LiChrolut EN cartridge during preconcentration, the nitrate peak observed was significantly reduced allowing quantification of the DCA peak, which was present in both preconcentrated water samples. As before, a standard addition curve was constructed over a concentration range of 0.0, 0.2, 0.4, 0.6 and 0.8 μ M of each of the HAs. Each of the spiked sample solutions were adjusted to below 0.3 pH units and preconcentrated in the usual manner. Peak heights for each of the HAs were plotted and resulting HA concentrations calculated. For the USEPA regulated haloacetic acids, the New Ross water sample contained 58 μ g/L of the five regulated HAs in total, which lay just under the USEPA maximum contamination limit. Excluding DCA, the total concentration of these five HAs was 34 μ g/L. Upon examination of the standard addition data obtained for the New Ross sample analysed without preconcentration, the total concentration of the five regulated HAs (without DCA), showed excellent agreement with this value at 40 μ g/L. The second water sample from Drogheda Co. Louth, Ireland was analysed in the same way by means of 25-fold preconcentration. Again, levels of MCA, TFA, DCA, CDFA and TCA were observed. The only regulated HAs with peak heights greater than LOD level were MCA, DCA and TCA and summed to a total of 13 μ g/L. CDFA and TFA were also observed and the total of all HA was quantified at 15 μ g/L. All standard addition curves displayed linearity (*Fig. 5.4*) with correlation coefficients above 0.98. Once more, all these figures can be found in *Table 5.3*. For standard addition curves, please refer to *Appendix A.4, Figs. A.4-3 and A.4-4*.

Table 5.3. HAs observed in three chlorinated drinking water supplies

Sample Name	HAs observed ($\mu\text{g/L}$)									Total
	MCA	MBA	TFA	DCA	CDFA	DBA	TCA	DCBA	CDBA	
<i>New Ross, Co. Wexford, Ireland^a</i>	<LOD	-	<LOD	-	<LOD	22	18	<LOD	<LOD	40
<i>Dublin City University, Co. Dublin Ireland^a</i>	3	-	-	-	1	44	-	-	-	48
<i>New Ross, Co. Wexford, Ireland^b</i>	4 ± 0.4	-	-	25 ± 2.5	3 ± 0.5	-	30 ± 3.9	<LOD	-	61 ± 7.3
<i>Drogheda, Co. Louth, Ireland^b</i>	1 ± 0.1	-	1 ± 0.2	8 ± 0.8	1 ± 0.15	-	4 ± 0.5	-	-	15 ± 1.8

^a Values calculated by standard addition without preconcentration

^b Values calculated by standard addition with preconcentration including standard errors calculated from Table 5.2

<LOD: Peaks observed less than LOD value (calculated as signal to noise ratio of 3:1)

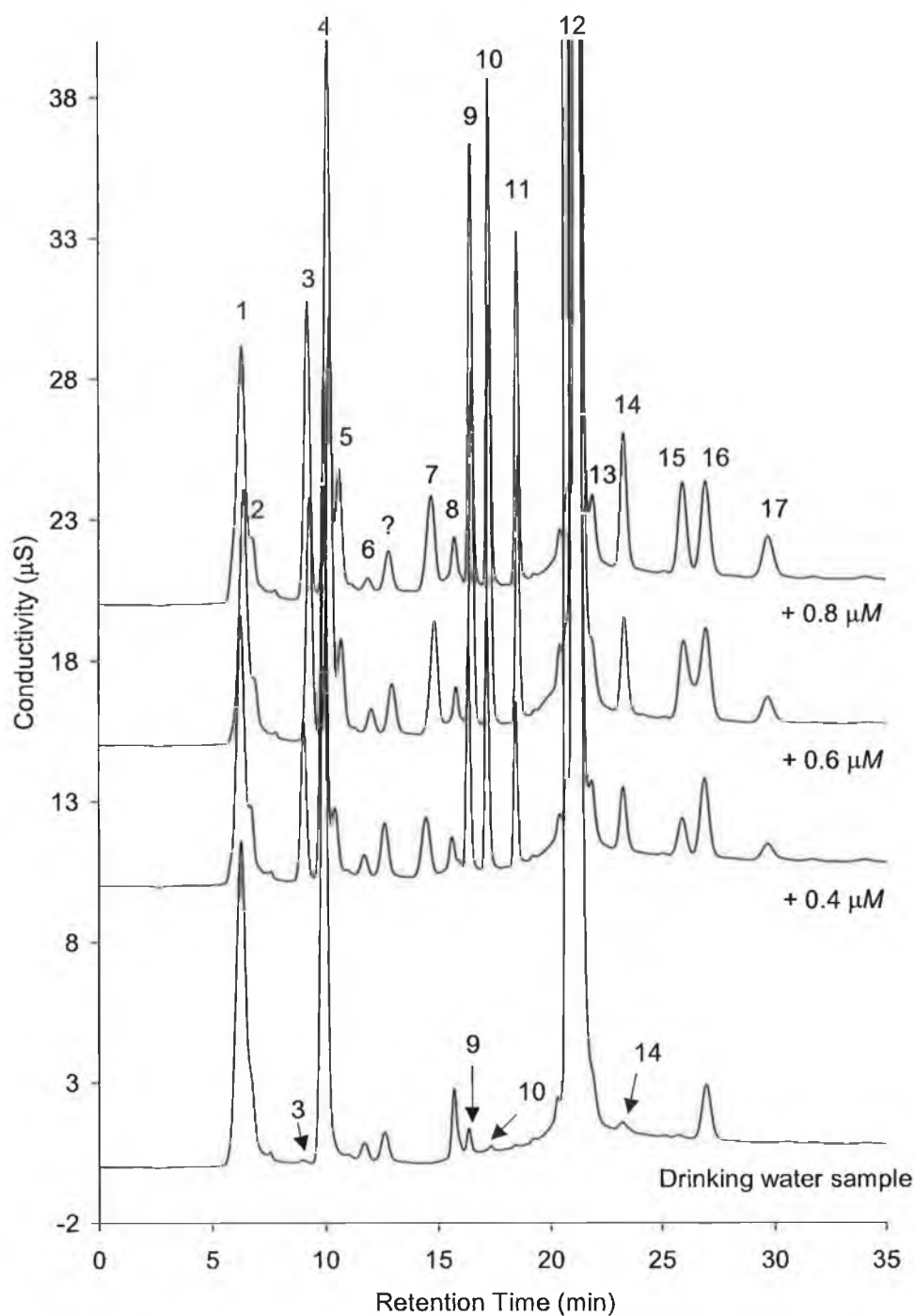


Fig. 5.4. Standard addition of HAs in drinking water from Drogheda, Co. Louth, Ireland. Sample and spiked samples preconcentrated 25 fold using SPE (LiChrolut EN). Elution Order: 1 = fluoride, 2 = formate, 3 = MCA, 4 = chloride. 5 = MBA. 6 = nitrite, 7 = TFA, 8 = nitrate, 9 = DCA, 10 = CDFA, 11 = DBA, 12 = sulphate, 13 = thiosulphate, 14 = TCA, 15 = DCBA, 16 = phthalate (Int. Std), 17 = CDBA. Concentration range = 0 – 0.8 μM HA.

5.3.4.3 Investigation into LiChrolut EN sorbent mass

In Chapter 3.0, an investigation was carried out into the elution profiles of five selected HAs from the LiChrolut EN phase. Considering that separations on the AS16 column were far superior to that of the AS11-HC column, it was decided that all nine HAs would be included in this next study. LiChrolut EN cartridges consist of a 3 mL housing containing two frits above and below 200 mg of the hypercrosslinked polymer. Subsequently, the sorbent from three fresh LiChrolut EN cartridges was removed with a spatula and placed in a weighing boat. From this, 400 mg of the isolated EVB-DVB sorbent was weighed on a balance and returned to the housing of one of the cartridges. Frits were placed both on the top and bottom of the sorbent and pressed tightly. This mass of sorbent corresponded to twice the mass contained within the commercially available cartridge.

The aim of this experiment was not only to plot elution profiles of all nine HAs, but to investigate whether doubling the sorbent mass would markedly increase percent recoveries. A standard of 0.2 μM MCA, MBA, TFA, DCA, CDFA, DBA, TCA and 0.4 μM DCBA and CDBA was prepared to 50 mL in Milli-Q water and then acidified to below pH 0.3. Preconcentration was carried out in the usual manner following the preconditioning steps outlined in Section 5.2.3. Once the 54.5 mL solution was passed through the cartridge, the sorbent was washed with 0.5 mL Milli-Q water as previous. The basis why 1 mL of Milli-Q water was not used here was due to the fact that the elution profiles of DBA, TCA, DCBA, CDBA and TCA were not determined and could elute earlier than expected, though unlikely since the fluorinated acids previously displayed the least affinity for the cartridge. Nevertheless, for direct comparison to the previous study, the choice for 0.5 mL Milli-Q wash was retained. Subsequently, 0.5 mL fractions of 10 mM NaOH were passed through the cartridge and collected in a vial for IC analysis. The elution profile can be observed in *Fig 5.5*. None of these fractions were passed through the MaxiClean cartridge series, as 0.5 mL volumes were insufficient for effective removal of chloride and sulphate alike.

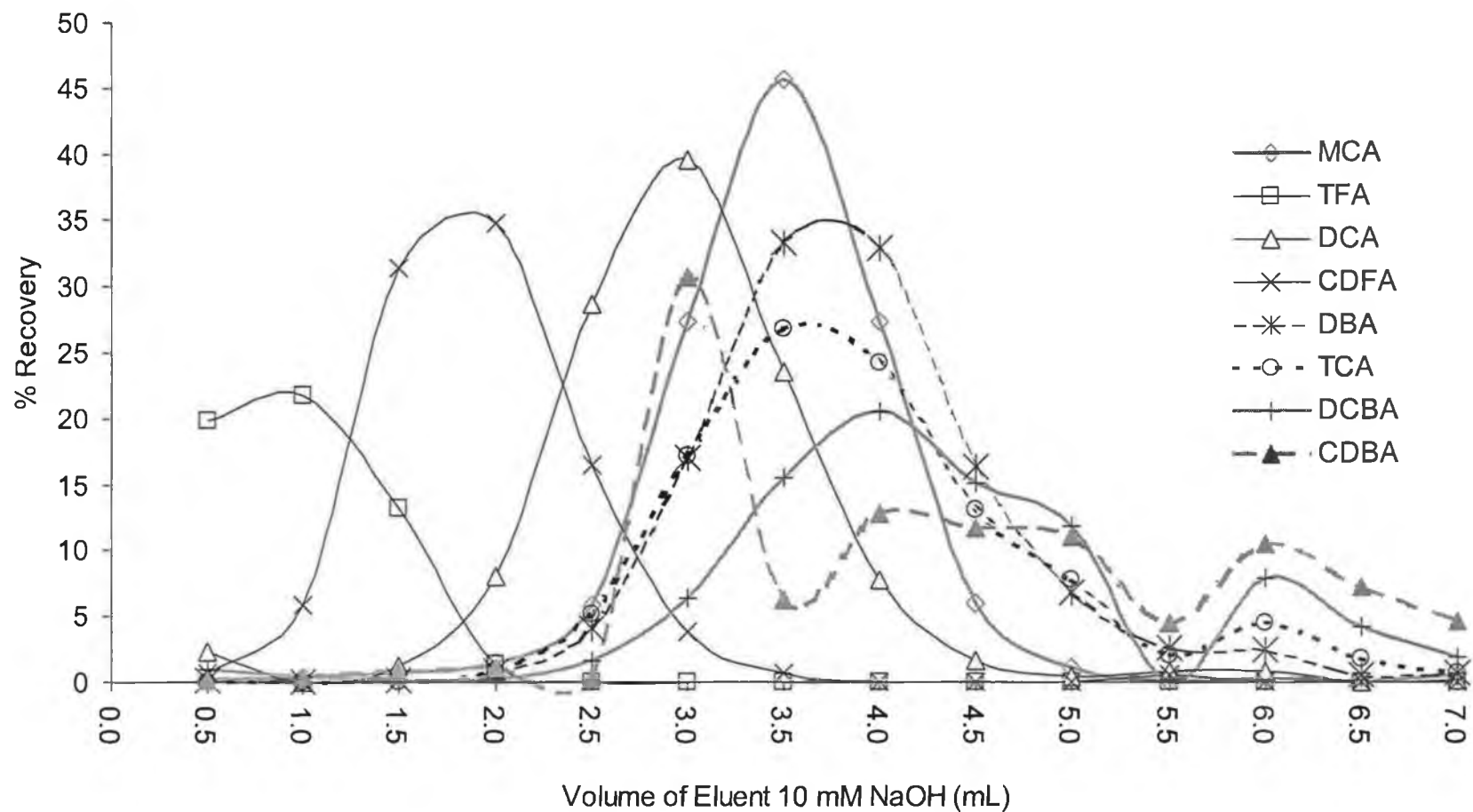


Fig 5.5. Elution profiles for eight HAs using 400 mg sorbent mass (double commercially available sorbent mass) in stepwise fractions of 0.5 mL of 10 mM NaOH

As can be observed from the profile, the fluorinated acids again show the least affinity for the cartridge with all TFA being eluted after 2 mL of 10 mM NaOH. CDFA was the next to elute with the majority of the bound acid being eluted in 4 mL of sorbent. CDBA eluted in a rather broad profile extending to the 14th fraction and its broadness matched that of DCBA. However, DCBA did not elute until the 8th fraction and displayed a stronger affinity for the cartridge. MCA, DCA, DBA and TCA eluted together in roughly 5 mL of 10 mM NaOH. Elution maxima for these four acids were DCA, MCA, TCA and DBA in order increasing elution volume. This elution profile suggests that when sorbent mass is doubled, the eluent volume required to remove them from the cartridge also roughly doubles. Percent recovery calculations were not possible for MBA, which still suffered slight coelution with residual chloride.

Another interesting point noted was that considering that some of the HAs eluted earlier and some eluted much later, the possibility to increase % recovery while maintaining a high preconcentration factor was possible by incorporating two elution steps. From the elution profile 2 mL of 10 mM NaOH was required to remove almost 100 % of the fluorinated acids. Following this 2 mL of eluent, the other HAs began to elute. This suggested that if the first 2 mLs were to be collected separately, a further 3.5 mL would elute almost 100 % of the other HAs, still leading to a 14.5-fold preconcentration factor. Collection of these two fractions of 2 mL followed by 3.5 mL of eluate in separate vials should have led to the same 25-fold preconcentration factor (for the first 2 mL fraction) for TFA and CDFA and a 14.5-fold preconcentration factor for the second 3.5 mL volume, assuming little or no portions of chlorinated or brominated HAs eluted in the previous 2 mL fraction with the fluorinated acids. However, the effect of doubling sorbent mass immediately showed a drop in preconcentration capability and thus would have led to higher detection limits regardless of improved % recoveries.

Nevertheless, the experiment was repeated with the same sorbent, which was washed with 6 mL MeOH and preconditioned with 6 mL of 200 mM H₂SO₄ prior to further use (washes and preconditioning reagent volumes were doubled alike for a double sorbent mass). The same concentration of HAs was prepared as to the previous study and preconcentrated at 2 mL/min. After a 2 mL wash of Milli-Q water, 2 mL of NaOH was passed through the cartridge and collected in a vial and injected onto the IC under the AS16 column method conditions. Accordingly, a further 3.5 mL fraction of 10 mM NaOH was passed through and similarly injected into the IC. Percent recoveries were calculated based on peak heights of the HAs in the preconcentrate versus an 100 % standard of 5 µM MCA, MBA, TFA, DCA, CDFA, DBA, TCA and 10 µM DCBA and CDBA. The results for percent recoveries derived for each HA in both fractions are given in *Table 5.4*. Surprisingly, the information derived from the % recovery data suggested that even though the theory was correct, showing low levels of the chlorinated and brominated acids in the first 2 mL fraction, the efficiency of preconcentration was still more pronounced when using the single 200 mg sorbent cartridge, with really only MCA and TFA showing higher percent recoveries. Furthermore, a higher detection limit was achieved with this method since the second fraction only corresponded to a 14.5-fold preconcentration factor.

Table 5.4 Comparison of single vs double sorbent mass as well as two-step elution

HA	Cumulative % Recovery from Elution Profile	Expected 100 % Standard Concentration (μM)	Concentration of Standard for Preconcentration (μM)	% Recovery from first 2 mL Fraction of 10 mM NaOH ^a	% Recovery from second 3.5 mL Fraction of 10 mM NaOH ^b	% Recovery of 200 mg sorbent ^c
MCA	113	5	0.2	6	84	65
MBA	N/A	5	0.2	N/A ^d	N/A ^d	63
TFA	56	5	0.2	77	35	17
DCA	115	5	0.2	8	82	84
CDFA	94	5	0.2	61	78	87
DBA	118	5	0.2	14	47	66
TCA	104	5	0.2	4	33	58
DCBA	87	10	0.4	6	18	30
CDBA	102	10	0.4	N/A ^e	N/A ^e	13

^abased on a 25-fold preconcentration factor.

^bbased on a 14.5-fold preconcentration factor.

^cfrom Table 5.2.

^ddue to interference from chloride.

^edue to poor signal intensity indicating a third elution step was possibly required specifically for CDBA

Since doubling sorbent mass doubled elution volume, it was considered that if eluent concentration was doubled, elution volume might have decreased to some extent. A similar experiment to the elution profile investigations was set up, with the exception that the eluent used in this work was 20 mM NaOH. Again, a standard of 0.2 μ M MCA, MBA, TFA, DCA, CDFA, DBA, TCA and 0.4 μ M DCBA and CDBA was prepared in Milli-Q water and preconcentrated on a fresh 400 mg sorbent cartridge. After a wash of 0.5 mL Milli-Q water, the bound HAs were eluted with stepwise fractions of 20 mM NaOH. The elution profile can be observed in *Fig 5.6(a)*. It can be clearly seen that doubling the eluting agent concentration did not induce more rapid elution of HAs from the cartridge with all HAs eluting in similar fractions to that of the 10 mM NaOH eluting agent. Therefore, doubling sorbent mass in an attempt to improve both % recovery and overall detection limits was not warranted in this case and the previously developed method using the 200 mg LiChrolut EN sorbent continued to be used in further analyses.

Along with the elution profiles for the HAs, the effect of elution volume was also assessed for the removal of excess sulphate from the sample. Peak heights for sulphate were plotted for both the 10 and 20 mM NaOH eluting agent and it was observed that when using the double sorbent mass that approximately 70 % of the excess sulphate could be removed with a wash step of 2 mL, which was double that of the 200 mg sorbent. This concurred with the original hypothesis that doubling sorbent mass, in fact doubled the volume required to remove the HAs and, accordingly, doubled the wash volume. The effect of increasing volume on the removal of excess sulphate can be seen in *Fig. 5.6(b)*.

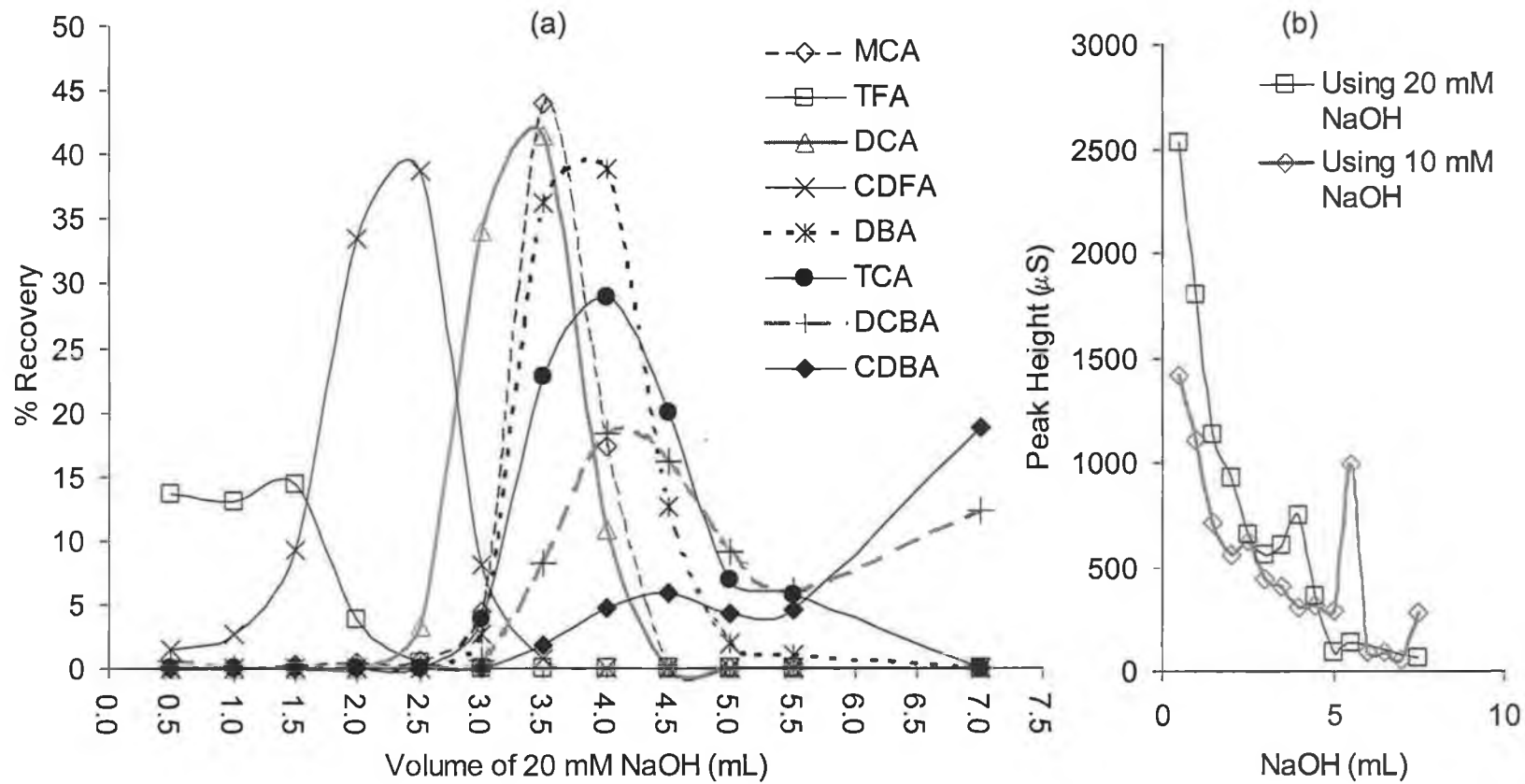


Fig 5.6 (a) Elution profiles for 8 HAs when using 20 mM NaOH as the eluting agent (b) the effect of increasing fraction number on excess sulphate removal associated with acidification step

5.4 Conclusions

By using the Atlas suppressor with hydroxide eluents at low flow rates, significantly lower detection limits for nine HA species were obtained than with the ASRS Ultra suppressor. Limits of detection without preconcentration were between 1.4 and 73.5 µg/L for a micro-bore IC method with only 100 µL injection volume. With solid phase extraction this was further reduced to a concentration range of 0.09 – 21.5 µg/L for the 9 HAS. When preconcentration was employed, a reduction in residual nitrate allowed identification and quantification of DCA. The developed method is indeed simple, practical and suitable for the routine analysis of treated drinking water samples.

When investigating the preconcentration elution profiles further, it was found that doubling the sorbent mass requires double the volume of eluting agent required to elute the HAs from the cartridge. Moreover, doubling the concentration of the eluting species had little or no effect on the elution profiles of the HAs and did not remove them in a shorter timeframe and in effect reduced the preconcentration capability and worsened limits of detection for the overall analysis. Furthermore, percent recoveries were only improved for MCA and TFA, which was not sufficient, allowing for the other reasons against making this a permanent alteration to the method. As a result it was concluded that the commercially available 200 mg sorbent cartridges were sufficient for the preconcentration step.

5.5 References

1. Y. Liu, S. Mou, J. Chromatogr. A, 997, (2003), 225.
2. Dionex AEES Atlas Suppressor Operations Manual
3. C. Sarzanini, M.C. Bruzzoniti, E. Mentasti, J. Chromatogr. A, 850, (1999), 197-211.
4. D. Martínez, J. Farré, F. Borrull, M. Calull, Journal of Chromatography A, 835 (1999) 187.
5. D. Martínez, F. Borrull and M. Calull, Journal of Chromatography A, 827 (1998) 105.
6. Y. Liu, Shifen Mou, Microchem. Journal, 75, (2003), 79.
7. Y. Liu, Shifen Mou, Chemosphere, (2004) In Press.

Chapter 6.0

Alternative detection modes to suppressed conductivity detection for HA analysis

"The first rule of intelligent tinkering is to save all the parts", Aldo Leopold

6.1 Introduction

Current modes of detection for ion chromatographic analysis have shown conductivity detection to dominate the research presented in the past few years with a steady increase in various types mass spectrometric detectors. In addition to these, other detection techniques have shown increased use with IC such as, amperometric, potentiometric, atomic emission and atomic fluorescence spectrometry [1]. Both UV-Vis [2, 3] and other more novel types such as conductive electroactive polymer modified electrodes [4] have shown direct application to HA analysis. UV detection at 210 nm has recently shown to be successful in combination with supported liquid micromembrane extraction (SLMME) to give impressive detection limits ranging from 0.02-2.69 µg/L for all nine chlorinated and brominated acetic acids with a 75-380 fold preconcentration factor [5].

However, direct or indirect UV detection has played a dominant role as the detector of choice more for CE determinations of HAs. Direct UV detection at 200 nm has been reported for application to HA analysis by Lopez-Avila *et al.* and quantification was possible at 100 ppb of all HAs with no preconcentration [6]. Less sensitive detection of HAs have been shown by Martinez *et al.* with indirect UV detection at 235 nm with 2,6 naphthalenedicarboxylic acid as carrier electrolyte [7].

Receiving the most attention in more recent years is IC with mass spectrometric detection (IC-MS). The determination of a wide range of analytes such as organic acids [8], illicit drug substances [9], agricultural chemicals [10] and water micropollutants [11], to name but a few, has shown to be possible with IC-MS. Generally suppressed ion exchange chromatographic methods require some sort of secondary volatilisation flow prior to the electrospray needle and/or a flow splitter for standard bore chromatography. Those that employ reversed phase liquid chromatography most often use organic solvent as a component of the mobile phase to aid separation and later volatilise the analytes. The benefits of mass spectrometric detection lie its analyte specific nature and makes it an invaluable tool for the analytical chemist. A discussion

of the recent advances in IC-MS technology for the detection of DBPs (HAs and oxyhalides) can be found in Chapter 1.0. Signals from IC-MS instruments can be observed in two forms (a) total ion chromatograms (TIC), which are acquisitions of the total number of ions per unit time over a selected m/z range and (b) selected ion monitoring (SIM) or extracted ion chromatograms (EIC), in which the analyst can select an individual mass corresponding to the analyte of interest and view its abundance over the course of the run. Sensitivity of mass spectrometric detection with IC separation has often shown to lie in the sub $\mu\text{g/L}$ range [12, 13] for the analysis of halogenated inorganic and organic compounds.

The aim of work presented here was to examine the suitability of added UV and electrospray mass spectrometric detectors for the direct analysis of HAs using the optimised suppressed ion chromatographic method. As part of this investigation, in depth optimisation of the ESI-MS parameters by direct infusion was required followed by development of sensitive MS detection of non-volatile analytes in aqueous eluents. UV wavelength optimisation, linearity and sensitivity studies were also required. The possibility of running all three detector types in series was considered followed by application to the analysis of real samples.

6.2 Experimental

6.2.3 Instrumentation

All chromatographic instrumentation and optimised conditions are given in Chapter 5.0, Section 5.2.1. For mass spectrometry, a Bruker Daltonics Esquire~LC electrospray octopole ion trap was employed complete with Bruker Daltonics NT 4.0 software run on separate Hewlett-Packard Kayak XA personal computer (Hewlett-Packard, Palo Alto, CA, USA) to UV and conductivity acquisitions. Optimised parameters for ESI-MS are listed in *Table 6.1*. Suppression was carried out in the external water mode. The Atlas and CR-ATC were connected to a secondary Waters 501 HPLC pump (Millipore-Waters, Milford, MA, USA), which supplied Milli-Q water at a flow rate of 0.30 mL/min. For direct infusion-MS a Cole Parmer 74900 series threaded screw syringe type pump was filled with sample and pumped at 250 μ L/hour. For IC-MS, the IC eluate was coupled to the electrospray via a T-piece supplied with a 0.12 mL/min flow of 100 % MeOH before entering the electrospray needle. The pump used for MeOH supply was a Hewlett-Packard HP100 micro-bore pump. Sample preconcentration with sulphate and nitrate removal was carried out as in Chapter 5.0, Section 5.2.3.

6.2.4 Chemicals

All reagents used were of analytical reagent grade purity. Sodium chloroacetate (98 %), bromoacetic acid (99 %+), sodium trifluoroacetate (98 %), sodium dichloroacetate (98 %), chlorodifluoroacetic acid (98 %), dibromoacetic acid (97 %), trichloroacetic acid (99 %+), bromodichloroacetic acid (neat) and dibromochloroacetic acid (neat) were all ordered from Aldrich (Milwaukee, WI, USA) along with all inorganic anions prepared from their respective sodium salts. Stock HA solutions were prepared to a concentration of 10 mM and stored in the refrigerator for a maximum of 2 weeks at 4 °C in the dark. Stock inorganic anion standards were prepared to a concentration of 1000 mg/L. All working standards were freshly prepared daily using diluent water from a Milli-Q purification system (Millipore, Bedford, MA, USA) with a

specific resistance of 18.3 MΩcm. Sulphuric acid used for acidification of preconcentration samples and standards was 99 % purity and also ordered from Aldrich. Methanol used for volatilisation was of MS grade and ordered from Romil (Cambridge, UK). A drinking water sample (1 L) for HA determinations was collected from the Dublin City University laboratory water supply as per Chapter 5.0, Section 5.2.3.

6.3 Results and Discussion

6.3.1 UV detection – wavelength optimisation

The Dionex AD20 was installed after the conductivity cell. A 4 μM HA standard was prepared in Milli-Q water and run at 190, 200, 210, 220, 230 and 240 nm. The resulting chromatograms were integrated and peak absorbances versus detector wavelength were plotted. From *Fig. 6.1* it can be observed that the HAs absorbed best in the low UV region at 190 nm. However, for realistic application to real samples, the wavelength chosen was not 190 nm, due to the onset of interference resulting from chloride. Chloride absorbance, as can be seen from *Fig 6.1*, dropped to roughly 20 % of its absorbance at 200 nm and no significant decrease in absorbance occurs from here onwards. Similarly, at 210 nm the absorbance of most of the HAs was up to 60 % lower than at 200 nm. The optimum wavelength combining sensitivity with reduced interference was therefore chosen to be 200 nm. Similar wavelength settings have been reported by Lopez-Avila *et al.* [3], but it does vary with other IC methods for this application using 210 nm as a less sensitive but increased specificity wavelength [2].

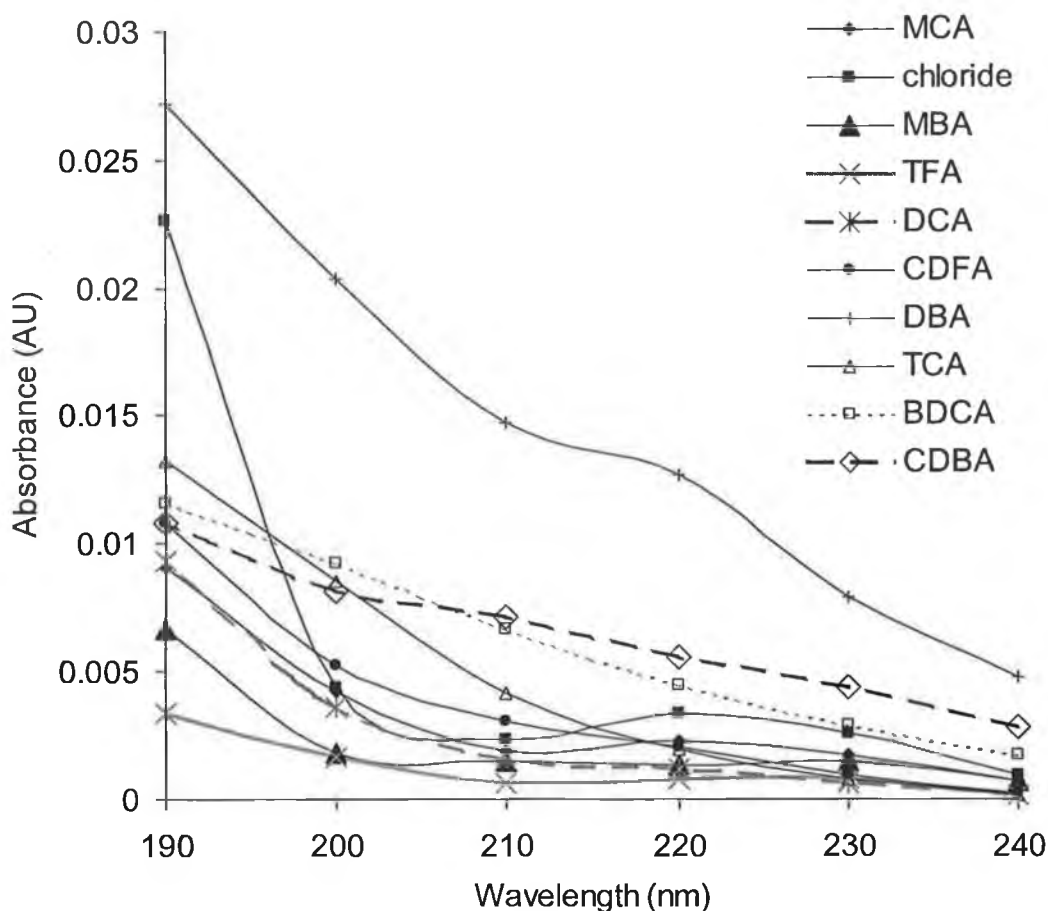


Fig. 6.1 UV absorbance wavelength optimisation for 4 μM standard of all HAs

During this experiment it was noted that the shape of the baseline was similar to that of the conductivity trace with an increase in absorbance over the course of the gradient, which was less pronounced at higher wavelengths suggesting a component of the eluent absorbed in this region. Since UV detection was carried out in series with suppressed conductivity in the auto-recycling mode, the eluent was expected to be a solution of analytes in pure water. Sensitivity measurements with the conductivity detector showed excellent suppression efficiency with the Atlas suppressor, so it was thought that this background interferent possibly arose from some component of the eluent generation process. However, this could not be conclusively proven with UV detection. Fig. 6.2 shows a separation of 4 μM HAs at all wavelengths listed above. Similarly, at low concentrations, observed MBA peaks were distorted due to a background absorbance dip just before the onset of the peak

possibly due to the low absorbance of chloride with respect to residual carbonate at this wavelength. For UV to be sensitive to low HA concentration levels and to be quantitative with reproducible results, this posed a problem as integration became difficult at low HA concentrations.

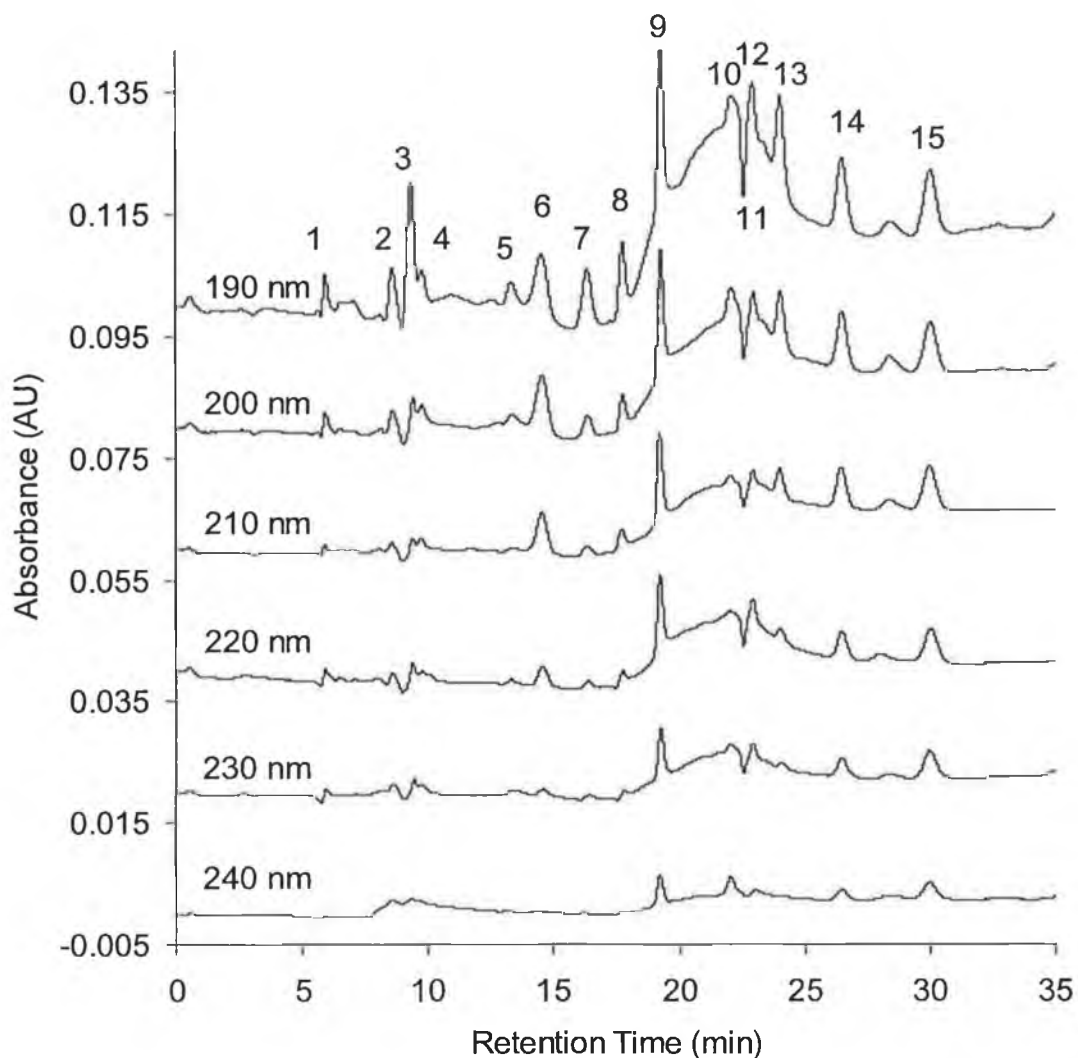


Fig 6.2 Chromatograms at each wavelength for a 4 μ M standard of 9 HAs. Offset 0.02 AU for clarity. Elution order: 1= acetate, 2 = MCA, 3 = chloride, 4 = MBA, 5 = TFA, 6 = nitrate, 7 = DCA, 8 = CDFA, 9 = DBA, 10 = carbonate, 11 = system peak, 12 = sulphate, 13 = TCA, 14 = DCBA, 15 = CDBA.

6.3.2 UV detector linearity and low limit sensitivity

With the wavelength now set at 200 nm, an investigation into detector linearity was carried out. A standard calibration series was set up comprising of concentrations of 2, 5, 7.5, 10, 15, 20 and 25 μM of all nine HAs with each run in triplicate. Linearity over this range was excellent with only TFA and MCA showing correlation coefficients < 0.99 . From the wavelength optimisation studies it was clear that UV detection was least sensitive for TFA and most sensitive for DBA, possibly explaining its slightly lower R^2 value. It was also noted that for the early eluters there existed a slight negative system peak prior to the chloride peak and made integration of MCA and MBA peak difficult at lower concentrations. Linearity correlation coefficients, slopes and intercepts, lower concentration standard deviation for triplicate runs and maximum detectable limit (MDL) of each concentration for this study are given in *Table 6.1*. The range was set for all HAs using this data. The lower limit of range was decided at 10 % RSD for triplicate runs or lower. All but MBA displayed percentage RSD values less than this value at the investigated 2 μM , concentration, which corresponded to a lower range of 185-433 $\mu\text{g/L}$ and for all nine HAs. As stated earlier, the presence of a background absorbing ion led integration difficulties for MCA and MBA at low concentrations and also this concentration range was not low enough to permit direct detection of these HAs in drinking water unlike with suppressed conductivity alone (see *Fig. 6.3*). Nitrate in direct detection methods would also have caused major effect as it absorbs strongly at 214 nm and would have completely masked TFA and possibly DCA. Quantitative analysis using suppressed conductivity and UV detection would have been successful when preconcentration was employed, but the strong UV absorbance of inorganic nitrogen containing compounds at 200 nm would have still been an issue with UV chromatograms detecting even the slightest presence of nitrate or nitrite. The conductivity detector offered a more resolute chromatogram with less interference and baseline disturbances than with UV detection and was also more sensitive in all cases (from MDL studies). For calibration curves, please refer to *Appendix A.5, Fig. A.5-1*.

Table 6.1 Linearity data for Dionex AD20 UV detector for 2, 5, 7.5, 10, 15, 20 and 25 μM of all nine HAs run in triplicate along with MDL.

	R^2	Slope (10^{-5} AU.L/mol)	Intercept (10^{-5} AU)	%RSD 2 μM standard	MDL ^a (mg/L)
MCA	0.9892	3	1.5	0.96	0.46
MBA	0.9936	5	-2.0	47.40	1.03
TFA	0.9887	1	2.0	0.90	1.69
DCA	0.9994	14	0.6	5.21	0.27
CDFA	0.9994	12	2.0	2.73	0.32
DBA	0.9992	43	4.0	0.97	0.05
TCA	0.9994	20	2.0	2.13	0.08
DCBA	0.9991	19	-0.1	0.69	0.26
CDBA	0.9940	12	1.0	7.73	0.41

^amaximum detectable limit for all species carried out by sequential dilution of standard until peak either breached 3:1 S:N ratio or peak disappeared because of interference or was unintegrable.

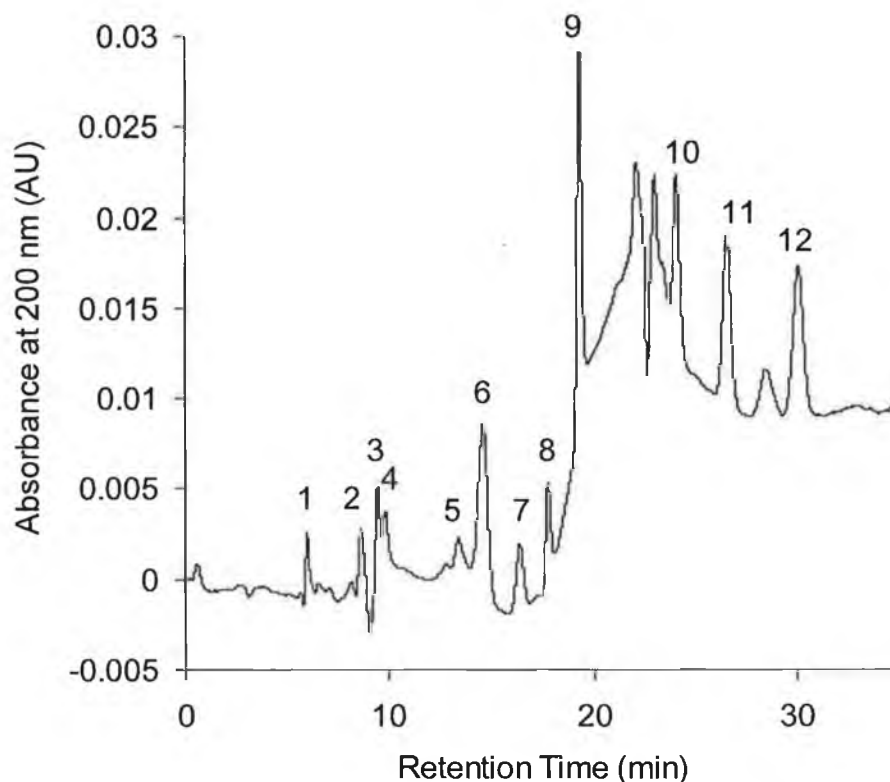


Fig 6.3 A 4 μM standard of 9 HAs with UV detection showing interference from chloride combined with background contaminant making integration of MBA and MCA difficult at low levels along with significant background signal rise over gradient run. Elution order: 1 = acetate, 2 = MCA, 3 = chloride, 4 = MBA, 5 = TFA, 6 = nitrate, 7 = DCA, 8 = CDFA, 9 = DBA, 10 = TCA, 11 = DCBA, 12 = CDBA.

6.3.3 Direct Infusion – Mass Spectrometry

In order to achieve maximum sensitivity, the mass spectrometer itself was first fine-tuned for HA analyses. Coupling the IC to an electrospray system will be discussed later in Section 6.3.4. A concentrated solution of seven HAs was prepared in a mixture of 71.5:28.5 water:methanol and infused at a flow rate of 250 $\mu\text{L}/\text{hour}$ using a threaded screw-type injector with a 250 μL glass syringe attached. DCBA and CDBA were not included in this optimisation, due to availability.

The resultant mass spectra showed clear signals for all analytes over all mass ranges. Each individual acid was then prepared in the water:MeOH solvent and all detector parameters were individually optimised. The Bruker Esquire~LC software allowed automatic tuning of the instrument for a particular m/z value by optimising each parameter sequentially and in triplicate, taking the previous optimised parameter and presetting its value before it optimised the next. Although it would have been preferable to have charts of this data included here, it was not possible with this software and final optimised parameters were merely noted. The parameters optimised were,

1. Capillary voltage (V)
2. End plate offset (V)
3. Capillary exit offset (V)
4. Skimmer 1 (V)
5. Octopole (V)
6. Octopole Δ (V)
7. Trap drive
8. Skimmer 2 (V)
9. Octopole RF (Vpp)
10. Lens 1 and 2
11. Nebulizer pressure (psi)
12. Dry gas flow (L/min)
13. Dry gas temperature ($^{\circ}\text{C}$)

The optimum MS parameters were determined for all seven HAs and are listed in Table 6.3. All HAs required high capillary voltages of 4200 V or greater and end plate offset voltages of between -500 ($[\text{DBA-H}]^-$) and -1200 V ($[\text{CDFA-H}]^-$ and $[\text{TFA-COOH}]^-$). The intensities for all analytes increased when dry gas flow and nebulizer pressure were set at their maximum operating value of 8 L/min and 55 psi. Importantly, the running cost of using up to 8 L/min of nitrogen drying gas for these extremely polar analytes was extensive and would not suit all laboratory environments economically. Trap drive levels of between 29 and 45 were required for all HAs. The manufacturer's notes recommended preset trap drive values of up to 50 for a m/z range of 50-400. The higher the trap drive level, the more optimal the conditions for higher m/z values. Capillary exit offset remained constant for all HAs at -50 V and similarly for skimmer 1, all HAs with the exception of $[\text{DBA-COOH}]^-$ required -15 V for optimal operation. The optimisation of focussing parameters markedly improved analyte signal intensity; especially lens 2, which varied significantly from 30 to 85 with both the type of HA and individual fragment. Similarly, skimmer 2 when optimised improved analyte sensitivity significantly.

It was noted that for each of the HAs there existed in some cases up to three discernable peaks corresponding to the deprotonated or pseudo molecular ion $[\text{M-H}]^-$, the decarboxylated form $[\text{M-COOH}]^-$ and a dimerised form $[\text{2M-H}]^-$ of each HA. These three ion forms have previously been reported by Roehl *et al.* [14] and the m/z chosen for maximum sensitivity single ion monitoring of each HA varied with the degree of halogenation. Structures for these fragments can be observed in *Fig. 6.4*.

Table 6.2 Optimised mass spectrometer conditions for HA analysis. All optimised parameters carried out at 8 L/min drying gas, 300°C dry gas temperature and 55 psi nebulizer pressure.

m/z	HA [Ion type]	Capillary Voltage (V)	End Plate Offset (V)	Skim 1	Cap. Exit Offset (V)	Octopole (V)	Octopole Δ (V)	Trap Drive	Skim 2 (V)	Oct RF (Vpp)	Lens 1	Lens 2
68.9	TFA [M-COOH] ⁻	4500.0	-1200	-15	-50	-1.00	-1.30	39.02	-4.67	50.00	4.44	49.51
82.9	DCA [M-COOH] ⁻	4500.0	-1005	-15	-50	-1.00	-1.30	34.07	-8.11	50.00	4.36	54.10
92.9	MCA [M-H] ⁻	4500.0	-592	-15	-50	-1.00	-0.96	35.77	-5.41	50.00	2.27	30.00
112.9	TFA [M-H] ⁻	4500.0	-730	-15	-50	-1.00	-1.36	38.61	-6.64	50.00	4.42	51.80
118.7	TCA [M-COOH] ⁻	4352.5	-695	-15	-50	-1.00	-1.76	45.15	-4.43	50.00	2.23	30.00
126.7	DCA [M-H] ⁻	4500.0	-546	-15	-50	-1.00	-0.50	29.25	-5.16	54.10	7.99	71.31
128.8	CDFA [M-H] ⁻	4500.0	-1200	-15	-50	-1.00	-0.50	35.39	-6.39	50.00	2.20	30.00
136.9	MBA [M-H] ⁻	4254.1	-1051	-15	-50	-1.33	-2.05	43.11	-5.66	86.89	7.50	85.08
162.9	TCA [M-H] ⁻	4500.0	-970	-15	-50	-3.49	-1.30	32.45	-4.18	50.00	2.23	30.00
172.6	DBA [M-COOH] ⁻	4254.1	-660	-29	-50	-1.00	-0.50	41.06	-6.86	50.00	6.71	66.72
216.6	DBA [M-H] ⁻	4254.1	-500	-15	-50	-4.54	-0.50	38.19	-2.95	86.89	4.81	60.98
<i>Average</i>		<i>4419.5</i>	<i>-831.7</i>	<i>-16</i>	<i>-50</i>	<i>-1.58</i>	<i>-1.09</i>	<i>37.46</i>	<i>-5.50</i>	<i>57.08</i>	<i>4.47</i>	<i>50.86</i>

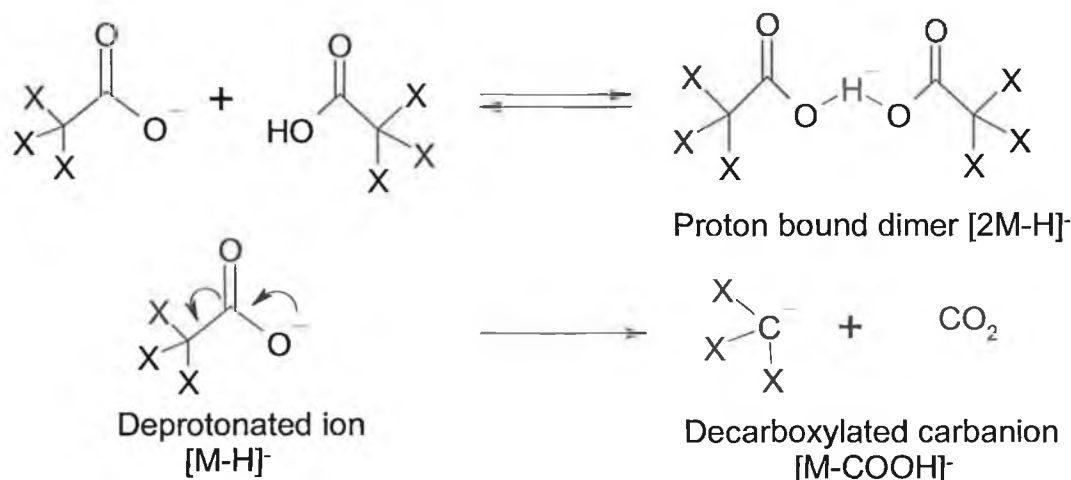


Fig 6.4 Observed pseudo molecular ion $[M-H]^-$, decarboxylated $[M-COOH]^-$ and dimerised forms $[2M-H]^-$ of each HA where X = F, Cl, Br or H [15].

Fig. 6.6 shows the mass spectra obtained for the three homogeneously halogenated chlorinated acids. The spectra shown here were averages of 20 individual mass spectra to give a more accurate representation of the compounds. MCA appeared clearly at m/z 92.9 and 94.9 in a 3:1 ratio showing the isotopic relative abundance of Cl^{35} and Cl^{37} for a compound containing one chlorine atom. For DCA, the $[M-H]^-$ peak occurred at m/z 126.8 with two further peaks, one at m/z 128.8 ($[Cl^{35}Cl^{37}CH_2COO]^-$ and $[Cl^{37}Cl^{35}CH_2COO]^-$) and a much smaller peak at 130.8 (corresponding to $[Cl^{37}_2CH_2COO]^-$). The ratio for a compound containing two chlorine atoms is generally 9:6:1 for the M, M+2 and M+4 peaks [16, 17]. The presence of two isotopic chlorines gave rise to *linear superposition* of individual chlorine atom isotopic patterns. The ratio for the pseudo molecular ion here was approximately 5:4:1 which did not correlate well with the accepted ratio, but when the decarboxylated fragment was examined, it agreed more conclusively that the compound contained two chlorine atoms. This second series of peaks for the decarboxylated form was observed at m/z 82.9, 84.9 and 86.9 and, as stated previously, at the 9:6:1 ratio. Also, the m/z 82.9 peak was visibly more intense than the pseudo molecular ion peak at m/z

126.7 suggesting that the decarboxylated form of the acid was more stable at the optimum conditions for DCA. For TCA, a trichlorinated compound, the three forms of the acid were present; the pseudo molecular ion at m/z 162.9 followed by the decarboxylated ion at m/z 118.7 and the dimerised form at m/z 322.5. Even more pronounced than with DCA, the decarboxylated ion shows the most sensitivity for MS analysis with also the emergence of the dimerised form, which was previously not observed with the mono- and dihalogenated anions. The spectra suggested that the degree of halogenation was a key factor in whether the most abundant ion was the pseudo molecular ion or the decarboxylated fragment. As will be shown, the dimerised form did not play a significant role and was only used for qualitative analysis if at all. However, a higher abundancy for this dimer ion was observed with an increase in the degree of halogenation and concurred with work published by Roehl *et al.* [14]. The effect of superposition of isotopic patterns can be seen in Fig.6.5.

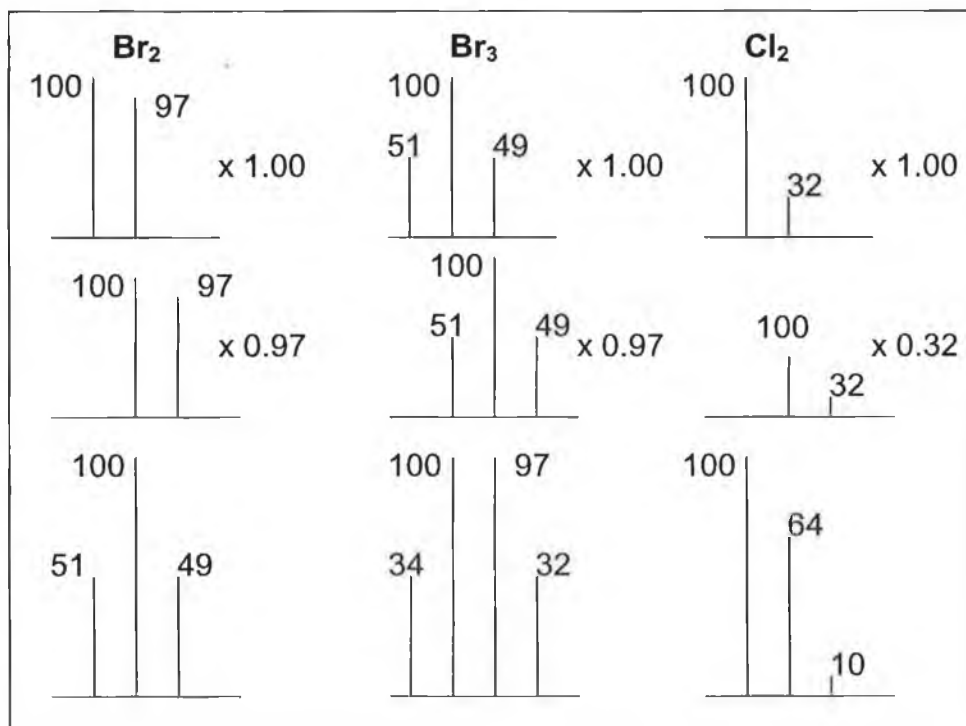


Fig. 6.5 Linear superposition of bromine and chlorine peak patterns [5]

The contribution of bromine and chlorine to M, M+2, M+4, M+6 etc. are given by the binomial expansion in Equation 6.1.

$$(a + b)^n = a^n + na^{n-1}b + \frac{n(n-1)a^{n-2}b^2}{2!} + \frac{n(n-1)(n-2)a^{n-3}b^3}{3!} + \dots + \dots$$

Equation 6.1

Therefore taking a and b to be 1 and 0.32 for the isotopic ratio of Cl^{35} and Cl^{37} respectively, the ratios of the peaks observed for TCA (where $n = 3$) should be 1: 0.96: 0.31: 0.03. The peaks observed for the pseudo molecular ion and decarboxylated fragment for TCA in *Fig. 6.6* show some correlation to this ratio for a compound containing three chlorine atoms.

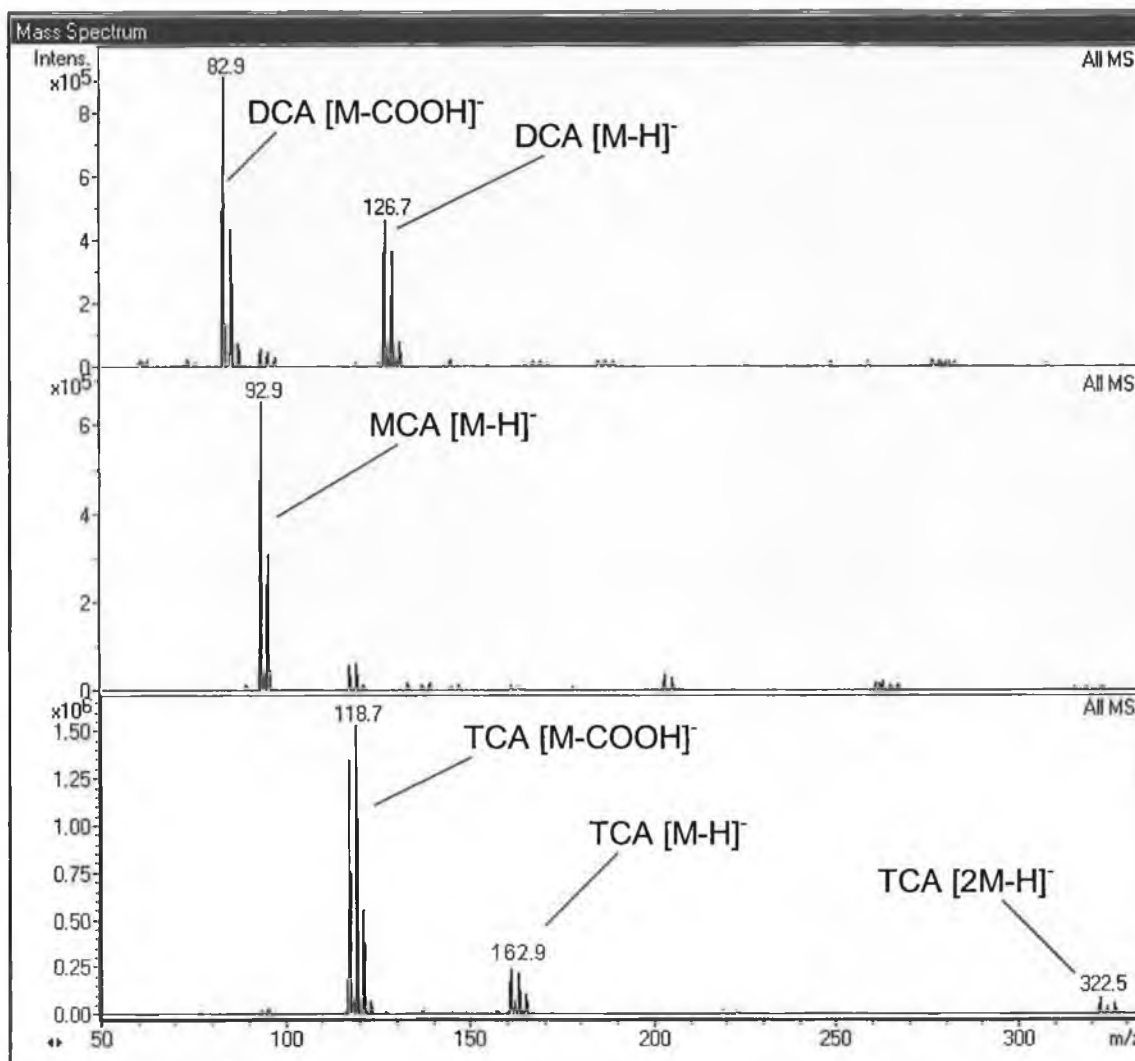


Fig. 6.6 Mass spectra for directly infused standard of MCA, DCA and TCA.

Correspondingly, individual solutions of each of the two brominated acids MBA and DBA were infused at 250 μ L/hour. Mass spectra show similar results to that of the chlorinated acids, albeit with different ratios for isotopic peaks corresponding to Br⁷⁹ and Br⁸¹ (Fig. 6.7). The MBA pseudo molecular ion was observed as a doublet at m/z 136.9 and 138.9 depending on the isotope of bromine. Also observed was loss of bromine at m/z 78.8.

The mass spectrum obtained for DBA was a little more complex with a distinct bromine signature triplet observed for the pseudo molecular ion at m/z 216.7 along with a similar triplet for the decarboxylated ion at m/z 172.6. The

isotopic abundance of bromine is 97 parts of Br⁸¹ for every 100 parts Br⁷⁹[4]. Therefore, a monobrominated species should contain a doublet comprising of a peak at the molecular mass as well as an M+2 peak similar to that of the mass spectrum obtained for MBA. For a dibrominated species these peaks undergo linear superposition similar to the multichlorinated acids according to Equation 6.1. A peak with 100 % intensity was observed at the molecular ion mass followed by its doublet at M+2 (but at 97 % intensity). The contribution of the second Br⁸¹ peak causes linear superposition resulting in a triplet of approximately 1:2:1 intensity ratio. As expected, the dibrominated species was observed as a triplet with this ratio. Unlike the DCA, the emergence of the dimerised form occurred with the dibrominated species in this case. As found with the chlorinated acids, it seemed that the degree of halogenation played a key role in formation of this ion, but yet again occurred at such a low relative intensity not to be of any qualitative or quantitative use.

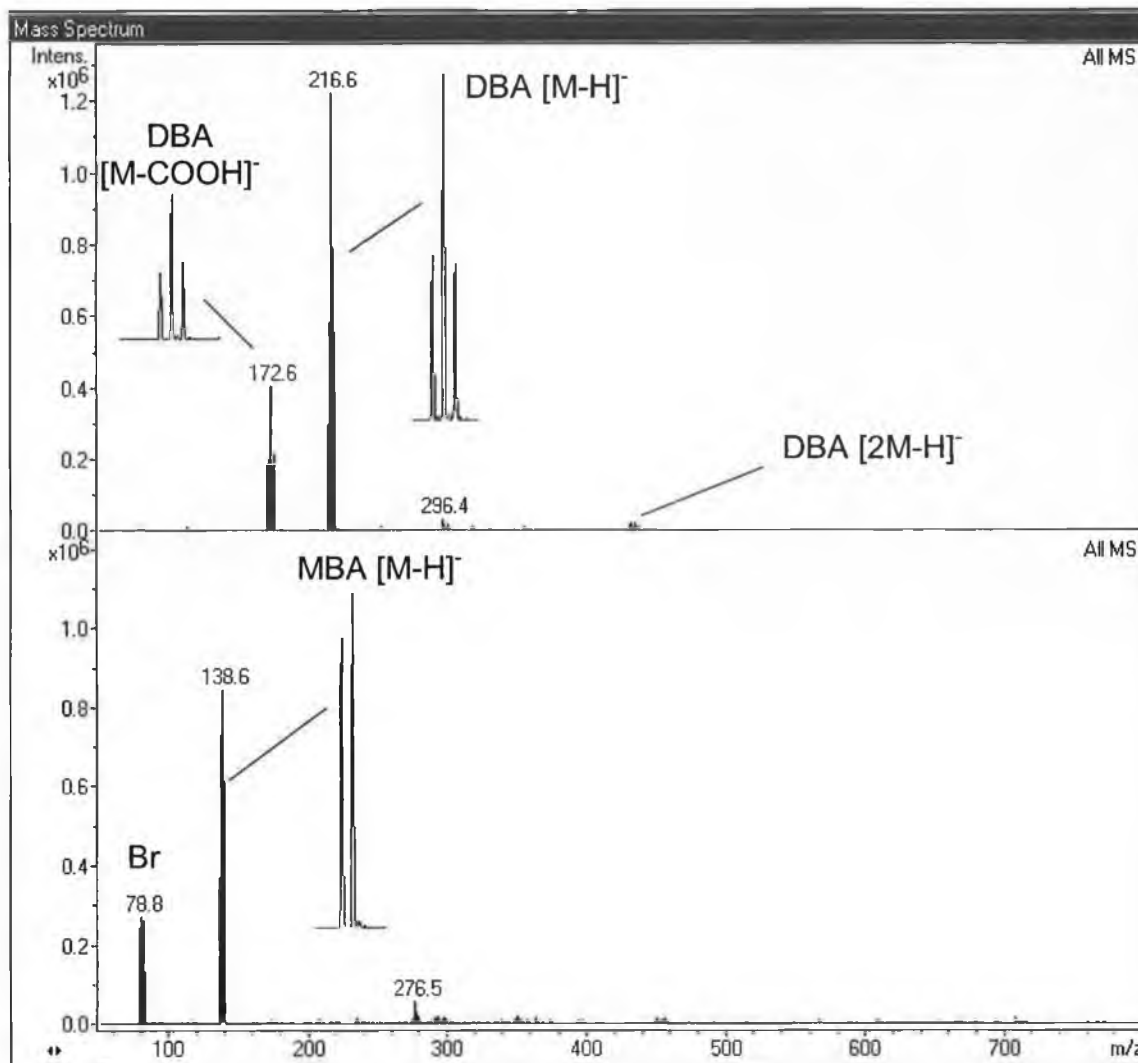


Fig 6.7 Direct infusion mass spectra for MBA and DBA at 250 μ L/hour

The two fluorinated species were infused last. Trifluoroacetic acid was expected to be observed as a singlet peak taking into consideration that fluorine does not have any naturally occurring isotope. This was indeed the case with a clear peak observed at m/z 112.9 along with the decarboxylated singlet peak at m/z 68.9. The heterogeneously halogenated CDFA was observed as the pseudo molecular ion at m/z 128.8 along with its decarboxylated fragment at 84.9 and the dimer form at 258.7. The pseudo molecular ion and fragment peaks were observed as doublets separated by 2 mass units and were due to the presence of isotopic Cl^{35} and Cl^{37} in a ratio of approximately 3:1 respectively. The mass spectra for the fluorinated compounds can be seen in Fig 6.8.

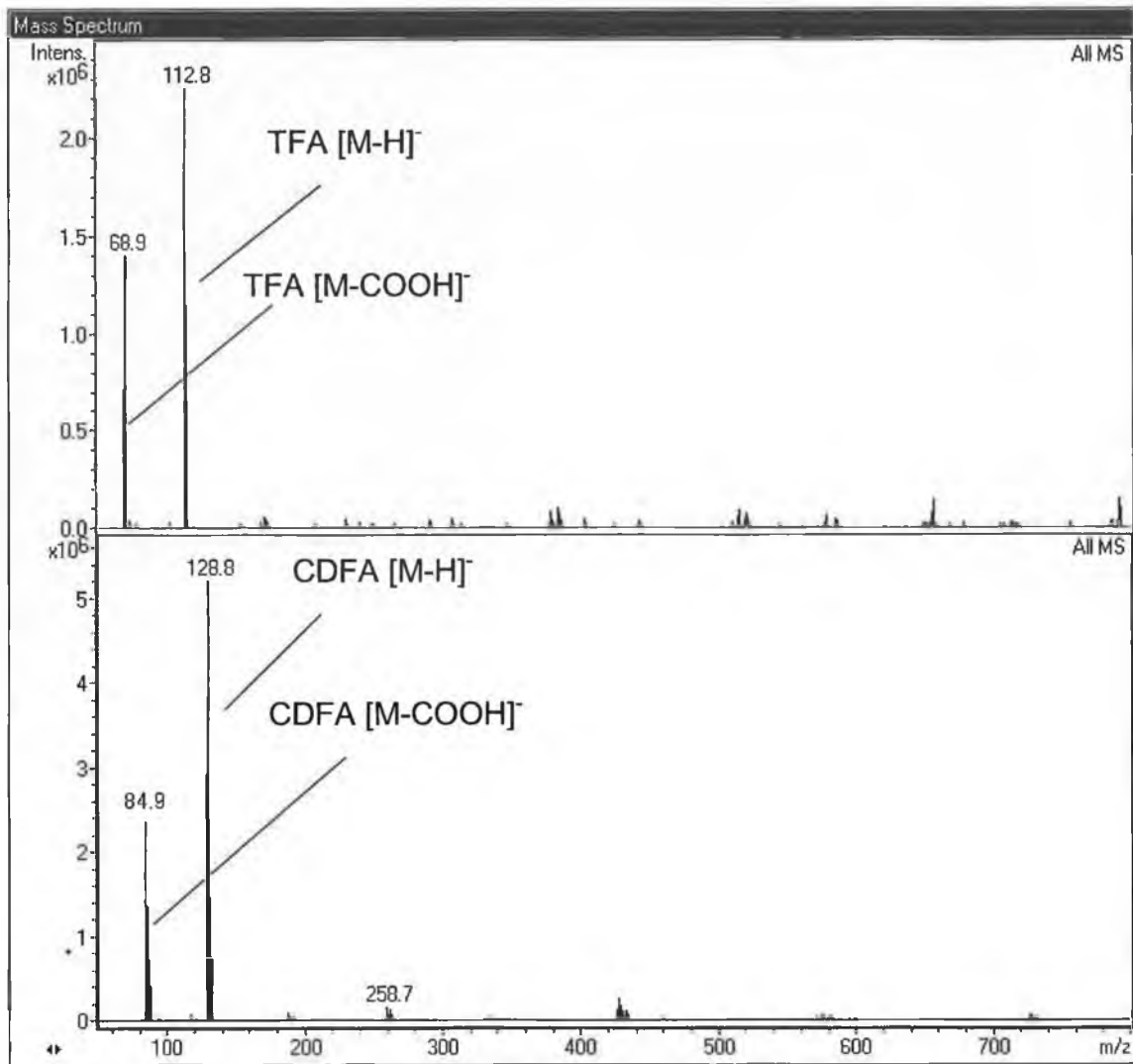


Fig. 6.8 Direct infusion mass spectra for TFA and CDFA (Flow rate = 250 $\mu\text{L}/\text{hour}$)

6.3.4 Ion chromatography-mass spectrometry optimisation

6.3.4.1 Elimination of background interference

To this point there was some speculation as to some form of interferent species in the background eluent. Neither conductivity nor UV detection could conclusively establish this except for observed baseline disturbances and a reduction in overall retention time for all HAs observed for electrolytically generated eluents. Coupling the IC to the electrospray needle was carried out by configuration of the suppressor and CR-ATC to the external water mode. The secondary Waters HPLC pump was employed to deliver Milli-Q water to the regenerative inlet on the Atlas, which in turn was plumbed to the regenerant inlet of the CR-ATC in order to maintain the same degree of suppression and carbonate removal. The regenerant flow rate was also set to match the eluent flow rate at 0.3 mL/min. Initial separations when carried out in the single ion monitoring (SIM) mode showed visible peaks for some, but not all of the HAs.

However, it was noticed that a large peak at m/z 182.9 caused significant interference and was present at high intensity and could have possibly contributed to analyte suppression resulting in poor sensitivity. As can be observed from *Fig 6.9*, the total ion chromatogram (TIC) for the separation of 9 HAs behaved similar to an indirect detection method. For each HA eluted, a decrease in total ion signal intensity was observed. When the SIM trace was acquired over the run time of the experiment, the same effect was noticed for this m/z value. Therefore, it was concluded that the interferent anion was a component of the eluent and not of the sample. Milli-Q water was investigated for contamination by injecting 100 μ L onto the IC at the optimum conditions. Background conductivity of the pure Milli-Q was within accepted limits and no large contamination peaks were observed during the separation, except for the residual chloride mentioned previously. No reference was made to generation of interferent species, or any other species therefore, relating to a peak at m/z 182.9 in the manufacturer's manual [18]. The eluent generator cartridge was also within its specified lifetime of 2 years and was still efficient to >70 % capacity.

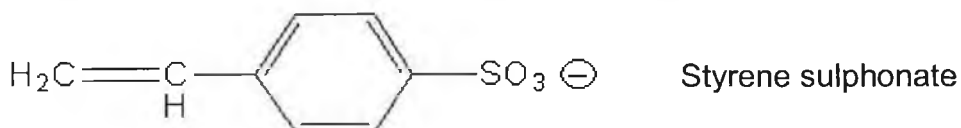
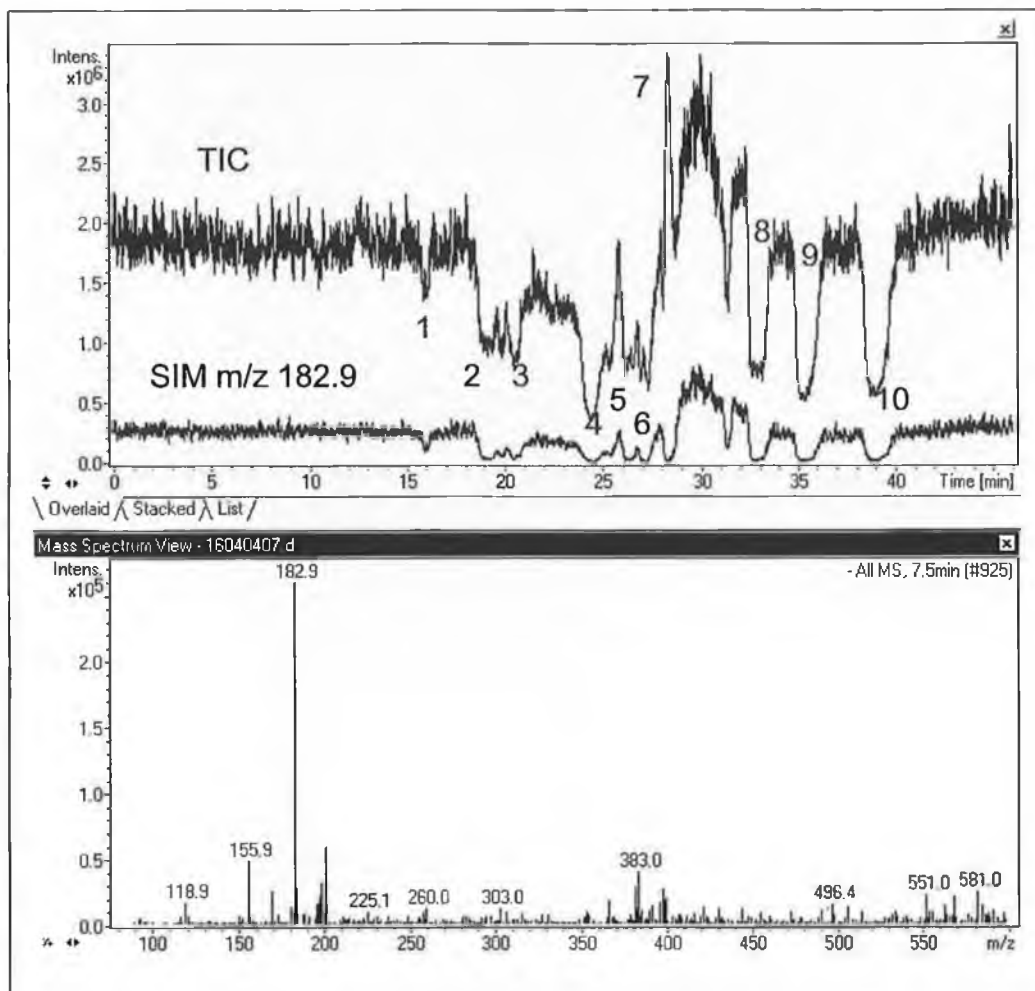


Fig 6.9 TIC and SIM traces of interferent species at m/z 182.9 resulting from leached styrene sulphonate into the electrolytically generated eluent during a separation of $100 \mu\text{M}$ standard of nine HAs. Elution order: 1= fluoride, 2 = MCA, 3 = MBA, 4 = TFA, 5 = DCA, 6 = CDFA, 7 = DBA, 8 = TCA, 9 = DCBA, 10 = CDBA.

It became clear that the cause of this large background interference was due to styrene sulphonate resulting from the eluent generation process. Styrene sulphonate leached from the membrane into the eluent and was an unavoidable flaw in the instrumentation design. The use of an eluent generator

was not warranted given the styrene sulphonate interference. Therefore, it was decided to revert to manually prepared eluents for the remainder of this work, although the CR-ATC was retained. The efficiency of carbonate removal from the system was invaluable to achieving similar detection limits to that reported in Chapter 5.0 with conductivity detection. In Chapter 4.0, a comparison between manual and electrolytically generated eluents showed variance in retention times for all analytes. With the use of mass spectrometry it was now possible to allocate a cause for this. Since styrene sulphonate was a bulky anion and leached into the eluent over time, it may have coated the column surface, thus reducing retention times for all analytes and would only have been removed by column cleanup procedures. Since the column was used for neat and preconcentrated drinking water samples, column cleanup was carried out every 3-4 months as a precaution and to maintain column efficiency. The column may have required cleaning at the point of the comparison experiment due to styrene sulphonate adsorption. However, fortunately the column had been subjected to numerous runs with the eluent generator and the fault was identified.

6.3.4.2 *Optimum parameters for simultaneous detection of nine HAs*

The chromatography system was again set up in the external water suppression mode with eluate passing from the conductivity cell to the electrospray needle. Like before, the secondary Waters HPLC pump was employed to deliver Milli-Q water to regenerate the Atlas suppressor and CR-ATC. However, in the following investigations the eluent generator was not used and two eluent reservoirs of 2.5 and 20 mM NaOH were prepared from the stock 50 % w/v solution.

The optimum parameters listed in *Table 6.1* were set to the optimum for the [TCA-COOH]⁻ ion, as it was the most abundant form of the analyte with the overall weakest intensity of all HAs. Initial separations showed acceptable conductivity measurements similar to that reported in Chapter 5.0, but sensitivity of the MS measurements in the total ion chromatogram (TIC) mode were poor, even with a 100 µM standard of all nine HAs. Higher sensitivity was

possible in the SIM mode and concentrations of 15 μM could easily be detected, although the SIM chromatograms did not display superiority over the detection limits offered by conductivity detection at this stage in the development. The TIC and the SIM traces were also free from the styrene sulphonate background interference.

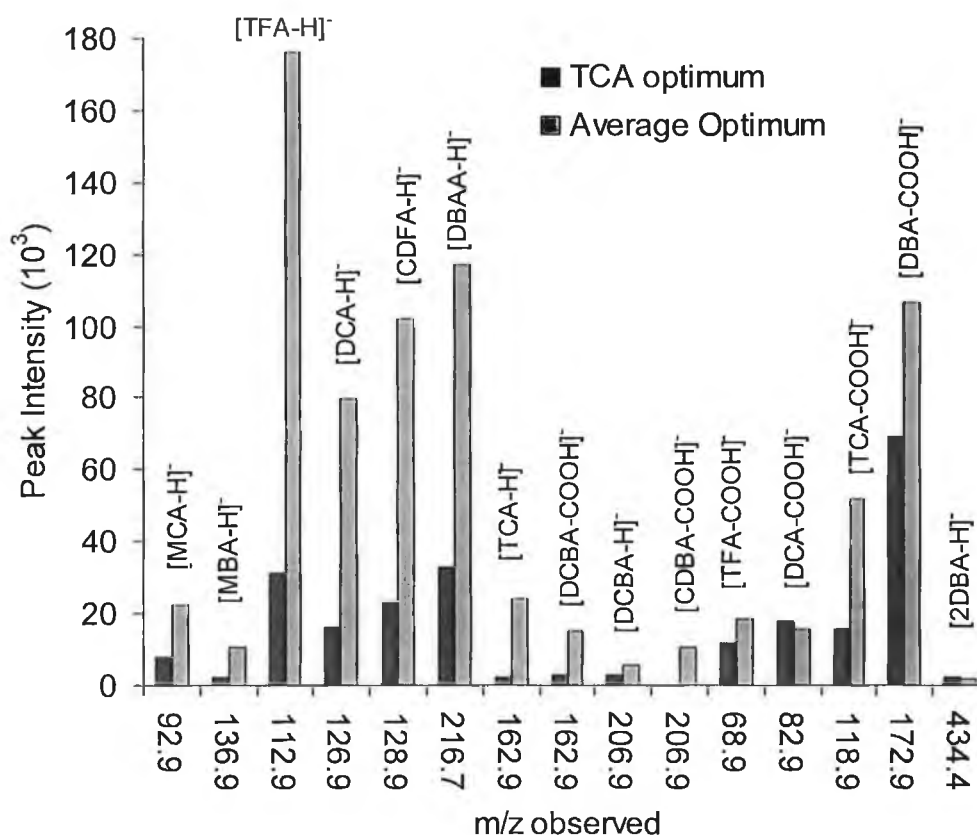


Fig. 6.10 Comparison of intensities at average MS conditions for all nine HAs versus TCA optimum conditions

It was found that the optimum MS conditions for TCA analysis caused sensitivity to suffer for the other HAs. A 15 μM standard was injected at both the TCA optimum and overall average conditions to investigate whether TCA sensitivity would drop significantly at average conditions while improving the sensitivity of the MS to all other species. Fig 6.10 shows the comparison of intensities of all species at optimum conditions for TCA and at average conditions. Surprisingly, all intensities improved significantly with the exception of the [DCA-COOH]⁻ peak at m/z 82.9 and [2DBA-H]⁻ at m/z 434.4 when the

average of all the optimum conditions for all HAs was taken. In the case of TFA, intensities improved by a factor of six which was a significant improvement.

6.3.4.3 *Addition of volatilising solvent*

In an attempt to further improve the sensitivity of the MS for the routine analysis of HAs, the addition of a tertiary pump flow of organic solvent was considered. This was achieved by inserting a T-piece into the flow of eluate prior to the MS interface. Solvent was set to flow in an antagonistic flow direction to IC eluate. Once the two flows had converged, the overall flow exited the T-piece at right angles to the two inlet flows through approximately 20 cm of micro-bore PEEK tubing to the electrospray needle. The solvent chosen for this was methanol, as it had shown to improve volatility of polar HAs over other organic solvents like isopropanol or acetonitrile. The flow of methanol was delivered using the Hewlett-Packard HP1100 micro-bore pump capable of delivering solvent flows of below 0.1 mL/min. The flow of solvent was varied over a range of 0.05 to 0.2 mL/min ($n=7$) maintaining the optimum IC separation flow of 0.30 mL/min. A HA standard of 15 μM was prepared in Milli-Q water and injected in duplicate onto the IC at optimum conditions. An initial rise in sensitivity, albeit quite small, due to the volatile solvent was observed for some, but not all of the HAs (see *Fig 6.11*). For example, there was no change in analyte intensity for the $[\text{DBA-COOH}]^-$ peak at m/z 172.6. Following this and above a total flow rate of 0.15 mL/min, a sharp decrease in sensitivity was observed showing that a critical flow rate had been reached for efficient electrospray generation. At this point the flow was too great and the majority of sample went to waste. It was decided to use 0.12 mL/min of solvent flow, leading to a total flow of 0.42 mL/min.

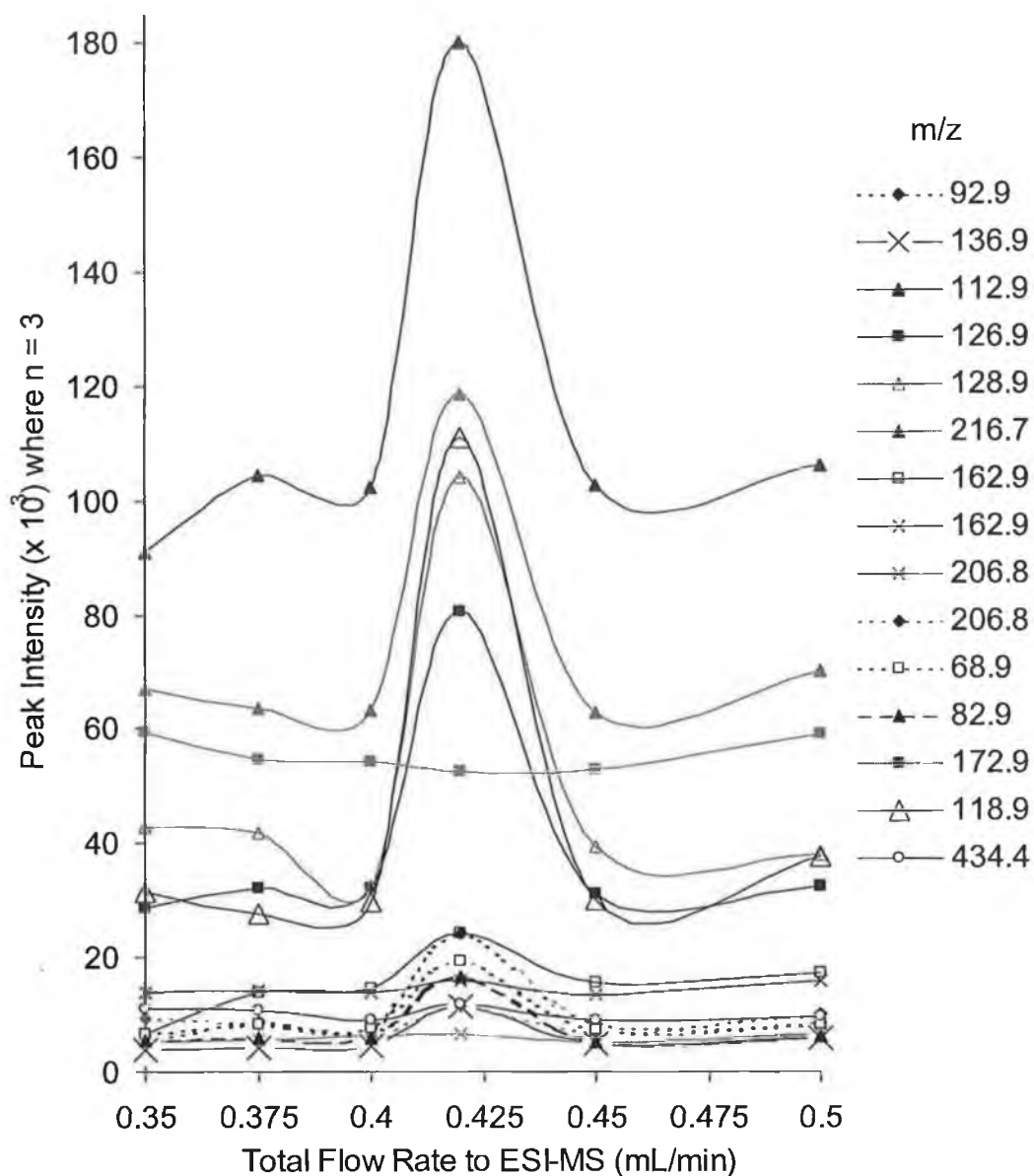


Fig. 6.11 Optimisation of total flow to electrospray needle comprising of 0.30 mL/min IC eluate (fixed) and additional 0.05, 0.075, 0.1, 0.12, 0.15 and 0.2 mL/min MeOH.

6.3.4.4 Optimisation of % MeOH in total flow

From using the secondary flow it was quite simple to see that the secondary MeOH flow had an effect on analyte intensity. In order to fine-tune this further, the effect of % MeOH in the total 0.42 mL/min flow was examined. The volatilising solvent was mixed with Milli-Q water to give overall MeOH percentages of 0, 5, 10, 15, 20, 25 and 30 % in the total 0.42 mL/min flow rate.

Again, a fresh 15 μM standard of the nine HAs was prepared and injected in duplicate onto the IC at optimum conditions. The resulting peak intensities for most abundant ion for each HA were plotted versus % MeOH in Fig. 6.12. It was noted that over the percentage range there was an increase in intensity to almost double that of the purely aqueous inflow. However, the increase seemed to be quite staggered and did not rise linearly. Any increase in tubing length or bore, may have caused unnecessary band broadening effect sensitivity. Nevertheless, the results showed a definite improvement in sensitivity to the HAs when the volatilising solvent was 100 % MeOH.

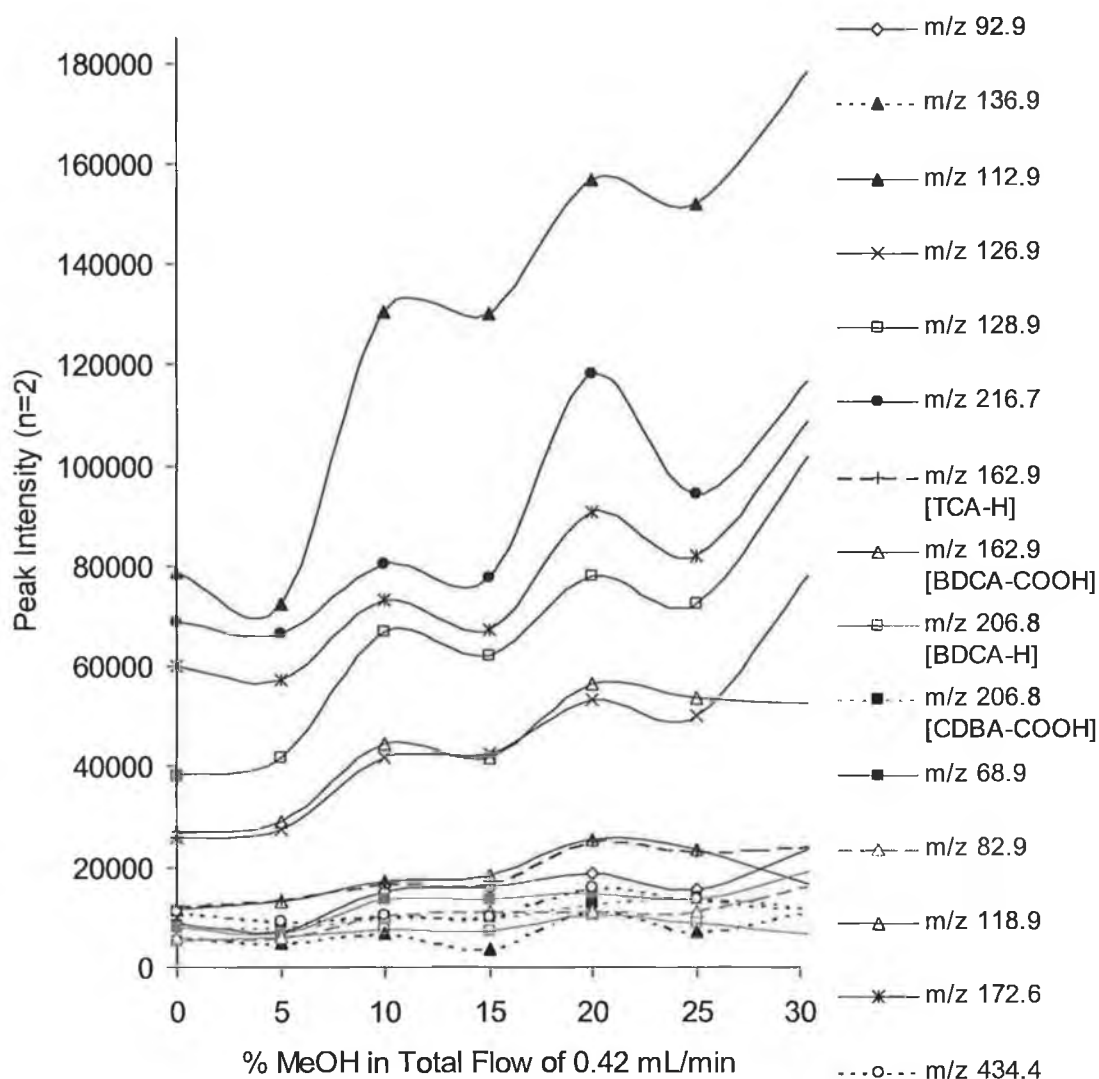


Fig 6.12 Effect of % MeOH on signal intensity at total flow rate

6.3.6.5 Improvement in UV chromatogram with manually prepared eluent

In order to assess the improvement of removing the eluent generator, the effect on the UV chromatogram was assessed since it displayed the most significant interference from styrene sulphonate. A 4 μM standard was prepared as before and injected onto the IC. The resultant chromatogram seemed freer from interference and the baseline rise over the total run was reduced (see Fig 6.13). However, the interference from chloride remained and still caused difficulty with integration of MBA and MCA. The only explanation for this was that there still existed some residual sulphate and chloride, which was not completely removed by the CR-ATC and which could not have been suppressed resulting in negative system peaks for sulphate and chloride.

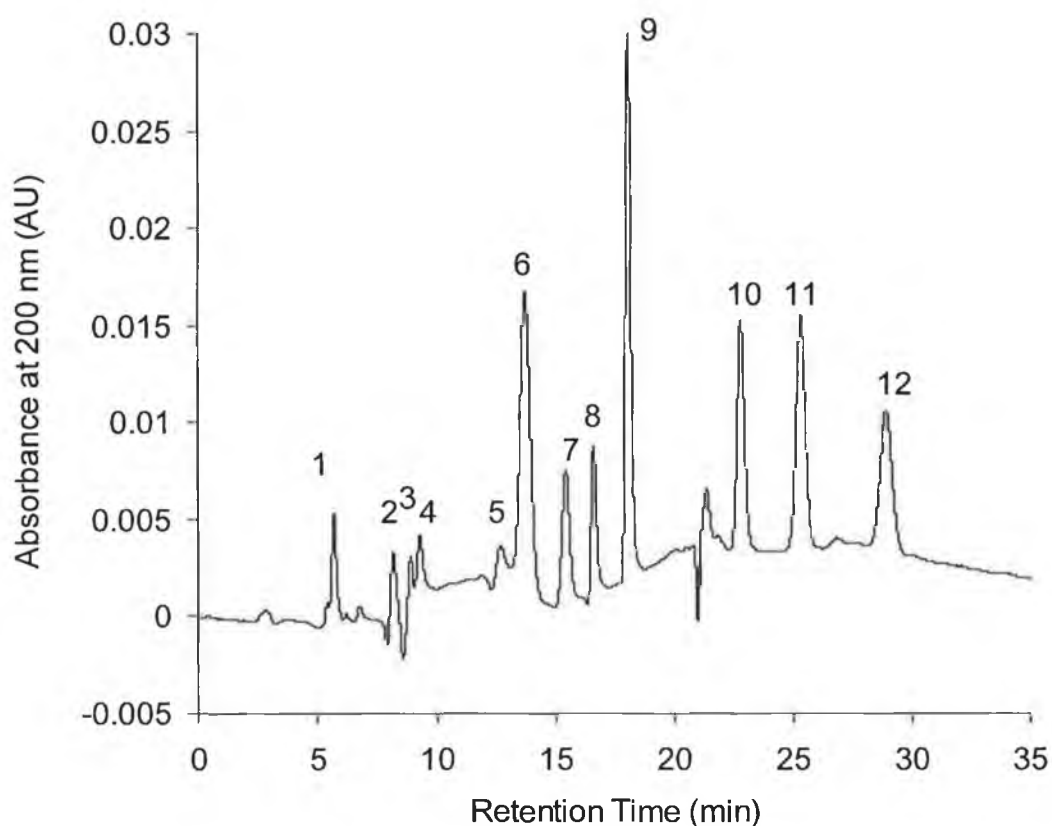


Fig. 6.13 Improvement in baseline stability for UV detection with manually prepared eluents.

6.3.5 Trends in observed ion types for each HA

Fig. 6.14 shows the separation of a standard of 15 μM of the nine HAs using mass spectrometric detection at all the optimised parameters thus far. As can be seen, peaks were observed both in the TIC and in SIM mode. Most interestingly are the highest abundance ions for each fragment of each HA. All pseudo molecular ions were present with the exception of CDBA at m/z 251.2, but was clearly observed as its decarboxylated fragment at m/z 206.9. Similarly, the pseudo molecular ion intensities for DCBA and TCA were significantly less than for their decarboxylated forms at m/z 162.9 and 118.9 respectively. DBA exhibited most stability as its decarboxylated form also. Both monohalogenated species were only present in their pseudo molecular ion forms. However, although trihalogenated species of chlorine and bromine displayed this stability as their decarboxylated form, TFA was present predominantly as its pseudo molecular ion also.

Table 6.3. % Intensity of each fragment for all nine HAs

HA	% Intensity		
	$[\text{M-H}]^-$	$[\text{M-COOH}]^-$	$[\text{2M-H}]^-$
MCA	100	-	-
MBA	100	-	-
TFA	100	10	3
DCA	100	20	3
CDFa	100	10	11
DBA	90	100	14
TCA	-	100	9
DCBA	-	100	15
CDBA	-	100	16

Table 6.3. shows the % abundance to the base peak for each fragment of each HA. From the mass spectral data, the indication that not only did the degree of halogenation play an important role in which fragment was most stable, but also the type of halogen substituted. Put simply, purely homogeneously fluorinated TFA showed most stability as the pseudo molecular

ion, chlorinated species displayed most stability ranging from monochlorinated pseudo molecular ion with an increase in abundance of the decarboxylated ion towards the trichlorinated species. Similarly with the brominated species, decarboxylated ion emerged as dominant with the dibrominated acid. This trend was possibly due to the electron rich halogens, which can supply electrons to stabilise a charge on its neighbouring carbon and thus form a stable decarboxylated ion. As bromine > chlorine > fluorine with respect to electron content, the appearance of a dominant $[M-COOH]^-$ ion from the results presented here suggested this to be accurate with dibrominated species displaying the most abundance as the decarboxylated ion before either chlorinated or fluorinated species.

Likewise, trends were apparent with the appearance of dimerised species. There was most increase in dimer stability associated with increasing degree of bromination, followed by chlorination and fluorination respectively. If a species contained two different halogen types, the larger halogen(s) contributed most to dimer stability. For instance, the intensity of the dimer ions for CDBA, DCBA and TCA are of the order CDBA > DCBA > TCA, the presence of a bromine atom significantly contributed to the dimer ion intensity even though all three were trihalogenated species.

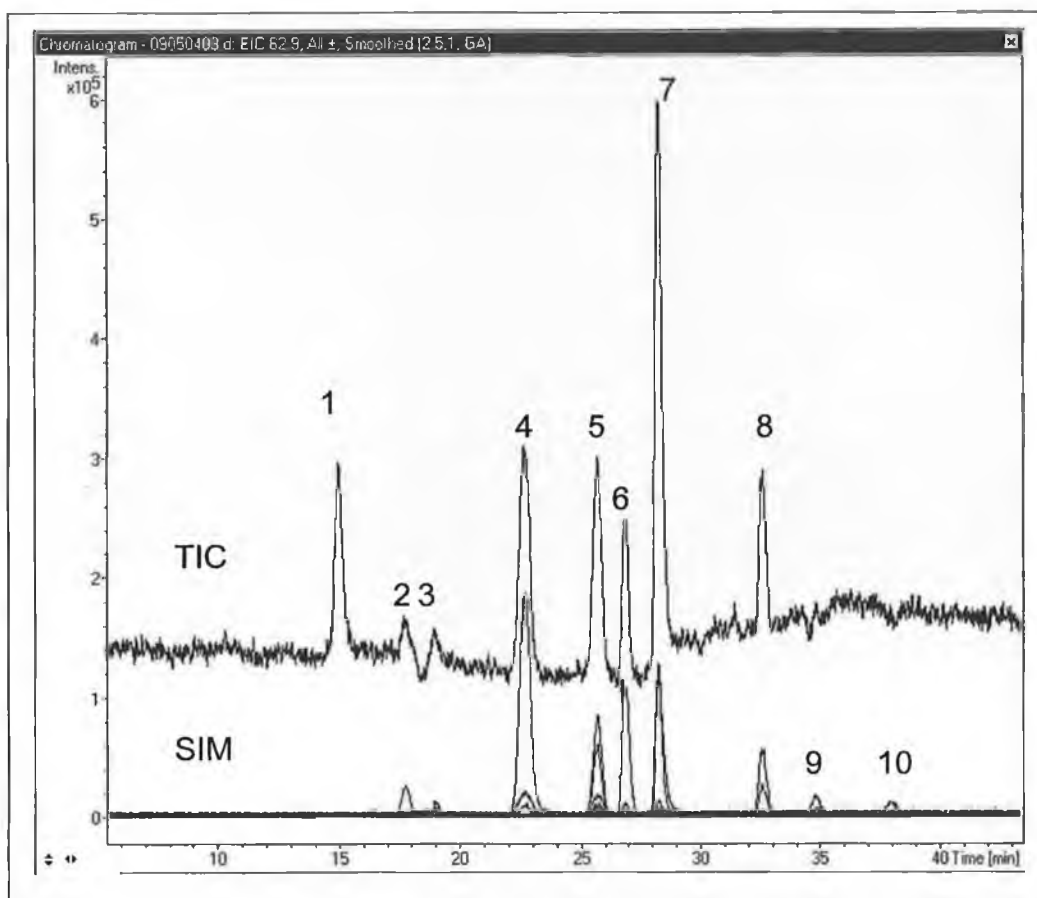


Fig 6.14. TIC and SIM traces for $15\mu\text{M}$ standard of 9 HAs. Elution order: 1 = fluoride, 2 = MCA (SIM m/z 92.9), 3 = MBA (SIM m/z 136.9), 4 = TFA (SIM m/z 112.9, 68.9, 226.8), 5 = DCA (SIM m/z 126.9, 128.9, 92.9, 254.8), 6 = CDFA (SIM m/z 128.9, 84.9, 258.8), 7 = DBA (SIM m/z 216.9, 172.9, 434.4), 8 = TCA (SIM m/z 162.9, 118.8, 326.6), 9 = DCBA (SIM m/z 206.8, 162.9, 414.6) 10 = CDBA (SIM m/z 251.2, 206.8, 503.4).

6.3.6 Analysis of a drinking water sample using suppressed ion chromatography with conductivity, UV and ESI-MS detection

The combination of all three detector types was considered in this investigation. Bearing in mind that the sensitivities of both mass spectrometric and UV detectors were not as low as for conductivity detection, the use of the preconcentration procedure developed in Chapter 3.0 was applied. A sample of laboratory drinking water was collected and spiked with 1 μM of the nine HAs. Fortifications were made by adding the appropriate amount of the 10 mM of individual HA stock solutions to a 50 mL volumetric flask and diluting to 50 mL with sample. This solution was then further diluted 1/10 with sample in a 50 mL volumetric flask to give an overall dilution factor of 1/1000. This sample was then subjected to 25-fold preconcentration with SPE followed by the chloride and sulphate removal procedure. Once more, eluate from the Atlas was connected to the conductivity cell, the UV cell and via the T-piece to the electrospray mass spectrometer. Volatilising solvent was set to 0.12 mL/min as before and the suppressor and CR-ATC were operated in the external water mode at a flow of 0.30 mL/min of Milli-Q water.

The resulting conductivity, UV, TIC and SIM chromatograms for the sample are shown in *Figs. 6.15 and 6.16* clearly showing the presence of the preconcentrated acids. The UV trace still suffered a baseline rise due to interference present in the eluent, as did the conductivity trace. This was most likely due to the fact that the combination of 3 detectors in series caused excessive backpressure (>2500 psi) to the IC system, which caused malfunction of the CR-ATC as the membrane within began to disintegrate. Similarly, the Atlas suppressor began to leak when all three detectors were used in series. An advantage of the AEES Atlas suppressor over membrane based suppressors like the ASRS Ultra became evident here. Because the suppressor itself consisted of a series of monolithic discs, the internal suppression bed seemed to be able to withstand high backpressures. When the pressure limit was exceeded for a short period of time, the Atlas swelled and leaked, but did not suffer permanent damage once the pressure was relieved. However, the CR-ATC was permanently damaged and the whole unit

was replaced. Therefore, it was decided not to run conductivity, UV and electrospray mass spectrometry simultaneously from this point forward. Conductivity measurements were sensitive enough without the addition of another non-analyte specific detector like UV detection. Thus to reduce this damaging high backpressure, only conductivity detection was used in conjunction with ESI-MS.

Three detectors did offer a multitude of data about the sample itself. Some peaks were detected with UV at quite high levels that were previously not observed with the conductivity detector. For instance, in *Fig 6.16 (b)* a peak eluted just before sulphate (peak 13) with comparable absorbance to that of some of the HAs in the sample. This peak was not observed in the conductivity trace at any quantifiable level. Similarly, conductivity signals for the peaks eluting after CDBA showed poor sensitivity as opposed to the UV trace, in which three distinct peaks were observed. On inspection of the TIC and the SIM traces (*Fig. 6.15*), the masses of these unknown compounds were determined and some were assigned possible identities. Coeluting with the peaks corresponding to acetate and fluoride, were two other masses at m/z 88.9 and 174.6 and were similar in mass to anions expected to elute at this early stage such as lactate and iodate. Phthalate was observed at peak 14 at m/z 164.8 and could have arose from plasticiser used for the manufacture of the LiChrolut EN cartridges that may have leached into the sample during preconcentration. Phthalate was used in Chapter 5.0 as an internal standard for use as a retention time marker for interference with DCBA. The three unknown peaks eluting last from both conductivity and UV traces (denoted with ? symbols) were examined and m/z values for the last two were assigned as 172.8 and 200.8 respectively, but mass spectra of these peaks did not allow elucidation of structure. Signal intensity was not sufficient enough to identify the m/z value for first of these three peaks. Fortunately, there seemed to be no interference with the HAs at all and all of the preconcentrated HAs were observed at their different masses. *Fig 6.15* also shows the SIM chromatograms for the most abundant ions separately and were qualitatively detected at this level with acceptable sensitivity.

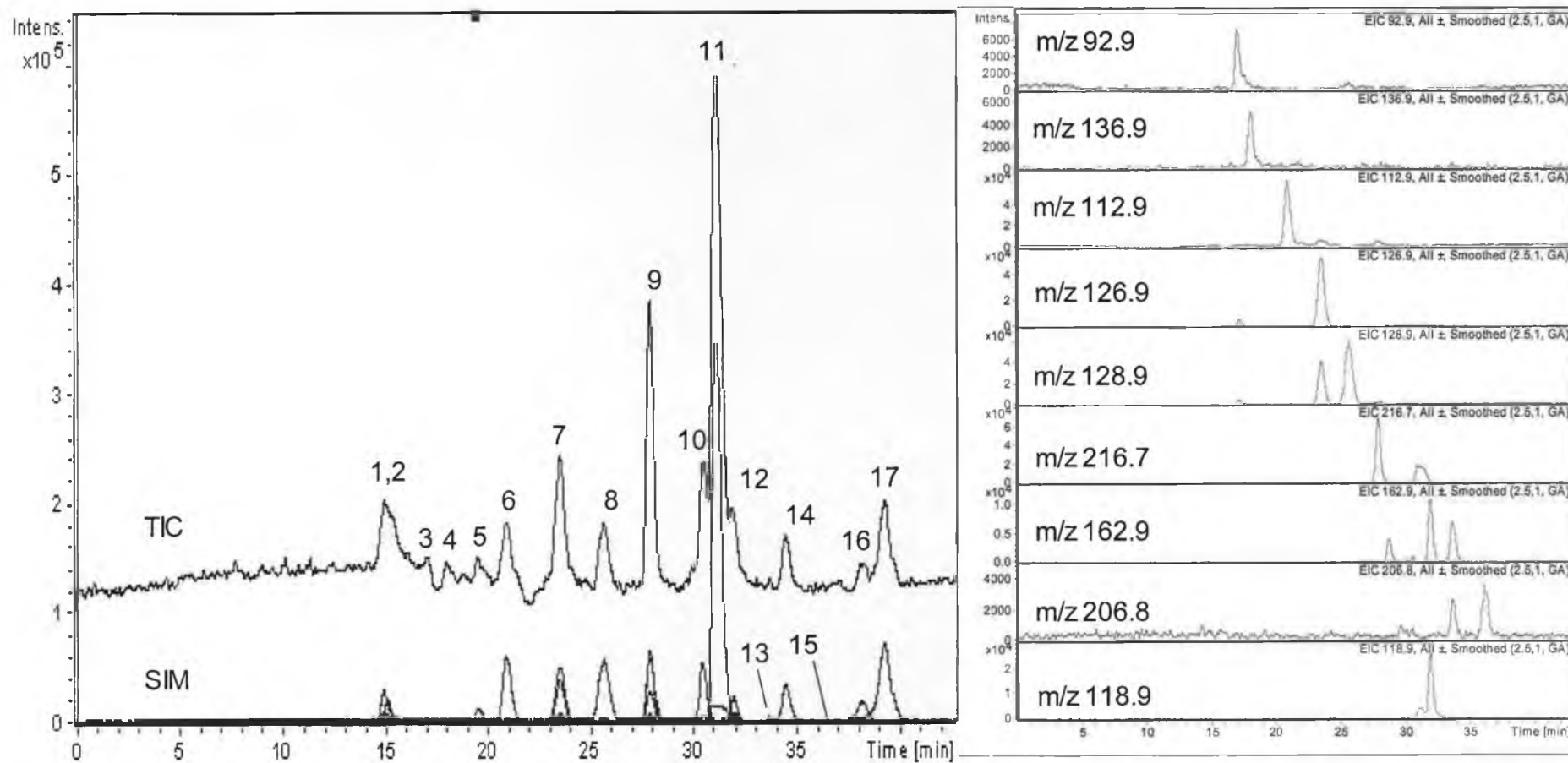


Fig 6.15. Figure left: TIC and SIM chromatograms for a preconcentration of drinking water spiked with nine HAs at 1 μM . Elution order: 1 = m/z 88.9, 2 = m/z 174.6, 3 = MCA, 4 = MBA, 5 = m/z 124.9, 6 = TFA, 7 = DCA, 8 = CDFA, 9 = DBA, 10 = m/z 198.8, 11 = sulphate, 12 = TCA, 13 = DCBA, 14 = m/z 164.8, 15 = CDBA, 16 = m/z 172.8, 17 = m/z 200.8. Figure right: SIM traces for most abundant ion for each HA. SIM traces smoothed with 2.5 point Gaussian averaging.

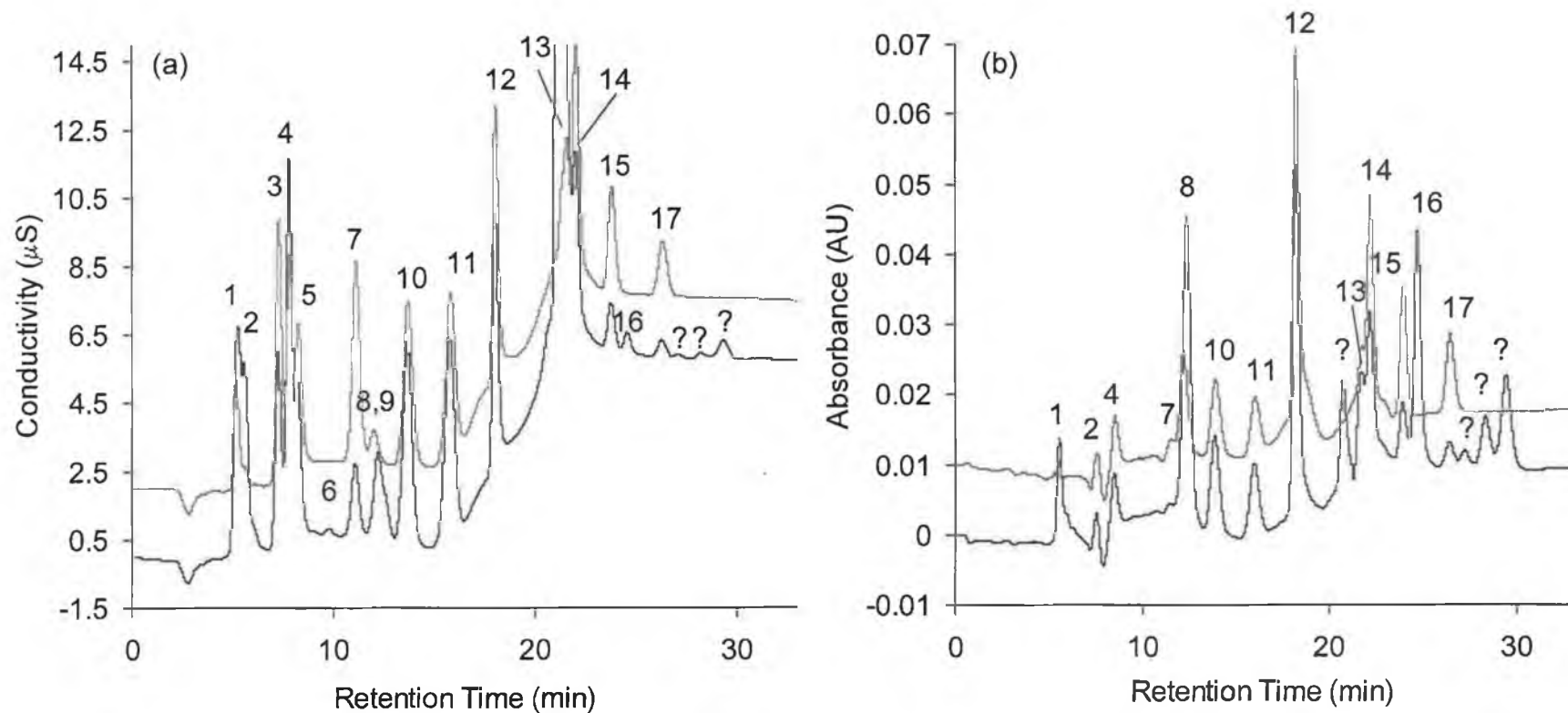


Fig. 6.16 Preconcentration of 1 μM spiked drinking water with (a) conductivity detection (overlaid with 15 μM standard offset by 2 μS) and (b) UV detection (overlaid with same 15 μM standard offset by 0.01 AU). Elution order: 1 = acetate, 2 = fluoride, 3 = MCA, 4 = chloride, 5 = MBA, 6 = nitrite, 7 = TFA, 8 = nitrate, 9 = bromide, 10 = DCA, 11 = CDFA, 12 = DBA, 13 = sulphate, 14 = TCA, 15 = DCBA, 16 = phthalate, 17 = CDBA.

6.4 Conclusion

Wavelength optimisation studies were carried out for UV detection and it was found that 200 nm was the most suitable for detection of HAs with minimal interference from chloride. Linearity and sensitivity were also assessed for UV detection and it was found that integration of MCA and MBA became difficult at low concentrations due to combined interference from eluent carbonate and sample chloride. Direct infusion was used to optimise the Bruker~LC mass spectrometer for seven HAs. Initial IC-MS separations suffered significant interference from styrene sulphonate, which resulted from the eluent generation process. As a result, the method reverted to manually prepared eluents. Sensitivity of the MS detector was found to be enhanced by passing IC eluate through a T-piece with a secondary flow of 100 % MeOH at a flow rate of 0.12 mL/min to increase volatilisation of HAs and boost sensitivity. Increasing the total flow to the electrospray above 0.42 mL/min was observed to reduce sensitivity of the MS for HAs. The percentage MeOH in the total flow was varied from 0 – 28.5 % and was found to approximately double MS sensitivity for all HAs. The application of conductivity, UV and electrospray mass spectrometric detection allowed the identification of HAs as low as 1 μ M in a preconcentrated drinking water sample and with further development showed the potential for more sensitive measurements. However, simultaneous usage of all three detectors caused excessive backpressures and resulted in malfunction of some IC components.

6.5 References

1. W.W. Buchberger, *TrAC*, 20, 6-7 (2001), 296-303.
2. C. Sarzanini, M.C. Bruzzoniti and E. Mentasti, *Journal of Chromatography A*, 850 (1999) 197.
3. V. Lopez-Avila, Y. Liu and C. Charan, *J. AOAC Intl.* 82 (1999) 689.
4. P. Akhtar, C.O. Too and G.G. Wallace, *Anal. Chim. Acta*, 341 (1997), 141-153.
5. D. Kou, X. Wang and S. Mitra, *Journal of Chromatography A*, 1055 (2004), 63-69.
6. V. Lopez-Avila, T van de Goor, B. Gaš and P. Coufal, *Journal of Chromatography A*, 993 (2003), 143-152.
7. D. Martínez, J. Farré, F. Borrull, M. Callull, J. Ruana and A. Colom, *Journal of Chromatography A*, 808 (1998), 229-236.
8. S.K. Johnson, L.L. Houk, J. Feng, D.C. Johnson and R.S. Houk, *Anal. Chim. Acta*, 341 (1997), 205-216.
9. K. Pilhainen, E Sippola and R. Kostianen, *Journal of Chromatography A*, 994 (2003), 93-102.
10. S.B. Mohsin, *Journal of Chromatography A*, 884 (2000), 23-30.
11. K.H. Bauer, T.P. Knepper, A. Maes, V. Schatz and M. Voisel, *Journal of Chromatography A*, 837 (1999) 117-128.
12. L. Charles, D. Pépin, *Journal of Chromatography A*, 804 (1998), 105-111.
13. W.W. Buchberger and W. Ahrer, *Journal of Chromatography A*, 850 (1999), 99-106.
14. R. Roehl, R. Slingsby, N. Avdalovic and P.E. Jackson, *Journal of Chromatography A*, 956 (2002) 245.
15. O. Debré, W.L. Budde and X. Song, *J. Am. Soc. of Mass Spectrometry*, 11 (2000), 809-821.
16. *Principles of Instrumental Analysis*, Skoog, Holler and Nieman, 5th edition, 1998.
17. McLafferty, Fred W. - *Interpretation of mass spectra* / Fred W. McLafferty, Frantisek Turecek. - 4th ed. Mill Valley, Calif: University Science Books, 1993.

18. Dionex Operators Manual, Eluent Generator Module and EluGen Hydroxide Cartridge, Document No. 031373, Revision 06, 8 July 2002.

Chapter 7.0

***Use of temperature programming to improve resolution of
inorganic anions, haloacetates and oxyhalides by suppressed
IC-ESI-MS***

*"Ah music... a magic far beyond anything done here"
-J.K. Rowling, creator of Harry Potter.*

7.1 Introduction

It can be stated without question, that within both past and present papers detailing the optimisation of HPLC separations, the parameter that has, and continues to receive, least attention is temperature. Often temperature is simply fixed at a set point to improve reproducibility of the chromatographic separation, and the effect upon the actual chromatographic selectivity is ignored.

In certain modes of HPLC, such as reversed-phase separations, the general responses to temperature are reasonably well understood, and the effect of temperature upon the retention and resolution of many organic species can be reliably predicted [1]. Within reversed-phase HPLC (RP-HPLC), in all but the most unusual cases, increases in temperature results in subsequent decreases in retention. With this in mind a small number of publications detailing the use of temperature programming in reversed-phase separations have appeared, mostly using an increase in column temperature to speed the elution of strongly retained solutes. These studies were the subject of a recently published review [2].

However, in modes of HPLC other than reversed-phase, such as IC, less predictable behaviour can be observed and contradictory effects and explanations are not uncommon, meaning further investigation is still merited. This is particularly the case with more complex simultaneous separations of inorganic, organic and varyingly charged ions, and even more so when mixed mode retention mechanisms may exist. There has been only a limited number of publications detailing temperature effects in ion exchange chromatography, either focusing on cation exchange [3-8] or anion exchange chromatography [9-13]. In the case of cation exchange, the most significant temperature effects upon both retention and selectivity have been seen with those ion exchangers which incorporate some degree of cation complexation [14], for example cation-exchangers bearing carboxylic [15], phosphonic [16,17], and more complex functionalities like iminodiacetic acid [18-19] or aminocarboxylic acids [3-20]. For the separation of anions on anion exchangers, temperature effects could be

described as less significant, and are mostly associated with changes in hydration radii of the anions and ion-exchange resins. For example, the enthalpy changes for halide ion-exchange reactions on strong PS-DVB based anion-exchangers are usually not higher than 3.3 kcal/eq [21].

In most cases the above studies have investigated temperature effects using isothermal separations, with very little attention paid to potential application of temperature programming. However, a limited number of studies have included temperature gradients in ion exchange separations. For example, Smith *et al.* [22] applied temperature gradients to decrease the capacity of 2,2,1-cryptand based anion exchange columns (the commercial product that has evolved from these early studies is the Dionex IonPac Cryptand A1 column). In this work the column capacity was based upon the nature of the complexed cation within the macrocycle and it was the binding of this cation that was affected most by the temperature gradient, with the effect of temperature upon interaction of the anion with the complex being secondary.

In suppressed IC of anions the use of hydroxide eluents is now common practice and the use of hydroxide eluent generators has also gained in popularity. When using suppression, particularly with hydroxide eluents, the ability to selectively manipulate retention becomes somewhat of a problem, as control of eluent chemistry is obviously limited. Thus alternative approaches need to be assessed. This is where temperature can prove useful. Temperature programming potentially can be used to adjust selectivity whilst simultaneously running isocratic or gradient hydroxide separations. In addition, this secondary temperature gradient causes little or no disturbance to the background signal because of heat dissipation in the suppressor module and temperature control in the conductivity cell.

In Chapter 2.0 and 4.0 the effect of isothermal separations was investigated and clearly showed that the optimisation of temperature proved vital for separation of HAs from inorganic anions. In this work, the potential of temperature programming to improve resolution of anionic species in chlorinated drinking water samples was assessed, namely common inorganic

anions, haloacetic acids as well as selected oxyhalides. A number of methods on the application of IC to HA analysis within drinking water have been published [23]. However, within these publications, those methods using hydroxide eluents with suppressed conductivity detection have all shown resolution of HAs from excess common anions to be problematical, particularly when applied to the analysis of real samples. Therefore, the response of HAs and other anionic species to temperature both under isocratic and gradient hydroxide conditions is assessed here and from these responses a suitable temperature programme to selectively manipulate retention was devised. The practical ability to do this was investigated with a comparison of two commercial column ovens and the final method applied to real sample matrices. Following this, analytical data was acquired for linearity, reproducibility and limit of detection for both conductivity and electrospray mass spectrometric detection and applied to analysis of a drinking water sample and a solid soil sample.

7.2 Experimental

7.2.1 Apparatus

Instrument models and components are all identical to those found in Chapter 6.0. All temperature experiments were carried out using suppressed conductivity detection using the AEES Atlas suppressor. Suppression was carried out in the auto-regeneration mode for all temperature experiments, except when using ESI-MS, where the suppressor was reconfigured to the external water mode.

The column temperature was regulated using the Dionex LC25 oven, which contained the injection valve, the suppressor, the guard and analytical columns and the conductivity cell. Temperature could be selected in 1 °C increments from 30-45 °C. For temperature gradient studies, actual column and oven temperatures were independently measured using an iButton sensor (Dallas Semiconductor Group, Dallas, TX, USA) placed within the oven to

record temperature data at 1 minute intervals and was sensitive to 0.5 °C changes in temperature. A Spark-Holland Mistral column oven (Spark-Holland, Emmen, The Netherlands) fitted with a monitored temperature readout (sensitive to 0.1 °C changes in temperature) was also used, for comparative temperature gradient work. This oven housed the guard and analytical columns, whilst the conductivity cell and injector remained in the Dionex LC25 (programmed with the same temperature profile) to ensure an equal amount of eluent pre-heating was seen with both column ovens and the conductivity cell temperature remained the same during comparative studies. For MS parameters, refer to Chapter 6.0.

7.2.2 Reagents

Analytical grade monochloroacetic acid (MCA), monobromoacetic acid (MBA), dichloroacetic acid (DCA), dibromoacetic acid (DBA), trichloroacetic acid (TCA), trifluoroacetic acid (TFA), chlorodifluoroacetic acid (CDFA), bromochloroacetic acid (BCA) dichlorobromoacetic acid (DCBA) and chlorodibromoacetic acid (CDBA), as well as the potassium salts of iodate, bromate, chlorite, chlorate, perchlorate, fluoride, chloride, and sulphate and the sodium salt of nitrate were obtained from Sigma-Aldrich (Gillingham, UK). All oxyhalides and HAs were prepared to a stock concentration of 10 mM and stored in a refrigerator at 4 °C until required for use for working standards. All inorganic anion stocks were prepared to a concentration of 1000 µg/L. All eluents were prepared from a 50 % solution of sodium hydroxide in water purchased from Sigma-Aldrich. All eluents and standards were prepared using diluent water from a Millipore water purification system (Millipore, Bedford, MA, USA) with a specific resistance of 18.3 MΩ cm. Eluents were passed through a 0.25 µm filter, followed by 15 minutes sonication prior to use.

7.2.3 Procedure

Temperature studies on isocratic separations were carried out at ambient, 30 °C, 35 °C, 40 °C and 45 °C. In all cases, the temperature within the oven was allowed to equilibrate for a 35-minute period between temperature

changes. When studying the effect of temperature on gradient separations, 37 °C was also included. Temperatures of above 45 °C were not studied to ensure the anion exchange columns were not damaged [13]. The use of micro-bore guard and analytical columns in this work minimised temperature equilibration times.

The optimum gradient separation method employed both a temperature gradient and a hydroxide concentration gradient. The column was initially allowed to equilibrate for 16 minutes between runs. Eluent concentration was kept at 1 mM for the first 20 minutes then ramped to 4 mM hydroxide over a 20-minute period, then to 20 mM hydroxide over 5 minutes. This hydroxide concentration was then maintained for a further 26 minutes. The initial temperature for the separation of early eluting anions was 30 °C. At 20 minutes the temperature was set at 45 °C and then returned to 30 °C at either 30 or 40 minutes, depending upon the sample.

Drinking water samples, where necessary, had sulphate and chloride removed by passing through a series of Alltech Maxi Clean cartridges (Alltech Associates, Deerfield, IL, USA) in the barium, silver and acid forms. These cartridges were preconditioned with 10 mL Milli-Q water, passed through at a flow rate of 1 mL/min, followed by the samples at the same flow rate. Samples of approximately 25 mL were taken by leaving the laboratory tap running for a period of 3 minutes, then rinsing the container three times with drinking water prior to collection, followed by immediate chloride and sulphate removal and injection. The preconcentration procedure using LiChrolut EN cartridges was used for selected water samples.

7.3 Results and Discussion

7.3.1 Effect of temperature on ion chromatography – theoretical considerations

There are kinetic and thermodynamic effects in IC, which can be attributed to changes of temperature. The kinetic effects are mainly associated with changes in the diffusion coefficients of solutes in mobile and stationary phases, and with changes in the rate of solute-sorbent reactions. These can be slower in ion exchange than in other modes of liquid chromatography, particularly if complexation is involved in the ion exchange process. Such kinetic effects are responsible for variations in column efficiency and peak symmetry.

The thermodynamics of the IC process is potentially more important to the chromatographer because of different solute responses due to temperature changes, which means temperature can be utilised as a real tool for the variation of separation selectivity.

As in Chapter 2.0, the effect of temperature, T , on retention factor, k , was described by the van't Hoff equation:

$$\ln k = \frac{\Delta H}{RT} + \frac{\Delta S}{R} + \ln \varphi \quad \text{Equation 7.1}$$

where ΔH is enthalpy change for the ion-exchange reaction, ΔS – entropy change, R – molar gas constant and φ is the phase volume ratio, a characteristic constant for a given column. If ΔS is a constant under the studied range of temperature, a plot of $\ln k$ vs. the reciprocal temperature $1/T$ should have a slope equal to $-\Delta H/R$. However, it should be noted that values of enthalpy calculated from the van't Hoff equation should not be considered as

standard enthalpy values ΔH° , as all data used for corresponding calculations cannot be obtained under conditions close to standard. For example, elevated pressure (50-70 bar) is always experienced within the chromatographic system.

The suitability of using the van't Hoff equation for the evaluation of enthalpy of sorbate-sorbent interactions is also limited by a number of other factors. Ideally the effects of temperature should be associated with solute-sorbate interactions of only a single definite type. In practice such single type interactions are rarely seen during chromatographic separations, so in the observed data it is necessary to take into account all possibilities for multi-mode interactions. To understand other limitations of the van't Hoff equation, possible changes in both the mobile and stationary phases should be considered as well as the possible changes in solute environment.

7.3.1.2 *Ion-exchanger*

Depending on rigidity and chemical nature of stationary phase, increases in temperature can change the porous structure of matrix, resulting in changes in basic parameters, such as dead volume and retention factors. The most dramatic effect of temperature upon the conformational mobility of polymer chains should take place in those ion-exchangers having low cross-linkage or in so-called gel-type ion-exchangers. The increased conformational flexibility of polymer chains combined with subsequent repulsion effects of charged functional groups attached to the polymer, may cause a partial redistribution of ion-exchange functional groups at the surface (or within the ion-exchanger) and hence induce changes in ion-exchange selectivity. If any such changes in the structure of the ion-exchanger take place it represents a change of ΔS , which causes difficulties in the evaluation of ΔH from the van't Hoff equation. To simplify this, the ΔS is usually accepted to be constant under experimental conditions.

In this particular investigation a Dionex IonPac AG16 (2 x 50 mm) guard and an IonPac AS16 (2 x 250 mm) analytical column were used for the

separation of a mixture inorganic anions and HAs. The IonPac AS16 column contains a 9 μm agglomerated anion-exchanger, consisting of a moderately sulphonated macroporous (200 nm) EVB-DVB polymer substrate bead with 55 % cross-linking, coated with a layer of alkanol quaternary ammonium functionalised 80 nm latex particles, with only 1 % cross-linking. According to the producer's data, the IonPac AS16 has an ion-exchange capacity of approximately 42.5 $\mu\text{equiv/column}$ and an ultra low hydrophobicity (related to the latex layer). The IonPac AG16 guard column is filled with 13 μm resin based of similar ion-exchange structure but based on micro-porous substrate and having a much lower capacity of 0.875 $\mu\text{equiv/column}$.

The low degree of cross-linking of the latex particles at the outer layer of the IonPac AS16 means the flexibility of the polymer chains bearing charged groups is increased at higher temperatures, so it is possible to expect redistribution of functional groups relative to each other, or relative to the oppositely charged, partly sulphonated surface of the more rigid central substrate with temperature changes.

7.3.1.2 *Mobile phase*

It is well established [24] that aqueous-based mobile phases exhibit a higher elution ability for hydrophobic solutes in reversed-phase separations under increased temperatures. On this basis, the use of overheated pure water as the mobile phase (up to 150 $^{\circ}\text{C}$) has become popular in RP-HPLC as a potential environmentally friendly replacement for water-organic solvent mixtures. In this current study there exists a definite probability of some degree of secondary hydrophobic interactions between particular HAs and the surface of EVB-DVB substrate of the IonPac AS16 resin. Therefore one can expect that the impact of such hydrophobic interactions will be less expressed at high temperatures. Mobile phase temperature effects on non-hydrophobic interactions, namely pure ion-exchange, are in the most part only seen with weak acid/basic eluents, where for example the dissociation constant is dependent upon temperature, which will subsequently affect eluent elution strength.

7.3.1.3 Solutes

There is a general conclusion that charged ions should have a decreased hydration radii at elevated solution temperatures. With all other conditions constant, this then would be the main reason for solute heat effects observed during ion-exchange interactions.

7.3.2 Van't Hoff plots

Initial temperature experiments were carried out on the IonPac AS16 column using isocratic conditions with a 20 mM hydroxide eluent. Three separate standards of the oxyhalides, the HAs and inorganic anions were prepared to 100 μ M concentration. The oxyhalides eluted in the order iodate, bromate, chlorate and perchlorate. For the investigation of the effect of temperature on the retention of each species under identical conditions, a relatively small temperature range from 30 °C to 45 °C was investigated ($n=5$) to avoid any possible column damage at higher temperatures [13], and to keep well within most operating parameters of most common column ovens. At each of the five temperatures investigated injections were carried out in triplicate to insure column equilibration had been achieved (see *Table 7.1*).

Hatsis and Lucy [12] have shown previously that the temperature effect upon anion exchange is dependent upon both eluent type (sodium carbonate or sodium hydroxide) and concentration, with the former having the larger effect. In the same study two anion exchange columns (IonPac AS11 and IonPac AS14) were compared using the same eluent and again considerable variation was seen.

Here, the effect of temperature upon a number of common inorganic anions, HAs and oxyhalides was investigated to provide information on the potential use of temperature and temperature gradients to improve resolution of anions from within each of these classes during ion chromatographic analysis of drinking waters. The test mixture included fluoride, chloride, nitrate, sulphate, MCA, MBA, TFA, DCA, CDFA, DBA, TCA, BDCA, CDBA, iodate, bromate,

chlorate and perchlorate. The results of this study are shown in *Fig. 7.1* with corresponding solute data, correlation coefficients, slopes and ΔH values shown in *Table 7.1*.

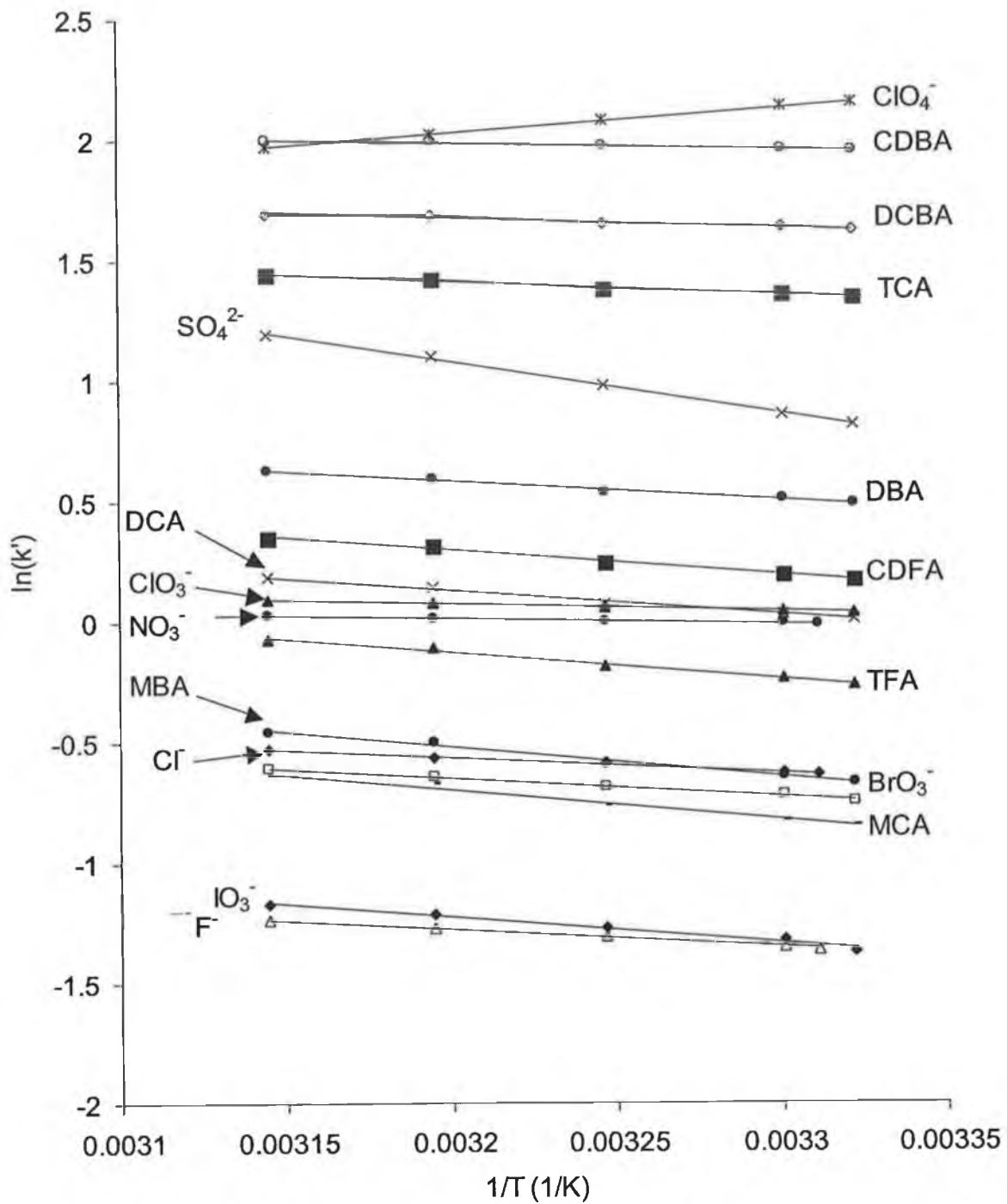


Fig. 7.1. Van't Hoff plots for 4 oxyhalides, 9 HAs and 4 inorganic anions using AS16 column with isocratic elution. Eluent = 20 mM NaOH.

Table 7.1 Slope data from van't Hoff plots, correlation coefficients, and ΔH values for oxyhalides, haloacetates and inorganic anions.

Anions	Log P	Van't Hoff Slope ^b	Correlation coeff. R ² (n=5) ^c	ΔH (kJ/mol) ^d
Inorganic anions				
fluoride	-	-744	0.993	-6.18
chloride	-	-636	0.998	-5.29
nitrate	-	-263	0.998	-2.18
sulphate	-	-2169	0.999	-18.03
Haloacetates				
MCA	0.22	-1282	0.989	-10.7
MBA	0.41	-1247	0.988	-10.4
TFA	0.50 ^a	-1119	0.989	-9.3
CDFA	0.82 ^a	-1037	0.991	-8.6
DCA	0.92	-1010	0.991	-8.4
DBA	1.69	-818	0.99	-6.8
TCA	1.33	-566	0.989	-4.7
DCBA	2.31	-428	0.984	-3.6
CDBA	2.91	-284	0.975	-2.4
Oxyhalides				
iodate	-	-1090	0.983	-9.1
bromate	-	-763	0.993	-6.4
chlorate	-	-332	0.998	-2.8
perchlorate	-	1008	0.999	8.4

^a Calculated in accordance with [26] all other taken from [27].

^b Data over 30 – 45°C (n=5), each data point collected in triplicate.

^c Calculated from linear regression of averaged retention data from triplicate injections.

^d Calculated using van't Hoff slope = $\Delta H/R$ and assuming ΔS to be constant.

Hatsis and Lucy in their study with IonPac AS11 made some conclusions about general temperature effects upon anions separated using the above anion exchangers [12]. These were; (i) weakly retained anions, such as iodate, bromate, nitrite, nitrate and bromide, were unpredictable and either showed increased or decreased retention with increasing temperature; (ii) Multiply charged anions such as sulphate and phosphate showed significant increases with increasing temperature; and (iii) Strongly retained singly charged anions

such as iodide and perchlorate showed significant decreases in retention with increasing temperature. From *Table 7.1* it is clear that in the work carried out here with the IonPac AS16 column, some similarities to these trends can be seen, particularly for the inorganic anions, where the more strongly retained nitrate is least affected by temperature and the doubly charged sulphate shows the largest increase in retention.

Upon close consideration of the oxyhalide and HA data, some interesting trends in temperature effects can also be observed. With the HAs, a strong correlation between retention and temperature effects can be clearly seen, with negative van't Hoff slope decreasing almost linearly with increased retention. To fully illustrate this, *Fig. 7.2(a)* shows a plot of slope (obtained from van't Hoff plots shown in *Fig. 7.1*, with retention data for each haloacetate taken at five different column temperatures in triplicate) against mean retention factor over the temperature range studied (average $\ln k$ for each HA over five column temperatures). As can be seen from the data shown the correlation is remarkable high, with a coefficient of $R^2 = 0.9899$. The retention order of the HAs and hence the magnitude of the temperature effect correlates very closely ($R^2=0.9088$) with the lipophilicity of the HAs ($\log P$, \log of *n*-octanol-water partition coefficient), with the least lipophilic species, namely MCA, showing the largest temperature effect, and the most lipophilic species, namely CDBA, showing the least effect. This is shown graphically as *Fig. 7.2(b)*. It is worthy of note that the lipophilicity of some of the HAs is in excess of some common organic acids typically considered to exhibit considerable lipophilicity, e.g. propionic acid ($\log P = 0.33$), butyric acid ($\log P = 0.79$) and heptanoic acid ($\log P = 2.42$). With this in mind, it is reasonable to assume that even on what is described as an 'ultra-low hydrophobicity column' such as the IonPac AS16, the lipophilic nature of the HAs still contributes somewhat to retention and selectivity and this is reflected in the relative responses to temperature. Unlike retention due to pure ion exchange, which for the most part increases with increasing column temperature (as for the common inorganic anions), retention due to such lipophilic interactions would be reduced at higher column temperatures, hence the relatively smaller increases in retention seen for the more lipophilic haloacetates.

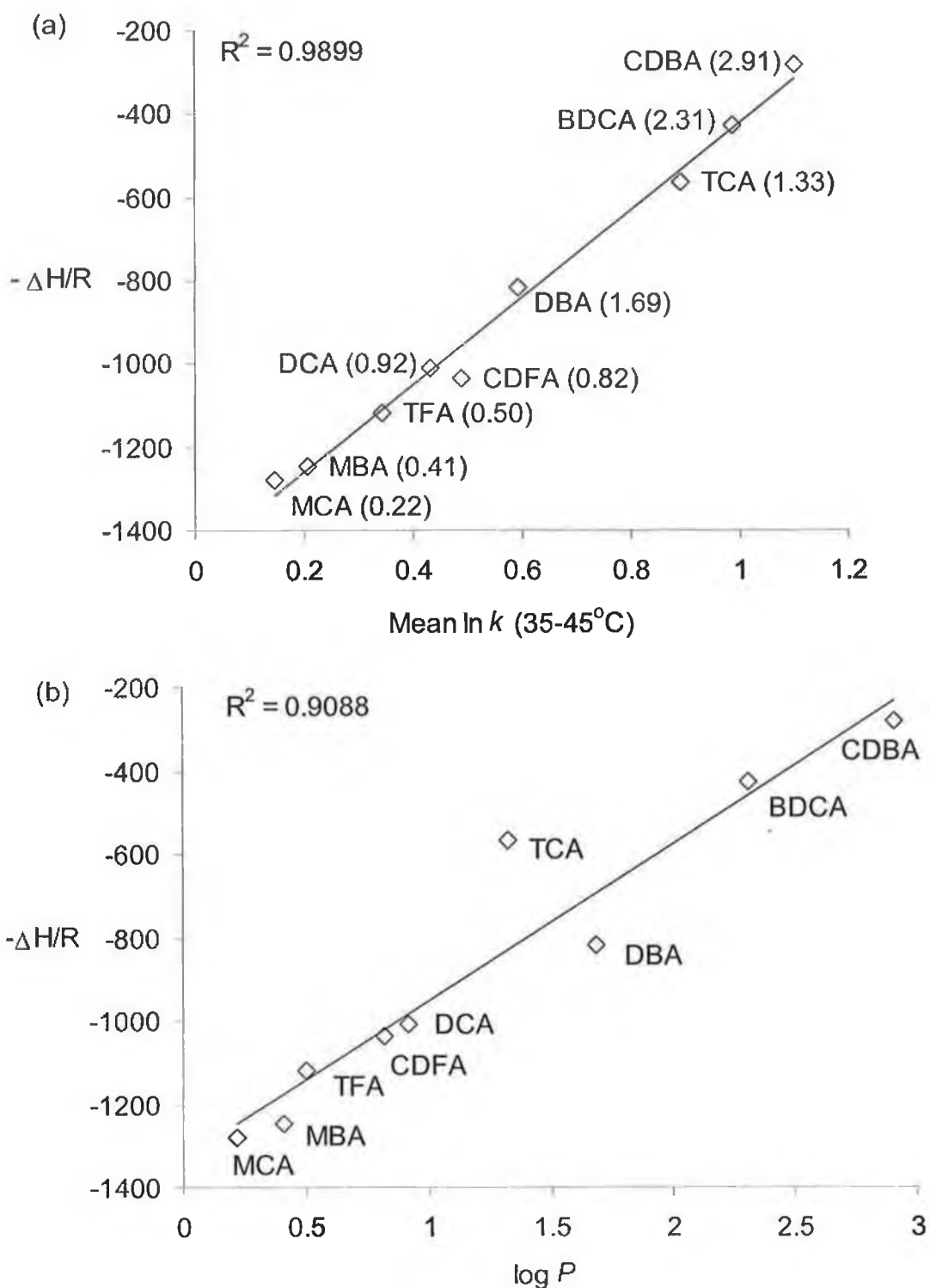


Fig. 7.2 (a) Plot showing the slope from van't Hoff plot against mean $\ln k$ for each HA over the temperature range 35 – 45 °C. Data shown in brackets = $\log P$ value or each anion. (b) Plot showing the slope from van't Hoff plot against $\log P$ for each HA.

7.3.3 Alteration of existing IC gradient method for separation of oxyhalides from HAs

The simultaneous separation of HAs, inorganic anions and oxyhalides was considered. A standard of all HAs and oxyhalides was prepared to 10 μM and injected onto the AS16 column using the method developed in Chapter 6.0. It was found that the only two oxyhalides to be regulated by governmental bodies, namely bromate and chlorate, coeluted with MCA and DCA respectively. Attempts were then made to separate bromate from MCA by reducing the initial concentration of the gradient to 1 mM NaOH and proved successful in separating bromate from MCA and chlorate from DCA, only when the temperature was lowered to 35°C (temperature not optimised). However, lowering the initial concentration caused longer runtimes and caused slight disimprovement in resolution of DCA and chlorate. It was decided to retain the initial concentration of the gradient at 1 mM to maintain the separation of MCA and bromate. Initiating the gradient at 20 minutes was then investigated by stepping the eluent concentration to 2.5 mM and then to 20 mM hydroxide after 20 minutes (the latter two eluent concentrations were similar to the method developed in Chapter 6.0). It was found that the gradient was not sufficient enough to allow the more hydrophobic anions to elute in an acceptable timeframe. Therefore, the second stage of the gradient was assessed and it was found that linearly increasing the hydroxide concentration to 4 mM after 20 minutes allowed separation of TFA and to a certain extent nitrate, chlorate and DCA in just over 40 minutes (*Fig. 7.3*). All this developmental work was carried out at 35°C, though column temperature was not optimised to this point.

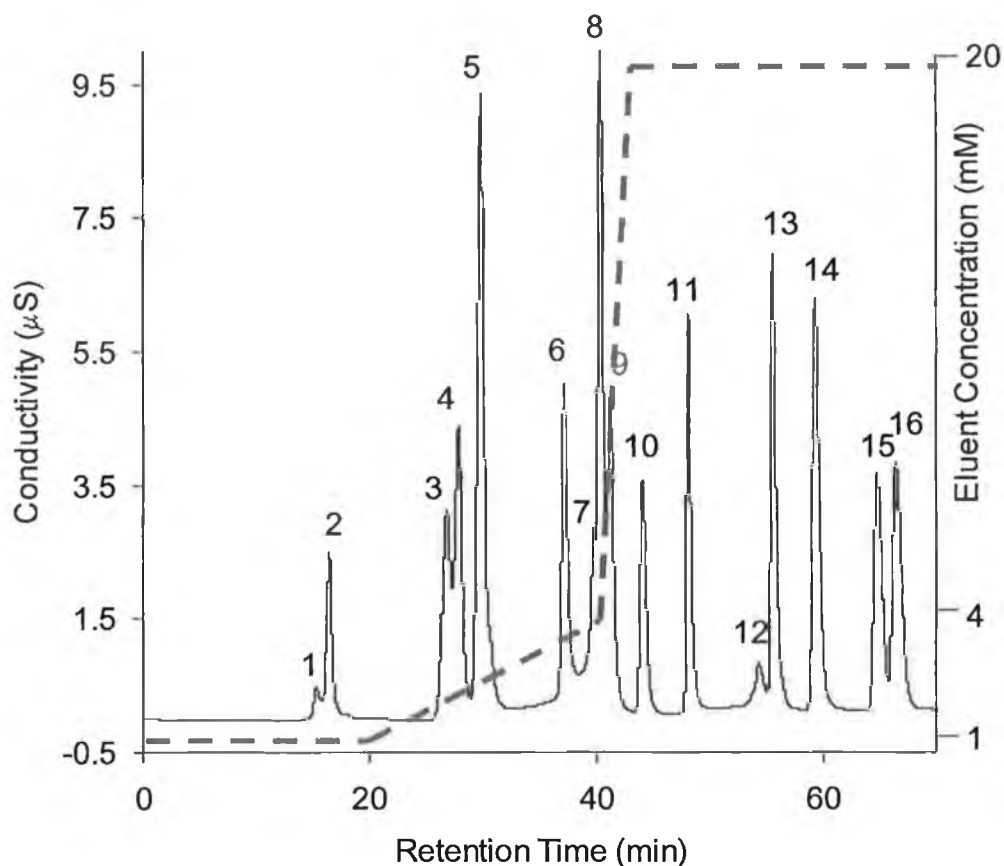


Fig. 7.3 Optimised gradient of 1 mM hydroxide for 20 mins, then linearly ramped to 4 mM over 20 mins followed by 5 minute linear increase to 20 mM hydroxide all at 35°C. Elution order: 1 = fluoride, 2 = iodate, 3 = MCA, 4 = bromate, 5 = chloride/MBA, 6 = TFA, 7 = nitrate, 8 = chlorate, 9 = DCA, 10 = CDFA, 11 = DBA, 12 = sulphate, 13 = TCA, 14 = DCBA, 15 = CDBA, 16 = perchlorate.

7.3.4 Effect of elevated temperature upon gradient IC separation

The current hydroxide gradient separation of common inorganic anions, HAs and oxyhalides was then run under increasing column temperatures between 30 and 45 °C ($n=5$) to evaluate effects upon selectivity, resolution and efficiency. As eluent strength has been shown previously to affect van't Hoff slopes [12] the data collected in Section 7.3.2 could not be used directly to predict changes in selectivity seen under eluent gradient conditions. The effect upon the optimised separation of the applied increase in column temperature can be seen in Fig. 7.4.

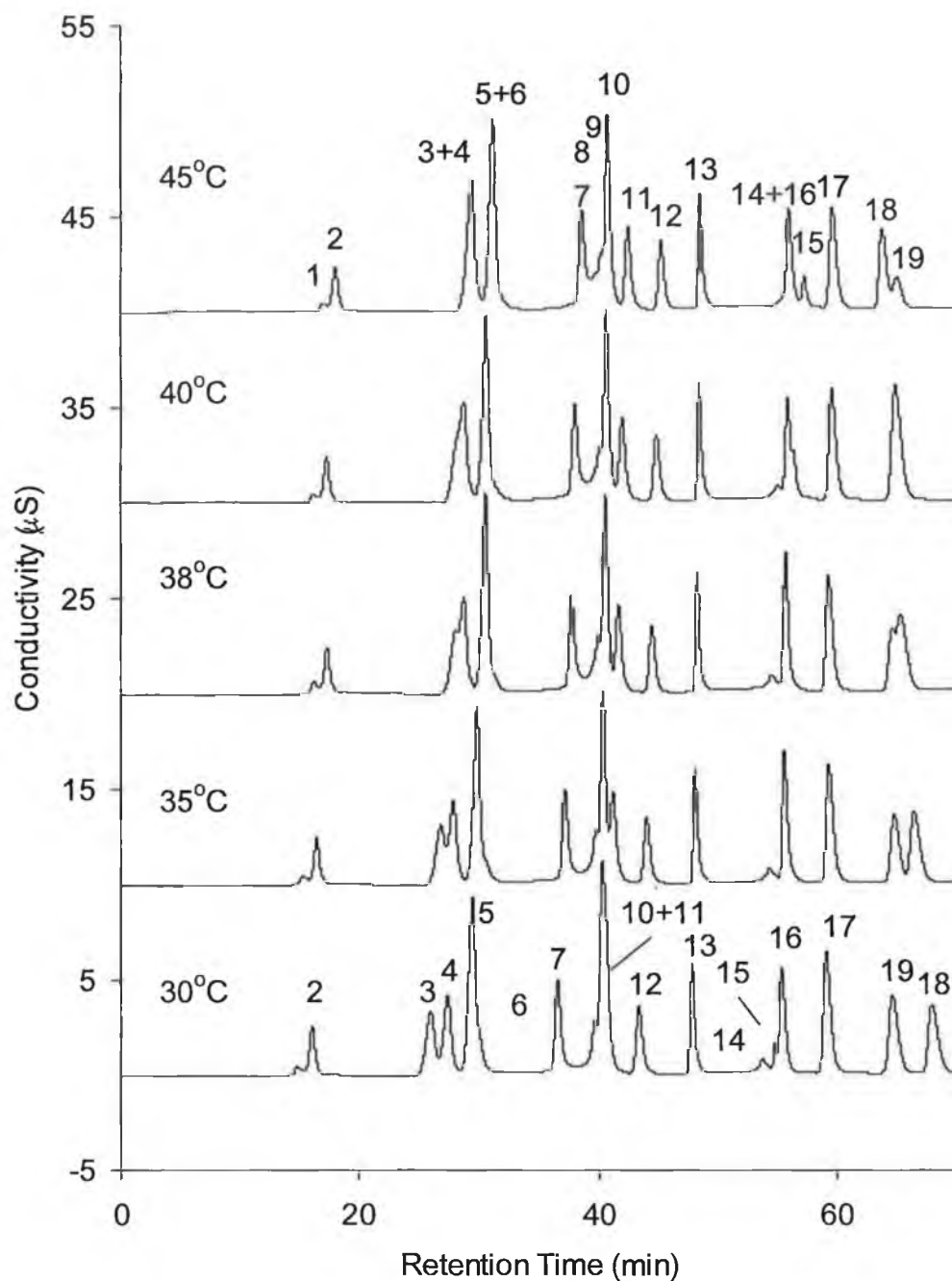


Fig. 7.4. Effect of increased column temperature upon the isothermal gradient separation of inorganic anions, oxyhalides and HAs. Eluent conditions = 1 mM NaOH 0 - 20 minutes, increased to 4 mM hydroxide over next 20 minute, then increased to 20 mM hydroxide over next 5 minutes. Peaks; 1 = acetate 2 = fluoride, 3 = MCA, 4 = bromate, 5 = chloride, 6 = MBA, 7 = TFA, 8 = nitrate, 9 = bromide, 10 = chlorite 11 = DCA, 12 = CDFA, 13 = DBA, 14 = carbonate, 15 = sulphate, 16 = TCA, 17 = BDCA, 18 = CDBA, 19 = perchlorate.

The chromatograms obtained show that complete resolution of all anions was not possible under any of the conditions investigated. It was also noticed that increasing temperature led to a decrease in resolution of peaks 1 to 6 (with the subsequent co-elution of MCA and bromate), an increase in the resolution of peaks 7-13 (allowing the resolution of chlorate and DCA), and a decrease in resolution of peaks 14 – 19 (causing coelution of carbonate and TCA, and CDBA and perchlorate). In summary, elevated column temperature had a detrimental affect upon resolution and the start and end of the chromatogram, whilst improving resolution of those peaks eluting at the centre. Clearly the observed trends indicated that an application of a temperature programme could be the solution to obtaining complete resolution.

7.3.5 Column oven performance

In order to apply a temperature gradient programme during a chromatographic run it is of great importance to be able to accurately and rapidly control column temperature [25]. Practically it is not trivial to accurately assess temperatures within analytical columns, as air temperatures within column ovens may not accurately reflect column temperatures. Therefore, to apply temperature programmes correctly, the performance of the column oven in controlling column temperature needed to be assessed. In an attempt to achieve a more accurate assessment of column temperature over time, a temperature sensor (iButton) was used which allowed surface temperatures to be monitored. This sensor was adhered to the analytical column itself, which was housed within a column oven whilst temperature programmes were applied. The sensor continuously measured the temperature of the actual column housing, whilst the column oven air temperature was simultaneously monitored by the column oven itself. Two commercial column ovens were available within this study and so their relative performance was assessed, these being the Dionex LC25 oven and a Spark-Holland Mistral oven (the Mistral oven contains peltier elements for more efficient heating and cooling, whereas the Dionex LC25 uses a simpler air conditioning scheme). To obtain an accurate comparison, lengths of pre-column tubing housed within each oven were kept equal and all samples were injected through a temperature controlled

injector. With the responses to increased temperature shown in *Fig. 7.4* in mind, temperature programmes starting at 30°C at $t=0$ and stepping to 45°C at $t=20$, and decreasing back to 30°C at either $t=30$ (10 min programme) or $t=40$ min (20 min programme), were investigated. *Figs 7.5(a)* and *(b)* show the column temperatures as measured by the iButton sensor over the two programmes for the two column ovens. As is clear from the figures shown, the performance of the two column ovens differed markedly, particularly upon cooling. In addition, it can be seen (*Fig. 7.5(a)*) that the actual column never reached the desired 45°C temperature in either oven within the 10 min programmed time, although the column within the Spark-Holland Mistral oven did reach a steady temperature of close to 45°C after 10 min during the 20 min programme. *Fig. 7.5(c)* shows the comparison of the column temperature within the Spark-Holland Mistral oven, with the actual oven temperature readout over the 10 min programme. From the comparison shown, it is clear that the column oven temperature readout cannot be relied upon for accurate temperature programming, and that the actual column temperature should be known if the dependable use of temperature programming is required. *Fig. 7.5(d)* shows the comparison of the iButton data when attached to the Spark-Holland Mistral oven wall and the Spark-Holland Mistral oven readout, showing good correlation.

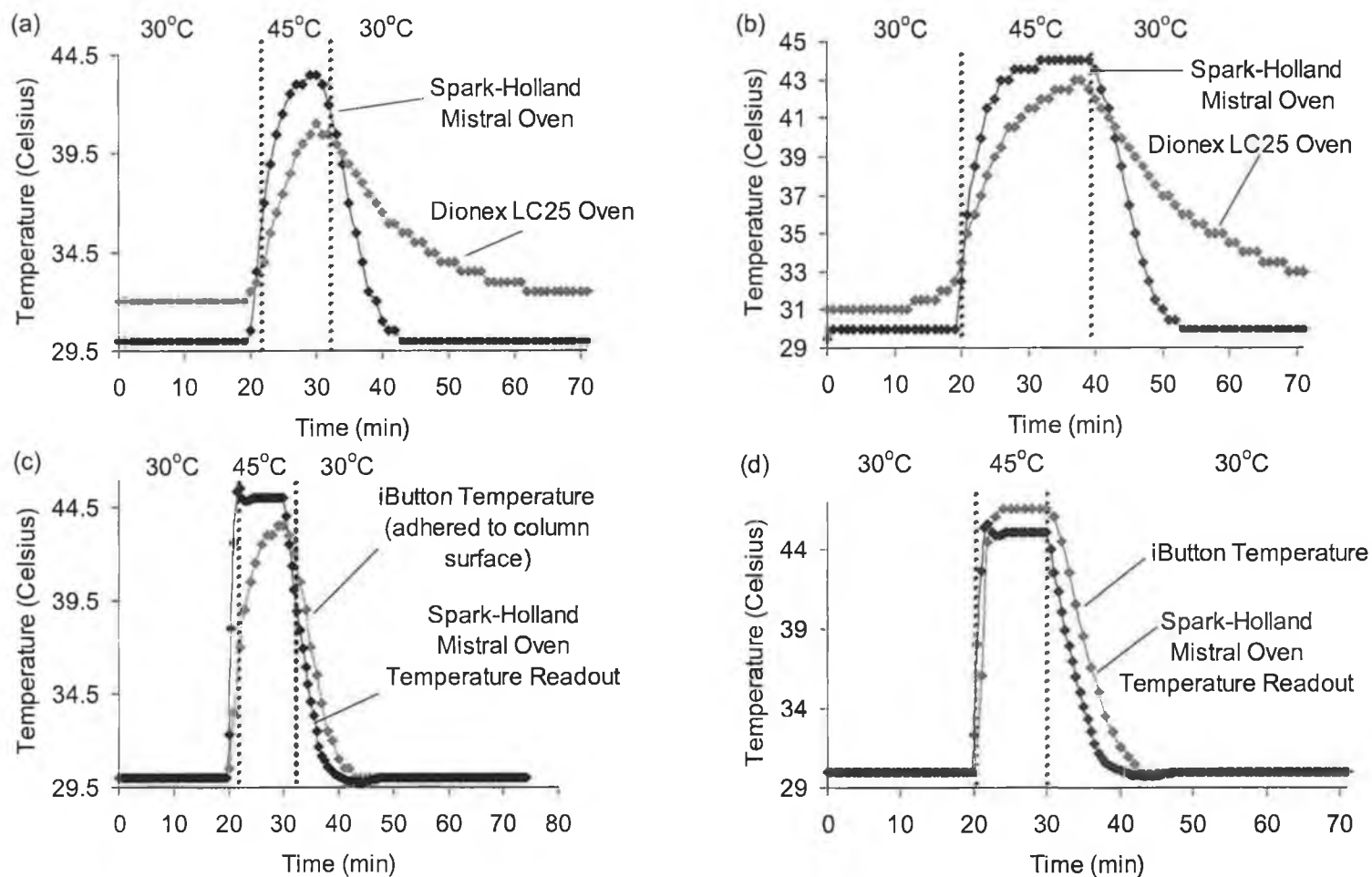


Fig. 7.5 (a-b) Column temperatures for columns held within column ovens during temperature programming cycles, recorded using iButton temperature sensor adhered to column surface. (c) Difference between the column oven readout and the column surface temperature. (d) Difference between the column oven readout and the column oven wall temperature.

7.3.6 Application of temperature program

With the use of the above performance data it was possible to apply temperature programmes to separations of standard solutions and spiked drinking water samples. Three programmes were applied, namely 30°C at $t=0$ and stepping to 45°C at $t=20$, and decreasing back to 30°C at either $t=30$ (10 min programme) or $t=35$ min (15 min programme), or 40 min (20 min programme). *Fig. 7.6* shows a chromatogram of a drinking water sample spiked with 20 µM of each of the HAs and selected oxyhalides resulting from the latter 20 min programme, obtained using the Mistral column oven. As can be seen from *Fig. 7.6*, improved resolution of peaks 3 to 6 was obtained through delaying the temperature increase for the first 20 min. After which the resolution of peaks 7 to 11 was gradually improved through increasing the time set at 45°C, with the 20 min programme (shown here) proving optimum. Maintaining the higher temperature for the full 20 min also results in the improved resolution of TCA and sulphate (as under these conditions TCA elutes after the large sulphate matrix peak), without negatively affecting the resolution of the CDBA and perchlorate.

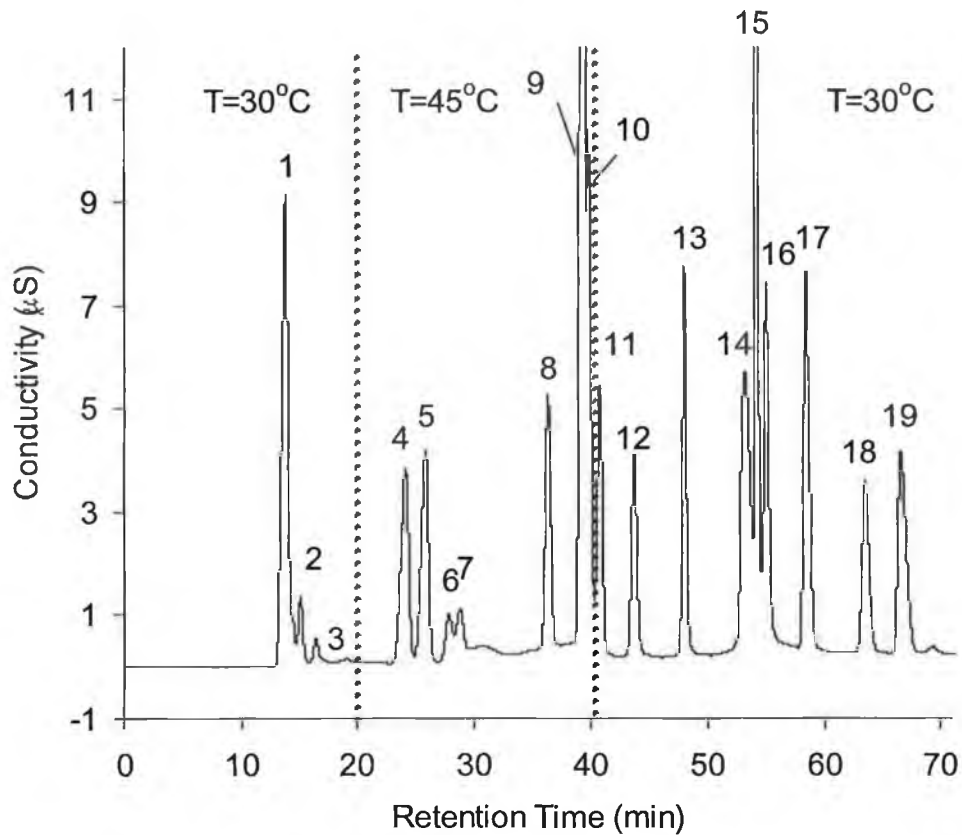


Fig. 7.6 Separation of HAs and oxyhalides in a drinking water sample ($20 \mu\text{M}$ spike of each HAs and oxyhalide, ex. CDBA = $32 \mu\text{M}$, BDCA = $40 \mu\text{M}$) using a hydroxide gradient with applied column temperature programming. Peaks; 1 = fluoride, 2 = iodate, 3 = chlorite 4 = MCA, 5 = bromate, 6 = chloride, 7 = MBA, 8 = TFA, 9 = nitrate, 10 = chlorate, 11 = DCA, 12 = CDFA, 13 = DBA, 14 = carbonate, 15 = sulphate, 16 = TCA, 17 = BDCA, 18 = CDBA, 19 = perchlorate.

An unspiked chlorinated drinking water sample was then analysed using the combined hydroxide and temperature programme. The freshly acquired sample was analysed directly following sulphate and chloride removal, and also analysed following the preconcentration method previously described. The resultant chromatograms are shown overlaid as Fig. 7.7(a) and (b), respectively. From the sample chromatograms it is clear that the combined using of the hydroxide gradient and the temperature programming results in excellent resolution of almost all peaks of interest. In the chromatograms shown the 10 min temperature programme was used to improve the resolution of the 8 peaks eluting after sulphate. As discussed previously, the preconcentration method used led to a reduction in sample fluoride, chloride, nitrate, bromide and carbonate, whilst recoveries for the HAs ranged from 16 % for TFA to 88 %

for CDFA. As the procedure uses sample acidification with sulphuric acid, there is also an increase in weak acid inorganic anions such as nitrite and phosphate, together with the appearance of several unknown peaks, probably due to weak organic acids. Quantification of the haloacetates was achieved using a 3 point standard addition. The results of which were MCA = 0.09 μM ($R^2 > 0.999$), DCA = 0.61 μM ($R^2 = 0.980$), MBA = 0.36 μM ($R^2 = 0.987$), DBA = 0.56 μM ($R^2 = 0.987$), TFA = 0.05 μM ($R^2 > 0.999$), CDFA = 0.50 μM ($R^2 = 0.985$), BDCA = 0.40 μM ($R^2 = 0.980$), CDBA = 0.15 μM ($R^2 = 0.959$).

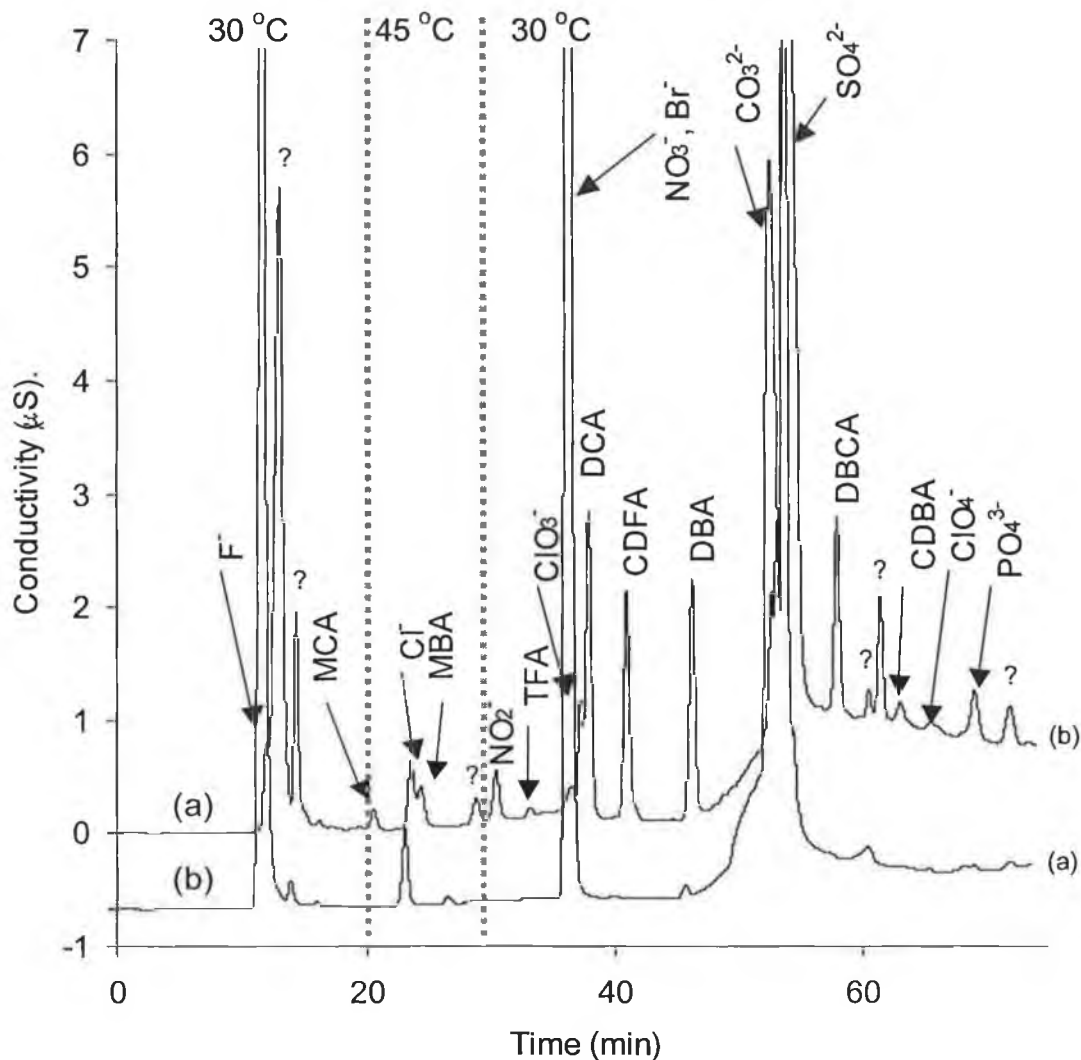


Fig. 7.7 Chromatograms showing the hydroxide gradient separation of inorganic anions, organic acids, oxyhalide and HAs in a chlorinated drinking water (a), and the same sample following preconcentration (b). Hydroxide gradient – as Figure 7.3.

7.3.7 Optimum method for suppressed ion chromatography with conductivity and electrospray mass spectrometry.

For application with conductivity detection alone, the method which utilised the temperature programme involving a temperature step to 45°C for 20 minutes in the Spark-Holland Mistral oven, obviously showed superior separation capability than for the 10 minute program with the Dionex LC25 oven. A 20 minute temperature program was not as practical with the LC25 oven as the inability for this oven to cool rapidly after 20 minutes was a major drawback and caused the separation of anions which eluted later to be compromised. However, when ESI-MS was required, the use of a second column oven was very cumbersome coupled with the fact that the instrument could not be left unattended as temperature steps were inputted manually at required times with the Mistral oven. Therefore, it was decided that the method using only the LC25 oven, with a 10 minute 45°C temperature program was to be taken as the optimum method for use with both conductivity and ESI-MS and as a result, its analytical performance characteristics were determined. Only if incorporation of the conductivity cell, the suppressor and the column along with software automation were possible with the Mistral oven, would this method have been chosen over a completely automated oven like the LC25, which could achieve all of these. Moreover, the use of ESI-MS did not require completely resolved peaks for identification of analytes. *Fig. 7.8* shows the optimum separation using suppressed conductivity with the LC25 oven temperature program.

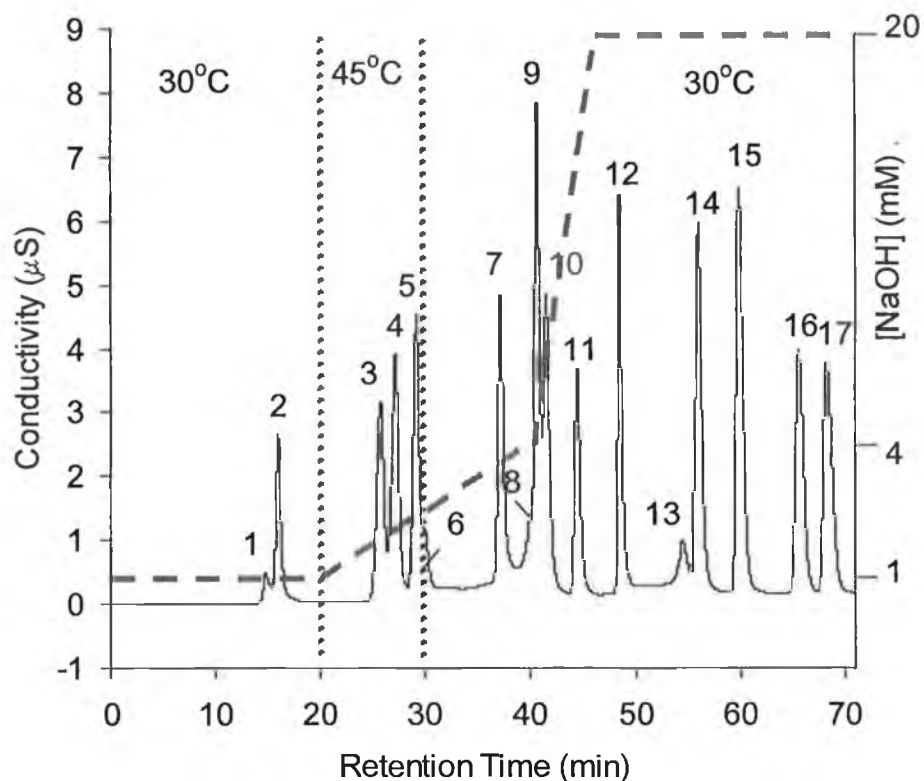


Fig 7.8 Optimum method for use with conductivity combined with ESI-MS detection using temperature program from 30-45°C at 20 minutes for a duration of 10 minutes. Also included is the hydroxide gradient profile (highlighted in grey). Elution order: 1 = fluoride, 2 = iodate, 3 = MCA, 4 = bromate, 5 = chloride, 6 = MBA, 7 = TFA, 8 = nitrate, 9 = chlorate, 10 = DCA, 11 = CDFA, 12 = DBA, 13 = carbonate, 14 = TCA, 15 = DCBA, 16 = CDBA, 17 = perchlorate. [Analytes] = 20 µM.

7.3.8 Analytical performance data for suppressed IC-ESI-MS and conductivity detection

7.3.8.1 Retention time reproducibility of dual gradient method

Clearly evaluation of precision is important if the application of temperature programmes (in combination with eluent gradients) is to be used routinely. Within the system used here, this was assessed through 30 repeat gradient runs, each carried out with the temperature programme applied. Fig. 7.9 shows the resulting retention data graphically with % RSD values for all retention times given. Given the long run times of the developed method, the data shown represents retention time reproducibility over an approximate 45 hr period and

is clearly most satisfactory. Peak area and peak height reproducibility is given in *Table 7.2* and shows that for 10 replicate runs, peak heights varied less than 4.1 % for all analytes with the exception of MBA at 9.2 %, which still suffered coelution from residual chloride in the Milli-Q water. Peak area reproducibility was slightly poorer for the same sample show variance of less than 7.6 % for all analytes, again with the exception of MBA at 11.7 %.

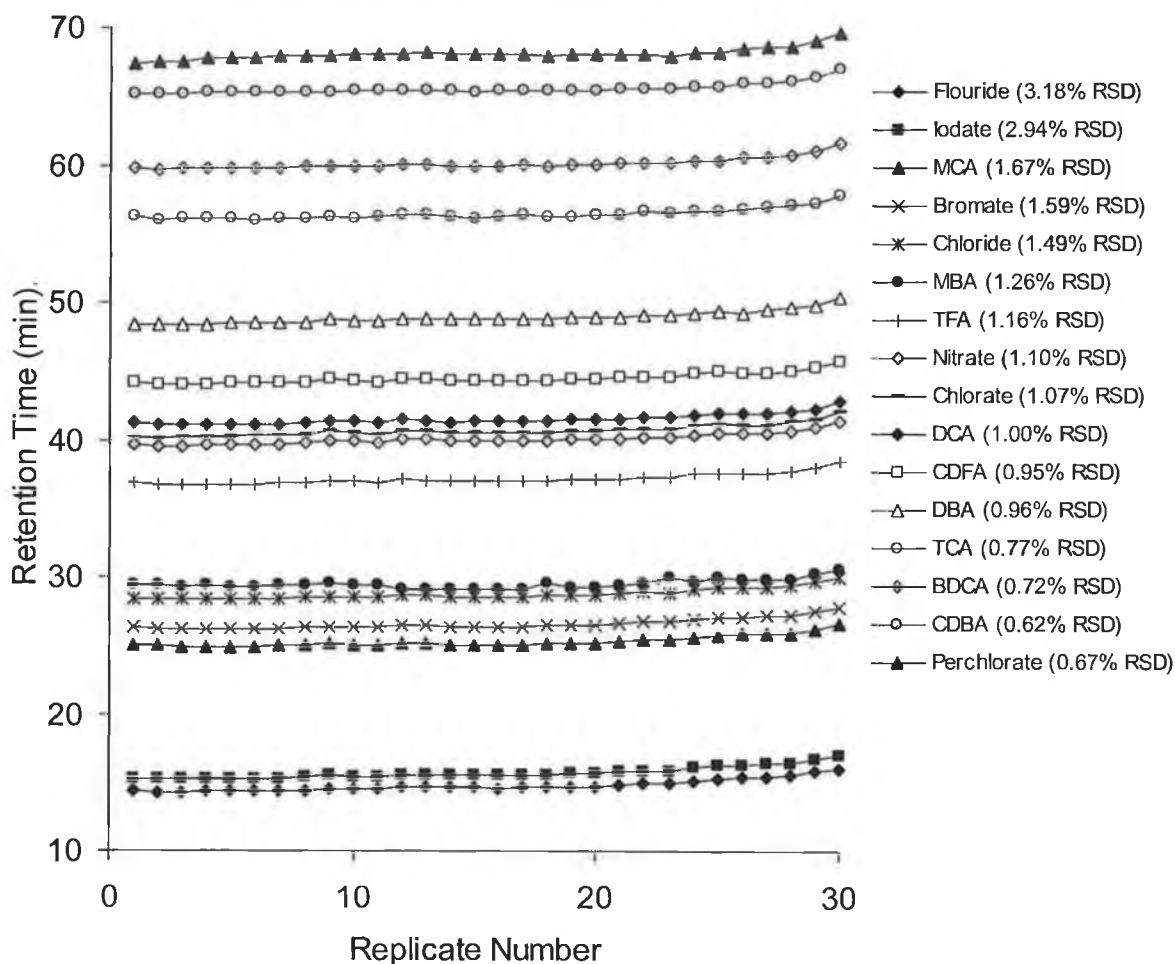


Fig. 7.9 Retention time repeatability for 30 repeat gradient runs with applied temperature programme using conductivity detection.

Table 7.2 Peak area and peak height reproducibility for n = 10 replications of a 2 µM standard of all analytes

Analyte	% RSD (Peak Area)	% RSD (Peak Height)
Iodate	5.8	2.5
MCA	5.9	3.1
Bromate	7.4	4.1
MBA	11.7	9.2
TFA	5.3	2.4
Chlorate	2.7	2.0
DCA	2.8	1.4
CDFA	3.6	1.8
DBA	7.6	3.7
DCBA	3.8	1.9
CDBA	6.0	2.5
Perchlorate	5.7	2.5

7.3.8.2 Linearity for suppressed conductivity and ESI-MS

For the assessment of linearity of both detectors using the optimum gradient method, a series of standards were prepared of both oxyhalides and HAs to concentrations of 0.05, 0.1, 0.2, 0.3 and 0.5 µM (for conductivity detector) followed by 5, 10, 15, 20 and 30 µM (for ESI-MS). Linearity for the conductivity detector was investigated using peak height and for ESI-MS using peak intensity. Also included in this mixture was BCA, which eluted just after CDFA with slight coelution. Standards for each were injected singly for conductivity detection, as extensive peak height and area reproducibility studies were already carried out throughout this work, and in duplicate for ESI-MS. Results from *Table 7.3* show that plots of peak height versus analyte concentration for the conductivity detector again showed acceptable correlation coefficients of greater than $R^2 > 0.99$ and displayed excellent linearity even to concentrations below 10 µg/L in most cases with the exception of MBA and TCA which coeluted with residual chloride and sulphate and could not be determined at this level. With regard to ESI-MS, linearity data was plotted for each of the

analytes corresponding to the following high abundance m/z values: m/z 92.9 ([MCA-H]⁻, [MBA-COOH]⁻), m/z 136.9 ([MBA-H]⁻), m/z 112.9 ([TFA-H]⁻), m/z 126.9 (BrO₃⁻, [DCA-H]⁻, [BCA-COOH]⁻), m/z 128.9 (Br⁸¹O₃⁻, [Cl³⁵Cl³⁷CHCOO]⁻, [CDFA-H]⁻, ([Cl³⁷BrCH]⁻ or [ClBr⁸¹CH]⁻)), m/z 174.9 (IO₃⁻, ([Cl³⁷BrCHCOO]⁻ or [ClBr⁸¹CH⁻COO]⁻)), m/z 216.7 ([DBA-H]⁻), m/z 162.9 ([DCBA-COO]⁻), m/z 206.8 ([CDBA-COOH]⁻), m/z 99 (ClO₄⁻), m/z 82.9 (ClO₃⁻, [DCA-COOH]⁻), m/z 84.9 (Cl³⁷O₃⁻, [Cl³⁵Cl³⁷CH]⁻), m/z 118.8 ([TCA-COOH]⁻), m/z 172.9 ([BCA-H]⁻, [DBA-COOH]⁻). As can be observed from *Table 7.4*, correlation coefficients did not display linearity as effectively as the conductivity detector for all m/z values, as all values were $\geq R^2$ 0.96. However, upon closer inspection all analytes displayed at least one ion type with $R^2 > 0.98$ with the exception of CDFA, TCA and DCBA. The results suggested that the ESI-MS could possibly only be used for qualitative purposes and considering resolution of most analytes with the conductivity detector was acceptable, that quantitative measurements should be carried out as before.

Table 7.3 Linearity data for conductivity detection over 50 – 500 nM analyte concentration (Linearity curves in Appendix A.6, Fig. A.6-1).

Analyte	Lower analyte conc. ($\mu\text{g/L}$)	R^2	Slope	Intercept
MCA	5	0.9996	0.0002	-0.0018
DCA	6	0.9913	0.0002	-0.0077
TCA	n.a.	n.a.	n.a.	n.a.
MBA	n.a.	n.a.	n.a.	n.a.
DBA	11	0.9984	0.0003	-0.0064
BCA	9	0.9986	0.0003	-0.0084
DCBA	10	0.9996	0.0006	-0.0045
CDBA	13	0.9992	0.0002	0.0001
TFA	6	0.9982	0.0002	0.0005
CDFFA	6	0.9962	0.0002	-0.0027
Iodate	9	0.9966	0.0002	0.0111
Chlorate	4	0.9986	0.0004	-0.0020
Perchlorate	5	0.9997	0.0003	-0.0004
Bromate	6	0.9994	0.0002	-0.0020

Table 7.4 Linearity data for extracted ion chromatograms for ESI-MS over 5 – 30 μM analyte concentration (refer Appendix A.6).

Analyte	R^2	Slope	Intercept	Appendix Fig.
[MCA-H] ⁻	0.9937	1138	1550	A.6-2 (b)
[MBA-H] ⁻	0.9921	296	579	A.6-2 (a)
[MBA-COOH] ⁻	0.9879	177	4256	A.6-2 (a)
[TFA-H] ⁻	0.9887	14217	22136	A.6-2 (c)
BrO ₃ ⁻	0.9890	6849	1812	A.6-2 (k)
[DCA-H] ⁻	0.9935	2845	117	A.6-2 (d)
[BCA-COOH] ⁻	0.9975	2727	1853	A.6-2 (f)
Br ⁸¹ O ₃ ⁻	0.9890	8095	1304	A.6-2 (k)
[CDFFA-H] ⁻	0.9745	960	1448	A.6-2 (e)
BrCl ³⁷ CHCOO ⁻ or Br ⁸¹ ClCHCOO ⁻	0.9894	4609	3852	A.6-2 (f)
IO ₃ ⁻	0.9854	10361	897	A.6-2 (k)
[DBA-H] ⁻	0.9868	6529	8135	A.6-2 (g)
[DCBA-COOH] ⁻	0.9666	1164	825	A.6-2 (i)
[CDBA-COOH] ⁻	0.9907	3748	-2241	A.6-2 (j)
ClO ₄ ⁻	0.9932	23511	72234	A.6-2 (k)
ClO ₃ ⁻	0.9939	11379	14310	A.6-2 (k)
[DCA-COOH] ⁻	0.9958	2601	419	A.6-2 (d)
Cl ³⁷ O ₃ ⁻	0.9793	3447	5786	A.6-2 (k)
ClCl ³⁷ CH ⁻ or Cl ³⁷ ClCH ⁻	0.9877	1731	-1432	A.6-2 (d)
[TCA-COOH] ⁻	0.9779	1585	-791	A.6-2 (h)
[DBA-COOH] ⁻	0.9967	17947	8188	A.6-2 (g)

Furthermore, included in *Tables 7.3 & 7.4* are the slopes and intercepts of linearity curves at each m/z . The intercepts are unusually high in most cases due to the fact that ion abundance, not peak height, versus analyte concentration was plotted. Therefore, the background ion abundance for each is included in these plots showing approximately the level of each ion present in the eluent. *Fig. 7.10* shows a separation of all analytes with the inclusion of BCA with no change to the original method. Chlorite was also originally included in the method for validation, but it was found that it decayed rapidly in Milli-Q water to chloride and oxygen, or oxidised to chlorate and required fresh standards to be prepared after relatively short periods of time. As a result chlorite determinations were not considered further. Chlorite is appears as peak 3 in the separation in *Fig. 7.10* and is only included here for completion.

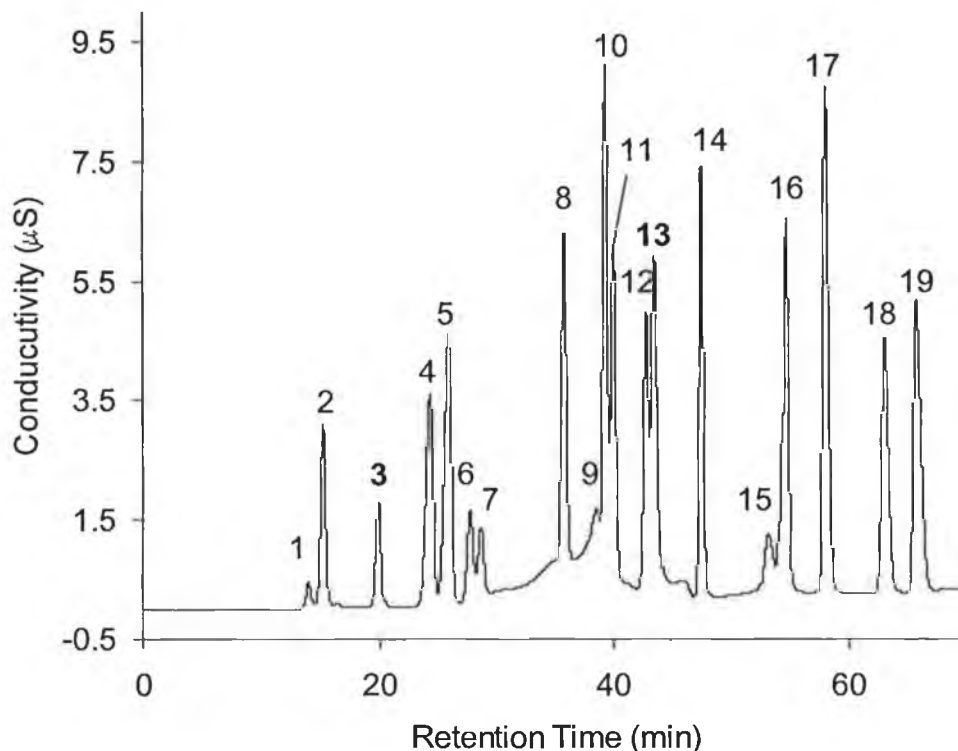


Fig 7.10 Separation of 20 μM standard of all analytes with BCA and chlorite (in bold). Elution order: 1 = acetate, 2 = iodate, 3 = chlorite, 4 = MCA, 5 = bromate, 6 = chloride, 7 = MBA, 8 = TFA, 9 = nitrate/bromide, 10 = chlorate, 11 = DCA, 12 = CDFA, 13 = BCA, 14 = DBA, 15 = carbonate, 16 = TCA, 17 = DCBA, 18 = CDBA, 19 = perchlorate.

7.3.8.3 LOD for conductivity detection

Since conductivity detection consistently showed the most practical application to direct detection of HAs and now oxyhalides in drinking water, the experiment was repeated incorporating the new temperature gradient. A fresh standard of 50 nM of all analytes was prepared in Milli-Q water and injected onto the IC at optimum conditions for $n=7$ replicate runs. Similarly, seven blanks (Milli-Q water) and seven eluent injections were carried out for accurate noise determinations with the suppressor operated in the external water mode. Noise levels were first taken over three sampled timeframes of (a) 8-10 (b) 34-36 and (c) 62-66 minutes from the Milli-Q blank runs, but it was found that, as reported earlier, large levels of acetate, chloride, carbonate and sulphate were observed. For more accurate determination of detector noise, the noise levels were taken from the 7 replicate eluent injections over the same timeframes and LODs calculated as a signal to noise ratio of 3:1 (*Fig 7.11*). Limits of detection are listed in *Table 7.5* for all analytes using external water mode suppression.

Table 7.5 Limits of detection for combined temperature and hydroxide gradient method.

Analyte	Noise (nS) ^a	LOD (nM) ^b	LOD (µg/L)
Iodate	0.3	7.8	1.4
Chlorite	0.3	11.7	0.8
MCA	0.3	5.4	0.5
Bromate	0.3	4.6	0.6
TFA	0.8	10.2	1.15
Nitrate	0.8	4.2	n.a.
Chlorate	0.8	7	0.6
DCA	0.8	3.8	0.5
CDFA	0.8	13.2	1.7
BCA	0.8	12	2.1
DBA	0.8	10.6	2.3
TCA	0.9	14.8	2.4
DCBA	0.9	12.1	2.5
CDBA	0.9	31.8	8.0
Perchlorate	0.9	9.7	0.96

^aNoise levels taken from 7 replicate eluent injections and measured over (i) 8-10 (ii) 34-36 and (iii) 62-66 minutes.

^bCalculated as S:N of 3:1 for 7 replicate 50 nM standards.

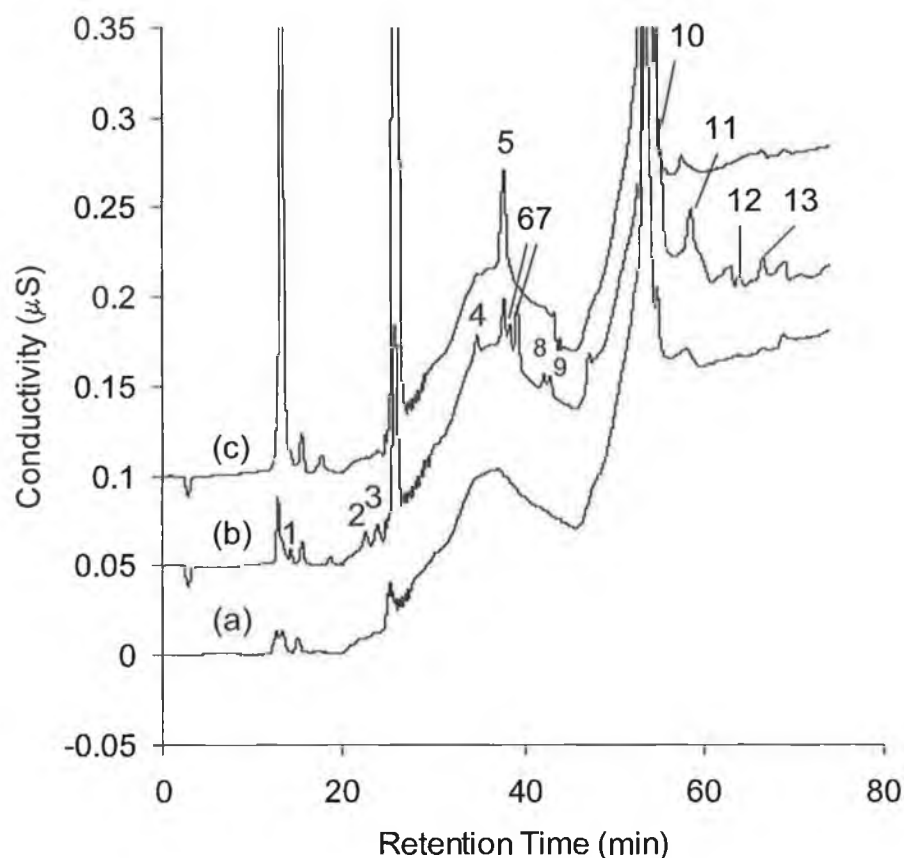


Fig 7.11 (a) eluent injection (b) near limit of detection 50 nM standard and (c) Milli-Q water injection. Elution order: 1 = iodate, 2 = MCA, 3 = bromate, 4 = TFA, 5 = nitrate, 6 = chlorate, 7 = DCA, 8 = CDFA, 9 = BCA, 10 = TCA, 11 = DCBA, 12 = CDBA, 13 = perchlorate.

Upon examination of all three traces in Fig 7.11 above, it can be observed that a baseline disturbance emerged over a timeframe of approximately 5 minutes beginning at a retention time of 25 minutes. This baseline disturbance was possibly due to the temperature program and possibly was the result of a temperature gradient across the diameter of the column causing differences in backpressure. Over the course of this limit of detection study this was observed in a repeatable manner and affected the determination of MBA. Unfortunately, the only remedy for using this method for the determination of MBA was to use the preconcentration method, to boost peak heights and to reduce overall interference. As part of another short study, the comparison of suppression carried out in the external water and auto-recycling modes was investigated. A standard of 80 nM of all analytes was

prepared in Milli-Q water and injected onto the IC with the suppressor configured for both regenerative modes. It was found surprisingly that detection limits seemed to be much better with the auto-recycling mode, with peak heights being enhanced slightly for all analytes. The pump used for external water mode was a rather antiquated Waters 501 series pump and may have contributed to this slight reduction in detection limits observed with external water mode suppression. Furthermore, in agreement with the previous study, both suppressor modes suffered the same baseline disturbance over the same timeframe, but slightly worse in auto-recycling mode despite improved sensitivity. An overlay of the two standards can be observed in Fig. 7.12.

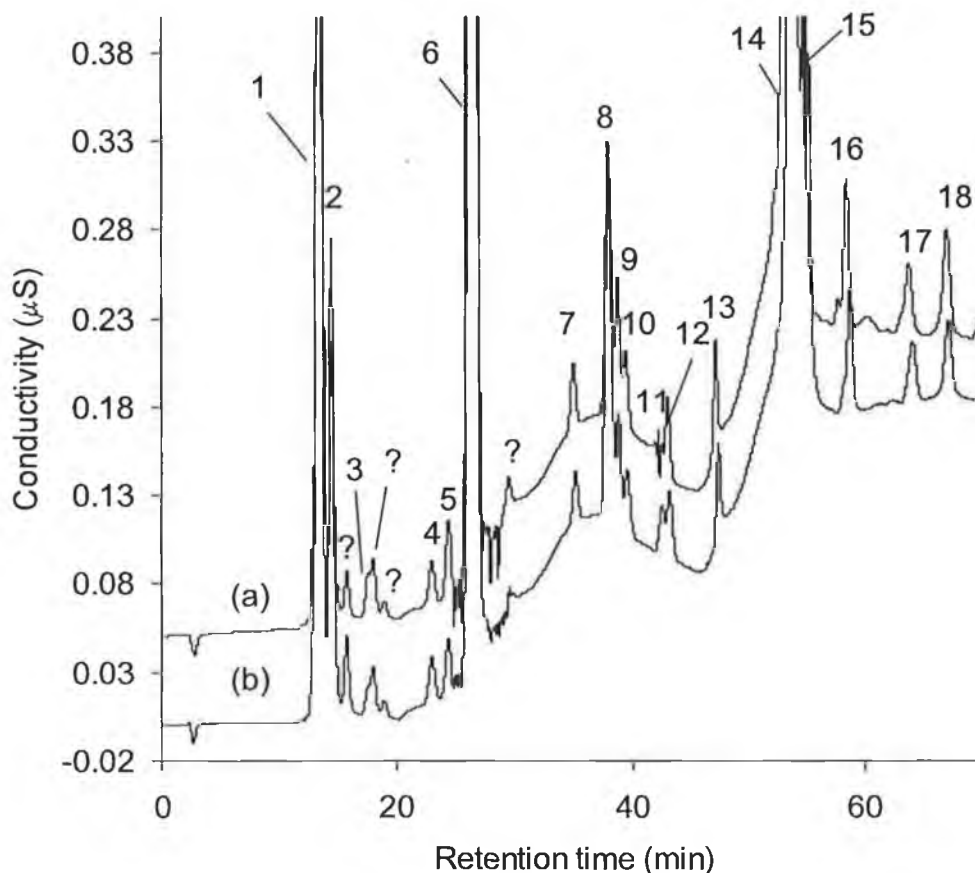


Fig. 7.12 Overlay of (a) 80 nM standard with suppression in auto-recycle mode and (b) same standard with suppression in external water mode. Elution order: 1 = fluoride, 2 = iodate, 3 = chlorite, 4 = MCA, 5 = bromate, 6 = chloride, 7 = TFA, 8 = nitrate, 9 = chlorate, 10 = DCA, 11 = CDFA, 12 = BCA, 13 = DBA, 14 = sulphate, 15 = TCA, 16 = DCBA, 17 = CDBA, 18 = perchlorate.

7.3.8.4 ESI-MS of oxyhalides and limit of detection

In a similar manner to conductivity limit of detection studies, a 10 μM standard was prepared of all analytes in Milli-Q water and injected at optimum IC and ESI-MS conditions. The most abundant ions for each HA and also the oxyhalides were then extracted from the TIC and noise measurements were made by taking five samples of noise from either side of each peak at each mass and calculating an average followed by a limit of detection. The background intensity was also taken into account when measuring peak signal intensities. It should be noted here that the optimum ESI-MS parameters were those listed in Chapter 6.0 for the HAs. Irish drinking water currently does not use ozonation as a means of disinfection and oxyhalides were only separated from HAs to ensure no false positive identifications in conductivity measurements. However, the method does offer significant use to countries with both disinfection types. Therefore, the ESI-MS conditions were not optimised for oxyhalides as HAs were the primary focus. Upon inspection of the TIC and SIM chromatograms, it became clear that the oxyhalides did not suffer significantly as a result of this and displayed particularly good responses in the mass spectra. In particular, the parameters allowed very sensitive detection of perchlorate at m/z 99 and 101. Perchlorate, which was highlighted in Chapter 1.0 as a known endocrine disruptor, has become of increased interest to researchers and governing bodies alike over the past number of years. *Fig. 7.13* shows a 10 μM HA and oxyhalide separation with all extracted ion mass chromatograms overlaid. Sensitivity for iodate was also high and was visible as a clear peak at m/z 174.9. Chlorate was monitored at m/z 82.9 and bromate at m/z 126.9. Limits of detection are given in *Table 7.6*.

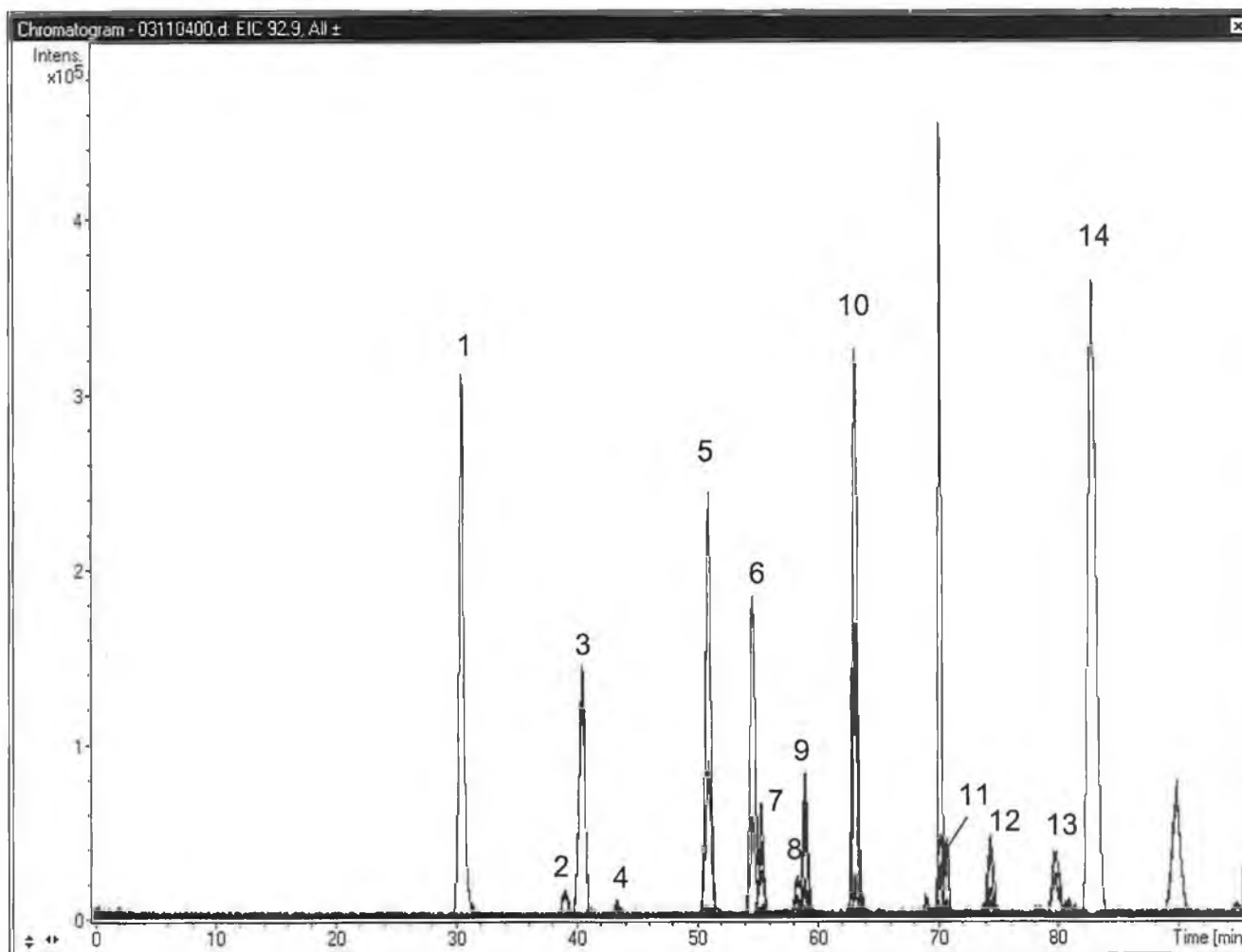


Fig 7.13 Extracted ion chromatograms for 10 μ M standard of all analytes. Elution order: 1 = iodate, 2 = MCA, 3 = bromate, 4 = MBA, 5 = TFA, 6 = chlorate, 7 = DCA, 8 = CDFA, 9 = BCA, 10 = DBA, 11 = TCA, 12 = DCBA, 13 = CDBA, 14 = perchlorate.

Table 7.6 Limits of detection for all analytes with ESI-MS

LOD (μM)	$[\text{M-H}]^-$	$[\text{M-COOH}]^-$	$[\text{M}]^-^a$	$[\text{M}]^-^b$
Iodate			0.1	
MCA	3			
Bromate			0.3	0.7
MBA	11			
TFA	0.4	0.3		
Chlorate			0.1	0.7
DCA	0.7	0.5		2.7
CDFFA	4			
BCA	1	1.6		1.9
DBA	0.4	0.3		
TCA	4	0.6		
BDCA	5	1.5		
CDBA		2		
Perchlorate			0.1	

LOD ($\mu\text{g/L}$)	$[\text{M-H}]^-$	$[\text{M-COOH}]^-$	$[\text{M}]^-^a$	$[\text{M}]^-^b$
Iodate			22	
MCA	313			
Bromate			39	93
MBA	1440			
TFA	39	19		
Chlorate			9	62
DCA	85	40		343
CDFFA	567			
BCA	174	205		
DBA	81	44		
TCA	599	74		
BDCA	1116	244		
CDBA		448		
Perchlorate			10	

^a LOD calculated as ion with chlorine/bromine in their most naturally occurring isotope

^b LOD calculated for M+2 peak for either Cl^{37} or Br^{81} isotopes

As can be observed from Table 7.6, only the LODs for TFA, DCA and DBA fall into the range of 0-60 $\mu\text{g/L}$ for haloacetic acids as proposed by the USEPA. The use of IC-ESI-MS as a standard tool for HA monitoring, still falls short of these requirements and still required the preconcentration method to allow detection of HAs at any quantifiable level. However, ESI-MS showed better sensitivity for the oxyhalides even though the MS parameters were not

optimised and were successful in detection of all oxyhalides at the low $\mu\text{g/L}$ level.

7.3.8.5 ESI-MS Reproducibility

Peak Intensities were investigated for reproducibility by preparing a 20 μM standard of all analytes and running on the IC-ESI-MS a total of six replications. Standard deviations, means and percent standard deviations can be found in *Table 7.7*.

Table 7.7 Reproducibility for peak intensities of a 20 μM oxyhalide and HA standard for $n = 6$ replicate runs.

m/z	Ion	Average Intensity (20 μM standard)	Standard Deviation (n=6)	%RSD
92.9	$\text{ClCH}_2\text{COO}^-$	25904	2436	9
136.9	$\text{BrCH}_2\text{COO}^-$	9962	1038	10
112.9	F_3CCOO^-	328798	21500	7
126.9	BrO_3^-	175246	20645	12
	$\text{Cl}_2\text{CHCOO}^-$	72358	6970	10
	ClBrCH^-	73489	3500	5
128.9	$\text{Br}^{81}\text{O}_3^-$	192810	22470	12
	$\text{Cl}^{37}\text{Cl}^{35}\text{CHCOO}^-$	51949	4839	9
	$\text{F}_2\text{ClCCOO}^-$	26785	2278	9
	$\text{Br}^{81}\text{ClCH}^-$ or $\text{BrCl}^{37}\text{CH}^-$	98170	9304	9
174.9	$\text{Br}^{81}\text{ClCHCOO}^-$ or $\text{BrCl}_{37}\text{CHCOO}^-$	30207	2756	9
	Br_2CH^-	258872	21354	8
	IO_3^-	261022	19403	7
84.9	$\text{Cl}^{37}\text{O}_3^-$	78688	6911	9
	$\text{Cl}^{37}\text{Cl}^{35}\text{CH}^-$	35537	3410	10
	F_2ClC^-	4341	444	10
82.9	ClO_3^-	273480	23925	9
	Cl_2CH^-	52320	4534	9
216.9	$\text{Br}_2\text{CHCOO}^-$	137922	17474	13
162.9	Cl_2BrC^-	25960	2395	9
206.8	ClBr_2C^-	92230	4888	5
172.9	Br_2CH^-	490889	40437	8
	BrClCHCOO^-	104856	8790	8
118.9	Cl_3C^-	37153	4826	13
99	ClO_4^-	558458	44024	8

As can be seen from *Table 7.7*, reproducibility for peak intensity was not as effective as the conductivity detector further outlining the fact that this particular model of mass spectrometer should really only be used for qualitative analyses. All quantitative analyte determinations should be carried out by conductivity detection. All %RSD values for the six replicate runs were between 5 and 13 % for all analytes.

7.3.9 *Application to real samples*

7.3.9.1 *Application to HA and oxyhalide determinations in soil*

The application of suppressed IC-conductivity-ESI-MS to the analysis of soil was considered. A sample of soil was taken from Co. Meath by digging approximately 10-15 cm into the earth and transferring soil to a glass-screw capped bottle. Sample was then transferred to a crucible and dried in an oven at 37°C for 24 hours. Considering that the oxyhalides and HAs are extremely soluble in water, the extraction procedure was relatively simple. A weight of 2.0 g of was measured out from the dried sample and placed in a conical Erlenmeyer flask. Exactly 20 mLs of Milli-Q water was added to the flask and the Erlenmeyer flask was left for 3 hours on an automatic shaker. The resulting solution in the Erlenmeyer flask was filtered using 0.45 µm vacuum filters and transferred to a vial. In parallel, a sample of soil was spiked with 0.5 µM of all analytes. Fortifications were made by preparing the desired concentration of all analytes in the 20 mL Milli-Q water solution used for extraction. When the neat sample was run with the dual gradient IC method and chromatograms obtained by conductivity detection were examined, peaks corresponding to the retention times of TFA, DCA, BCA, DBA, DCBA, CDBA and perchlorate were observed at various concentrations. Particularly evident were the peaks for BCA and DBA, which when compared to the 0.5 µM standard, seemed to be at a similar level of magnitude indicating that these HAs were above the USEPA limit of 60 µg/L. *Fig 7.14* shows an overlay of a spiked versus unspiked sample.

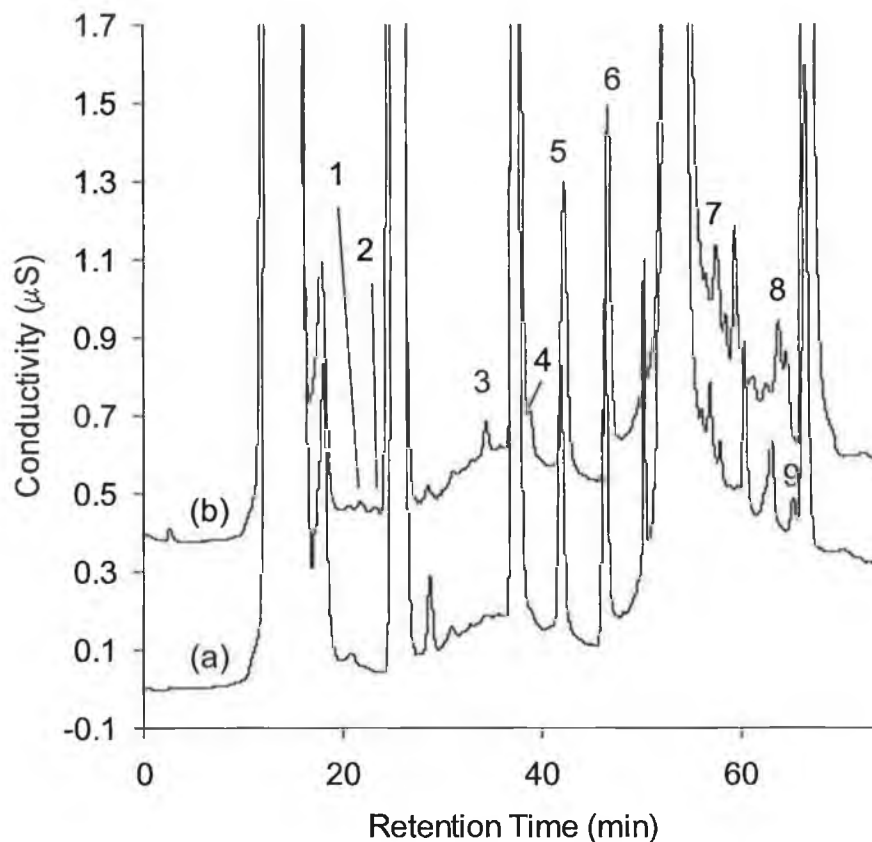


Fig. 7.14 (a) Unspiked soil extract (b) 0.5 µM spiked soil extract. Elution order: 1 = MCA, 2 = bromate, 3 = TFA, 4 = DCA, 5 = BCA, 6 = DBA, 7 = DCBA, 8 = CDBA, 9 = perchlorate.

The neat sample was run also using ESI-MS. From the resulting TIC, SIM was carried out for any peaks observed. No m/z values were present for either DBA or BCA. On closer inspection of the range m/z 79-81, a very small peak for loss of bromine appears at the retention time corresponding to BCA, indicating that BCA could be present, but that the ESI-MS was not sensitive enough to confirm for its ions $[M-H]^-$ and $[M-COOH]^-$. This highlighted the advantage of the ESI-MS over the conductivity detector in identifying a false positive result. The only m/z observed corresponding to an analyte mass, was m/z 99, corresponding to perchlorate. Confirmation of the presence of perchlorate was carried out by inspecting the $Cl^{37}O_4^-$ peak at m/z 101. For a compound containing one chlorine atom, the ratio of M and M+2 peak should be approximately 3:1. In this case the ratio was slightly higher at 100:43 and so did not agree entirely with the accepted ratio. In order to be certain, the

standards for linearity were examined over the concentration range 5-30 μM perchlorate for ratios of m/z 99 and 101. It was found that for all 5 standards in duplicate runs that the ratio of m/z 99-101 was 100:42.9 ($\pm 1.9\%$ for m/z 101), which clearly indicated that this peak was in fact perchlorate. The extracted ion chromatograms for all ions observed in the sample are shown in Fig. 7.15 along with the mass spectrum of the perchlorate peak.

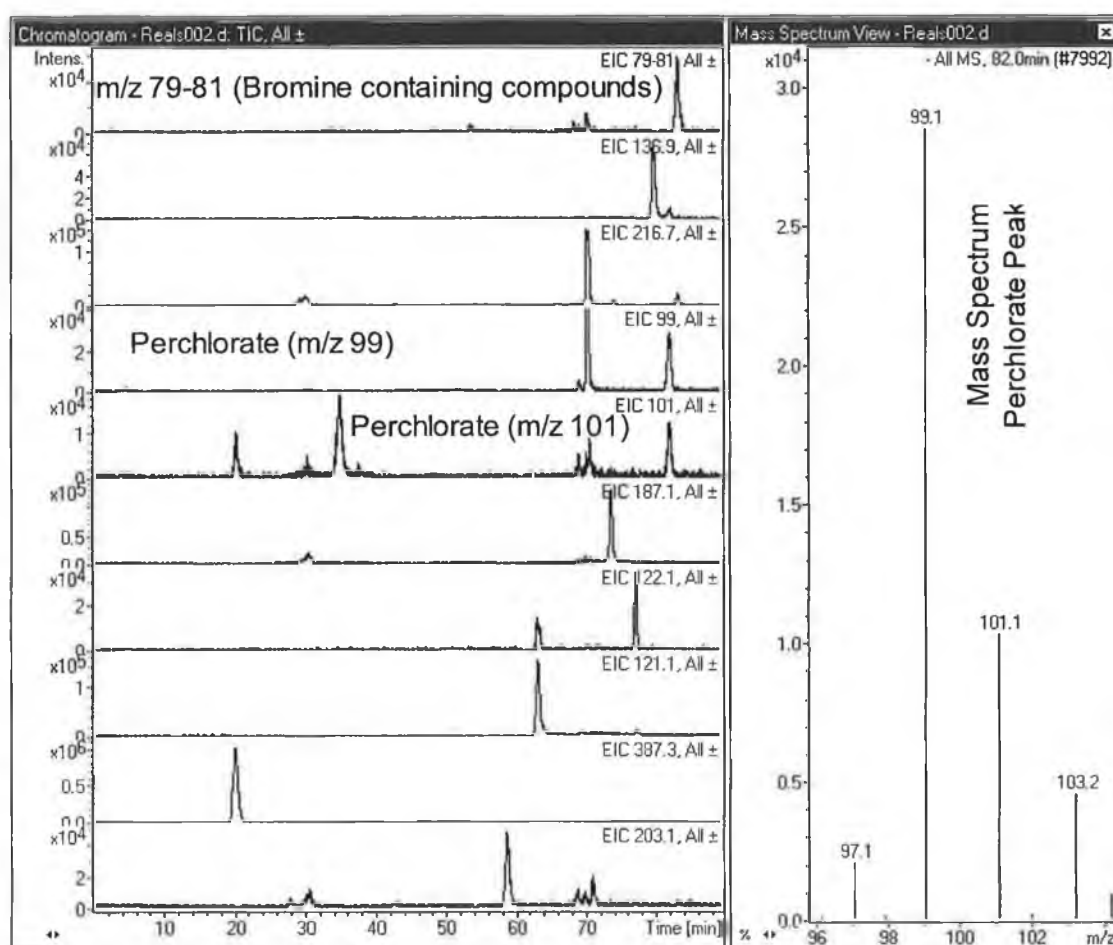


Fig. 7.15 Extracted ion chromatograms for each ion in TIC. (Right) mass spectrum for peak corresponding to perchlorate.

Following identification of perchlorate, a short standard addition quantification with ESI-MS was carried out by spiking the soil sample as before with 0, 2, 5, 9 and 17 μM of perchlorate and plotting peak intensity versus perchlorate concentration. The calibration curve shown in Fig. 7.16, shows that a best fit

curve for all points gave an R^2 value of 0.977 and for directing the curve through the unspiked sample data point, R^2 0.949. Clearly, improved linearity was displayed with the former. Taking the equation of the line into account, the concentration of perchlorate in the soil sample was 2.5 μM , 249 $\mu\text{g/L}$ or 2.5 $\mu\text{g/g}$ of soil. For the curve passing through the neat extract, the extrapolated equation of the line corresponded to a perchlorate concentration of 0.91 μM , 90 $\mu\text{g/L}$ or 0.90 $\mu\text{g/g}$ of soil and showed considerable variance.

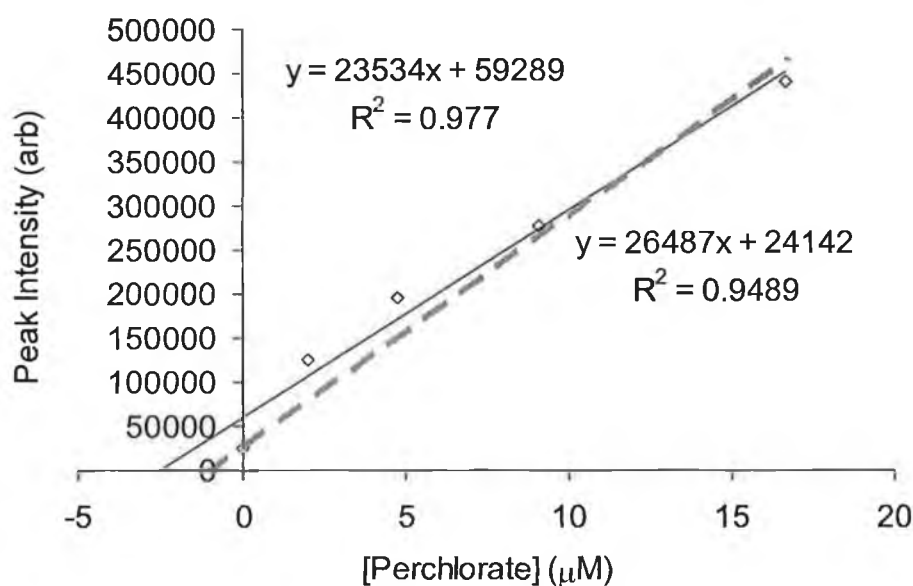


Fig 7.16 Standard addition curve for perchlorate in soil. Best fit curve for all data points shown in black, and for curve directed through unspiked sample data point in grey.

7.3.9.2 Suppressed IC-conductivity-ESI-MS of drinking water sample

A 1 L sample of laboratory drinking water was taken using the standard sampling procedure outlined in Chapter 5.0, Section 5.2.3 in late November of 2004 and was analysed for HA and oxyhalide content. The sample was first subjected to extraction of chloride and sulphate using the Maxi-Clean cartridge series as before and injected neat onto the IC using the applied hydroxide and temperature program. Upon inspection of the chromatogram obtained from the conductivity detector, very low levels of CDFA, DBA and perchlorate were observed. Following this, a 50 mL aliquot of sample was preconcentrated and cleaned in the usual manner and run with dual gradient suppressed IC-

conductivity-ESI-MS. Very distinct peaks corresponding to levels of MCA, MBA, TFA, chlorate, DCA, CDFA, BCA, DBA, DCBA, CDBA were observed and a very small peak for perchlorate was observed which coeluted with a preconcentrated component of the sample and was obscured. Fig. 7.17 shows the chromatograms obtained for unspiked samples with and without preconcentration.

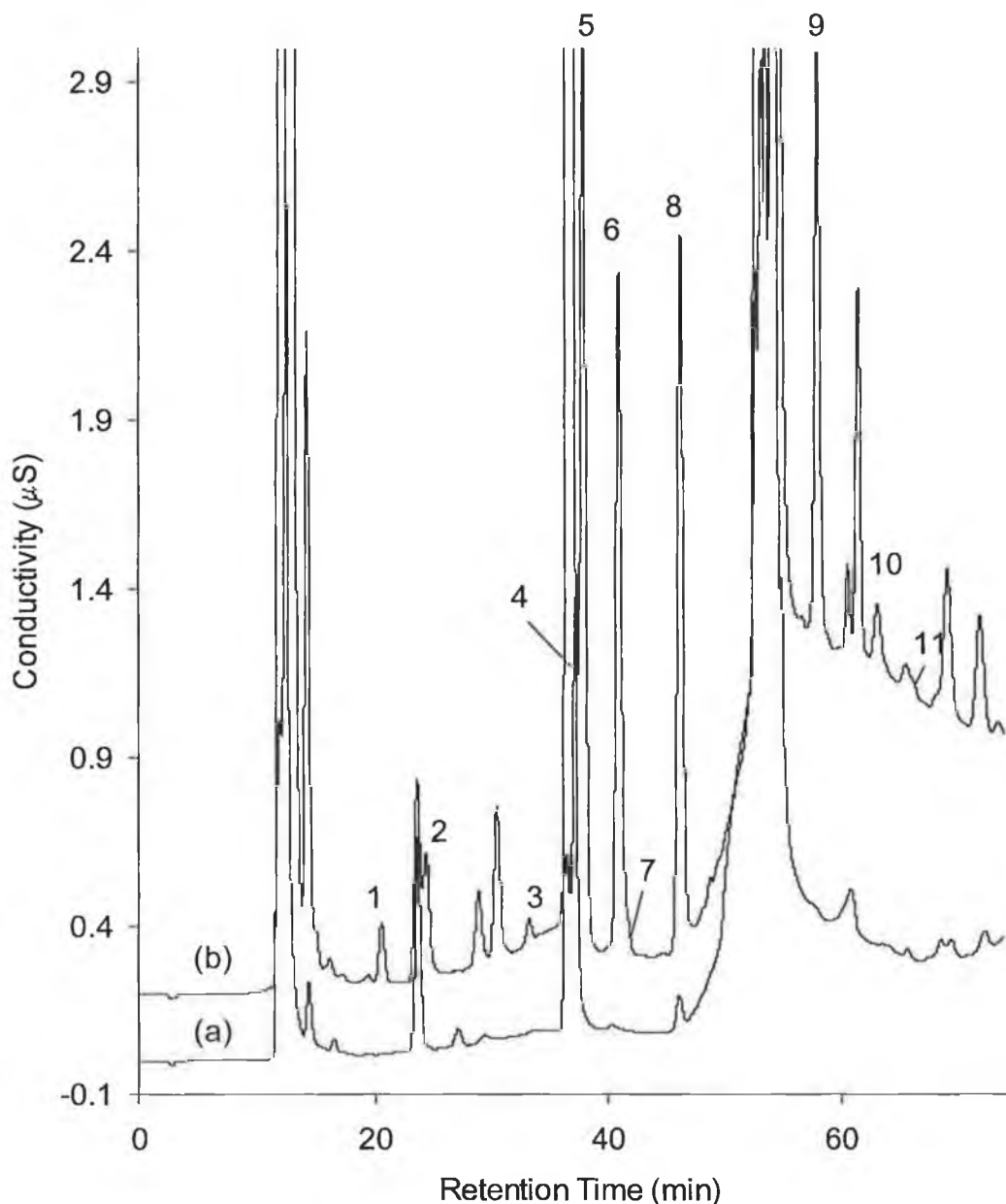


Fig 7.17 (a) neat drinking water sample with sulphate and chloride removed with Alltech SPE cartridges (b) preconcentrated neat drinking water sample. Elution order: 1 = MCA, 2 = MBA, 3 = TFA, 4 = chlorate, 5 = DCA, 6 = CDFA, 7 = BCA, 8 = DBA, 9 = DCBA, 10 = CDBA, 11 = perchlorate.

To conclusively identify all compounds observed from the preconcentrated sample, the extracted ion chromatograms were examined. Extracted m/z values of 126.9, 128.9, 172.9, 216.9, 82.9, 84.9, 99, 101 and 206.8 confirmed the presence of DCA, CDFA, DBA, chlorate, perchlorate and CDBA in the drinking water sample. In contrast to the soil sample, perchlorate was present at much lower levels and was visible at just below the LOD level. Additionally, from examination of the extracted ion chromatogram for bromine (m/z 79-81), the presence of MBA and DCBA was further shown at correlating retention times, though not with complete certainty. Examination of the EICs for MBA at m/z 136.9 and DCBA at m/z 162.9 show the presence of these two compounds, but at below limit of detection level (S:N 3:1). This evidence correlated well with the conductivity traces and highlighted the applicability of an analyte specific detector. In contrast to the previous soil sample the availability of the MS in this case allowed the positive identification of analytes. *Fig. 7.18* represents all the extracted ion chromatograms for all ions present in this drinking water sample after preconcentration with SPE.

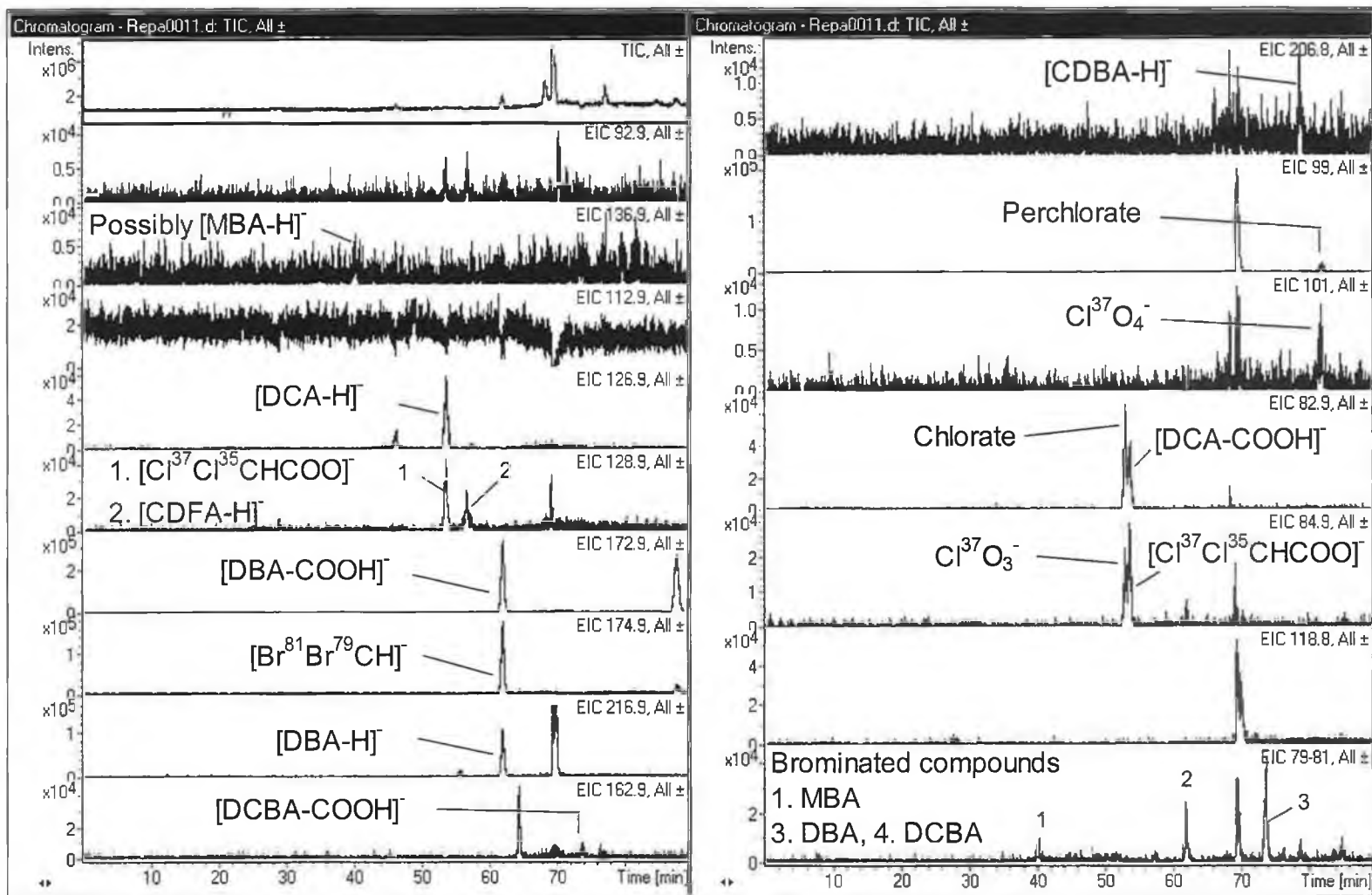


Fig 7.18 Extracted ion chromatograms for laboratory drinking water preconcentrated 25-fold showing presence of DCA, CDFa, DBA, chlorate, perchlorate, CDBA and possibly some DCBA and MBA.

To quantify the levels of HAs in this drinking water sample, a semi quantitative standard addition (by peak height) was carried out by spiking two 50 mL aliquots of sample with 1 and 2 μM of each analyte and preconcentrating in the usual manner. The oxyhalides were not quantified, as they did not preconcentrate reproducibly to allow standard addition. The sum total of all HAs in the drinking water sample was 12.83 $\mu\text{g/L}$ and was well within the specified limit of 60 $\mu\text{g/L}$ even for all analytes not included in the USEPA Stage I Disinfectants and Disinfectant By-products Rule. The levels of each observed HA are listed in *Table 7.8*.

Table 7.8. Semi-quantitative standard addition of HAs in laboratory drinking water sample.

HA	Concentration from standard addition (μM)	% Recovery and standard deviation ^a	Concentration in original water sample (μM)	Concentration in original water sample ($\mu\text{g/L}$)
MCA	0.37	65 \pm 10	0.006	0.53 \pm 0.05
MBA	0.36	63 \pm 28	0.006	0.78 \pm 0.22
DCA	0.61	84 \pm 10	0.007	0.92 \pm 0.09
CDFA	0.50	87 \pm 15	0.006	0.74 \pm 0.11
TFA	0.05	17 \pm 23	0.003	0.34 \pm 0.08
DBA	0.56	66 \pm 18	0.008	1.84 \pm 0.33
DCBA	0.40	13 \pm 4.6	0.031	6.39 \pm 0.29
CDBA	0.15	30 \pm 7.8	0.005	1.29 \pm 0.10
Total [HA]				12.8 \pm 1.27

^a From Chapter 5.0, Table 5.2

7.4 Conclusions

Better understanding of the temperature effects upon the ion exchange separation of oxyhalide and haloacetates has led to a practical and useful application of temperature programming to significantly improve the resolution of analyte peaks within a particularly complex sample. Some evidence for hydrophobic interactions between haloacetates and anion-exchanger IonPac AS16 were found. The final method, although longer than ideal, exhibits the resolution, efficiency and sensitivity required to determine the above species in actual drinking water samples (as shown), and as such is a real practical alternative to gas chromatographic methods for monitoring such disinfection by-product species. Adequate results were obtained for linearity of both detectors, with conductivity detection showing superior correlation coefficients. Limit of detection studies showed that conductivity detection still offered the highest sensitivity in contrast to MS. Reproducibility of the combined temperature and hydroxide gradient showed excellent % RSDs. With respect to peak area and height, conductivity detection showed better peak reproducibility for $n = 10$ replicate runs. Application of the method to two very different sample types was shown with perchlorate present in soil samples and the majority of the monitored analytes present in the drinking water sample at $12 \mu\text{g/L}$ concentration in total. The method indeed offers itself to the monitoring of HAs and oxyhalides in drinking water and when coupled to MS, significantly reduces the level of false positive results.

7.5 References

1. C.Zhu, D.M Goodall, S.A.C. Wren, *LC-GC Europe*, 17 (2004), 530
2. B.A. Jones, *J. Liq. Chromatogr. Related Techn.*, 27 (2004), 1331.
3. M.G. Kolpachnikova, N.A. Penner, P.N. Nesterenko, *Journal of Chromatography A*, 826 (1998), 15.
4. B. Paull, W. Bashir, *Analyst*, 128 (2003), 335.
5. M.A. Rey, C.A. Pohl, *Journal of Chromatography A*, 739 (1996), 87.
6. P.A. Kebets, K.A. Kuz'mina, P.N. Nesterenko, *Russian Journal of Physical Chemistry*, 76 (2002), 1481.
7. P. Hatsis, C.A. Lucy, *Analyst*, 126 (2001), 2113.
8. J. Chong, P. Hatsis, C.A. Lucy, *Journal of Chromatography A* 97 (2003), 161.
9. Y. Baba, N. Yoza, S. Ohashi, *Journal of Chromatography*, 348 (1985), 27.
10. N.E Fortier, J.S. Fritz, *Talanta*, 34 (1987), 415.
11. A.V. Pirogov, O.N. Obrezkov, O.A. Shpigun, *J. Anal Chem.*, 52 (1997), 152.
12. P. Hatsis, C.A. Lucy, *Journal of Chromatography A*, 920 (2001), 3.
13. R. Dybczynski, K. Kulisa, *Chromatographia*, 57 (2003), 475.
14. P. Jones, P.N. Nesterenko, *Journal of Chromatography A*, 789 (1997), 413.
15. W. Bashir, E. Tyrrell, O. Feeney, B. Pauli, *Journal of Chromatography A*, 964 (2002), 113.
16. M.J. Shaw, P.N. Nesterenko, G.W. Dicinoski, P.R. Haddad, *Australian Journal of Chemistry*, 56 (2003), 201.
17. M.J. Shaw, P.N. Nesterenko, G.W. Dicinoski, P.R. Haddad, *Journal of Chromatography A*, 997 (2003), 3.
18. A. Haidekker, C.G. Huber, *Journal of Chromatography A* 921 (2001), 217.
19. P.N. Nesterenko, P. Jones, *Journal of Chromatography A* 804 (1998), 223.
20. A.I. Elefterov, M.G. Kolpachnikova, P.N. Nesterenko, O.A. Shpigun, *Journal of Chromatography A*, 769 (1997), 179.

21. G.E. Boyd, Thermal effects in ion exchange reactions with organic exchangers: enthalpy and heat capacity exchanges, ion exchanges in the process industries, Society of Chemical Industry, London, 1970, p. 261.
22. R.G. Smith, P.A. Drake, J.D. Lamb, Journal of Chromatography, 546 (1991), 139.
23. B. Paull, L. Barron, Journal of Chromatography A, 1046 (2004), 1.
24. B.W. Yan, J.H. Zhao, J.S. Brown, J. Blackwell, P.W. Carr, Anal. Chem., 72 (2000), 1253.
25. R.G. Wolcott, J.W. Dolan, L.R. Snyder, Journal of Chromatography A, 869 (2000), 3.
26. SRC Environmental Fate Database, Syracuse Research Corporation, 2004.
27. D. Kou, X. Wang, S. Mitra, Journal of Chromatography A, 1055 (2004), 63.

Chapter 8.0

Final Conclusions and Summations

A number of distinct conclusions can be made upon close examination of the work presented here. It was clear that successful ion exchange chromatography with both columns required a well tailored eluent concentration gradient for adequate separation of HAs from existing mg/L concentrations of inorganic anions. The degree of hydrophobicity of TCA, DCBA and CDBA played an important role in determination of the overall analysis time. High concentrations of hydroxide were required to elute them and this unfortunately resulted in rather excessive run-times in all cases. The method developed using the agglomerated AS11-HC column yielded poor resolution of inorganic anions from trace HAs especially MBA from chloride. Initial work with this column clearly showed the requirement for preconcentration. As part of this study it was proposed that the hyper cross-linked EVB-DVB stationary phase of the LiChrolut EN allowed for a dual retention mechanism involving not only hydrophobic interactions, but also anion exchange mechanisms and requires very specific optimisation of total sample volumes to be preconcentrated, in this case, 50 mL. Elution profiles showed the affinity for the HAs for the stationary phase with fluorinated acids showing the least affinity. The LiChrolut EN cartridge was very rugged and it was possible to carry out 6 repeat concentrations on the same cartridge without any marked decrease in percent recovery. Later it was found that doubling sorbent mass only doubled volumes required to elute the bound HAs and doubling eluent NaOH concentration had little or no effect. It was also discovered that the preconcentration procedure gave rise to an inherent self-cleaning effect and successfully removed over 90 % of sample nitrate allowing determination of DCA. Overall percent recoveries were adequate for all of the five regulated HAs, but were poor for TFA and CDBA at 17 % and 13 %.

The merits of SPE with suppressed conductivity detection became apparent with the addition of the eluent generator module. Although sensitivity initially improved markedly with electrolytically generated eluents, it was later found to introduce leachates of styrene-sulphonate into the eluent causing a significant difference in retention data to those methods using manually prepared eluents. Furthermore, background interference with ESI-

MS detection was far too significant with electrolytically generated eluents. It was later found that improvements in sensitivity were due to the CR-ATC module, which was a component of the eluent generator. The CR-ATC was retained and was most significant in developing final methods using temperature programming, albeit with manually prepared eluents. Therefore, eluent generation was not considered to be suitable for the suppressed IC-ESI-MS analysis of HAs and was removed. Attempts to separate MBA and chloride were unsuccessful with the IonPac AS11-HC column, but showed clear improvement with the IonPac AS16 column. Overall, this column offered the more resolved chromatogram for all analytes and other solutes. Hydroxide eluents, using Dionex instrumentation, are generally suppressed using the ASRS Ultra series membrane suppressors. However, it was decided to compare this membrane suppressor to a cation exchange type suppressor using an internal bed of monolithic discs. Using low concentration gradients (≤ 20 mM in this case) it was found that the AEES Atlas suppressor was by far the most efficient suppressor and aided in obtaining far superior detection limits that were, in some cases, a 47-fold improvement in detectable analyte concentration. Using this suppressor, HAs could be quantified without preconcentration and the working range was between 1.4 and 73.5 $\mu\text{g/L}$ with direct injection. Although undesired, the introduction of a SPE sample pre-treatment procedure allowed the removal of interferent inorganic anions and was particularly efficient in the removal of 90 % of sulphate and 98 % of chloride. Coupling this sensitive suppressed conductivity method with the SPE preconcentration procedure, detection limits in the 0.1-21.5 $\mu\text{g/L}$ range were possible for all nine HAs, with all detection limits for the five regulated HAs ≤ 1.1 $\mu\text{g/L}$. Both of these methods were then applied to the determination of drinking water samples, in which HAs were quantified.

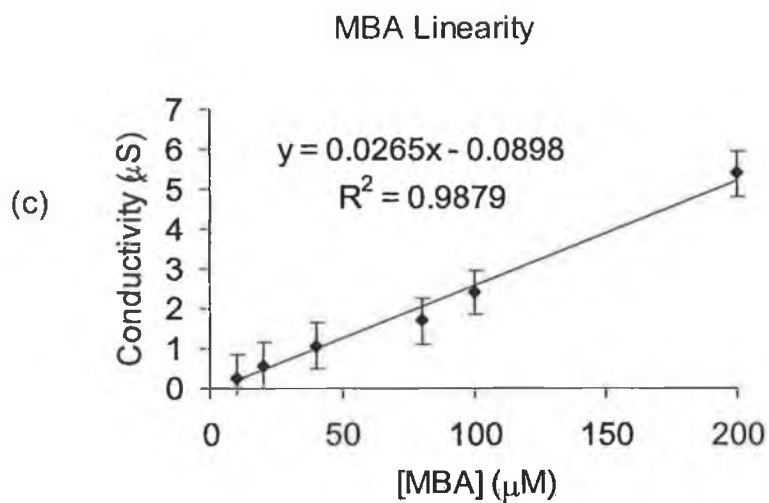
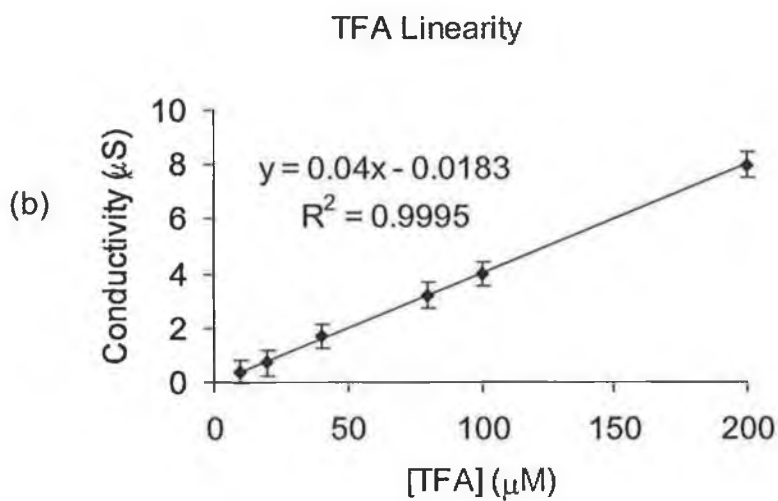
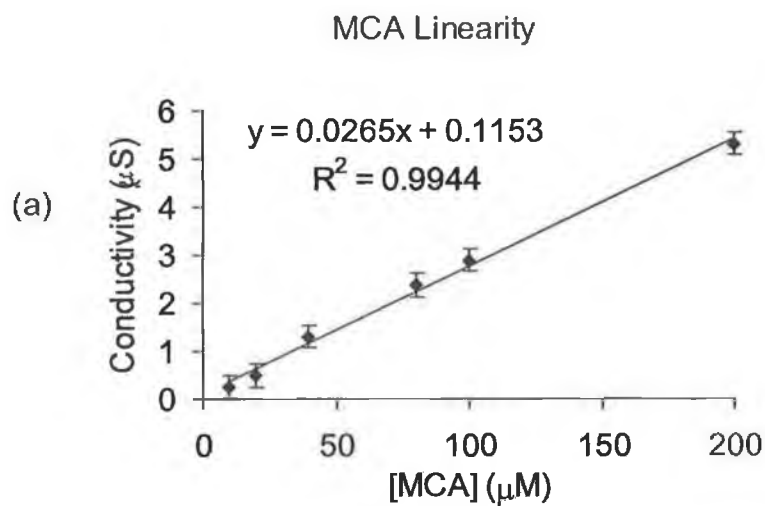
Alternative detection methods to suppressed conductivity were investigated and it was found that UV detection was not suitable, offering a poor chromatogram with distorted peak shapes and inadequate sensitivity at an optimised wavelength of 200 nm. Electrospray mass spectrometry was also investigated and, once optimised, offered a multitude of data about any

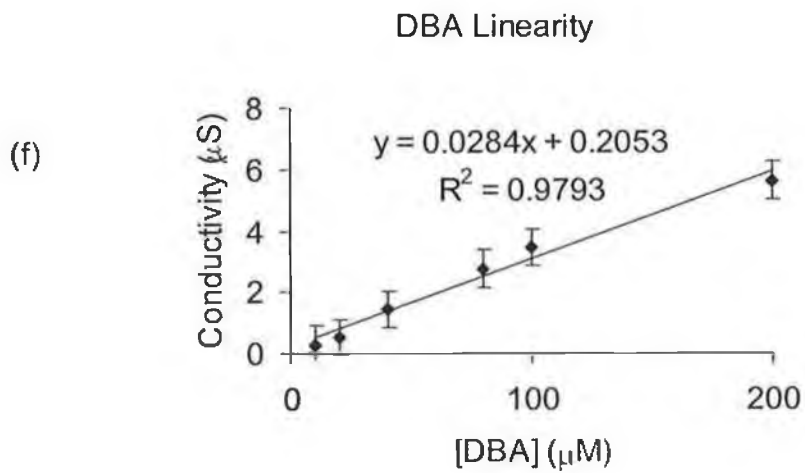
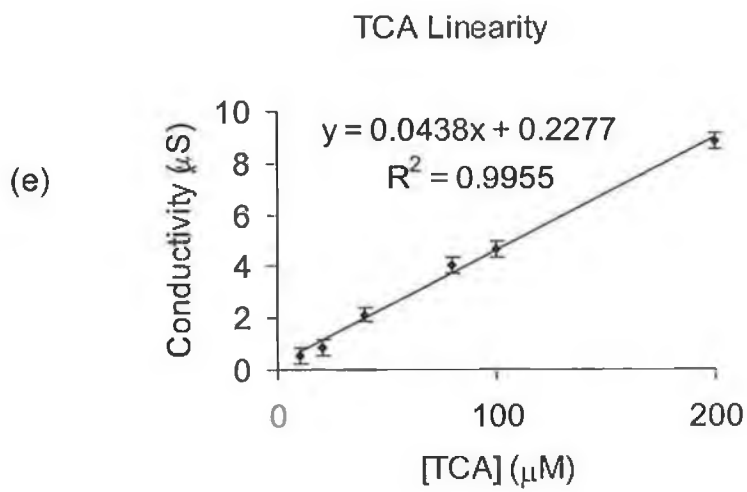
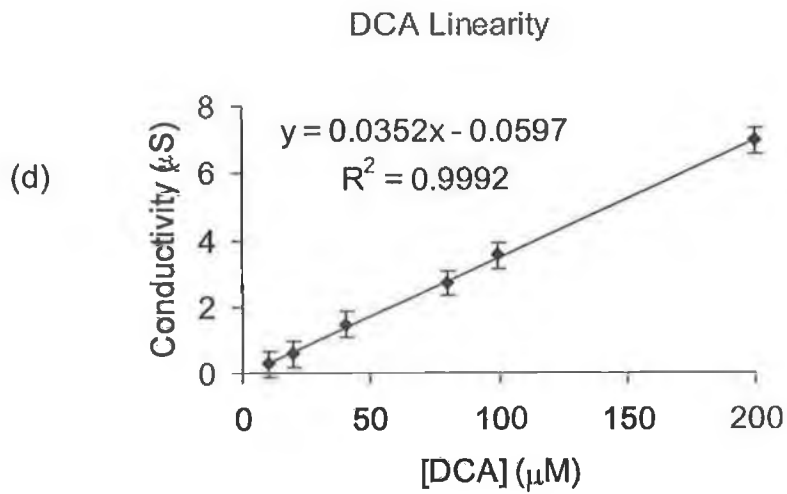
one sample or standard. Analytes existed as their pseudo molecular ion, $[M-H]^-$, decarboxylated fragment ion, $[M-COOH]^-$, and a dimerised ion form, $[2M-H]^-$. The combination of suppressed conductivity, UV and ESI-MS was applied to a spiked drinking water sample. Unfortunately, both the Atlas and the CR-ATC began to leak and clearly could not withstand the backpressure from three detectors in series. As a result, UV detection was not considered further.

The simultaneous separation of oxyhalides, inorganic anions and HAs was considered using the IonPac AS16 column. Separation of all analytes was not achieved at any one set oven temperature. Therefore, it was considered to incorporate a dual gradient of hydroxide concentration and oven temperature. The optimised method offered excellent reproducibility and improved the separation of all analytes. The analysis of perchlorate in soil was possible and was determined using both suppressed conductivity and ESI-MS detection following prior perchlorate extraction into Milli-Q water. This SPE-suppressed IC-conductivity-ESI-MS method was then applied to the analysis of drinking water. Sensitivity of ESI-MS was poorer than conductivity measurements and lay in the mid-high $\mu\text{g/L}$ range. Suppressed conductivity detection limits lay in the range 0.5-8.0 $\mu\text{g/L}$ for direct injection. Along with further improvements in sensitivity, could this dual detector method be used for routine monitoring of HAs and oxyhalides.

Overall, suppressed conductivity detection offered the most promising results and analysis of two separate groups of DBP was possible with one column with adequate resolution. Run-times were longer than desired, but considering the complex nature of the sample, separation was excellent. The preconcentration procedure was less complex, cumbersome and time-consuming than the USEPA proposed liquid-liquid extraction derivitisation and could be completed well within one IC run-time allowing once sample to be separated by IC, while the next sample was prepared. The applicability of IC to anionic DBP determinations in complex matrices has shown to be successful here and although, not as sensitive as either the GC-ECD or GC-MS methods, shows definite promise as an alternative.

Appendix A.1





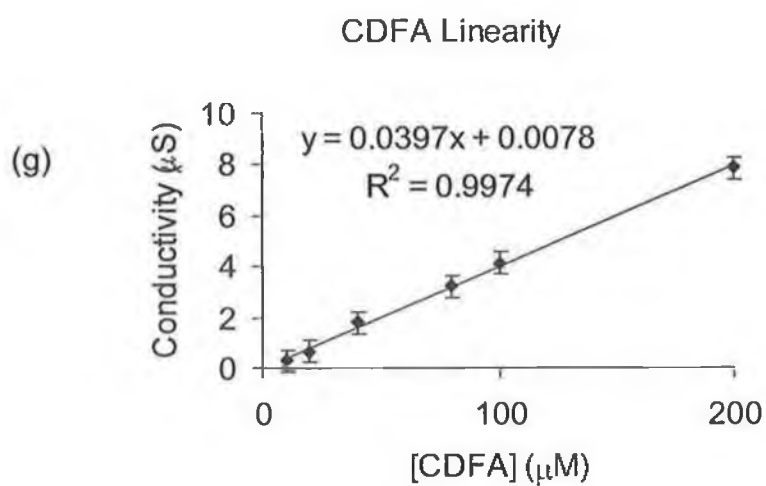


Fig. A.1-1 (a)-(g) Linearity Curves for seven HAs with optimised AS11-HC column method in Chapter 1.0, Section 2.3.7.1.

Appendix A.2

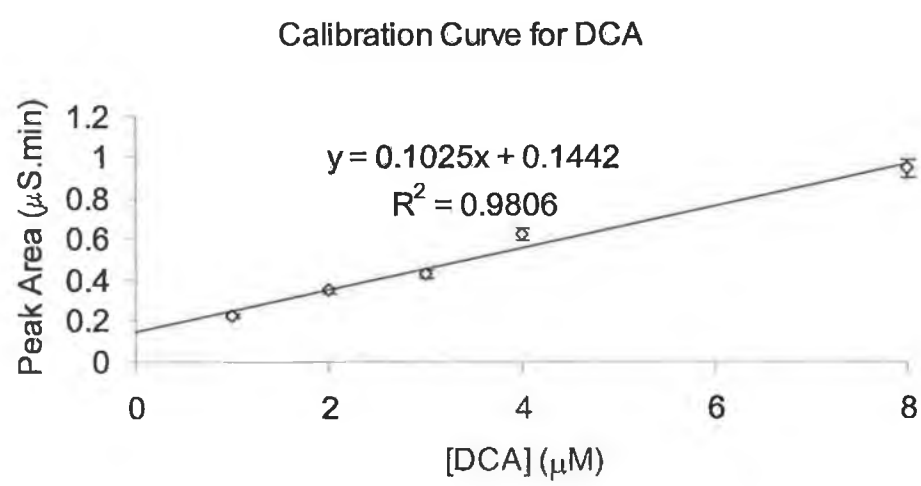
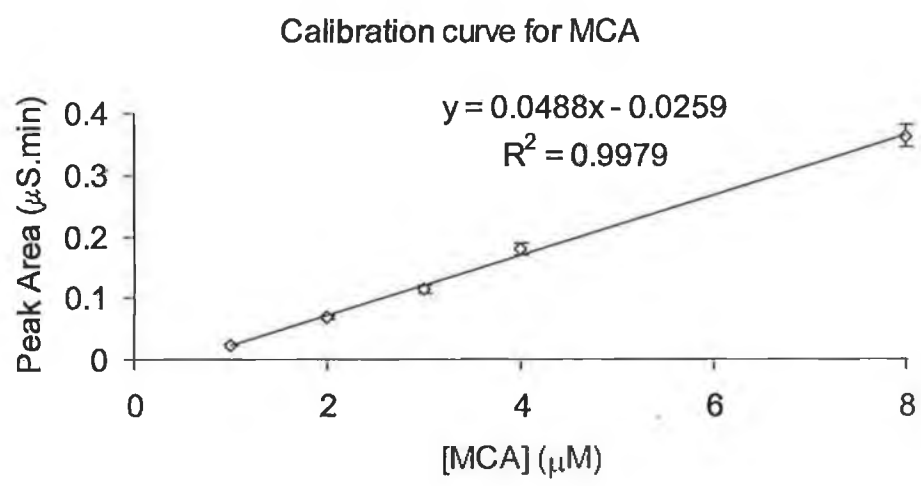
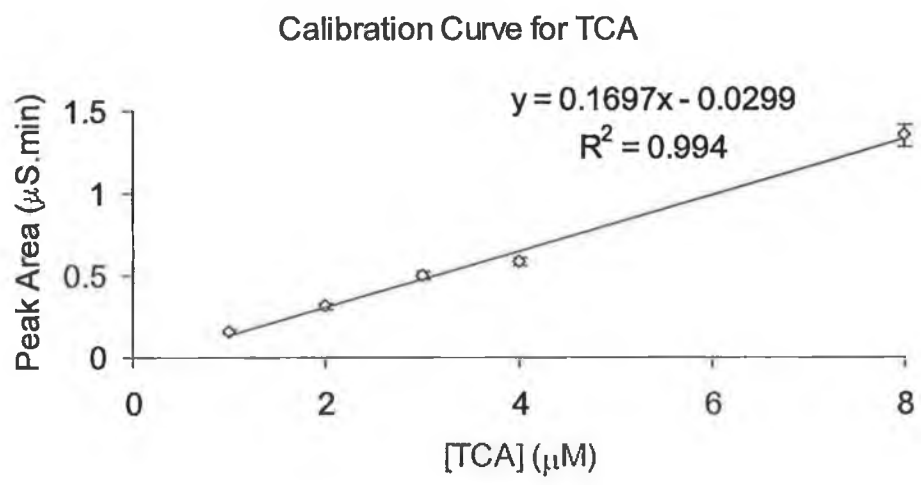
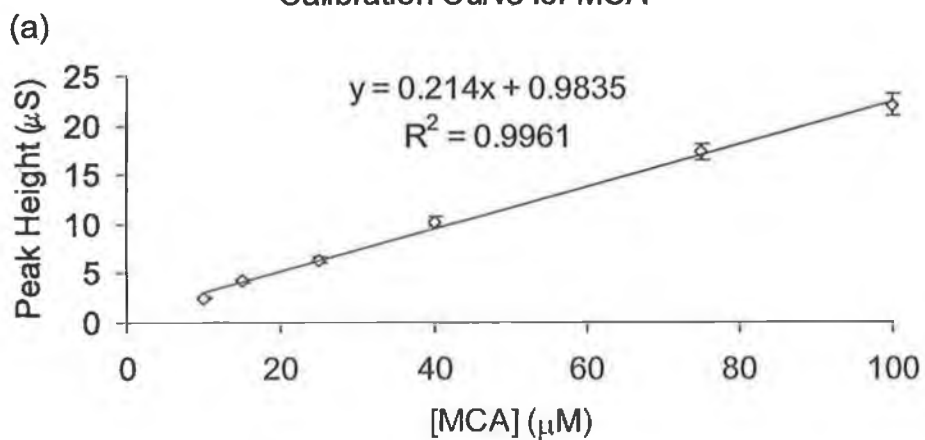


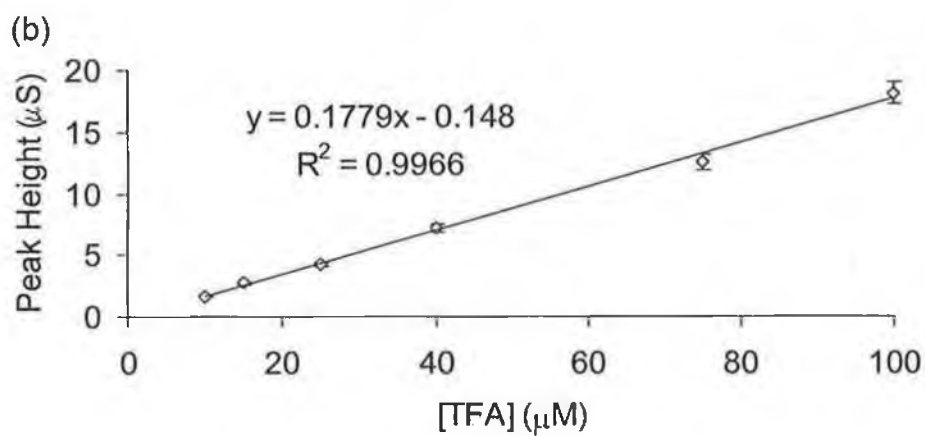
Fig. A.2-1 Calibration curves for quantification of identified HAs in drinking water sources in Table 3.3 in Chapter 3.0, Section 3.3.6.

Appendix A.3

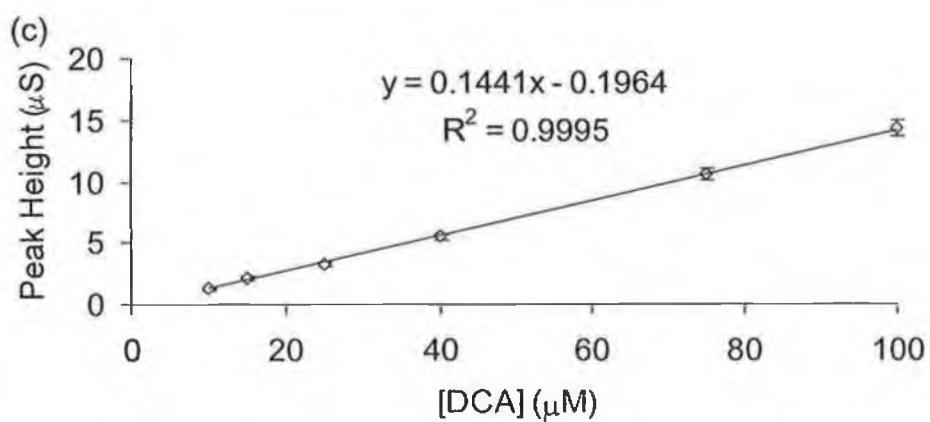
Calibration Curve for MCA



Calibration Curve for TFA



Calibration Curve for DCA



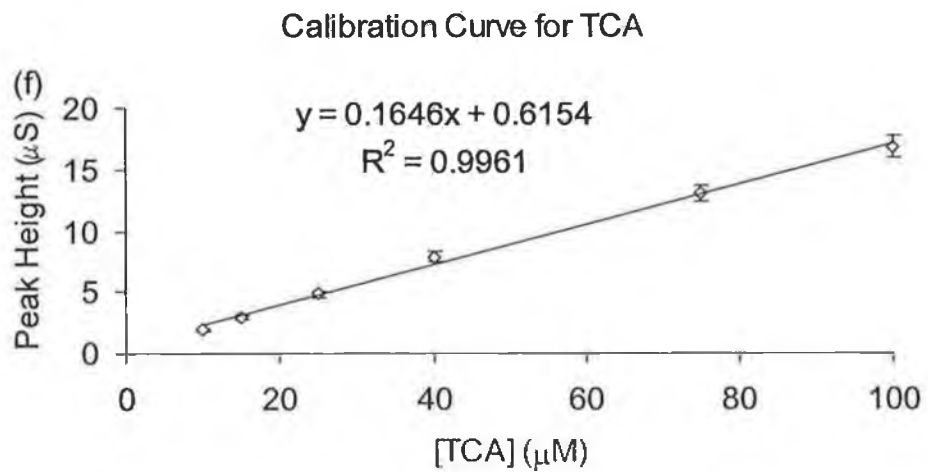
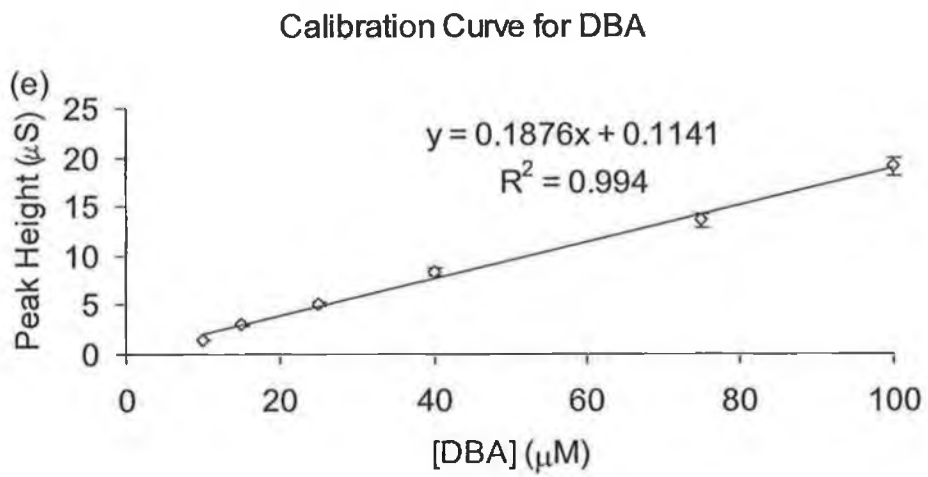
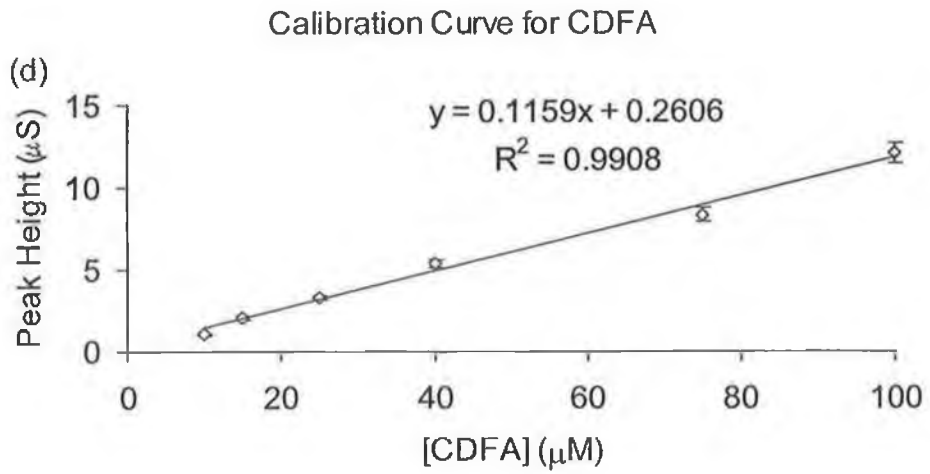


Fig. A.3-1 (a-f) Calibration curves for the determination of HAs observed in 5 drinking water samples in Chapter 4.0, Section 4.3.4.

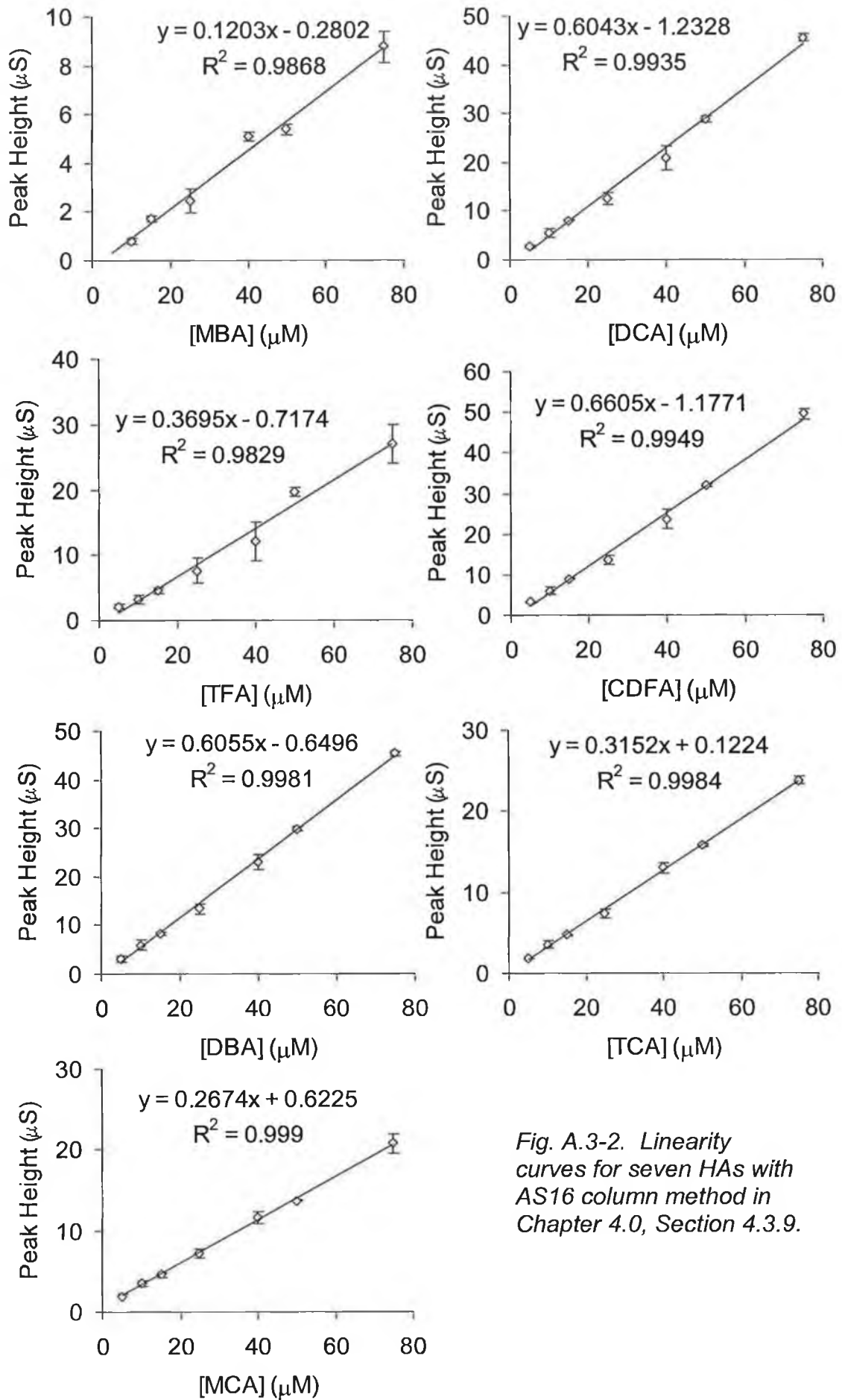


Fig. A.3-2. Linearity curves for seven HAs with AS16 column method in Chapter 4.0, Section 4.3.9.

Appendix A.4

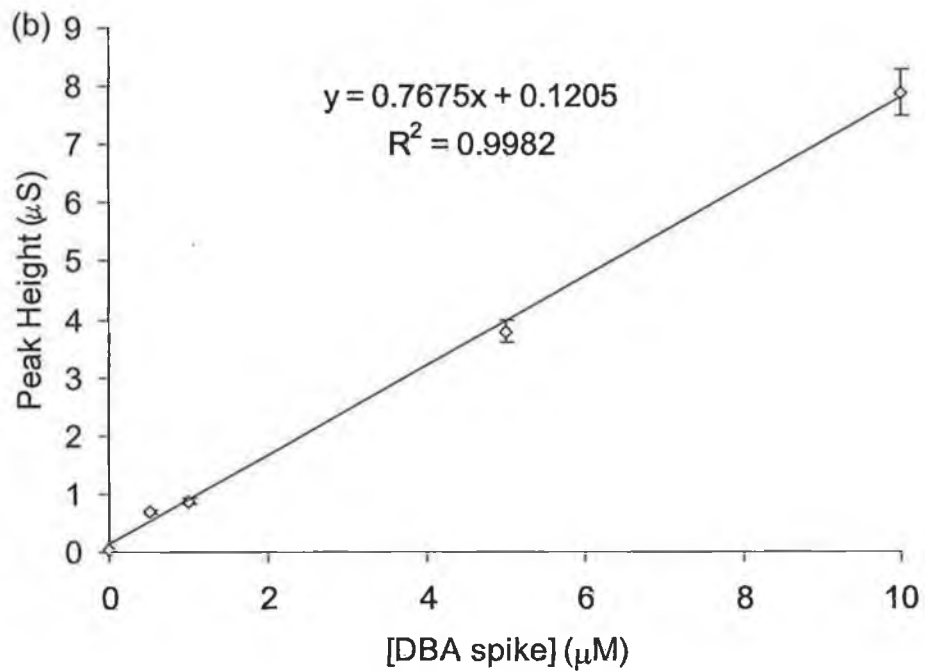
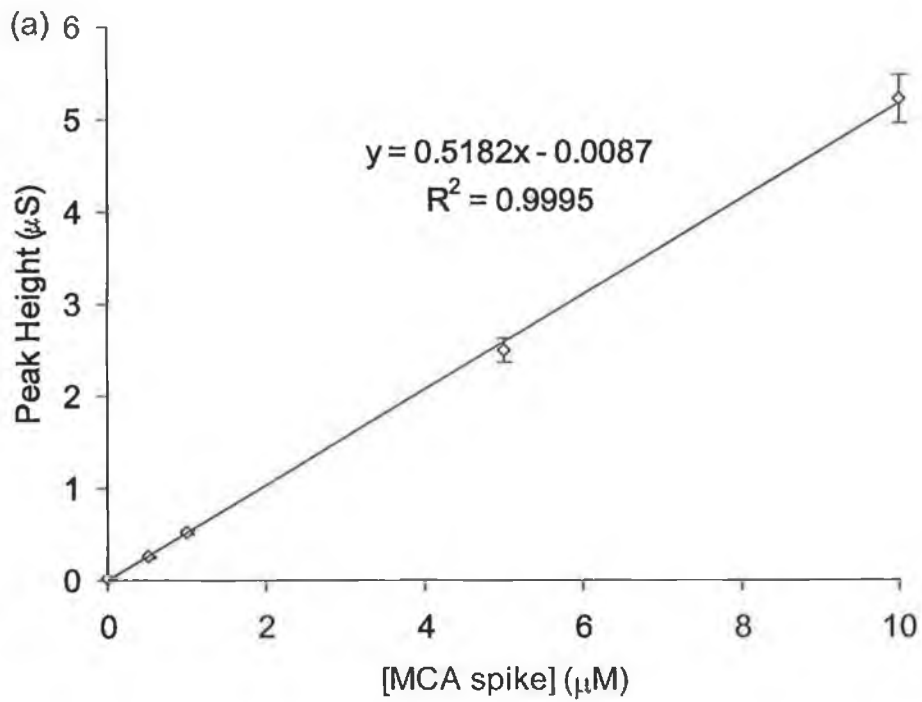


Fig. A.4-1 (a-b) Standard addition curves for direct determination of HAs in DCU drinking water sample in Chapter 5.0, Section 5.3.4.1.

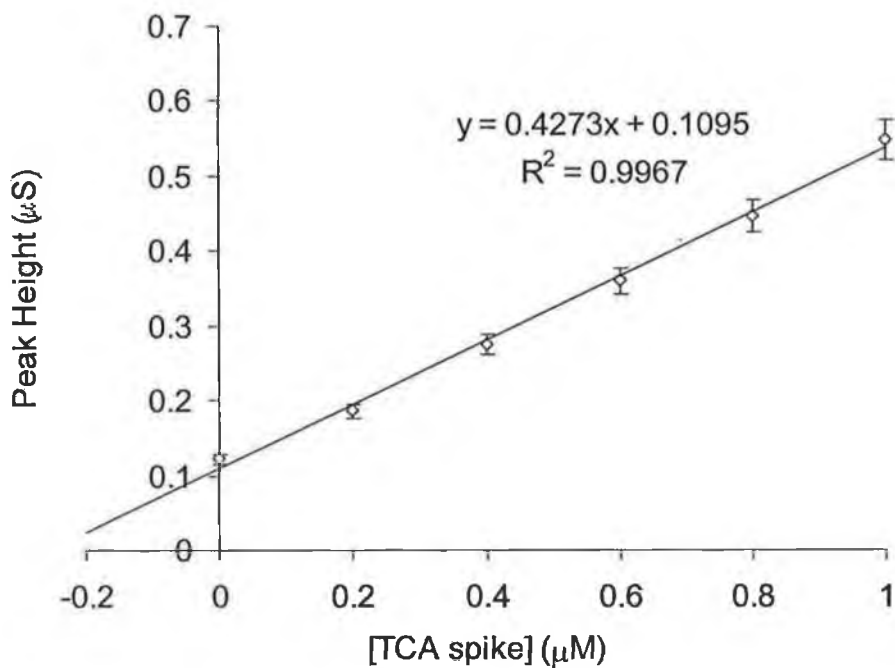
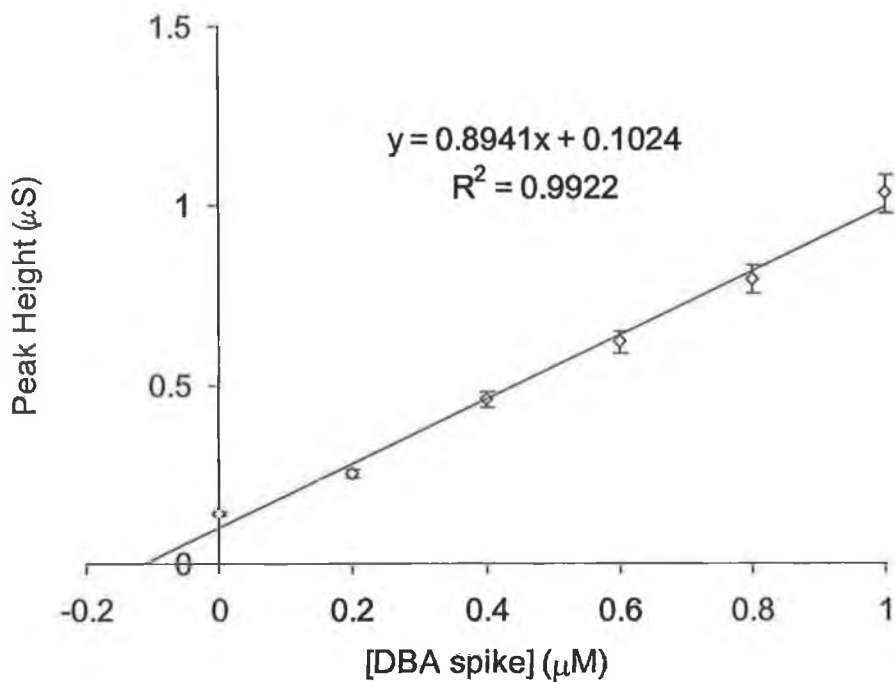


Fig. A.4-2 Standard addition for direct determination of MCA and TCA in drinking water sample from New Ross, Co. Wexford (Chapter 5.0, Section 5.3.4.1).

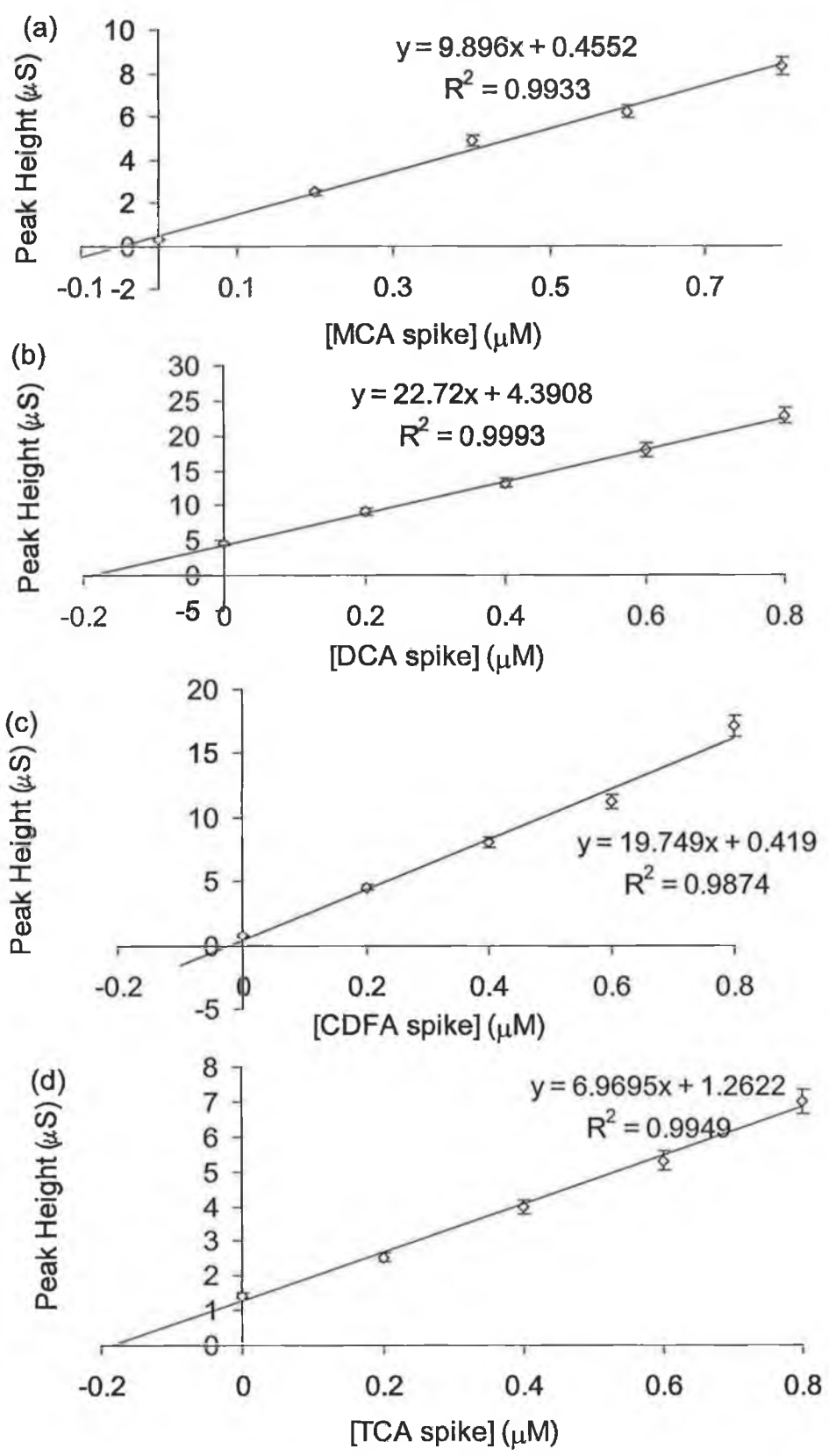


Fig. A.4-3 Standard addition curves for 25-fold preconcentrated New Ross drinking water sample for (a) MCA, (b) DCA, (c) CDFA and (d) TCA as in Chapter 5.0, Section 5.3.4.2.

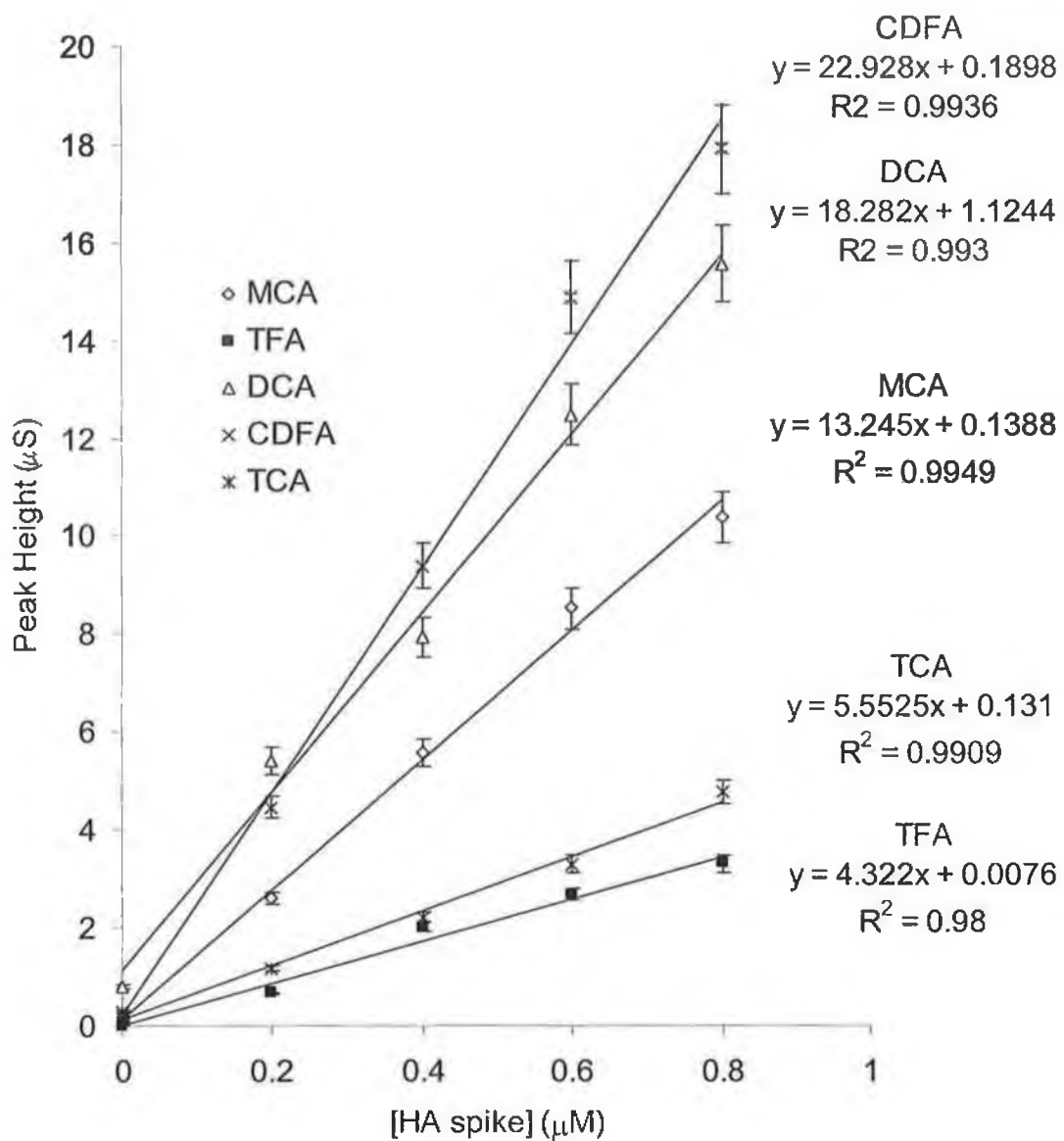


Fig. A.4-4 Standard addition curves for 25-fold preconcentrated sample of drinking water from Drogheda, Co. Louth. (Chapter 5.0, Section 5.3.4.2).

Appendix A.5

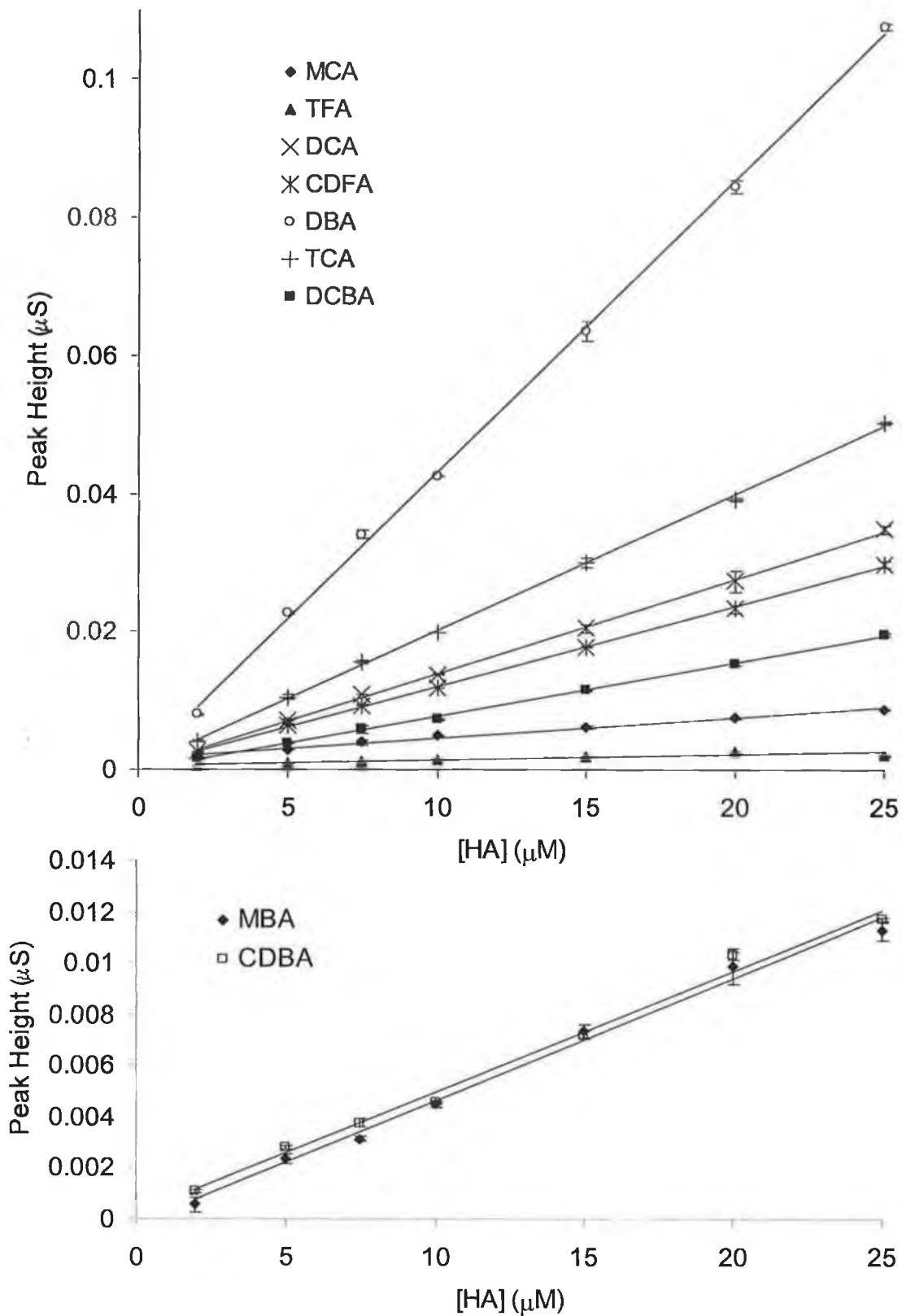


Fig. A.5-1 UV detector linearity for triplicate standards of all HAs over the range 2-25 μM . Correlation coefficients and trendline equations in Table 6.1.

Appendix A.6

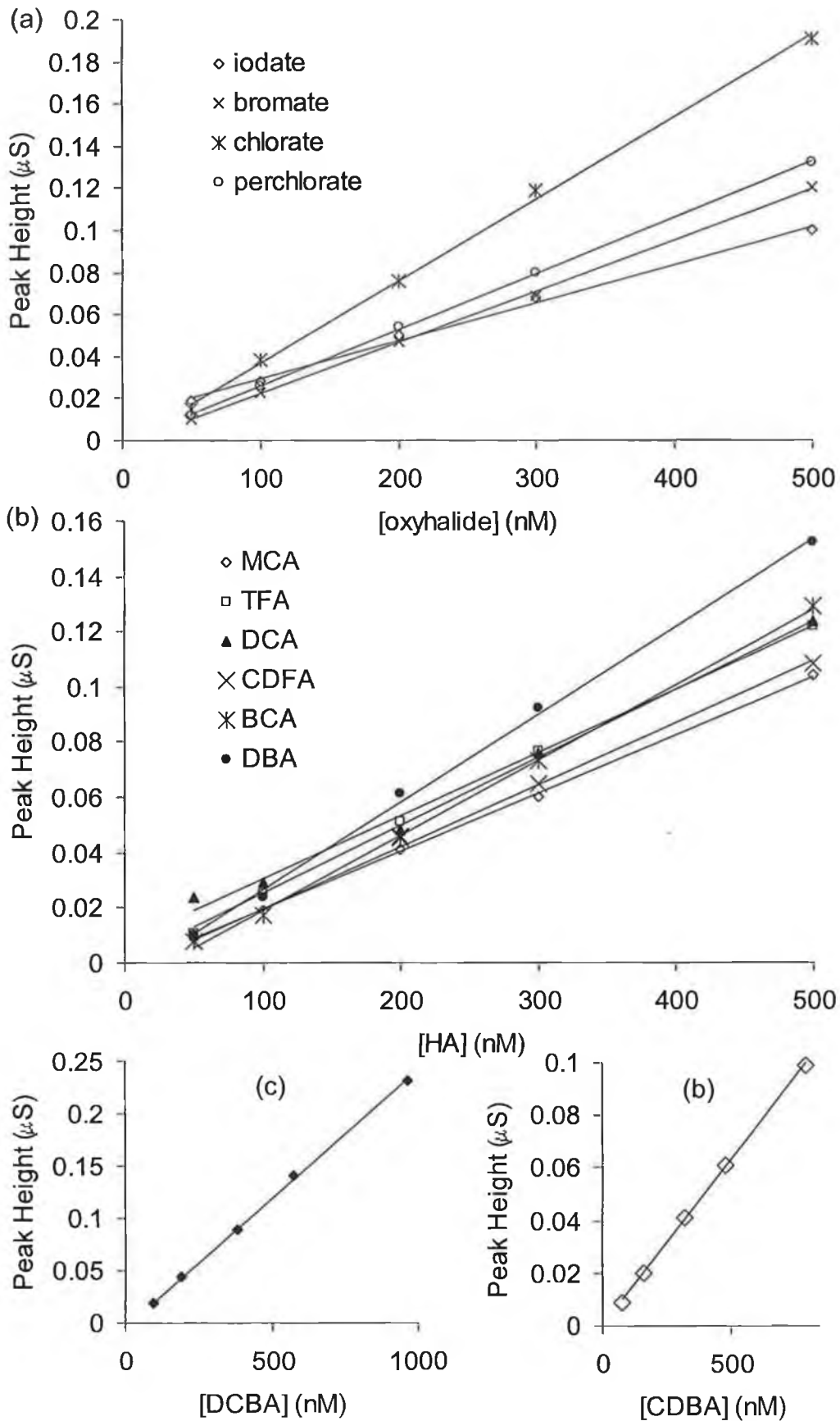
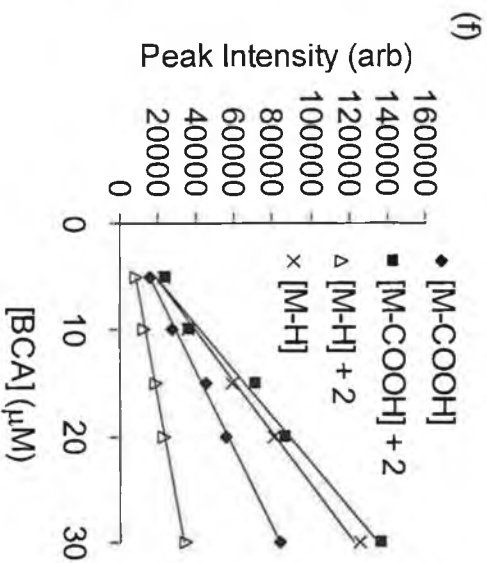
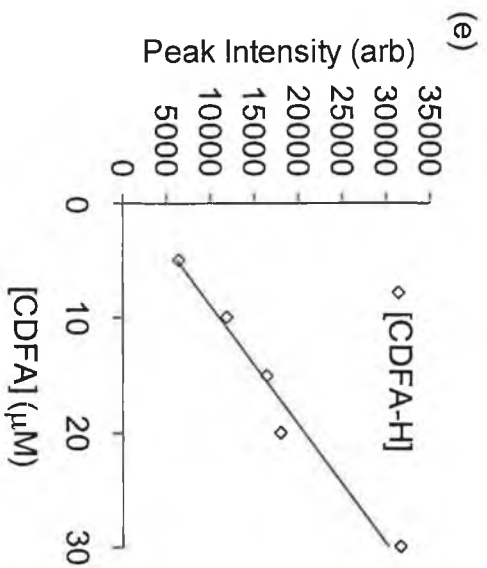
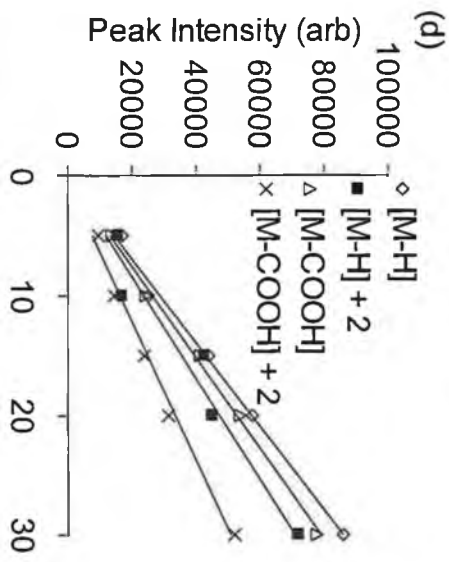
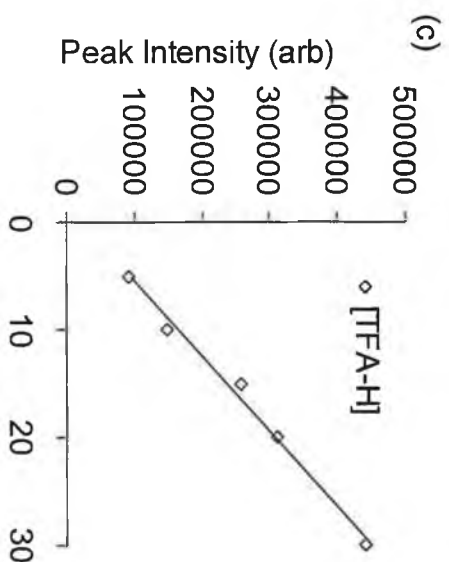
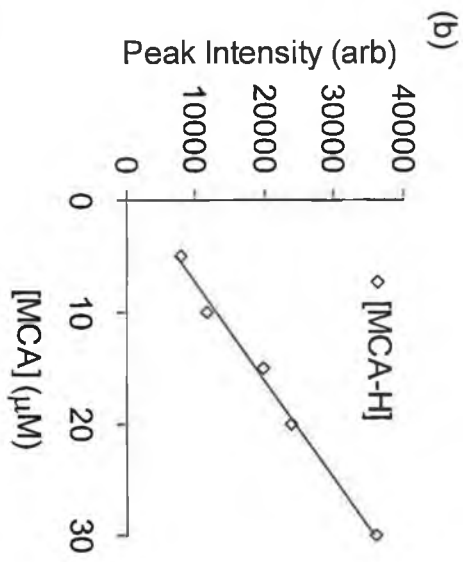
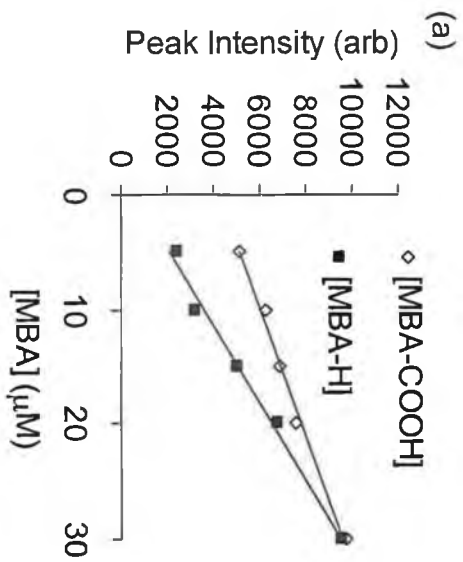


Fig. A.6-1 Linearity for all HAs and oxyhalides using optimised temperature program in Chapter 7.0, Section 7.3.8.2. For all correlation coefficients and trendline equations, refer to Table 7.3.

[TFA] (μM)

[DCA] (μM)





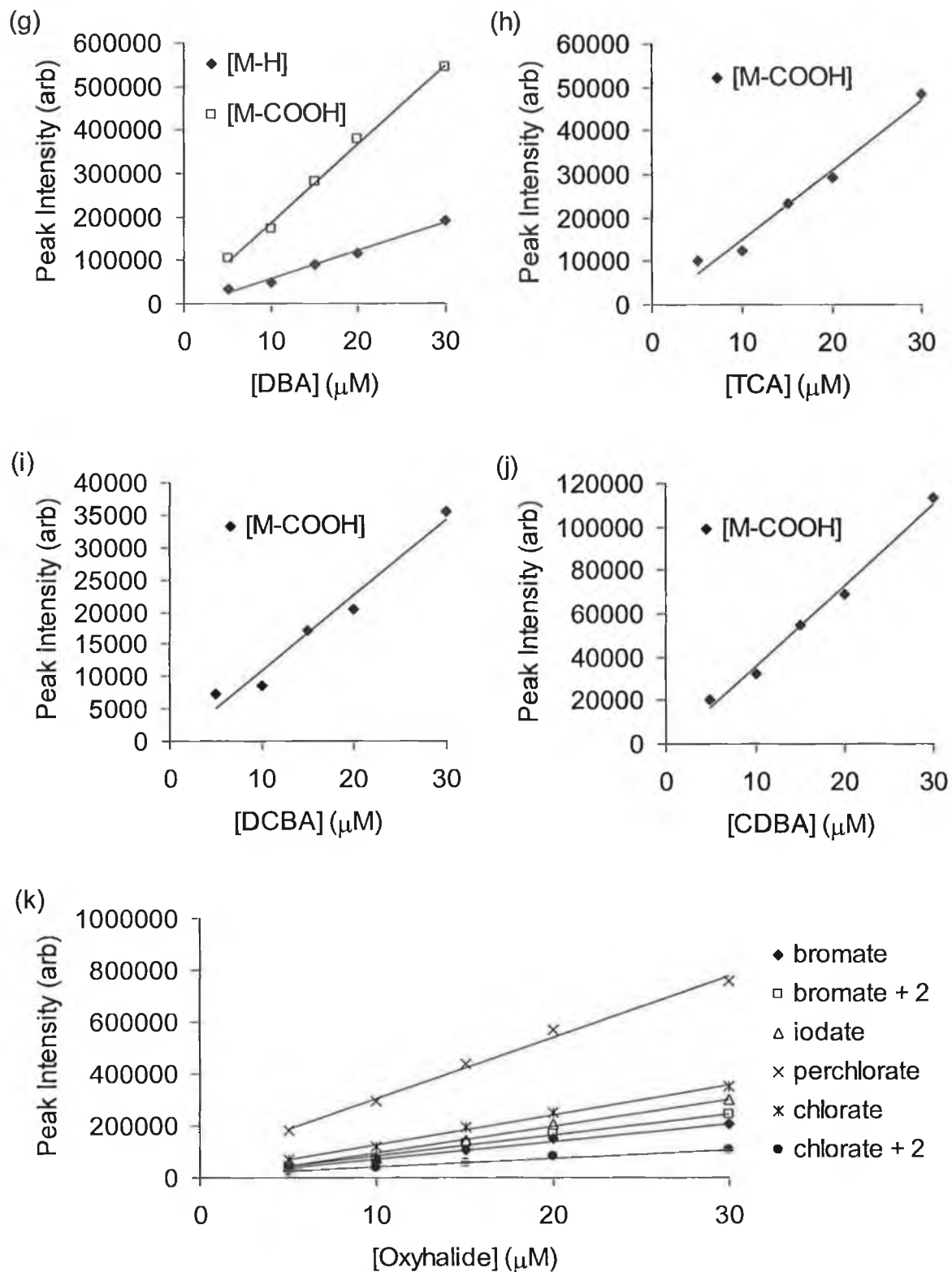


Fig. A.6-2 (a-k) ESI-MS detector linearity for all analytes using optimised temperature gradient in Chapter 7.0, Section 7.3.8.2. Values of m/z which include a chlorine or bromine isotope are denoted, "+2". All correlation coefficients and trendline equations can be found in Table 7.4.

Appendix A.7 Poster Presentations



Use of Temperature Programming to Improve Resolution of Haloacetic Acids and Oxyhalides in Drinking Water by Suppressed Ion Chromatography

Leon Barron, Pavel Nesterenko and Brett Paull

National Centre for Sensor Research, School of Chemical Sciences, Dublin City University, Glasnevin, Dublin 9, Ireland.



Fax: 00353-(1)-7005503; Tel: 353-(1)-7005060; E-mail:

Summary - The poster presents the first practical example of using temperature gradients to improve the resolution of complex anion mixtures in combination with hydroxide gradient ion chromatography. Temperature programming was used to improve selectivity in the gradient suppressed ion chromatographic separation of inorganic anions, haloacetic acids and oxyhalides in drinking water samples. The programme exploited varying responses of these anions to changes in temperature. Retention factors (k') for 17 anionic species were calculated from van't Hoff plots. For haloacetic acids, both the degree of substitution and log P values correlated well with the magnitude of the temperature effect, with monochloro- and monobromoacetic acids showing the largest effect ($\Delta H = -10.4$ to -10.7 kJ/mol), dichloro- and dibromoacetic acids showing a reduced effect ($\Delta H = -6.8$ to -8.4 kJ/mol) and trichloro-, tribromo- and chlorodibromoacetic acids showing the least effect ($\Delta H = -4.7$ to -2.4 kJ/mol). The effect of temperature on oxyhalides ranged from $\Delta H = 8.4$ kJ/mol for perchlorate to $\Delta H = -9.1$ kJ/mol for iodate. The effectiveness of a simple temperature programme was investigated to improve the resolution of closely retained species at the start, middle and end of the separation obtained using a previously optimised hydroxide gradient, in a real drinking water sample matrix. Retention time reproducibility of the final method ranged from 0.62 to 3.18% RSD ($n = 30$) showing temperature programming to be a practically important parameter to manipulate resolution.

1 - Temperature effect

Temperature programming was used to improve selectivity in the gradient suppressed ion chromatographic separation of inorganic anions, haloacetic acids and oxyhalides in drinking water samples. The programme exploited varying responses of these anions to changes in temperature. Retention factors (k') for 17 anionic species were calculated from van't Hoff plots. For haloacetic acids, both the degree of substitution and log P values correlated well with the magnitude of the temperature effect, with monochloro- and monobromoacetic acids showing the largest effect ($\Delta H = -10.4$ to -10.7 kJ/mol), dichloro- and dibromoacetic acids showing a reduced effect ($\Delta H = -6.8$ to -8.4 kJ/mol) and trichloro-, tribromo- and chlorodibromoacetic acids showing the least effect ($\Delta H = -4.7$ to -2.4 kJ/mol). The effect of temperature on oxyhalides ranged from $\Delta H = 8.4$ kJ/mol for perchlorate to $\Delta H = -9.1$ kJ/mol for iodate. The effectiveness of a simple temperature programme was investigated to improve the resolution of closely retained species at the start, middle and end of the separation obtained using a previously optimised hydroxide gradient, in a real drinking water sample matrix. Retention time reproducibility of the final method ranged from 0.62 to 3.18% RSD ($n = 30$) showing temperature programming to be a practically important parameter to manipulate resolution.

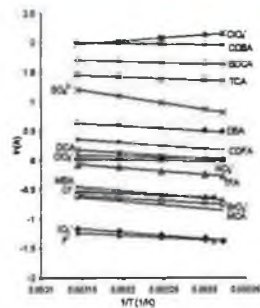


Figure 1. Van't Hoff plots for 9 haloacetic acids and 4 inorganic anions using AS16 column with ion chromatography. Eluent = 20 mM NaOH.

Table 1. Retention factors (k') for 17 anionic species at 15, 30, 45, 60, 75, 90, 105, 120, 135, 150, 165, 180, 195, 210, 225, 240, 255, 270, 285, 300, 315, 330, 345, 360, 375, 390, 405, 420, 435, 450, 465, 480, 495, 510, 525, 540, 555, 570, 585, 600, 615, 630, 645, 660, 675, 690, 705, 720, 735, 750, 765, 780, 795, 810, 825, 840, 855, 870, 885, 900, 915, 930, 945, 960, 975, 990, 1005, 1020, 1035, 1050, 1065, 1080, 1095, 1110, 1125, 1140, 1155, 1170, 1185, 1200, 1215, 1230, 1245, 1260, 1275, 1290, 1305, 1320, 1335, 1350, 1365, 1380, 1395, 1410, 1425, 1440, 1455, 1470, 1485, 1500, 1515, 1530, 1545, 1560, 1575, 1590, 1605, 1620, 1635, 1650, 1665, 1680, 1695, 1710, 1725, 1740, 1755, 1770, 1785, 1800, 1815, 1830, 1845, 1860, 1875, 1890, 1905, 1920, 1935, 1950, 1965, 1980, 1995, 2010, 2025, 2040, 2055, 2070, 2085, 2100, 2115, 2130, 2145, 2160, 2175, 2190, 2205, 2220, 2235, 2250, 2265, 2280, 2295, 2310, 2325, 2340, 2355, 2370, 2385, 2400, 2415, 2430, 2445, 2460, 2475, 2490, 2505, 2520, 2535, 2550, 2565, 2580, 2595, 2610, 2625, 2640, 2655, 2670, 2685, 2700, 2715, 2730, 2745, 2760, 2775, 2790, 2805, 2820, 2835, 2850, 2865, 2880, 2895, 2910, 2925, 2940, 2955, 2970, 2985, 3000, 3015, 3030, 3045, 3060, 3075, 3090, 3105, 3120, 3135, 3150, 3165, 3180, 3195, 3210, 3225, 3240, 3255, 3270, 3285, 3300, 3315, 3330, 3345, 3360, 3375, 3390, 3405, 3420, 3435, 3450, 3465, 3480, 3495, 3510, 3525, 3540, 3555, 3570, 3585, 3600, 3615, 3630, 3645, 3660, 3675, 3690, 3705, 3720, 3735, 3750, 3765, 3780, 3795, 3810, 3825, 3840, 3855, 3870, 3885, 3900, 3915, 3930, 3945, 3960, 3975, 3990, 4005, 4020, 4035, 4050, 4065, 4080, 4095, 4110, 4125, 4140, 4155, 4170, 4185, 4200, 4215, 4230, 4245, 4260, 4275, 4290, 4305, 4320, 4335, 4350, 4365, 4380, 4395, 4410, 4425, 4440, 4455, 4470, 4485, 4500, 4515, 4530, 4545, 4560, 4575, 4590, 4605, 4620, 4635, 4650, 4665, 4680, 4695, 4710, 4725, 4740, 4755, 4770, 4785, 4800, 4815, 4830, 4845, 4860, 4875, 4890, 4905, 4920, 4935, 4950, 4965, 4980, 4995, 5010, 5025, 5040, 5055, 5070, 5085, 5100, 5115, 5130, 5145, 5160, 5175, 5190, 5205, 5220, 5235, 5250, 5265, 5280, 5295, 5310, 5325, 5340, 5355, 5370, 5385, 5400, 5415, 5430, 5445, 5460, 5475, 5490, 5505, 5520, 5535, 5550, 5565, 5580, 5595, 5610, 5625, 5640, 5655, 5670, 5685, 5700, 5715, 5730, 5745, 5760, 5775, 5790, 5805, 5820, 5835, 5850, 5865, 5880, 5895, 5910, 5925, 5940, 5955, 5970, 5985, 6000, 6015, 6030, 6045, 6060, 6075, 6090, 6105, 6120, 6135, 6150, 6165, 6180, 6195, 6210, 6225, 6240, 6255, 6270, 6285, 6300, 6315, 6330, 6345, 6360, 6375, 6390, 6405, 6420, 6435, 6450, 6465, 6480, 6495, 6510, 6525, 6540, 6555, 6570, 6585, 6600, 6615, 6630, 6645, 6660, 6675, 6690, 6705, 6720, 6735, 6750, 6765, 6780, 6795, 6810, 6825, 6840, 6855, 6870, 6885, 6900, 6915, 6930, 6945, 6960, 6975, 6990, 7005, 7020, 7035, 7050, 7065, 7080, 7095, 7110, 7125, 7140, 7155, 7170, 7185, 7200, 7215, 7230, 7245, 7260, 7275, 7290, 7305, 7320, 7335, 7350, 7365, 7380, 7395, 7410, 7425, 7440, 7455, 7470, 7485, 7500, 7515, 7530, 7545, 7560, 7575, 7590, 7605, 7620, 7635, 7650, 7665, 7680, 7695, 7710, 7725, 7740, 7755, 7770, 7785, 7800, 7815, 7830, 7845, 7860, 7875, 7890, 7905, 7920, 7935, 7950, 7965, 7980, 7995, 8010, 8025, 8040, 8055, 8070, 8085, 8100, 8115, 8130, 8145, 8160, 8175, 8190, 8205, 8220, 8235, 8250, 8265, 8280, 8295, 8310, 8325, 8340, 8355, 8370, 8385, 8400, 8415, 8430, 8445, 8460, 8475, 8490, 8505, 8520, 8535, 8550, 8565, 8580, 8595, 8610, 8625, 8640, 8655, 8670, 8685, 8700, 8715, 8730, 8745, 8760, 8775, 8790, 8805, 8820, 8835, 8850, 8865, 8880, 8895, 8910, 8925, 8940, 8955, 8970, 8985, 9000, 9015, 9030, 9045, 9060, 9075, 9090, 9105, 9120, 9135, 9150, 9165, 9180, 9195, 9210, 9225, 9240, 9255, 9270, 9285, 9300, 9315, 9330, 9345, 9360, 9375, 9390, 9405, 9420, 9435, 9450, 9465, 9480, 9495, 9510, 9525, 9540, 9555, 9570, 9585, 9600, 9615, 9630, 9645, 9660, 9675, 9690, 9705, 9720, 9735, 9750, 9765, 9780, 9795, 9810, 9825, 9840, 9855, 9870, 9885, 9900, 9915, 9930, 9945, 9960, 9975, 9990, 10005, 10020, 10035, 10050, 10065, 10080, 10095, 10110, 10125, 10140, 10155, 10170, 10185, 10200, 10215, 10230, 10245, 10260, 10275, 10290, 10305, 10320, 10335, 10350, 10365, 10380, 10395, 10410, 10425, 10440, 10455, 10470, 10485, 10500, 10515, 10530, 10545, 10560, 10575, 10590, 10605, 10620, 10635, 10650, 10665, 10680, 10695, 10710, 10725, 10740, 10755, 10770, 10785, 10800, 10815, 10830, 10845, 10860, 10875, 10890, 10905, 10920, 10935, 10950, 10965, 10980, 10995, 11010, 11025, 11040, 11055, 11070, 11085, 11100, 11115, 11130, 11145, 11160, 11175, 11190, 11205, 11220, 11235, 11250, 11265, 11280, 11295, 11310, 11325, 11340, 11355, 11370, 11385, 11400, 11415, 11430, 11445, 11460, 11475, 11490, 11505, 11520, 11535, 11550, 11565, 11580, 11595, 11610, 11625, 11640, 11655, 11670, 11685, 11700, 11715, 11730, 11745, 11760, 11775, 11790, 11805, 11820, 11835, 11850, 11865, 11880, 11895, 11910, 11925, 11940, 11955, 11970, 11985, 12000, 12015, 12030, 12045, 12060, 12075, 12090, 12105, 12120, 12135, 12150, 12165, 12180, 12195, 12210, 12225, 12240, 12255, 12270, 12285, 12300, 12315, 12330, 12345, 12360, 12375, 12390, 12405, 12420, 12435, 12450, 12465, 12480, 12495, 12510, 12525, 12540, 12555, 12570, 12585, 12600, 12615, 12630, 12645, 12660, 12675, 12690, 12705, 12720, 12735, 12750, 12765, 12780, 12795, 12810, 12825, 12840, 12855, 12870, 12885, 12900, 12915, 12930, 12945, 12960, 12975, 12990, 13005, 13020, 13035, 13050, 13065, 13080, 13095, 13110, 13125, 13140, 13155, 13170, 13185, 13200, 13215, 13230, 13245, 13260, 13275, 13290, 13305, 13320, 13335, 13350, 13365, 13380, 13395, 13410, 13425, 13440, 13455, 13470, 13485, 13500, 13515, 13530, 13545, 13560, 13575, 13590, 13605, 13620, 13635, 13650, 13665, 13680, 13695, 13710, 13725, 13740, 13755, 13770, 13785, 13800, 13815, 13830, 13845, 13860, 13875, 13890, 13905, 13920, 13935, 13950, 13965, 13980, 13995, 14010, 14025, 14040, 14055, 14070, 14085, 14100, 14115, 14130, 14145, 14160, 14175, 14190, 14205, 14220, 14235, 14250, 14265, 14280, 14295, 14310, 14325, 14340, 14355, 14370, 14385, 14400, 14415, 14430, 14445, 14460, 14475, 14490, 14505, 14520, 14535, 14550, 14565, 14580, 14595, 14610, 14625, 14640, 14655, 14670, 14685, 14700, 14715, 14730, 14745, 14760, 14775, 14790, 14805, 14820, 14835, 14850, 14865, 14880, 14895, 14910, 14925, 14940, 14955, 14970, 14985, 15000, 15015, 15030, 15045, 15060, 15075, 15090, 15105, 15120, 15135, 15150, 15165, 15180, 15195, 15210, 15225, 15240, 15255, 15270, 15285, 15300, 15315, 15330, 15345, 15360, 15375, 15390, 15405, 15420, 15435, 15450, 15465, 15480, 15495, 15510, 15525, 15540, 15555, 15570, 15585, 15600, 15615, 15630, 15645, 15660, 15675, 15690, 15705, 15720, 15735, 15750, 15765, 15780, 15795, 15810, 15825, 15840, 15855, 15870, 15885, 15900, 15915, 15930, 15945, 15960, 15975, 15990, 16005, 16020, 16035, 16050, 16065, 16080, 16095, 16110, 16125, 16140, 16155, 16170, 16185, 16200, 16215, 16230, 16245, 16260, 16275, 16290, 16305, 16320, 16335, 16350, 16365, 16380, 16395, 16410, 16425, 16440, 16455, 16470, 16485, 16500, 16515, 16530, 16545, 16560, 16575, 16590, 16605, 16620, 16635, 16650, 16665, 16680, 16695, 16710, 16725, 16740, 16755, 16770, 16785, 16800, 16815, 16830, 16845, 16860, 16875, 16890, 16905, 16920, 16935, 16950, 16965, 16980, 16995, 17010, 17025, 17040, 17055, 17070, 17085, 17100, 17115, 17130, 17145, 17160, 17175, 17190, 17205, 17220, 17235, 17250, 17265, 17280, 17295, 17310, 17325, 17340, 17355, 17370, 17385, 17400, 17415, 17430, 17445, 17460, 17475, 17490, 17505, 17520, 17535, 17550, 17565, 17580, 17595, 17610, 17625, 17640, 17655, 17670, 17685, 17700, 17715, 17730, 17745, 17760, 17775, 17790, 17805, 17820, 17835, 17850, 17865, 17880, 17895, 17910, 17925, 17940, 17955, 17970, 17985, 18000, 18015, 18030, 18045, 18060, 18075, 18090, 18105, 18120, 18135, 18150, 18165, 18180, 18195, 18210, 18225, 18240, 18255, 18270, 18285, 18300, 18315, 18330, 18345, 18360, 18375, 18390, 18405, 18420, 18435, 18450, 18465, 18480, 18495, 18510, 18525, 18540, 18555, 18570, 18585, 18600, 18615, 18630, 18645, 18660, 18675, 18690, 18705, 18720, 18735, 18750, 18765, 18780, 18795, 18810, 18825, 18840, 18855, 18870, 18885, 18900, 18915, 18930, 18945, 18960, 18975, 18990, 19005, 19020, 19035, 19050, 19065, 19080, 19095, 19110, 19125, 19140, 19155, 19170, 19185, 19200, 19215, 19230, 19245, 19260, 19275, 19290, 19305, 19320, 19335, 19350, 19365, 19380, 19395, 19410, 19425, 19440, 19455, 19470, 19485, 19500, 19515, 19530, 19545, 19560, 19575, 19590, 19605, 19620, 19635, 19650, 19665, 19680, 19695, 19710, 19725, 19740, 19755, 19770, 19785, 19800, 19815, 19830, 19845, 19860, 19875, 19890, 19905, 19920, 19935, 19950, 19965, 19980, 19995, 20010, 20025, 20040, 20055, 20070, 20085, 20100, 20115, 20130, 20145, 20160, 20175, 20190, 20205, 20220, 20235, 20250, 20265, 20280, 20295, 20310, 20325, 20340, 20355, 20370, 20385, 20400, 20415, 20430, 20445, 20460, 20475, 20490, 20505, 20520, 20535, 20550, 20565, 20580, 20595, 20610, 20625, 20640, 20655, 20670, 20685, 20700, 20715, 20730, 20745, 20760, 20775, 20790, 20805, 20820, 20835, 20850, 20865, 20880, 20895, 20910, 20925, 20940, 20955, 20970, 20985, 21000, 21015, 21030, 21045, 21060, 21075, 21090, 21105, 21120, 21135, 21150, 21165, 21180, 21195, 21210, 21225, 21240, 21255, 21270, 21285, 21300, 21315, 21330, 21345, 21360, 21375, 21390, 21405, 21420, 21435, 21450, 21465, 21480, 21495, 21510, 21525, 21540, 21555, 21570, 21585, 21600, 21615, 21630, 21645, 21660, 21675, 21690, 21705, 21720, 21735, 21750, 21765, 21780, 21795, 21810, 21825, 21840, 21855, 21870, 21885, 21900, 21915, 21930, 21945, 21960, 21975, 21990, 22005, 22020, 22035, 22050, 22065, 22080, 22095, 22110, 22125, 22140, 22155, 22170, 22185, 22200, 22215, 22230, 22245, 22260, 22275, 22290, 22305, 22320, 22335, 22350, 22365, 22380, 22395, 22410, 22425, 22440, 22455, 22470, 22485, 22500, 22515, 22530, 22545, 22560, 22575, 22590, 22605, 22620, 22635, 22650, 22665, 22680, 22695, 22710, 22725, 22740, 22755, 22770, 22785, 22800, 22815, 22830, 22845, 22860, 22875, 22890, 22905, 22920, 22935, 22950, 22965, 22980, 22995, 23010, 23025, 23040, 23055, 23070, 23085, 23100, 23115, 23130, 23145, 23160, 23175, 23190, 23205, 23220, 23235, 23250, 23265, 23280, 23295, 23310, 23325, 23340, 23355, 23370, 23385, 23400, 23415, 23430, 23445, 23460, 23475, 23490, 23505, 23520, 23535, 23550, 23565, 23580, 23595, 23610, 23625, 23640, 23655, 23670, 23685, 23700, 23715, 23730, 23745, 23760, 23775, 23790, 23805, 23820, 23835, 23850, 23865, 23880, 23895, 23910, 23925, 23940, 23955, 23970, 23985, 24000, 24015, 24030, 24045, 24060, 24075, 24090, 24105, 24120, 24135, 24150, 24165, 24180, 24195, 24210, 24225, 24240, 24255, 24270, 24285, 24300, 24315, 24330, 24345, 24360,



Reagentless IC of Haloacetic Acids in Drinking Water and Preconcentration with SPE



Leon Barron and Brett Paull
National Centre for Sensor Research,
Dublin City University, Ireland
Email



Recently, there has been increased concern that chlorine, used as a biocide in water treatment, can lead to the formation of halogenated organic compounds upon reaction with natural organic matter. These so-called disinfectant by-products (DBPs) include the group of compounds collectively known as haloacetic acids (HAAs). The presence of HAAs in drinking water is of major concern due to their potential carcinogenic and mutagenic effects. A suppressed ion chromatographic method was developed for the analysis of (MBAA) monobromo-, (DBAA) dibromo-, (MCAA) monochloro-, (DCAA) dichloro-, (TCAA) trichloro-, (CDFAA) chlorodifluoro- and (TFAA) trifluoroacetic acids in drinking water using a Dionex EG40 eluent generator equipped with a continuously regenerating anion trap column (Dionex, Sunnyvale, CA, USA). A Dionex 250 x 2 mm AS11HC anion exchange column was employed using a gradient of 10–100 mM potassium hydroxide as eluent combined with suppressed conductivity detection. For ultra-trace determinations of HAAs, preconcentration was necessary and was investigated using Merck Lichrolut EN SPE Cartridges (Merck, Darmstadt, Germany). This methodology was then applied to drinking water samples.

1. Haloacetic Acid Formation

The presence of disinfectant by-product (DBPs) has recently been regulated by the USEPA (Method 502 Series) with MCLs of 60 µg/L in total for monochloro-, dichloro-, trichloro-, monobromo- and dibromoacetic acids (HBAA). Only 40% of DBPs have been classified to date. Increased formation of HAAs is primarily related to high dosage chlorination and elevated levels of Natural Organic Matter (NOM).

2. Reagentless IC of Haloacetic Acids

The optimised separation conditions involved eluent supplied by a Dionex EG40 eluent generator with a gradient of KOH from 10–100 mM (Fig. 1). Suppression was carried out by a Dionex ASRS Ultra suppressor at a current of 50 mA. Separators were carried out on the microbore Dionex AS11HC anion exchange column at a flow rate of 0.30 mL/min and an elevated temperature of 45°C. Table 1 shows the analytical performance characteristics for this method using an injection volume of 100 µL.

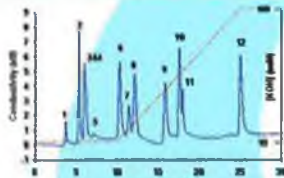


Fig. 1 Separation of 7 HAAs. Elution order: 1 = Fluoride, 2 = MCAA (15 µM), 3 = Chloride/MBAA (15 µM), 4 = Nitrate, 5 = TFAA (15 µM), 6 = Nitrate, 7 = DCAA (15 µM), 8 = CDFAA (15 µM), 9 = CDFAA (15 µM), 10 = DBAA (15 µM), 11 = Sulphate, 12 = TCAA (15 µM).

Table 1 Analytical performance data for reagentless IC of seven HAAs for linearity and repeatability of retention times

HAA	Linearity (R ²)	Repeatability (RSD)
MCAA	0.9961	0.48
TFAA	0.9966	0.97
DCAA	0.9995	0.86
CFAA	0.9908	0.43
DBAA	0.994	0.23
TCAA	0.9961	0.18

3. Boosting Detection Limits with Reagentless IC

The EG40 eluent generator (KOH) was equipped with a Continuously Regenerating Anion Trap Column to reduce background noise and to remove carbonates from the hydroxide eluent. Fig. 1 and Table 2 show the improvements in LODs for all seven HAAs as well as background noise reduction.

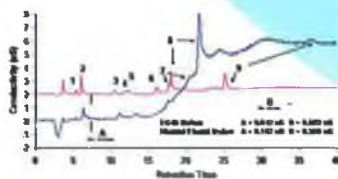


Fig. 2 Overlay of reagentless ICs separation of 7 HAAs with separation using manually prepared eluents. Elution order: 1 = MCAA (0.5 µM), 2 = chloride, 3 = TFPA (0.75 µM), 4 = Nitrate, 5 = DCAA (0.75 µM), 6 = CDFAA (1.0 µM), 7 = DBAA (1.0 µM), 8 = Sulphate, 9 = TCAA (2.5 µM). Both separators employed the chromatographic conditions listed in Section 2.

Table 2 Comparison of LODs using manually prepared eluents and generated eluents with EG40 using 100 µL injection volume

HAA	Absolute LOD using Manually Prepared Eluents (µg/L)	Absolute LOD using EG40 Generated Eluent (µg/L)
MCAA	1	1
MBAA	5	not available
TFAA	6	6
DCAA	9	7
CFAA	19	13
DBAA	32	7
TCAA	40	14

4. Preconcentration of HAAs by Solid Phase Extraction

In order to detect HAAs at a level equivalent in drinking water, it was necessary to employ a preconcentration step. Preliminary studies have been reported by Martínez *et al.* and Sarzani *et al.* [1,2]. The method proposed by these workers was further investigated here using a Merck Lichrolut EN SPE cartridge. Preconcentration factors of 1, 2 and 3 mL/min were investigated and results show that 2 mL/min was optimum for a 50 mL spiked sample. Seven 0.5 mL fractions of eluent were collected and treated onto the IC and the % recovery calculated to optimise the minimum quantity of NaOH required to preconcentrate samples to a maximum. It was found that 2 mL of 10 mM NaOH removed all 7 HAAs sufficiently.

Table 3 % Recoveries for 7 HAAs using the Merck Lichrolut EN cartridge and repeatability after six preconcentrations on separate cartridges

HAA	% Recovery
MCAA	64.52 ± 3.22
MBAA	82.81 ± 8.87
TFAA	16.87 ± 1.98
DCAA	84.83 ± 4.15
CFAA	86.53 ± 6.87
DBAA	Not available
TCAA	58.32 ± 4.98

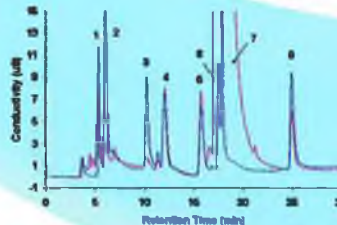


Fig. 3 Blue Trace Standard of 25 µM HAAs (Expected 100% preconcentration). Elution order: 1 = MCAA, 2 = MBAA, 3 = TFPA, 4 = DCAA, 5 = CDFAA, 6 = DBAA, 7 = Sulphate, 8 = TCAA. Blue Trace: Preconcentration of 50 mL of 1 µM MCAA, MBAA, TFAA, DCAA, CDFAA, DBAA and TCAA to 2 mL of 10 mM NaOH.

5. Real Samples

Drinking water samples were taken from three locations within Dublin City and one satellite. HAAs observed were the mono- and dichlorinated acetic acids and are listed in Table 4 below and were quantified by use of calibration curve methodology.

Table 4 Observed concentrations of HAAs from 4 separate drinking water sources (n=6)

Source	HAA	Concentration (µg/L)
Dublin City University, North Dublin City, Ireland	MCAA	2.36 ± 0.88
	DCAA	7.77 ± 0.24
	TCAA	30.23 ± 0.88
Dunshaughlin, South Dublin City, Ireland	MCAA	6.14 ± 0.81
	DCAA	45.15 ± 1.84
Finghridge, South Dublin City, Ireland	DCAA	48.81 ± 1.78
	DCAA	18.54 ± 0.85

Standard Addition

A sample of preconcentrated drinking water was run at optimum conditions. The observed HAAs (DCAA and standard addition) was carried out by preconcentrating samples spiked with 0, 0.2, 0.4, 0.8 and 1.0 µM of DCAA. Fig. 4 shows the obtained standard addition curve.

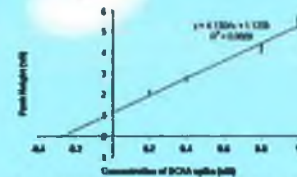


Fig. 4 Standard addition curve for preconcentration of drinking water containing DCAA. Quantification of the HAAs yielded 4 µg/L DCAA.

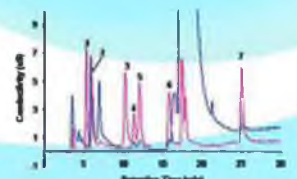


Fig. 5 Blue Trace Preconcentration of drinking water showing levels of DCAA (80 µg/L), CDFAA (20 µg/L), TCAA (24 µg/L). Spiked trace: 15 µM standard of HAAs: 1 = MCAA, 2 = Chloride, 3 = TFPA, 4 = Nitrate, 5 = DCAA, 6 = CDFAA, 7 = TCAA.

6. Conclusion

Reagentless Ion Chromatography with preconcentration offers a simple and sensitive methodology for the determination and quantification of HAAs in tap waters. Merck Lichrolut EN SPE cartridges display adequate preconcentration capabilities for real samples and, in future works, in the coupling of the suppressed IC method to a mass spectrometer to improve detection selectivity.

References

- [1] D. Martínez, J. Fari, F. Borral, M. Celis, J. Ruano, A. Colom. *Journal of Chromatography A*, 1998, 809, 229-236.
- [2] C. Sarzani, M. C. Brucacci, E. Mantas, *Journal of Chromatography A*, 1999, 860, 197-211.



Direct detection of trace haloacetic acids in drinking water using micro-bore ion chromatography

Leon Barron and Brett Paull
National Centre for Sensor Research, School of Chemical Sciences,
Dublin City University, Dublin 9, Ireland.
Email: Brett.Paull@dcu.ie



A highly sensitive gradient micro-bore ion chromatographic method was developed with electrolytically generated hydroxide eluents for the simultaneous determination of low ppb levels of monochloro- (MCAA), monobromo- (MBAA), trifluoro- (TFAA), dichloro- (DCAA), chlorodifluoro- (CDFAA), dibromo- (DBAA), trichloro- (TCAA), bromodichloro- (BDCAA) and chlorodibromooacetic acids (CDBAA) in chlorinated drinking waters. The possibility of using a Dionex Atlas suppressor (Dionex Corp., Sunnyvale, CA, USA) with hydroxide eluents was investigated in order to further reduce baseline noise levels and permit direct conductivity detection of trace haloacetic acids (HAAs) in drinking water samples. This Atlas suppressor displayed a significant reduction in noise levels compared to alternative suppressors, reducing noise by a factor of 15 in some cases, allowing trace HAAs to be seen with direct 100 µL injection of treated water with prior chloride and sulphate removal. Where necessary, solid phase extraction was employed to preconcentrate samples and lowered the overall detection limit to between 0.08 – 21.5 µg/L of HAAs. Standard addition curves for three drinking water samples were carried out for both direct injection and preconcentration methods. R² values for both standard addition methods were > 0.90. HAAs content for the three drinking water samples from Dublin City University, New Ross, Co. Wexford and Drogheda, Co. Louth were 46.5 µg/L, 58.3 µg/L and 12.6 µg/L respectively.

1. Instrumentation

- Dionex DK800 IC
- Analytical column: Dionex IonPac AS16 (20 x 2 mm)
- Flow Rate: 0.30 mL/min
- Suppressor: Dionex Atlas at 19 mA
- Eluent Generator Gradient:
 - >2.6 mM KOH for 10 minutes
 - >2.6 mM KOH for 6 minutes
 - >20 mM KOH for 20 minutes
- Injection Volume: 100 µL
- Oven Temp: 40°C
- Software: Dionex Peak Net

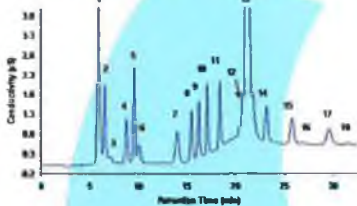


Fig. 1. 2 µM standard of 2 HAAs. Elution Order: 1 = fluoride, 2 = formate, 3 = chloride, 4 = MCAA, 5 = chlorite, 6 = MBAA, 7 = TFAA, 8 = nitrate, 9 = DCAA, 10 = CDFAA, 11 = DBAA, 12 = carbonate, 13 = sulphate, 14 = TCAA, 15 = BDCAA, 16 = phosphite, 17 = CDBAA, 18 = phosphate.

2. Improved detector sensitivity with monolithic ion exchange suppressor [1]

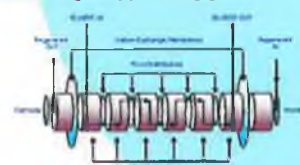


Fig. 2. Schematic of the Dionex Atlas suppressor.

The Dionex Atlas suppressor (Fig. 2) is conventionally used for low conductivity eluents such as carbonate/bicarbonate but will suppress hydroxide up to 25 mM at a low of 1.0 mL/min. When compared to an Ultra suppressor, which is usually more efficient at hydroxide suppression, detector noise with the Atlas proved 15-21 times better in some cases (See Table 1). Furthermore, the Atlas pumps higher back pressures and allows coupling of the IC to electrolytic generation systems.

Table 1. Analytical Performance Characteristics for Direct Injection of HAAs and LODs with Solid Phase Extraction Method [1]

HAAs	MBAA	TFAA	DCAA	CDFAA	DBAA	TCAA	BDCAA	CDBAA
Retention Time (min)	5.5	6.5	8.0	9.5	11.0	12.5	14.0	15.5
Peak Height (µS)	1.11	0.20	0.20	1.04	0.80	0.80	0.80	0.80
Detection Limit (µg/L)	0.05	0.1	0.1	0.1	0.1	0.1	0.1	0.1
LOD (µg/L)	0.1	0.1	0.1	0.1	0.1	0.1	0.1	0.1

1. Not listed on 2.5 µg/L standard.
2. Standard on 0.1 µg/L standard.
3. Standard on 0.1 µg/L standard.
4. Standard on 0.1 µg/L standard.
5. Standard on 0.1 µg/L standard.

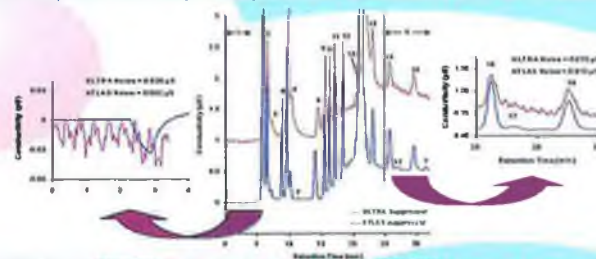


Fig. 3. Comparison of HAA separations with both Atlas and Ultra suppressors. Elution Order: 1 = fluoride, 2 = formate, 3 = chloride, 4 = MCAA, 5 = chlorite, 6 = MBAA, 7 = nitrate, 8 = TFAA, 9 = nitrate, 10 = DCAA, 11 = CDFAA, 12 = DBAA, 13 = carbonate, 14 = sulphate, 15 = TCAA, 16 = BDCAA, 17 = phosphite, 18 = CDBAA, [HAA] = 2 µM.

Fig. 4. Standard addition of HAAs in drinking water from Drogheda, Co. Louth, instead employing both preconcentration and ion stacking methods.

Real and spiked samples preconcentrated 25 fold using SPE (UChroUTEN).

Elution Order: 1 = fluoride, 2 = formate, 3 = MCAA, 4 = chloride, 5 = MBAA, 6 = nitrate, 7 = TFAA, 8 = nitrate, 9 = DCAA, 10 = CDFAA, 11 = DBAA, 12 = sulphate, 13 = phosphate, 14 = TCAA, 15 = BDCAA, 16 = phosphite (In Std), 17 = CDBAA.

Concentration range = 0 – 0.8 µM HAA.

Standard addition curve correlation coefficients for all HAAs observed 0.98.

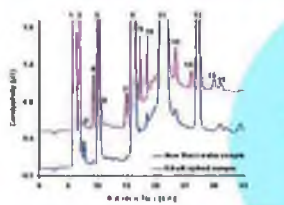


Fig. 4. Sample of drinking water supply from New Ross, Co. Wexford, Ireland passed through chloride and sulphate removal cartridges only and run on IC with overlay of 0.8 µM HAA spiked water sample. Elution Order: 1 = fluoride, 2 = formate, 3 = chloride, 4 = MCAA, 5 = chlorite, 6 = MBAA, 7 = TFAA, 8 = nitrate, 9 = CDFAA, 10 = DBAA, 11 = sulphate, 12 = TCAA, 13 = BDCAA, 14 = phosphite, 15 = CDBAA, 16 = phosphate.

3. Solid Phase Extraction [2]

Where preconcentration was necessary 50 mL samples were first added to less than pH 0.3 (pH of TFAA) with sulphate as a Merck Ultra Pure cartridge was used for the preconcentration procedure and were first preconditioned with 3 mL 0.1M NaOH followed by 3 mL 200 mM H₂SO₄. Samples were passed through at a low rate of 2 mL/min and following a wash of 1 mL Milli-Q water, were eluted with 2 mL 10 mM NaOH. In order to remove excess chloride and sulphate, a series of Altech MaxClean cartridges, were preconditioned with 10 mL Milli-Q water and the 2 mL extract was passed through at 1 mL/min. The first 1 mL of eluate was discarded and the rest collected in a vial for IC analysis. The % recoveries for this method are listed in table 2.

Table 2. % Recoveries for SPE Method [2]

HAAs	MBAA	TFAA	DCAA	CDFAA	DBAA	TCAA	BDCAA	CDBAA
Recovery (%)	100	100	100	100	100	100	100	100
Standard Deviation (%)	1.5	1.5	1.5	1.5	1.5	1.5	1.5	1.5

4. Quantification of HAAs in Drinking Water

Quantification of HAAs in 4 samples was carried out with and without the preconcentration procedure using standard addition (Fig. 5). When the preconcentration procedure was used, DCAA determinations were possible due to the fact the nitrate does not preconcentrate and so lead to a 'washout' effect. All samples were within the USEPA MCL of 80 µg/L for the sum total of MCAA, DCAA, TCAA, MBAA and DBAA (Table 3). However, in the case of the New Ross sample, levels of unregulated brominated haloacetic acids increased the total HAA concentration to 81 µg/L.

Table 3. Quantification of HAAs by Standard Addition [1]

HAAs	MBAA	TFAA	DCAA	CDFAA	DBAA	TCAA	BDCAA	CDBAA
New Ross	4.80	4.80	4.80	23.5	17.2	4.80	4.80	26.0
Drogheda	0.8	0.8	0.8	0.8	0.8	0.8	0.8	0.8
New Ross	0.3	0.3	0.3	0.3	0.3	0.3	0.3	0.3
Drogheda	1.5	1.5	1.5	1.5	1.5	1.5	1.5	1.5

1. Values include 10% relative standard deviation.
2. Values include 10% relative standard deviation.
3. Values include 10% relative standard deviation.

5. Conclusion

By using the Atlas suppressor with hydroxide eluent at low flow rates, significantly lower detection limits for the HAA species were obtained than with the ASRS Ultra suppressor. Limits of detection without preconcentration were between 14 and 735 µg/L for a micro-bore IC method with only 100 µL injection volume. With solid phase extraction on the water further reduced to a concentration range of 0.08 – 21.5 µg/L for the HAAs. When preconcentration was employed, a reduction in residual nitrate allowed identification and quantification of dibromooacetic acid. The developed method is indeed simple, practical and suitable for the routine analysis of treated drinking water samples.

1. Dionex Atlas Atlas suppressor is suitable for use in low flow rate systems.
2. Dionex Atlas Atlas suppressor is suitable for use in low flow rate systems.
3. Dionex Atlas Atlas suppressor is suitable for use in low flow rate systems.





Suppressed Ion Chromatography of Haloacetic Acids in Drinking Waters and Preconcentration using Solid Phase Extraction

Leon Barron and Brett Paul

National Centre for Sensor Research, School of Chemical Sciences, Dublin City University, Ireland
Email:

DCU

Recently, there has been increased concern that chlorine, used as a biocide in water treatment, can lead to the formation of halogenated organic compounds upon reaction with natural organic matter. These so-called disinfectant by-products (DBPs) include the group of compounds collectively known as haloacetic acids (HAAs). The presence of HAAs in drinking water is of major concern due to their potential carcinogenic and mutagenic effects. A suppressed ion chromatographic method was developed for the analysis of (MBAA) monobromo-, (DBAA) dibromo-, (MCAA) monochloro-, (DCAA) dichloro-, (TCAA) trichloro-, (CDFAA) chlorodifluoro- and (TFAA) trifluoroacetic acids in drinking water. A Dionex 250 x 2 mm AS11HC anion exchange column (Dionex, Sunnyvale, CA, USA) was employed using a gradient of 10–100 mM sodium hydroxide as eluent combined with suppressed conductivity detection. Studies of linearity, repeatability and limits of detection were carried out. For ultra-trace determinations of HAAs, preconcentration was necessary and was investigated using Merck LichroChel EN SPE Cartridges (Merck, Darmstadt, Germany). Percent recovery studies, capacity studies and repeatability were carried out to determine suitability of this SPE cartridge for real sample analysis.

1. Haloacetic Acid Formation

The presence of disinfectant byproduct HAAs has recently been regulated by the USEPA (Method 552 Series) with MCLs of 60 µg/L in total for monochloro-, dichloro-, trichloro-, monobromo- and dibromooacetic acids (HAAS). Prior to the discovery of HAAs, only trihalomethanes were covered by legislation. Following extensive research it was shown that there exists a definite problem with a wide range of DBPs as shown in Fig. 1 below. Increased formation of HAAs is primarily related to high dosage chlorination and elevated levels of Natural Organic Matter (NOM).

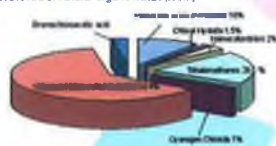


Fig 1. Classifiers of disinfectant byproducts leading to formation of water.

2. Suppressed Ion Chromatography

In the work presented here an ion chromatographic method has been developed which is suitable for the determination of HAAs in drinking water. The optimal separation conditions involved a gradient of NaOH from 10–100 mM over 10 minutes for a duration of 15 minutes. Eluent concentration was then kept constant for a further 15 minutes. Sequential runs were followed by an equilibration time of 10 minutes. Suppression was carried out by a Dionex ASRS Ultra suppressor at a current of 50 mA. Separations were carried out on the monobromo ion exchange column at a flow rate of 0.30 mL/min and an elevated temperature of 35°C. Reproducibility studies show that for successive injections that retention times vary less than 1.6% for the 7 HAAs.

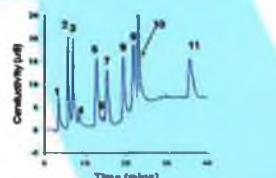


Fig 2. Separation of 7 HAAs. Elution order: 1 = Fluoride, 2 = MCAA (0.2 mM), 3 = MBAA (0.2 mM), 4 = Nitrate, 5 = TFAA (0.2 mM), 6 = Nitrite, 7 = DCAA (0.2 mM), 8 = CDFAA (0.2 mM), 9 = DBAA (0.2 mM), 10 = Sulphate, 11 = TCAA (0.2 mM).

HAAs	Aspirin LOD (ng)
MCAA	4
MBAA	6
TFAA	6
DCAA	8
CDFAA	19
DBAA	33
TCAA	40

Table 1. Absolute limits of detection for seven HAAs including HAAS. IC loop size for this experiment was 100 µL. For detector response for all HAAs was linear over a range of 10 µM to 200 µM and all R² values were greater than 0.98.

3. Preconcentration of HAAs by Solid Phase Extraction

In order to detect HAAs at a level expected in drinking water, it was necessary to employ a preconcentration step. Preliminary studies have been reported by Martínez *et al.* and Sazanov *et al.* [1–2]. The method proposed by these workers was further investigated here using a Merck LichroChel EN SPE cartridge. The cartridge was first washed with 2 mL MeOH and then conditioned with 2 mL of 200 mM H₂SO₄. Samples to be preconcentrated were adjusted to pH 0.3 with concentrated H₂SO₄. Preconcentration flow rates of 1, 2 and 3 mL/min were investigated and results show that 2 mL/min was optimum for a 50 mL spiked sample. Prior to elution using NaOH, the cartridge was washed with 1 mL MilliQ water to remove excess sulphate. Seven 0.5 mL fractions of eluent were collected and injected onto the IC and the % recovery calculated.

Fig 3 shows the minimum volume of NaOH required to desorb and elute each of the bound HAAs. The less hydrophobic the HAA, the less eluent required to desorb. It was found that 2 mL of 10 mM NaOH adequately removed all 7 HAAs and interfered less with separation than 1 mL of MeOH and other organic solvents used previously [1–2]. When the concentration of the preconcentrator eluent NaOH was increased so did % recovery, but with a significant inter-ferent peak at 2.80 minutes.

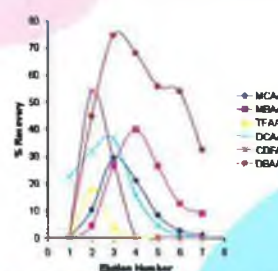


Fig 3. Successive fractions of 0.5 mL 10 mM NaOH to desorb and elute bound HAAs from the LichroChel EN cartridge.

It should be noted that TCAA was not included in the above elution study, as the more hydrophobic acids have poorer % recoveries and optimum was based on their performance, instead of that of TCAA, which has an increasing % recovery with increasing volume of sample preconcentrated as can be seen in Fig 4. For capacity studies, 10, 20, 50 and 250 mL of tap water were spiked with 5 µM MCAA, MBAA, TFAA and DCAA and 30 µM CDFAA, DBAA and TCAA and preconcentrated to 2 mL of 10 mM NaOH.

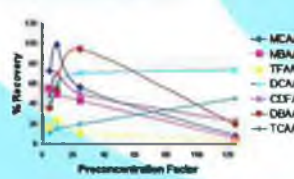


Fig 4. Capacity study for LichroChel EN SPE Cartridges.

Observations show that a higher preconcentration factor of tap water samples tend more reliably to the cartridge than the brominated and trichlorinated forms.

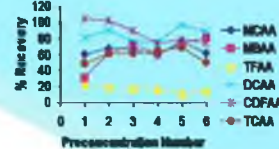


Fig 5. Durability of Merck LichroChel EN cartridge over 6 successive preconcentrations.

For repeat preconcentration experiments it was necessary to determine the durability of the PS-CyB cartridge stationary phase. Six successive repeat preconcentrations were carried out at the concentration listed in the capacity study, and injected onto the IC to determine the effect of low pH on the SPE phase. Fig 5 shows that after six repeat injections, % recoveries for all HAAs were still high and that the polymeric stationary phase is not affected significantly by low pH.

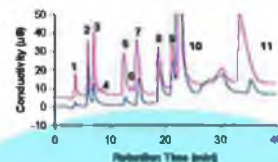


Fig 6. Lower Tapwater Standard of 0.1 mM HAAs. Elution order: 1 = Fluoride, 2 = MCAA, 3 = MBAA, 4 = Nitrite, 5 = TFAA, 6 = Nitrate, 7 = DCAA, 8 = CDFAA, 9 = DBAA, 10 = Sulphate, 11 = TCAA.

Fig 6 shows an overlay of preconcentrated 20 mL spiked drinking water sample (spiked at 0.1 mM) levels of fluoride and fluoride have been reduced as a result of preconcentration. Fig 7 shows a preconcentration of an unspiked drinking water sample and shows levels of DCAA. According to EU regulations, DCAA should not be present in drinking water.

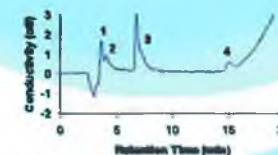


Fig 7. Preconcentration of 50 mL of drinking water sample to 2 mL of 10 mM NaOH at a preconcentration flow rate of 2 mL/min. Order of elution: 1 = Fluoride, 2 = NaOH Interferent, 3 = chloride, 4 = DCAA. Injection volume 100 µL.

4. Conclusion

Suppressed Ion Chromatography with preconcentration offers a suitable methodology for the determination and quantification of HAAs in tap waters. Merck LichroChel EN SPE cartridges display adequate preconcentration capabilities for real samples and future work lies in the coupling of the suppressed IC method to a mass spectrometer for improved detection sensitivity.

References
[1] O. Martínez, J. Fariñ, F. Brindl, M. Cid, L.J. Rues, A. Cobos, *Journal of Chromatography A*, 1998, 800, 229-235.
[2] C. Sazanov, M. C. Bruzzone, E. Minisci, *Journal of Chromatography A*, 1999, 860, 167-171.



Is our water safe to drink? Ion chromatography-electrospray mass spectrometry of oxyhalides and haloacetates in drinking water



Leon Barron and Brett Paul
National Centre for Sensor Research, School of Chemical Sciences, Dublin City University, Ireland
email: brett.paul@dcu.ie

Recently, there has been increased concern that chlorine and ozone, used as disinfectants in water treatment, can lead to the formation of halogenated organic compounds and oxyhalides upon reaction with natural organic matter. These so-called disinfectant by-products (DBPs) include the group of compounds collectively known as haloacetic acids (HAAs) and the oxyhalides. The presence of HAAs in drinking water of major concern due to their potential carcinogenic and mutagenic effects. A suppressed IC method was developed for the analysis of (MBA) monobromo-, (DBA) dibromo-, (MCA) monochloro-, (DCA) dichloro-, (TCA) trichloro-, (CDFA) chlorodifluoro-, (TFA) trifluoro-, (CBA) chlorobromo-, (DCBA) dichlorobromo- and (CDBA) chlorodibromoacetates as well as iodate, chlorate, bromate and perchlorate in water by ion chromatography combined with various modes of detection. Perchlorate although not a DBP but occurs frequently in fertilisers and is a known endocrine disruptor. A Dionex (250 x 2 mm) AS16 anion exchange column (Dionex, Sunnyvale, CA, USA) was employed using a gradient of 1–20 mM sodium hydroxide as eluent combined with suppressed conductivity detection and mass spectrometry. This optimum method was applied to the determination of HAAs and oxyhalides in drinking water and a soil sample. For ultra-trace determinations of HAAs, preconcentration was necessary and was investigated using Merck LiChrolut EN SPE Cartridges (Merck, Darmstadt, Germany).

1. Suppressed Ion Chromatography with Conductivity Detection

Suppressed ion chromatography was carried out on a Dionex DSS00 complete with LC25 oven and CD20 conductivity detector. The suppressor used was a Dionex AEES Atlas (4 mm) monolithic cation exchange type suppressor operated at 18 mA from an SC20 suppressor controller. Fig. 1 shows the separation of 20 µM of 9 HAAs and 4 oxyhalides. A temperature program was used of 30°C for 20 mins, then stepped to 45°C for 10 minutes followed by 30°C for the remainder of the run. Re-equilibration was 16 minutes after a gradient run of 1 mM NaOH for 20 mins followed by linear ramping to 4 mM NaOH over 20 mins and then to 20 mM over 5 minutes. Injection volume: 100 µL. This method was sensitive to a lower limit of 0.49–7.9 µg/L for all analytes and displayed excellent linearity above R²=0.98, also for all analytes. Retention time repeatability of this temperature gradient method was less than 3% for all analytes when n = 30 replicate runs.

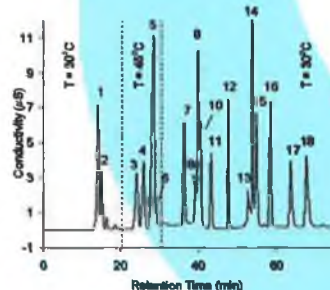


Fig. 1. Separation of 20 µM of nine HAAs and 4 oxyhalides in Milli-Q water. Elution order: 1 = acetate, 2 = iodate, 3 = MCA, 4 = bromate, 5 = chlorate, 6 = MBA, 7 = TFA, 8 = ribrate, 9 = chlorate, 10 = DCA, 11 = CDFA, 12 = DBA, 13 = carbonate, 14 = sulphate, 15 = TCA, 16 = DCBA, 17 = CDBA, 18 = perchlorate

2. Solid Phase Extraction

SPE was carried out for preconcentration of HAAs. 50 mL samples were acidified to < pH 0.3 and preconcentrated at 2 mL/min on Merck LiChrolut EN cartridges. For removal of excess sulphate (from acidification) and chloride the sample was passed through Alltech Max Clean IC-Ba (2), IC-Ag and IC-H cartridges [1]. Overall % recoveries were above 50% with the exception of TFA, DCBA, CDBA at 17, 30 and 13% respectively.

[1] "Determination of haloacetic acids in drinking water using a suppressed micro-bore ion chromatography with solid phase extraction", Leon Barron and Brett Paul, J. Chrom. A, 522 (2004), 153–161

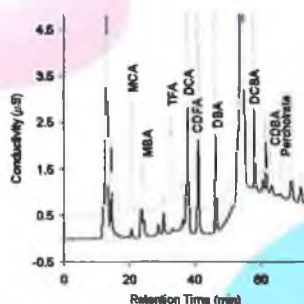


Fig. 2. Preconcentration of laboratory drinking water and overlaid with 1 µM spiked preconcentrate of all analytes. Offset by 0.5 µS for clarity.

Fig. 2 shows a preconcentration of drinking water overlaid with a 1 µM spiked preconcentrate. Levels of MCA, MBA, TFA, DCA, CDFA, DCBA, DBA, and perchlorate were found at above the USEPA maximum contamination limit of 60 µg/L for the sum of MCA, DCA, TCA, MBA and DBA. Above 60 µg/L, these compounds can adversely affect human health. The maximum contaminant limit for perchlorate is 10 µg/L.

3. Ion Chromatography-Electrospray Ionisation Mass Spectrometry of Real Samples

IC was coupled to a Bruker Daltonics Esquire-LC electrospray octopole ion trap mass spectrometer and applied to detection of real samples. Fig. 3 (left) shows a spiked drinking water sample of 2 µM of the 9 HAAs and 4 oxyhalides. Fig. 3 (right) shows perchlorate extracted from a soil sample and separated on the IC with a visible peak at min 99 and 101.

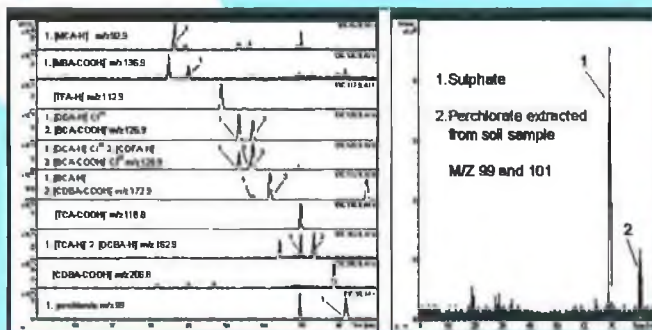


Fig. 3 (Left) Extracted Ion Chromatograms for 2 µM spiked preconcentrated drinking water sample of all ten HAAs and perchlorate. (Right) Presence of perchlorate in soil sample. Sol sample was dried at 40°C and perchlorate was extracted into 20 mL Milli-Q water.

4. Conclusions

Suppressed IC-ESI-MS has shown to offer a multitude of data about one sample. Moreover, it was sensitive to low µg/L concentrations of all analytes with conductivity detection and when preconcentration was employed the MS could easily detect low µg/L levels of all analytes. The reported high levels of HAAs and oxyhalides become more and more of an issue every day. Regulations are less stringent in Europe than the USA, but without reliable analytical methods, Irish drinking water cannot be monitored for the presence of harmful DBPs.

5. Acknowledgements

The authors would like to thank Enterprise Ireland for funding this project.